APPLICATION OF COMPUTER-AIDED DESIGN TO MICROSTRIP CIRCUITS

by

M. HOSSEINI B.Sc. Dip. Ed., M.Sc.

A thesis submitted for the degree of Doctor of Philosophy at

The University of Warwick, England.

July 1977.

SUMMARY

The work is based on a facility which has been developed in the Department of Engineering and presently is concerned with computer correction, optimization and computer-aided design of microwave integrated circuits.

The characterization of distributed elements on microstrip, particularly for use with a computer analysis/optimization package present a considerable challenge, making the analysis of microwave circuits difficult. Here, the network analyzer, in conjunction with automatic computer corrected S-parameter measurement, is utilized to characterize the discontinuity in terms of its properties at the external terminals. Some empirical expressions have been obtained for the effects of abrupt change in centre conductors of microstrip lines.

The generally accepted numerical techniques for evaluating microstrip parameters in conjunction with the computer-aided design packages are no longer useful. The reason for this is that a numerical routine has to be called upon numerous times, which makes it impossible in an optimization program. This was initially overcome by developing an algorithm, which allows for the evaluation of conductor and dielectric losses, as well as dispersion effects.

While the use of good analysis programs were essential, the limited capabilities associated with fast analysis algorithms often significantly reduce the efficiency of the design procedure. An algorithm was then developed to evaluate the two-port parameters of a multi-terminal circuit, which halves the number of iterations in comparison with conventional nodal analysis routines.

It was therefore decided to include junction parasitics and the above parameters in the optimization work. First some modifications were made on current optimization methods to be adopted for the design of microwave integrated circuits. Two programs were then developed, one applied to the design of several amplifiers on microstrip, utilizing gallium arsenide F.E.T.'s as well as bipolar transistors. The other program is used to

characterize two-port active as well as passive devices.

Initially a preliminary circuit was designed using a unilateral device model. Optimization was used to modify the circuit performance to meet the desired specification, by varying the element values. It was then possible to construct such an optimized circuit with the confidence that it would perform in a manner close to that which was predicted.

DECLARATION

The work described in this Thesis has not been submitted to any other University for a degree. Some of the material presented has been published or may be published in the future.

Use has been made of publications relevant to this work and references to such cases have appropriately been given. All other work and conclusions are due to the author unless otherwise stated.

ACKNOWLEDGEMENTS

I wish to express my gratitude to Professor J.A. Shercliff, Chairman of the Department of Engineering of the University of Warwick, and Professor J.L. Douce, for the facilities provided for conducting these investigations, the U.K. Science Research Council and the Ministry of Science and Higher Education of Iran for the financial support.

The work was supervised by Dr. H.V. Shurmer, and I wish to thank him for his guidance during the past three years and for his assistance during the preparation of the manuscript.

As I am a handicapped person, confined to a wheelchair, thanks are also due to my brother, Mr. M. Hosseini, for pushing my wheelchair and helping on many odd occasions.

During this time I have had the opportunity of meeting people who worked in the same field and discussing with them certain technical aspects of the problem. I take this opportunity of acknowledging their assistance.

In the Department of Engineering, Dr. M.K. McPhun for many useful discussions, particularly both Mr.and Mrs. DaSilva, for tolerating my all-too-frequent late-night visits and their very warm attitude. Mr. A.J. Hulme, Mrs. K.A. Stoneman and Miss L. Harvey for computing assistance. Thanks are also due to Mr. L. Baker, Mr. W.R. Davis, and Mrs. E. Ludford for their very warm attitude and many technical assistances.

In the School of Electronic Engineering, University College of North Wales, Professor I.M. Stephenson and B. Easter for many useful discussions on equivalent circuits of microstrip discontinuities.

In the Allen Clark Research Centre, Plessey Company Ltd., Mr. J.A. Turner, Dr. R.A. Soares (now at C.N.E.T., France), Mr. H.E.G. Luxton, Mr. D.A. Abbott and Dr. R.S. Butlin, for the use of GaAs F.E.T.'s devices and fabrication of microwave amplifiers and many useful discussions.

Finally, I would like to thank Mrs. Joan Carrington for the decipherment of the handwritten manuscript and typing the thesis.

CONTENTS

1

INTRODUCTION

Microstrip, because of its light weight, small dimensions and easy processing capability, is being increasingly used for microwave circuit design up to J-band frequencies. The original version, called the 'stripline', was introduced more than two decades ago around 1949. As early as March 1955 a special issue of IRE was published as "Transactions on Microwave Theory and Techniques", it was devoted entirely to the subject of microwave strip circuits. These early investigations into the properties of microstrip lines generally did not stimulate widespread acceptance of the technique, due to the ease with which line discontinuities could excite radiation and unwanted modes. Recent years have seen the rapid rise in importance of miniature microwave integrated circuits, which are usually planar in structure. Fig. 1.1 shows this structure; it consists of

a narrow strip conductor separated from a parallel conducting ground plane by an intervening and supporting dielectric material.

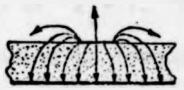

FIG. 1.1 MICROSTRIP STRUCTURE WITH FIELD.

The planar nature of microstrip lines immediately caused renewed attention to the microstrip technique. Moreover, the use of high dielectric constant substrate materials allows smaller overall circuit size as well as tending to bind the fringing fields more tightly to the centre conductor. These facts, plus the advantages of convenience and low batch fabrication costs, have tended to lessen the previous objections and finally allowed microstrip to achieve a posit... of widespread application.

From the general field theory [1], the characteristic solution of electric and magnetic field components in this structure may be expressed in terms of a scalar potential ϕ which is given by:

$$\nabla_t^2\phi + (K^2 - \beta^2)\phi = 0 \qquad \text{in the free space} \qquad (1.1a)$$

$$\nabla_t^2\phi + (\varepsilon_r K^2 - \beta^2)\phi = 0 \qquad \text{in the substrate} \qquad (1.1b)$$

subscript t indicates transverse, that is for x and y components only, so that the vector operator ∇_t may be written as follows:

$$\nabla_t = \vec{a}_x \frac{\partial}{\partial x} + \vec{a}_y \frac{\partial}{\partial y} \qquad (1.2)$$

The other quantities are $K = 2\pi/\lambda$, where λ is the free-space wavelength, and β the propagation constant.

In the case of free space ($\varepsilon_r = 1$), the potential ϕ satisfies the Laplace equation in the cross section and does not generate

longitudinal electric or magnetic field components. Hence, the lowest order mode is the TEM-mode. However in practice $\varepsilon_r > 1$, so to solve Equation (1.1) it may be regarded as a perturbation of the limiting case of $\varepsilon_r = 1$. The effect of this perturbation is small when the operation frequency is low. The quasi-TEM approximation may then be regarded as a zero-order solution to the exact equation shown in (1.1). The simplification applied above is not valid for higher values of K., as at higher frequencies spurious propagating modes introduce a dispersive effect which makes the simple TEM model inaccurate. Chapter 8 will illustrate this problem more fully and also presents an algorithm for evaluating the parameters of open microstrip line, which leads to calculation of conductor and dielectric losses, as well as dispersion effects [2].

In most micro strip networks the lines are necessarily finite in length and width, consequently this introduces discontinuity problems. Thus, for design purposes, the lines must be characterized and the parasitic junction effects evaluated in useful terms and parameters. If the circuit designer is not relying on "cut-and-try" methods, he requires accurate information concerning the discontinuity effects to be used in the alternative method of computer-aided design (CAD). To co-operate this information with CAD packages, it will be necessary to present results by formulae rather than by tables and curves. Chapter 9 presents a method for calculating the transmission properties of the discontinuities and considering also the frequency dependence of the microstrip lines. The method is far more powerful when used in conjuction with the additional facility of automatic computer corrected S-parameter measurements. The object of this chapter is also to establish the effects of various discontinuities that frequently occur in microwave integrated circuits. It provides

also an introduction to various methods of calculating discontinuity effects. Taking account of the various parameters and parasitic junction effects in microstrip circuits, the final design may be carried out by a computer-aided design approach.

The analytical adjustment of the circuit parameters, for a complex network, coupled with the use of measurement characterization data, can be very effective in an effort to achieve a final design which meets desired performance without requiring experimental adjustment of the circuit parameters. In most cases this can only be accomplished by the use of computer aided design [3].

The initial effort to use the computer as a design tool was made in the well-established area of filter synthesis[4]. In these now-classical approaches, filter design was separated into two main steps. The first step was to approximate a given set of design specifications by a system transfer function.

The second step was to realize this transfer function by a connection of ideal circuit elements. Typically, however, when physical elements were used to build the circuit, the actual performance deviated significantly from that which was desired.

The first attempt to solve this problem was made by M.R. Aaron[5], when he suggested that the computer could be a useful aid. He proposed using a least-squares approach for improving upon the design obtained in each step of the classical synthesis approach.

Today, computer programs permit determination of nominal component parameters values and also their maximum permitted spreads in relation to given tolerances on circuit response functions. This is done particularly when a large number of identical circuits must be produced. This is made possible by the availability of analysis

routineswhich, besides being rapid, also allow precise determination of network functions in conjunction with device modelling techniques and characterization data. An analysis routine, whether or not used in conjunction with optimization techniques, can provide the designer with an efficient means of combining empirical data with theoretical element models. This analysis/optimization routine is needed to simulate and optimize the performance of many microwave circuits. The specific need for this capability, rather than the "cut-and-try" approach, is to provide the engineer with an "automatic test bench" in which ideas are tried until a satisfactory result is achieved, resulting in a high degree of cost effectiveness in most applications.

For many requirements, however, no straightforward synthesis exists; this is true particularly in networks containing active devices, in which the designer's experience and intuition are brought to bear in choosing a circuit to meet the requirements. In many problems the effect of parameter values on performance is complicated and the designer needs extra knowledge to determine parameter changes and so improve performance. In this case a set of instructions may be written into a CAD program which could direct a synthesis process. Depending on the requirements, such instruction routines may solve: a) the approximation problem and exit when a suitable transfer function has been obtained; b) it may perform the realization only from a given transfer function; c) it may carry out the whole task, obtaining the circuit directly from the specifications. The network is repeatedly analyzed and its performance is compared with specifications. If necessary, the parameters are adjusted in a systematic way to reach the desired performance.

A flow chart of an analysis/optimization routine is shown in Fig. 1.2.

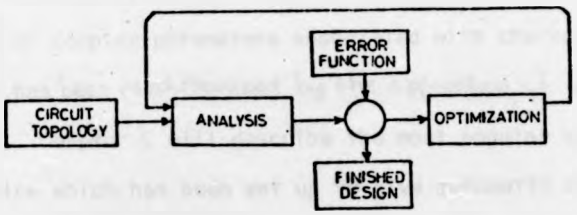

FIG. 1.2 A FLOW CHART OF COMPUTER-AIDED DESIGN.

Presently, there are many analysis/optimization routines in a variety of programming languages [6]. The optimization routines range from various direct search to sophisticated gradient methods. No attempt will be made to provide complete discussion of their operation here, since Chapter 2 will be devoted to more thorough analyses of some of these systems.

In principle the analysis algorithm invariably occupies the bulk of the computer time, being called upon to re-compute the overall network response each time the parameters are varied. It is therefore essential that this algorithm be made efficient which in turn influences the choice of network analysis method. In Chapter 3, various types of analysis routine are reviewed critically in terms of efficiency and cost when applied to microwave problems. Also in this Chapter an algorithm is presented for evaluating two -port network parameters, which halves the number of iterations in an analysis/optimization program.

An important consideration in CAD, the result of device characterization has enabled the designer to accurately simulate circuit performance with the aid of measured data. It is

in these areas that the measurements are so tedious manually, that automation via a digital computer is warranted. As many types of microwave instrumentation have become increasingly sophisticated, the treatment of complex parameters associated with characterization measurements has been revolutionized by the application of on-line measurements. Chapter 4 will describe the most popular computerized instrumentation which has been set up to give automatic on-line characterization by scattering parameters of 2-port microwave devices. In this system, errors inherent in the hardware, together with those arising from transitions, mounting arrangements, etc., at each frequency are evaluated and stored in the computer. Subsequent runs using test pieces to be characterized are carried out at the same frequency steps. The computed errors can be then subtracted from the measured data to give corrected results[7].

Errors in the S-parameters measurements of active or passive devices make them difficult to characterize. Any accurate measurement can only be carried out on the automatic network analyzer using the full two-port correction facilities. In the case of microstrip circuits and most two port active devices, an additional error is introduced by the parasitics of the coaxial-to-microstrip adapters. Chapter 5 will describe a technique which utilizes the coaxial standards available for use with the automatic network analyzer.

The various microstrip circuits involved in all experiments were carried out using nominally 0.025" thick 99.6% alumina substrates (MRC superstrate) with dielectric constant $\varepsilon_r = 9.8$. Chapter 6 describes the fabrication technique which has been adopted to construct the microstrip networks. Circuits were fabricated on

1" × 1" substrates using nichrome/gold conducting films of 5 microns approximate thickness.

The usefulness of theoretical calculation of microstrip parameters is severely limited by the accuracy with which the dielectric constant of the substrate material can be specified, at microwave frequencies. Thus, Chapter 7 covers the measurement technique which enables a check on the validity of theoretical data and provides data where the theory is not yet fruitful.

Finally, in Chapter 10 an optimization program is presented which includes algorithms for dispersion and losses in microstrip. A facility also exists within the program for converting transmission line elements from their air lengths and characteristic impedances to dimensions compatible with microstrip substrates. The optimization routine combines pseudo-random and conjugate gradient pattern search techniques, to improve the chances of finding a global minimum solution to multimodal problems. The optimization of several bipolar and GaAs F.E.T. amplifiers shows the program's ability to produce good results from poor starting values. In this Chapter two analysis programs will also be described; one uses the two-port chain matrix method and handles eight basic types of circuit elements for dealing with the microstrip circuits and the other utilizes the nodal analysis algorithm which has been developed by the author dealing mainly with the modelling of devices.

REFERENCES

1. COLLIN, R.E. "Field theory of guided waves," McGraw Hill, New York (1960).
2. HOSSEINI, N.M., and H.V. SHURMER ,"MICPA-Evaluation of microstrip line parameters", Electron. Lett. Vol. 12, No. 19, 15th Sept. (1976) pp.496-497.
3. HOSSEINI, N.M. and H.V. SHURMER, "Computer-aided design of microwave integrated circuits", Submitted to J. of Electronic and Radio Engineer. Special issue on microwave integrated circuits, December (1977).
4. GUILLEMIN, E.A. "Synthesis of passive network", John-Wiley & Sons, Inc. New York,(1957)
5. AARON, M.R. "The use of least squares in system design", IRE Trans. Circuit Theory, Vol. CT-3 (1956) pp. 224-231.
6. HOSSEINI, N.M., SHURMER, H.V. and SOARES, R.A."OPTIMAL-A program for optimising microstrip networks", Electron. Lett. Vol. 12, No.8, 15th April (1976), pp. 190-192.
7. SHURMER, H.V., LUXTON, H.E.G. HOSSEINI, N.M. and STONEMAN, K.A. "The application of an on-line computer to microwave measurement". IMEKO VII , Vol. No. 2, 10-14 May (1976), London, Paper, BEL/211.

OPTIMIZATION METHODS FOR MICROWAVE CIRCUITS

In problems where the synthesis procedures of classical circuit theory are inapplicable, optimization techniques may often provide a solution. They are generally iterative in nature, the network being analyzed repeatedly, performance compared with the specifications and the parameters adjusted systematically until success is achieved. Without this last qualification, of course, the analysis-cum-adjustment process degenerates into a computer aided cut-and-try method, the equivalent of the screwdriver-adjustment technique used by "on-the-bench" designers. As anyone who has attempted this procedure knows, convergence via cut-and-try is hopeless for circuits with several variable parameters. For this reason the sophisticated analysis methods of Chapter 3 should be supplemented by equally clever

techniques which enable the designer to improve his initial or intermediate results.

Depending on the requirements, an optimization program may solve only the approximation problems and exit when a suitable transfer function has been obtained. It may, alternatively, perform the realization only, from a given transfer function. Finally, it may carry out the whole task, obtaining the circuit directly from the specifications. However, this is not always a foolproof process. Even though the computer may be quite effective in modifying element values, a proper choice of circuit topology is usually left to the designer, such a choice being essential if a final design is to be achieved with elements which are readily physically realizable.

It is not intended to give here a complete account of optimization techniques, as they are dealt with in the literature [1-5]. The main purpose is rather to review various methods which can be applied to microwave integrated circuit design. First, the basic ideas of optimization are discussed. This is followed by classifying these methods into three categories, with a discussion of each one. Finally a criterion is given, devised by the author, for choosing any particular technique. The chapter ends with an examination of how the current optimization program may be improved and extended for designing circuits.

2.1 BASIC IDEAS OF OPTIMIZATION.

'In a broad sense, optimization means finding the combination of a group of variables which sets a function equal to its optimum, usually either at the minimum or maximum value of the function. The function may be linear or non-linear, with or without constraints on the range of values from which the variables are chosen. For meaningful supervision of the optimization process, the proper performance evaluation function must be chosen and a satisfactory description of it provided. This usually means that the function to be minimized, or maximized, (called the 'error function') must adequately describe the final desired response. The objective function thus generated will be an error function of some type (e.g. mean square, Tchebyschev error, etc.). This then will be the dependent variable which the optimization process will seek to optimize.' A frequently used error function, for various responses such as transducer gain, input and output VSWR, is the following least pth formulation

$$\epsilon = 1/p \sum_{\omega} (W_1(j\omega)|\rho_{in}(j\omega)|^P + W_2(j\omega)|\rho_{out}(j\omega)|^P + W_3(j\omega)|G_t(j\omega) - G_d(j\omega)|^P) \qquad (2.1a)$$

An error function which includes both gain and noise figure may be written as:

$$\epsilon = 1/p \sum_{\omega}(W_1(j\omega)|NF(j\omega)|^P + W_2(j\omega)|G_t(j\omega) - G_d(j\omega)|^P \qquad (2.1b)$$

where

W_1, W_2 and W_3 are the weighting factors.

G_T and G_d are calculated and desired gain respectively.

ρ_{in} and ρ_{out} are input and output VSWR respectively

NF is the noise figure and P is an integer even number.

The least Pth error function is sometimes referred to as the least Pth 'objective function'. For example, an ideal objective in amplifier design is to minimize the least Pth maximum deviation of the actual response from the specified performance. Fig. 2.1 shows a response function satisfying an amplifier specification.

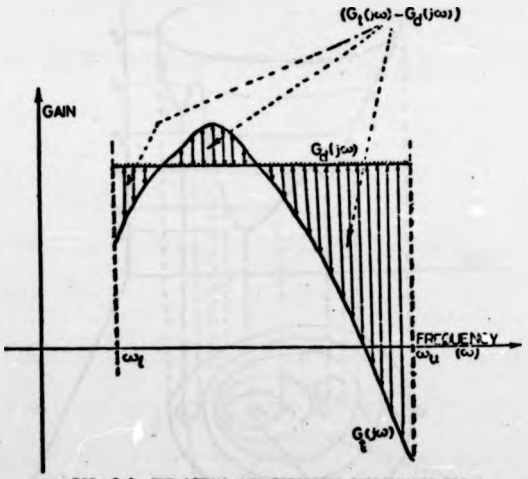

FIG. 2.1 THE ACTUAL AND SPECIFIED PERFORMANCE FOR A TYPICAL AMPLIFIER, WHERE G_d IS DESIRED GAIN, G_t IS COMPUTED GAIN, and ω_L, ω_U ARE LOWER AND UPPER FREQUENCY BOUNDS RESPECTIVELY.

It frequently happens that the objective function has more than one optimum, in which case it is called a "multi-modal" function, as distinct from a "uni-modal" function, which has only a single optimum. If several optima exist (of different value), the most extreme one is referred to as the "global" optimum while others are called "local" optima. Fig. 2.2 illustrates a surface which represents the error function of an organization.

As mentioned before, an optimization method is essentially a set of procedures for systematically generating a sequence of vectors or points

$\tilde{x}_o, \tilde{x}_1, \tilde{x}_2, \ldots \tilde{x}_k, \ldots$ in a subset such that:

$$\varepsilon(\tilde{x}_o) > \varepsilon(\tilde{x}_1) > \varepsilon(\tilde{x}_2) \ldots > \varepsilon(\tilde{x}_k) \ldots \qquad (2.2)$$

and evaluating their effectiveness in locating optimum points.

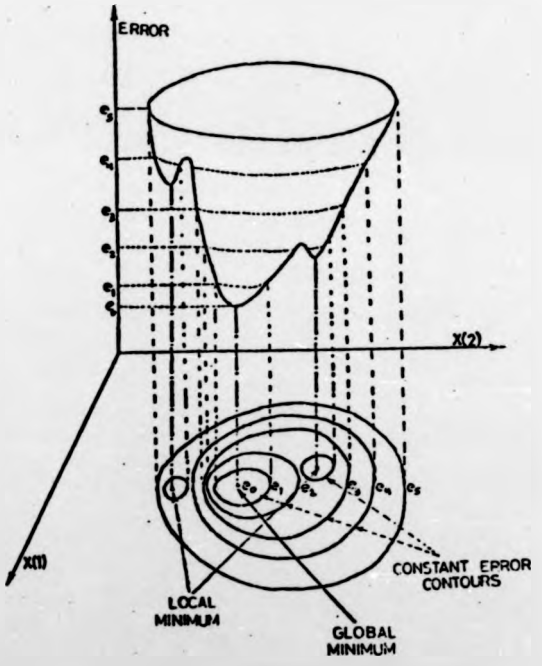

FIG. 2.2 ERROR FUNCTION OF MULTI-MODAL PROBLEMS MAY HAVE LOCAL AND GLOBAL MINIMUM.

Naturally, the methods which converge are of greater interest, i.e. methods which generate the optimum points in a finite number of steps, or in which points come sufficiently close to the optimum after a finite number of $\tilde{x}$'s.

In generating such sequences of points, a starting value $(\tilde{x}_o)$ must be chosen, which satisfies any constraints which may exist.

Once a point is chosen, two decisions must be made before the next point can be generated. Firstly, a direction must be picked in which the next point can be generated and secondly a step size must be decided, to be taken in the chosen direction. Any descent method generates $[\tilde{x}_k]$ by the following equation:

$$\tilde{x}_{k+1} = \tilde{x}_k + t_k \tilde{d}_k \qquad k = 0, 1, \ldots \qquad (2.3)$$

where $\tilde{d}_k$ is the direction and $|t_k d_k|$ is the step size.

The mechanism of generating sequences of points and their effectiveness in locating the optimum point depend very much on the function to be optimized and on the amount of information which is available for generating the next guess at the optimum point.

2.2 CURRENT OPTIMIZATION METHODS

Roughly speaking, we may classify the optimization methods into three categories:

A - The methods using only the functional values.

B - The methods making use of first-order derivatives as well.

C - The methods which also require knowledge of second-order derivatives.

These derivatives may be computed analytically, or numerically, depending on the methods. The methods in category (C) will generate points that are sufficiently close to the optimum point in some sense in the least number of steps. This does not mean, however, that they are the most efficient methods in terms of computer time. In microwave theory the function $\varepsilon(\tilde{x})$ is so complex that its second derivatives may not be obtainable explicitly by an analytical method and even their numerical approximation may be very crude. Thus evaluation of derivatives may consume

more computer time than would be needed to evaluate the function at several points.

Typically, mathematical functions which describe microwave circuit behaviour are non-linear. Dropping the methods of categories (C), the applicable methods then are categories (A) and (B), which may be classified into one of the following two groups.

2.2.1 DIRECT SEARCH

The methods in Category (A), which do not require the calculation of gradients but rather depend on function evaluation at various combinations of variables are classified into this group. The direct search methods cover several strategies i.e. grid and random search, which do not rely on directions, and pattern search, which relies on the direction of greatest improvement. However, they will be discussed briefly, each one in turn, as follows:-

GRID SEARCH. This method does not rely on gradients or directions and basically involves choosing a large number of independent variable sets and evaluating the dependent variable. Fig. 2.3 shows how the variable range is broken up into small segments and the function is repeatedly evaluated until the lowest function value is found.

RANDOM SEARCH. This method may also be classified in this group where a compound number of random function evaluations are done to locate an optimum within some range of the true optimum for a given factor.

PATTERN SEARCH. This method relies on the direction of greatest improvement. Fig. 2.4 shows a typical technique where the function is initially evaluated at and around some starting point and a finite step is then taken in the direction where the greatest improvement is detected.

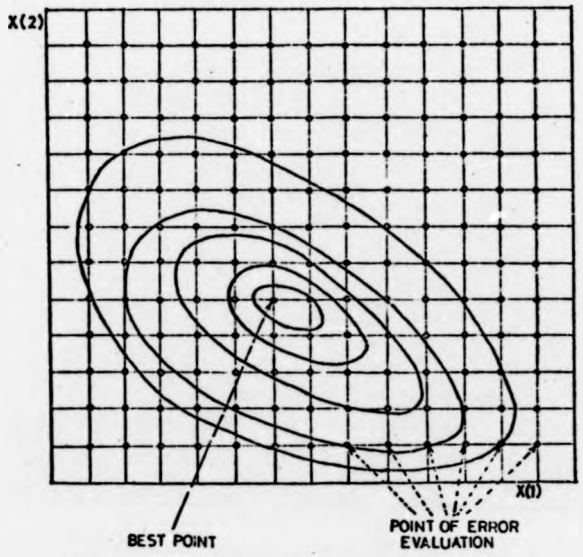

FIG. 2.3 GRID SEARCH METHODS DO NOT RELY ON GRADIENTS.

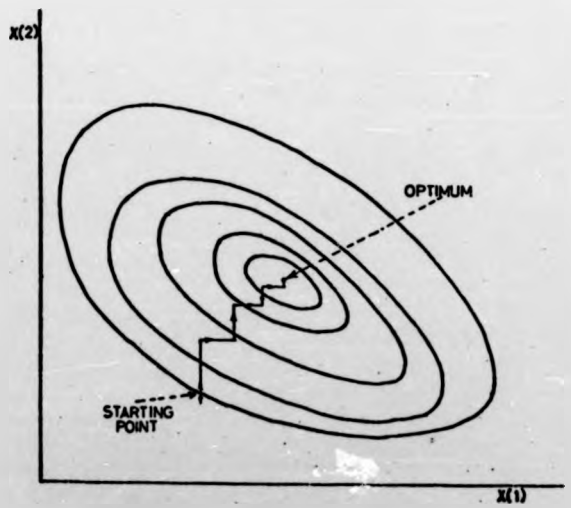

FIG. 2.4 A PATTERN SEARCH RELIES ON THE DIRECTION OF GREATEST IMPROVEMENT.

This method is much more efficient than grid and random techniques, and has found great application in microwave circuits[5]. One of strategies, called "DIRECT SEARCH", has been described by Hooke and Jeeves[6]. The procedure is started by evaluating the error at the starting point (base) and a set of exploratory moves are made along the co-ordinate axes in order to determine the direction in which the minimum lies. A pattern move is then made along the direction selected by a successful move, in the hope that the previous success will be repeated. When a pattern move and subsequent exploratory moves fail, the parameter increments are reduced and the whole procedure restarted at that base point. The search is terminated when increments fall below prescribed levels.

A similar technique called "SPIDER", in which the exploratory moves are made in randomly chosen orthogonal directions, has been described by Emery and O'Hagan[7].

Another technique that appears to be very efficient in terms of computer running time is called the "SIMPLEX" method[8]. The error function is evaluated at $(n + 1)$ mutually equidistant points in the space of the n independent variables, such points being said to form the vertices of a simplex. The method then determines the vertex at which the error function has the largest value, and refects this vertex in the centroid of the reflection. If reflection has produced a new optimum point, then further steps in this direction test for any success. However, if reflection gives a worse point then a contraction takes place.

Finally, another method in this group is called "RAZOR" search[9]. This strategy begins with a modified version of the pattern search

until it fails. A random point is selected automatically in the neighbourhood and a second pattern search is initiated until this one also fails. The method has been proposed to deal with valleys along which a path of discontinuous derivatives lies.

2.2.2. GRADIENT BASED METHODS.

The values of first order partial derivatives of the error function with respect to the independent variables are used in selecting the search direction. Several known techniques exist in this group, the most popular strategies being described as follows:

STEEPEST DESCENT. By mathematical definition, a function will increase fastest along the direction of gradient and the most rapid decrease can be found along the negative direction [4]. This direction is known as the direction of steepest descent. In this method first a gradient direction is computed which points toward the greatest improvement in the optimum along the line. This is followed by finding a new gradient direction and another line search along that direction. Fig. 2.5 shows the performance of this method.

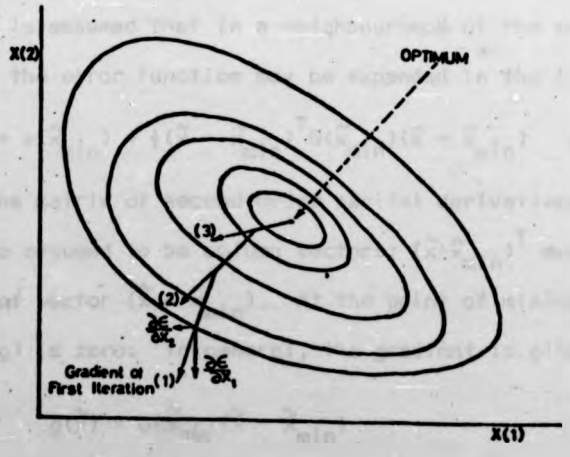

FIG. 2.5 GRADIENT SEARCH METHODS TAKE PARTIAL DERIVATIVES OF ERROR FUNCTION IN SELECTING THE SEARCH DIRECTION.

The process is repeated until no further improvement can be found. The gradient is defined as the vector sum of the partial derivatives

$$\bar{g} = \left(\frac{\partial \varepsilon}{\partial x_1}, \frac{\partial \varepsilon}{\partial x_2}, \frac{\partial \varepsilon}{\partial x_3}, \ldots \frac{\partial \varepsilon}{\partial x_n}\right) \qquad (2.4)$$

The method of steepest descent is very slow. Various modifications have been made to speed up the procedure[10], but near the optimum it still tends to slow down drastically. However, some gradient methods (e.g. direct search method) find the optimum of the function along the direction of search instead of taking a fixed step in this direction. Suppose that starting from $\tilde{x}_o$, vectors $\tilde{x}_1, \ldots, \tilde{x}_k$ have been generated, where the next vector $\tilde{x}_{k+1}$ is chosen somewhere on the ray emanating from $\tilde{x}_k$ in the direction $\tilde{d}_k$ in (2.3), then t_k is determined by solving the corresponding one-dimensional optimization problem[4].

VARIABLE METRIC METHOD. The most popular strategy based on gradient technique was proposed by Davidson[11]. This method is known as 'VARIABLE METRIC'. The underlying method, described by Fletcher and Powell[12], is based on the variable metric technique. It is assumed that in a neighbourhood of the required minimum $\tilde{x}_{min}$, the error function may be expanded in the form:

$$\varepsilon(\tilde{x}) = \varepsilon(\tilde{x}_{min}) + \tfrac{1}{2}(\tilde{x} - \tilde{x}_{min})^T G(\tilde{x}_{min})(\tilde{x} - \tilde{x}_{min}) \qquad (2.5)$$

where G, is the matrix of second-order partial derivatives. The vectors are assumed to be column vectors; $(\tilde{x}-\tilde{x}_{min})^T$ means the transpose of vector $(\tilde{x} - \tilde{x}_{min})$. At the point of minimum, the gradient (g) is zero. In general, the gradient is given by

$$g(\tilde{x}) = G(\tilde{x}_{min})(\tilde{x} - \tilde{x}_{min}) \qquad (2.6)$$

Assuming now that the symmetric matrix G is positive definite, the following equation holds true:

$$\tilde{x} - \tilde{x}_{min} = G^{-1}(\tilde{x}_{min}) \cdot g(\tilde{x}) \qquad (2.7)$$

If $G^{-1}(x_{min})$ were available, it would allow $\tilde{x}_{min}$ to be calculated in one step.

To approach $G^{-1}(x_{min})$, a method of successive linear search in the G-conjugate direction is used (see Appendix A).

CONJUGATE DIRECTION METHOD - The conjugate direction method is in fact similar to the gradient method, but the difference is that each new direction of search forms a part of the iteration cycle. In this method the new values of $\tilde{x}_{k+1}$ are found by using

$$\tilde{x}_{k+1} = \tilde{x}_k + t_k \tilde{P}_k \ , \qquad (2.8)$$

where $\tilde{P}_k = H_k \tilde{d}_k$, the matrix H_k being updated at every iteration. The matrix H_k rotates the direction of search from that of the gradient to a new directions, $\tilde{P}_o, \tilde{P}_1, \ldots . \tilde{P}_{n-1}$ so that G-orthogonality is satisfied. The underling method has been described by Fletcher and Reeves[13]. From the Taylor expansion (2.5), the gradient is seen to be as (2.6). The condition for the gradient to vanish is:

$$G(\tilde{x}_{min}) \cdot \tilde{x} = G(\tilde{x}_{min}) \cdot \tilde{x}_{min} \qquad (2.9)$$

For the solution of these equations, direction $\tilde{P}_o, \tilde{P}_1, \ldots$ are generated such that G-orthogonality is satisfied (see ch. 10).

2.3 A POSSIBLE CRITERION

Because there are so many optimization methods, it is not generally possible to single out a particular method as the one to be used in every case. Some judgement, experience, or preliminary exploration may be necessary to find a method that will solve the optimization problem in a routine manner if possible.

A few attempts at comparison studies have been made by several computing centres. These, however, tend to make objective comparisons much more difficult, since different computing centres have different computing hardware and software .

One attempt was made by Fletcher [14] to examine the relative efficiency of a few direct search methods on various test functions. The test functions were designed to prove difficult to minimize. For example, one of those is a parabolic valley proposed by Rosenbrock [15]., viz:-

$$f(x_1, x_2) = 100\,(x_2 - x_1^2)^2 + (1 - x_1)^2$$

with starting values $\underset{\sim}{x}_o = (-1.2, 1.0)$

For each test function he plotted $\log_{10}(f - f_{min})$ against the number of linear minimizations. His conclusion was that most techniques became unworkable as the number of variables increased. This situation arises from the fact that at each iteration, many of the linear minimizations are made repeatedly in limited subspaces, permitting only restricted progress to the minimum.

The situation with regard to the problem of microwave optimization is somewhat different. Microwave error functions are usually complex and have many local extremes, so these sequential methods may converge to the nearest local minimum, ignoring neighbouring minima, which may be better. Thus it may be seen that one of the criteria is ACCURACY, i.e. how close are the final objective function values and the minimum vectors to the true minima. Although there are no absolute guarantees of a "global minimum" by most pattern search methods, this does not become really restrictive; if the response meets the designer's criteria, that minimum is acceptable. Another compara tive study has been made by Colville[16], in which he asked over thirty participants to submit test problems and to solve those problems chosen for the study. The selected problems were varied in size and structure and represent typical examples of current applications of nonlinear programming.

The criteria which he put on each solution were as follows:

(a) How much time is required to program and set up the problem?

(b) How much time is required to execute the problem solution?

(c) How many function and constraint evaluations are required?

(d) Are partial derivatives calculated? If so, how? Analytically or numerically?

An overall summary of results was that the methods in category (c) were much more efficient than either the direct search methods or the small step gradient methods. It should be emphasized that this observation is fairly obvious. But as previously noted the methods of category (C) are not applicable to microwave optimization problems.

2.4 CONCLUSIONS.

In general, the direct and pattern optimization techniques are based on "sequential" or linear search algorithms in which points previously generated are used in determining the new directions of search. Although extremely efficient in determining the minima of unimodal functions, a sequential search technique will converge to the nearest local minimum, ignoring neighbouring minima which may be superior.

As cost is a very important consideration in the selection of an optimization algorithm for use in an industrial application, the author and his colleagues[17] have been using a very large step direct-search technique. Although very efficient in producing an acceptable result from a poor starting value, for multivariable problems, the penalty paid here is that the convergence rate is slow where initial values are near to the optimum. Fig. 2.6, shows the gain of an amplifier versus frequency which has been optimized with a large step, pseudo-random strategy. It can be seen the convergence rate tends to slow down after three cycles. This is because the technique requires several variables in order to "hop" randomly from minima to

minima until one of a satisfactory depth has been located.

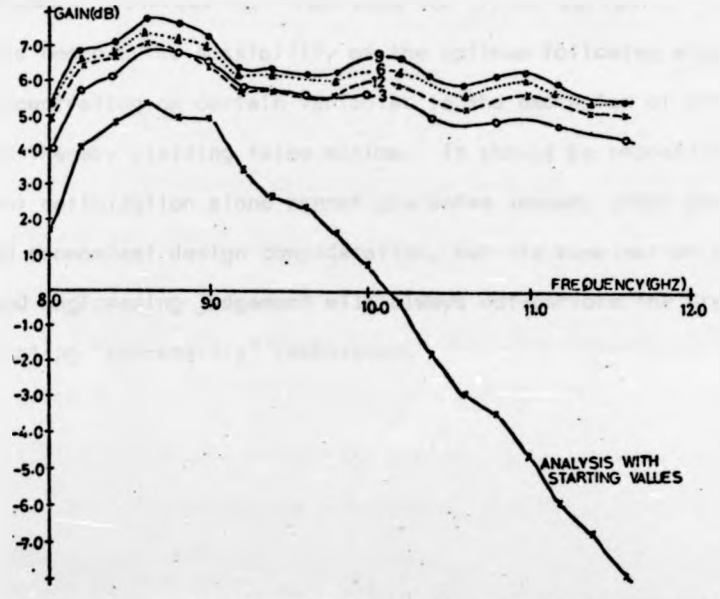

FIG. 2.6 THE CONVERGENCE RATE OF LARGE STEP LINEAR SEARCH IS SLOW FOR DESIGNS WHOSE INITIAL VALUES ARE NEAR TO THE OPTIMUM.

By using two or three different strategies of optimization[18], one may increase the accuracy of approach to the true minimum. It is also desirable to reduce the execution time, particularly when the starting points are near to the position of the minimum. To these ends the author and his colleagues have used a combination of 'large step direct search' with 'conjugate gradient pattern search' techniques. To improve the chances of finding a global minimum solution to multi-modal problems (as encountered in amplifier optimization), a limited number of random searches are also employed. The nonunilateral properties of GaAS F.E.T.

and bipolar transistors in microwave amplifier circuits means that the elements all interact to some degree with each other which affects the overall response. For this reason, the pseudo-random sequence technique has been used for chosen variables [19,20]. This reduces the possibility of the optimum following algorithm concentrating on certain variables to the exclusion of others, and thereby yielding false minima. It should be emphasized that optimization alone cannot guarantee success under practical and economical design consideration, but its combination with good engineering judgement will always out-perform the previously existing "cut-and-try" techniques.

REFERENCES

1. WILDE, D.J. and BEIGHTLER, C.S. "Foundations of optimization", Prentice-Hall, Inc., Chapters 4, 5, 6, 7, 8 (1967) pp. 99-425.

2. PIERRE, D.A. "Optimization theory with application", John Wiley & Sons., New York (1969).

3. AOKI, M. "Introduction to optimization techniques. Fundamentals and applications of non-linear programming", MacMillan Company, New York, (1971).

4. BOX, M.J., DAVIES, D., and SWANN, W.H. "Non-linear optimization techniques", Oliver and Boyd, Edinburgh, U.K., (1969).

5. BANDLER, J.W. "Optimization methods for computer-aided design", I.E.E.E. Trans. Microwave Theory and Techniques, Vol., MTT-17, No. 8, August (1969), pp. 533-552.

6. HOOKE, R., and JEEVES, T.A. "Direct search-solution of numerical and statistical problems", J. ACM, Vol. 8, April (1961), pp. 212-229.

7. EMERY, F.E., and O'HAGAN, M. "Optimal design of matching network, for microwave transistor amplifiers", I.E.E.E. Trans. Microwave Theory and Techniques, Vol. MTT-14, pp. 696-698, December (1966).

8. NELDER, J.A., and MEAD, R. "A simplex method for function minimization", Computer J. Vol. 7 , pp.308-313, January (1965).

9. BANDLER, J.W. and MacDONALD, P.A., "Optimization of microwave networks by razor search", I.E.E.E. Trans. Microwave Theory and Techniques, Vol. MTT-17, No. 8, pp. 552-562, August (1969).

10. AGNEW, D. "Gradient based optimization", Notes associated with a one-day seminar, Imperial College, Department of Electrical Engineering, London, 12th February (1975).

11. DAVIDSON, W.C. "Variable metric methods for minimization", Argonne National Laboratory Report, ANL-5990, Revised November (1959).

12. FLETCHER, R. and POWELL, M.J.D. "A rapidly convergent descent method for minimization", Computer Journal, Vol. 6, iss. 2., pp. 163-168, (1963).

13. FLETCHER, R. and REEVES, C.M."Function minimization by conjugate gradients", Computer Journal, Vol. 7, pp.149-154 (1964).

14. FLETCHER, R. "Function minimization without evaluating derivatives", Computer Journal, Vol. 8, iss. 1., pp.33-41, April (1965).

15. ROSENBROCK, H.H. "An automatic method for finding the greatest or least value of a function", Computer Journal, Vol. 3, pp.175-184 (1960).

16. COLVILLE, A.R. "A comparative study of nonlinear programming codes", Technical Report No. 320-2949, IBM New York Scientific Centre, June (1968).

17. HOSSEINI, N.M., SHURMER, H.V., and SOARES, R.A. "OPTIMAL- a program for optimising microstrip networks"., Electron.Lett. Vol.12, No. 8, 15th April (1976), pp. 190-192.

18. HOSSEINI, N.M. "Computer-aided microwave circuit design". Internal report, University of Warwick, May 1976.

19. HOSSEINI, N.M., SHURMER, H.V. "Parameter evaluation and optimisation for microstrip", I.E.E. Colloquium on microwave integrated circuit, Digest No. 1976/93, London 28 October (1976), pp. 4/1-3.

20. SOARES, R. A. "Amplifier design using bipolar transistors", London University, Ph.D. Thesis (1974).

3

COMPUTER AIDED - ANALYSIS METHODS

In any combined circuit analysis/optimization computer program, the analysis subroutine plays a dominant role. The associated algorithm invariably occupies the bulk of the computer time, being called upon to re-compute the overall network response each time the parameters are varied. It is therefore essential that this algorithm be made efficient, which in turn influences the choice of network analysis method.

Several analytical methods have been used in the study and design of microwave circuits. This Chapter begins by discussing the indefinite admittance matrix (IAM) as being most appropriate for combinations of two and three terminal networks. This is followed by a detailed exposition of an analysis algorithm developed by the author, which is very useful, particularly for modelling transistors and other active devices. A critical review of the general two-port chain matrix is described next, this being eminently suitable, both on account of its high efficiency

and adaptability for programming. In relation to minimizing the computing time and memory size, some consideration is given to sparse-matrix techniques. The chapter ends with a discussion of the adjoint network approach, followed by the author's conclusions.

3.1 MULTI-TERMINAL CIRCUIT ANALYSIS

Sometimes it is advantageous to use a combination of matrix techniques, rather than a single procedure[1]. The former approach may be particularly useful where different types of network are involved which have a common node or ground connection. An example illustrative of the approach is described, involving use of the indefinite admittance matrix (IAM) in combination with a definite impedance matrix[2].

The short circuit admittance matrix[Y], for a two terminal admittance y connected between nodes i and j of an n-node network, is given by:

$$[Y] = \begin{array}{c} \begin{matrix} i & j \end{matrix} \\ \begin{bmatrix} y & -y \\ -y & y \end{bmatrix} \begin{matrix} i \\ j \end{matrix} \end{array} \qquad (3.1)$$

Consider now a three-terminal device added into the network at nodes 1, 2 and 3, where the third terminal is at the reference or ground potential, as indicated in Fig. 3.1.

FIG. 3.1 DEVICE WITH ADMITTANCE PARAMETERS MEASURED WITH RESPECT TO TERMINAL 3.

From superposition theory[2], it is easy to show that the IAM will be given by:

$$[Y]=\begin{bmatrix} y_{11} & y_{12} & -(y_{11}+y_{12}) \\ y_{21} & y_{22} & -(y_{21}+y_{22}) \\ -(y_{11}+y_{21}) & -(y_{12}+y_{22}) & y_{11}+y_{12}+y_{21}+y_{22} \end{bmatrix} \qquad (3.2)$$

It should be noted that, any particular terminal of the added device may be selected as the reference terminal. For example, with a bipolar transistor, it would be equally admissible to use as the reference terminal either the base, emitter or collector.

Suppose now, the IAM of an n-node circuit is being entered in a manner such that the ground node is placed in the last row. The next m rows from the bottom denote the grounded voltage source nodes, and the first $\ell = n - m$ rows represent the actual elements. This ordered indefinite admittance matrix is depicted in (3.3).

$$[\tilde{Y}] = \begin{matrix} n-m \\ m \\ 0 \end{matrix} \begin{bmatrix} \tilde{y}_{\ell\ell} & \tilde{y}_{\ell s} & \tilde{y}_{\ell g} \\ \tilde{y}_{s\ell} & \tilde{y}_{ss} & \tilde{y}_{sg} \\ \tilde{y}_{g\ell} & \tilde{y}_{gs} & \tilde{y}_{gg} \end{bmatrix} \qquad (3.3)$$

Solving (3.3) for the first $n-m$ rows, we then get:

$$\tilde{I}_\ell = \tilde{y}_{\ell\ell}\,\tilde{v}_\ell + \tilde{y}_{\ell s}\,\tilde{v}_s \qquad (3.4)$$

where $\tilde{I}_\ell$ denotes the independent current source connected to the first ℓ nodes, $\tilde{v}_s$ the grounded independent voltage source and $\tilde{v}_\ell$ the unknown voltage of the first ℓ nodes. The matrix $\tilde{y}_{\ell\ell}$ may be decomposed into two matrices of a lower $[L]$ and an upper triangular

[U] such that $\tilde{y}_{\ell\ell} = LU$. If we now get:

$$LU\ \tilde{V}_{\ell} = \tilde{I}_{eq} \tag{3.5}$$

Then $\tilde{I}_{eq} = \tilde{I}_{\ell} - \tilde{y}_{\ell s}\ \tilde{v}_{s}$ may be solved by forward and backward substitution[9].

3.1.1 ANALYSING LARGE CIRCUITS.

In order to analyze very large circuits, one may divide the circuit into subcircuits calculating for each of them one of its n-port matrices. Subsequently, the subcircuits are interconnected and so the matrix relative to the ports of the complete circuit is determined.

Once the IAM of a subcircuit is established it may be divided into internal and external nodes. By eliminating the variables relative to the internal nodes, one obtains the IAM matrix relative to the external nodes.

Every IAM matrix may be partitioned into the following equation

$$\begin{bmatrix} \tilde{I}_e \\ \tilde{I}_i \end{bmatrix} = \begin{bmatrix} \tilde{y}_{ee} & \tilde{y}_{ei} \\ \tilde{y}_{ie} & \tilde{y}_{ii} \end{bmatrix} \begin{bmatrix} \tilde{V}_e \\ \tilde{V}_i \end{bmatrix} \tag{3.6}$$

where $\tilde{I}_e$ and $\tilde{V}_e$ are the vectors of the currents and voltages relative to the external nodes, and $\tilde{I}_i$ and $\tilde{V}_i$ are those relative to the internal nodes. If nothing is to be connected to the internal terminals then $\tilde{I}_i = 0$ and solving (3.6) for $\tilde{V}_i$ in terms of $\tilde{V}_e$ i.e:-

$$V_i = -\tilde{y}_{ii}^{-1}\ \tilde{y}_{ie}\ \tilde{V}_e \tag{3.7}$$

The current $\tilde{I}_e$ is then given by:

$$\tilde{I}_e = (\tilde{y}_{ee} - \tilde{y}_{ei}\ \tilde{y}_{ii}^{-1}\ \tilde{y}_{ie})\ \tilde{V}_e \tag{3.8}$$

which may be written:

$$\tilde{I}_{eq} = \tilde{y}_e \tilde{v}_e \tag{3.9}$$

with

$$\tilde{y}_e = \tilde{y}_{ee} - \tilde{y}_{ei} \tilde{y}_{ii}^{-1} \tilde{y}_{ie} \tag{3.10}$$

which represents the IAM with respect to the external ports of each subcircuit. When the subcircuits are connected together the IAM for the external nodes of the complete circuit is calculated using the same procedure[3].

3.1.2 COMPUTATION OF TWO-PORT PARAMETERS.

In a vast number of network problems, however complicated the network, the relationship between electrical properties at an output port and an input port is the item of predominant interest. It is therefore desirable to compute the two-port parameters of such a network.

The author has developed an alternative procedure which halves the number of iterations required in the evaluation of any two-port parameters.

This section describes how, with the aid of a simple algorithm, a relatively inexperienced computer programmer can apply the relevant procedures to typical multiterminal circuit analysis. This is very useful, particularly for modelling transistors and various other active and passive devices.

Consider a network in which there are n independent node-pairs, labelled sequentially, 1, 2, ... i, ... o, ... (n-1), n, where i and o are those terminal pairs acting as input and output ports respectively. It may be necessary to consider only these node-pairs

and ignore all others, we can use one of the standard forms of two-port parameters to represent the network between the input and output ports. If the representation is to be in the form of Z-parameters, for example, it is required to find the elements of the Z-matrix of eqn. (3.11).

$$\begin{bmatrix} V_i \\ V_o \end{bmatrix} = \begin{bmatrix} Z_{ii} & Z_{io} \\ Z_{oi} & Z_{oo} \end{bmatrix} \begin{bmatrix} I_i \\ I_o \end{bmatrix} \tag{3.11}$$

The IAM for the n-independent node-pairs would be of the form

$$[I] = [Y]\,[V] \tag{3.12}$$

where all the elements of $[I]$ are zero except for I_i and I_o. If the node n is being taken as the reference we may obtain a non-singular matrix $[Y_{n-1}]$ by removing from $[Y]$ the nth row and column. Provided that the determinant of this matrix is non-zero we may then obtain the inverse of the admittance matrix $[Y_{n-1}]$, and hence re-write eqn. (3.11)

$$[V] = [Z]\,[I] \tag{3.13}$$

The matrix eqn. (3.13) represents (n-1) simultaneous equations. Since, however, there are only four unknowns, we may reduce these to two equations only, i.e. the ones involving the independent variables, thus relating to the input and output terminals. Hence factorising the $[Y_{n-1}]$ matrix into the lower triangular matrix $[L]$ and upper triangular matrix $[U]$ with diagonal elements of unity, the jth column of these matrices may be calculated via the following algorithm [4]:

$$u_{ij} = (y_{ij} - \sum_{k=1}^{i-1} \ell_{ik}\, u_{kj})/\ell_{ii} \qquad i < j$$

$$\ell_{ij} = y_{ij} - \sum_{k=1}^{j-1} \ell_{ik}\, u_{kj} \qquad i \geq j \tag{3.14}$$

where u_{ij} and ℓ_{ij} are the elements of $[U]$ and $[L]$ respectively, utilising

$$\left[Y_{n-1}\right]^{-1} = [U]^{-1}\,[L]^{-1} \tag{3.15}$$

Now the problem is to invert the triangular matrices $[L]$ and $[U]$. The inverse of a lower (upper) triangular matrix is also a lower (upper) triangular matrix [5].. Now let $[L]^{-1} = [\ell'_{ij}]$ with $\ell'_{ij} = 0$, $i < j$ and let $\tilde{L}_i$ and $\tilde{L}_j^{-1}$ be respectively, the ith column of $[L]$ and the jth row of $[L]^{-1}$. Then for $1 \leq k \leq n$:

$$\begin{aligned} \tilde{L}_k^{-1}\,\tilde{L}_k &= \ell'_{kk}\,\ell_{kk} = 1 \\ \tilde{L}_k^{-1}\,\tilde{L}_j &= \sum_{i=j}^{k} \ell'_{ki}\,\ell_{ij} = 0 \qquad j = k-1,\ k-2,\ \ldots,\ 1 \end{aligned} \tag{3.16}$$

from which may be calculated ℓ'_{ki}, $i = k,\ k-1,\ \ldots,\ 1$ for any k, thereby obtaining all the elements of $[L]^{-1}$. The algorithm is as follows:

$$\begin{aligned} \ell'_{kk} &= 1/\ell_{kk} \qquad k = 1,\ \ldots,\ n \\ \ell'_{kj} &= (-\sum_{i=j+1}^{k} \ell'_{ki}\,\ell_{ij})/\ell_{jj} \qquad j = k-1,\ \ldots,\ 1 \end{aligned} \tag{3.17}$$

similarly we may calculate $[U]^{-1} = [u'_{ij}]$ the only difference being the fact that the diagonal elements of $[U]$ are unity. The

calculation of $[L]^{-1}$ and $[U]^{-1}$ followed by the matrix multiplication $[U]^{-1}\,[L]^{-1}$, gives the following algorithm:

$$z_{ij} = \sum_{k=1}^{n} u'_{ik}\, \ell'_{kj} \qquad (3.18)$$

It is, of course, a matter of routine transformation to obtain any other desired set of two-port parameters from these, e.g. scattering or transmission parameters. In summary, evaluation of two-port parameters by conventional means, requires two separate runs by a nodal analysis program. For example in the case of s-parameters it means that with a generator connected to port i only s_{ii} and s_{oi} can be evaluated. Similarly by removing the generator from port i and connecting to port o, s_{io} and s_{oo} can be evaluated. It was shown that this algorithm may be used to evaluate the S-parameters in one run, and this halves the number of iterations required in a typical analysis/optimization program.

3.2 TWO-PORT MATRIX METHOD.

Often one realises that a certain function of a network is formed by cascade connection of two or more simpler networks. By repeated application of this operation the general circuit parameters may be computed for any number of two-port networks in cascade. For only two types of parameters the final matrix is equal to the product of the individual two-port elements. One is the well-known [ABCD] parameters[5], and the other is TRANSFER SCATTERING-PARAMETERS. The latter one is usually defined entirely from a wave point of view rather than voltage and current[6-7]. The scattering parameters cannot be used in chain

matrices as a result of the decision to take reflected waves as dependent variables and incident waves as independent. Therefore, Transmission parameters [T] set, which have properties similar to those of the [ABCD] set, may be used in the analysis routine. In order to analyse completely a network, the measured s-parameter set of an active device must normally be converted to the [ABCD] or [T] set using the following relationships[6]. (Assuming both input and output normalization constants are equal to Z_o).

$$[ABCD] = \frac{1}{2S_{21}} \begin{bmatrix} (-\Delta s + s_{11} - s_{22} + 1) & Z_o(\Delta s + s_{11} + s_{22} + 1) \\ (1/Z_o)(\Delta s - s_{11} - s_{22} + 1) & (\Delta s - s_{11} - s_{22} + 1) \end{bmatrix} \quad (3.19)$$

Conversion from [S] to [T] set would be

$$[T] = \frac{1}{S_{21}} \begin{bmatrix} -\Delta s & -S_{22} \\ S_{11} & 1 \end{bmatrix} \quad (3.20)$$

where $\Delta s = s_{11} s_{22} - s_{12} s_2$.

One of the interesting and powerful features of this method, other than the speed of computation, is the ability to store matrix representations of individual network elements in the computer memory. Individual element types and related data may be specified as integral parts of an overall network topology. Each type is coded, enabling the program to call upon the necessary algorithm to compute the [ABCD] or [T] set for that element and for the total network, chaining these elements in the correct sequence and computing their matrix product. Once a given element matrix is stored there is no need to recompute unless new values are specified by the user or possibly by an optimization routine.

The stored invariant element data may be rapidly recalled, maintaining a high degree of overall program efficiency.

3.3 SPARSE MATRIX TECHNIQUES.

The admittance matrix of [Y] described in section 3.1 for a typical ten-node electric circuit contains fewer than 50-per cent nonzero elements. As the number of circuit nodes increases the percentage of non-zero terms drops, so that at 100 nodes typical circuits contain 5 per cent nonzero elements [8]. For efficient utilization of high-speed memory, and to allow for practical solution of very large circuits, storage may be allocated for only the nonzero terms of the admittance matrix. It is also worth mentioning that where less than 30% of the matrix entries are nonzero one should consider storing the entries of nonzero elements [9].

The most obvious method of compacting data is simply to store the row and column numbers of each nonzero valued position in two vectors, and the value in a third vector. As an example of one of the basic storage techniques consider the matrix

$$[Y]=\begin{bmatrix} y_{11} & y_{12} & 0 & 0 & y_{15} \\ 0 & y_{22} & 0 & y_{24} & 0 \\ 0 & 0 & y_{33} & 0 & y_{34} \\ y_{41} & 0 & 0 & y_{44} & 0 \\ 0 & 0 & y_{53} & 0 & y_{55} \end{bmatrix} = \begin{bmatrix} 1 & 2 & 0 & 0 & 3 \\ 0 & 4 & 0 & 5 & 0 \\ 0 & 0 & 6 & 0 & 7 \\ 8 & 0 & 0 & 9 & 0 \\ 0 & 0 & 10 & 0 & 11 \end{bmatrix} \qquad (3.21)$$

The information concerning the nonzero element value and its position may be stored as two vector arrays NRO, and NCO.

These two vectors, which may each be called a pointer array, before node renumbering would contain the following numbers:

Row locator	Column identifier	Term identified
NRO(1) = 1	NCO(1) = 1	y(1) = y_{11}
NRO(2) = 4	NCO(2) = 2	y(2) = y_{12}
NRO(3) = 6	NCO(3) = 5	y(3) = y_{15}
NRO(4) = 8	NCO(4) = 2	y(4) = y_{22}
NRO(5) = 10	NCO(5) = 4	y(5) = y_{24}
	NCO(6) = 3	y(6) = y_{33}
	NCO(7) = 5	y(7) = y_{34}
	NCO(8) = 1	y(8) = y_{41}
	NCO(9) = 4	y(9) = y_{44}
	NCO(10)= 3	y(10)= y_{54}
	NCO(11)= 5	y(11)= y_{55}

The number stored in position I of the NRO array, represents the starting location in the second pointer array, NCO. Where the values are associated with terms of row I in the [Y] matrix.

As it can be seen, for example NRO(2) = 4 indicates that the first element in row 2 is the fourth element of NCO. NCO(4) gives its column position and y(4) gives its element value. So by means of the system of pointers, the whole nonzero elements of any network are rapidly accessible[8]. It is also worth mentioning that the optimal ordering of the equation in the [Y] matrix is of vital importance to minimize the production of new non-zero terms when decomposing the original matrix[Y] [4]. As an example consider the following matrix with its L-U decomposition:

$$[Y] = \begin{bmatrix} y_{11} & y_{12} & y_{13} & y_{14} \\ y_{21} & y_{22} & 0 & 0 \\ y_{31} & 0 & y_{33} & 0 \\ y_{41} & 0 & 0 & y_{44} \end{bmatrix} = \begin{bmatrix} 1 & 0 & 0 & 0 \\ \ell_{21} & 1 & 0 & 0 \\ \ell_{31} & \ell_{32} & 1 & 0 \\ \ell_{41} & \ell_{42} & \ell_{43} & 1 \end{bmatrix} X \begin{bmatrix} u_{11} & u_{12} & u_{13} & u_{14} \\ 0 & u_{22} & u_{23} & u_{24} \\ 0 & 0 & u_{33} & u_{34} \\ 0 & 0 & 0 & u_{44} \end{bmatrix} \quad (3.20)$$

As it can be seen all the [L] and [U] elements are nonzero, and six nonzero values were created in [L] and [U] which were zero valued in [Y]. Thus the sparsity of [L] and [U] depend on the ordering of the equations and the solution variables. To illustrate, now consider [Y] and its L-U decomposition which is a result of interchanging columns and rows 1 and 4 of the [Y] matrix viz:

$$[Y] = \begin{bmatrix} y_{44} & 0 & 0 & y_{41} \\ 0 & y_{22} & 0 & y_{21} \\ 0 & 0 & y_{33} & y_{31} \\ y_{14} & y_{13} & y_{12} & y_{11} \end{bmatrix} = \begin{bmatrix} 1 & 0 & 0 & 0 \\ 0 & 1 & 0 & 0 \\ 0 & 0 & 1 & 0 \\ \ell_{41} & \ell_{42} & \ell_{43} & 1 \end{bmatrix} \begin{bmatrix} u_{11} & 0 & 0 & u_{14} \\ 0 & u_{22} & 0 & u_{24} \\ 0 & 0 & u_{33} & u_{34} \\ 0 & 0 & 0 & u_{44} \end{bmatrix} \quad (3.21)$$

so the nonzero structure has been maintained throughout the L-U decomposition by optimal ordering of the equations. This may be done by searching to see if there are any rows with only one non-zero off-diagonal term. If one is found, it is numbered first, those with two non-zero terms second, etc., and finally those with the most non-zero terms last.

3.4 ADJOINT NETWORK & SENSITIVITIES.

In Chapter two it was indicated that the gradient optimization methods on average perform better. They require the gradient of the objective function with respect to the set of adjustable parameters in the circuit. This gradient of error function may be obtained either analytically or numerically using some finite difference scheme. In the case of the latter one it is usually inferior to the best direct search methods[10]. This inferiority stems from the inaccuracy of the estimated derivatives, which results in the selection of a poorer direction than would be obtained using analytic derivatives. Hence, in this section the analytic gradient evaluation of error function will be discussed by means of the adjoint network.

The basic idea for evaluating gradient, it may also be called sensitivites, is a general network theorem by Tellegen[11]. The theory itself has no apparent application to sensitivity problems, making discovery of its significance independently in [12] and [13] all the more remarkable.

Consider a linear time-invariant network N, with branch voltage and current denoted by $v_n(t)$, $i_n(t)$ respectively. Now let $\hat{N}$ be another network with branch voltage and current denoted by $\hat{v}_n(t)$ and $\hat{i}_n(t)$ respectively. The network $\hat{N}$, known as the adjoint of N, has the same structure as N, but possib ly different types of elements between corresponding nodes.(see Fig. 3.2.)

Upon application of Tellegen's theorem[12]

$$\sum_n v_n(t)\,\hat{i}_n(t) \equiv 0 \quad \text{and} \quad \sum_n i_n(t)\hat{v}_n(t) \equiv 0 \tag{3.22}$$

where the summation is taken over all branches of the networks N and $\hat{N}$.

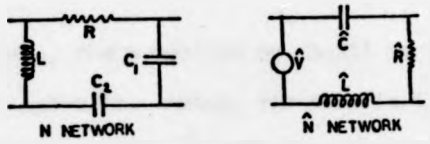

FIG. 3.2 NETWORKS WITH SIMILAR STRUCTURE.

Now let the voltage and current in N have a perturbation of $\Delta v_n(t)$ and $\Delta i_n(t)$. Since Tellegen's theorem is independent of element value, then it must still be satisfied, so that:

$$\sum_n [v_n(t) + \Delta v_n(t)]\,\hat{i}_n(t) \equiv 0$$

and

$$\sum_n [i_n(t) + \Delta i_n(t)]\,\hat{v}_n(t) \equiv 0 \tag{3.23}$$

combining (3.22) and (3.23) yields:

$$\sum_n \Delta v_n(t)\,\hat{i}_n(t) \equiv 0 \quad \text{and} \quad \sum_n \Delta i_n(t)\,\hat{v}_n(t) \equiv 0 \tag{3.24}$$

Finally, and most importantly:

$$\sum_n [\Delta v_n(t)\hat{i}_n(t) - \Delta i_n(t)\hat{v}_n(t)] \equiv 0 \tag{3.25}$$

This equation in fact is the key to evaluation of all sensitivities of a network.

As an example, consider a 2-port network N with its adjoint network $\hat{N}$ as indicated in Fig. (3.3).

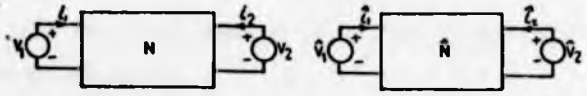

FIG. 3.3 TWO CIRCUITS OF IDENTICAL TOPOLOGY, N IS ORIGIN NETWORK AND $\hat{N}$ ITS ADJOINT NETWORK.

As previously, the summation on (3.25) is taken over all branches of the networks. Hence, the term in (3.25), corresponding to the branches of N and $\hat{N}$ which are the port terminations, can be separated from those relevant to internal branches, to yield:-

$$\Delta i_1 \hat{v}_1 - \Delta v_1 \hat{i}_1 + \Delta i_2 \hat{v}_2 - \Delta v_2 \hat{i}_2 = -\sum_k (\Delta i_k \hat{v}_k - \Delta v_k \hat{i}_k) \qquad (3.26)$$

when the summation now is taken only over internal branches.

Suppose now a two-terminal component (Z_k) is subject to change, then, $\Delta v_k = \Delta i_k Z_k + \Delta Z_k i_k$ and (3.26) may be rewritten as follows:

$$\Delta i_1 \hat{v}_1 - \Delta v_1 \hat{i}_1 + \Delta i_2 \hat{v}_2 - \Delta v_2 \hat{i}_2 = -\sum_k (\hat{v}_k - Z_k \hat{i}_k) \Delta i_k - \hat{i}_k i_k \Delta Z_k \qquad (3.27)$$

The quantity Δi_k is of no interest, thus it may be eliminated by choosing $\hat{v}_k = Z_k \hat{i}_k$. Consider now the network N excited by a voltage source at port 1 and the voltage (Δv_2) at the open-circuited port 2 is the response of interest. By suitably terminating N and $\hat{N}$ as shown in Fig. (3.4), the left hand side of (3.27), except ΔV_2, may be forced to be zero.

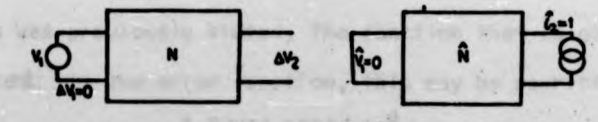

FIG. 3.4 TERMINATIONS REQUIRED TO SET CERTAIN TERMS TO ZERO ON EQUATION (3.27).

In this case the final form of (3.27) for a two-terminal components impedance becomes

$$\frac{\Delta V_2}{\Delta Z_k} = - i_k \hat{i}_k \tag{3.28}$$

This expression indicates how the sensitivity of output voltage to a small change in an impedance may be calculated through two circuit analyses, one of the original network N, and the other the adjoint network $\hat{N}$. The expression describing the adjoint element, associated with the all element types of network N, may be manipulated in a similar manner[15-16].

The procedure has also indicated how the adjoint network may be constructed from the original network, this is summarized as follows:

(a) - the branch impedance matrix $\hat{Z}_{ba}$ of the adjoint is related to the branch-impedance matrix Z_{ab} of the original network N by $Z_{ab} = \hat{Z}_{ba}$;

(b) the original source is removed and replaced with a short circuit if it was voltage source, and an open circuit if it was a current source;

(c) A one ampere current source is connected to the response terminal of the adjoint network. In this case, however, (i.e. only 2-terminal components) in which N and $\hat{N}$ are identical. It has been shown that the computational cost can also be reduced virtually to that of a single analysis[14].

As was previously stated, the function that is going to be optimized is the error function, this may be rewritten as

$$\epsilon = \frac{1}{p} \sum W(j\omega)(D(j\omega))^p \tag{3.29}$$

where $D(j\omega) = (G_t(j\omega) - G_d(j\omega))$ and the symbols are as defined in (2.1).

If the network is modified slightly, by changing the element x_l to $x_l + \delta x_l$, this produces changes in $G_t(jw)$ and therefore in the error function ε. For this given adjustable element the first-order variation in equation (3.29) would be as follows:

$$\frac{\partial \varepsilon}{\partial x_l} = \text{Re} \sum W(j\omega) |D(j\omega)|^{p-2} (D^* \frac{\partial D}{\partial x_l}) \qquad (3.30)$$

where 'Re' stands for the real part and '*' denotes the complex conjugate. Now D may be expressed as a function of a particular response, for example the forward transmission (s_{21})

$$D = s_{21} - s_{21}^{o} \qquad (3.31)$$

where $s_{21} = 2\sqrt{R_s G_L} \times \frac{v_o}{v_{in}}$, and v_o is the voltage across the load of G_L, v_{in} is the generator voltage and R_s is the real part of the generator impedance Fig. (3.5). Thus (3.30) becomes

$$\frac{\partial \varepsilon}{\partial x_l} = \text{Re} \sum W(j\omega) |s_{21} - s_{21}^{o}|^{p-2} (s_{21} - s_{21}^{o})^* \frac{2\sqrt{R_s G_L}}{v_{in}} \frac{\partial v_o}{\partial x_l} \qquad (3.32)$$

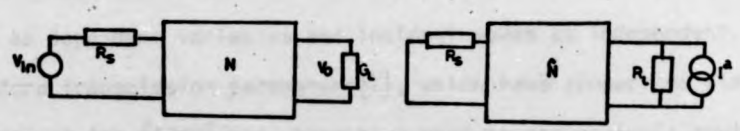

FIG. 3.5 ORIGIN (N) AND ADJOINT ($\hat{N}$) NETWORK MODEL.

If I^a in the adjoint network of Fig. (3.5) is excited where

$$I^a = W(j\omega) |s_{21} - s_{21}^{o}|^{p-2} (s_{21} - s_{21}^{o})^* \frac{2\sqrt{R_s G_L}}{v_{in}}$$

Then the gradient of the error function is reduced to the expression (3.28) for an impedance element. Similarly for other responses, the adjoint models may be derived by the same technique.

3.5 CONCLUSIONS.

In the course of the development of any computer analysis program, two conflicting requirements emerge, one is to perform the analysis as quickly as possible, by making the program highly specific, the other is to relate the method of computation to the general usage capability of the program. The methods most frequently adopted by analysis programs of linear circuits in the frequency domain have been described, giving greater attention to those best suited for use in microwave circuits. A comparison of the above methods indicates that the two-port chain matrix is quite fast but it is not really suitable for a multi-terminal network.

In the developing of a computer analysis/optimization program by the author and his colleague[17], the S-parameter approach was chosen, since it is ideally suited to the above requirements. It is obvious that the inability to use S-parameters in chain matrices is the result of the decision to take reflected waves as dependent variables and incident waves as independent. Therefore transmission parameters[T], which have properties similar to those of the [ABCD] set, have been used in the analysis routine. The calculations required for the transformation from [S] to [T] are slightly less complex than those required from [S] to [ABCD] sets. For a higher evaluation efficiency, the [T] set have therefore been used for cascading.

An algorithm has been described which may be applied to evaluate any two-port parameters of a network. The algorithm is particularly suitable for modelling active or passive devices in conjunction with an optimization.routine. In particularly, it was demonstrated how a relatively inexperienced programmer can apply the relevant procedures to multi-terminal circuit analysis, so halving the number of iterations required in a typical 2-port parameter evaluation.

The conclusion of chapter two indicated that the gradient techniques are superior to other types of optimization techniques. They require the gradient with respect to the set of adjustable parameters in the circuit. The adjoint network described in this Chapter (3) is the most efficient approach for the computation of the gradient of a particular response with respect to adjustable parameters in the circuit. It has been shown also how the error of different responses may be computed by means of an adjoint network, this is summarized as follows:

An approximate network is postulated, and the desired response is found, together with error (ε), and all currents or branch voltages ($v_{k\ell}$), by solving the network. The adjoint network is then built and solved, leading to all currents and voltages ($\hat{v}_{\ell k}$) in this network. Finally, from the computed voltages the gradient of error function ($\frac{\partial \varepsilon}{\partial x}$) with respect to the adjustable element x is evaluated. The error may then be optimised by one of the gradient techniques previously described.

REFERENCES

1. MARCHENT, B.G. "Interactive computer programs for the computer aided design of linear microwave circuits", Ph.D. Thesis, University of Warwick, July (1973).

2. WEINBERG, L. "Network analysis and synthesis", McGraw-Hill, New York, (1962), pp.44-59.

3. MURRAY-LASSO, M.A. "Analysis of linear integrated circuits by digital computer using black-box techniques", Ch 4 of HERSKOWITS, G.J. "Computer-aided integrated circuit" McGraw-Hill, New York, 1968

4. CALAHAN, D.A. "Computer-aided network design", McGraw-Hill, New York, (1972).

5. RALSTON, A. "A first course in numerical analysis", McGraw Hill, New York, (1965), pp.445-448.

6. WEINBERG, L. "Fundamentals of scattering matrices", Elect. Technol, (New York), vol. 80, No.1 (1967) pp.55-72.

7. HEWLETT-PACKARD "S-parameter Design" Application Note 154 April (1972).

8. BERRY, R.D. "An optimal ordering of electronic circuit equation for a sparse matrix solution", I.E.E.E. Trans. on circuit Theory, vol. CT-18 January (1971) pp.40-50.

9. BRYANT, P.R., "Numerical techniques - Gaussian elimination and the LU algorithm". Notes associated with one-day seminar on sensitivity and tolerance, Imperial College, London, 12th February (1975).

10. BOX, M.J., DAVIES, D., and SWANN, W.H., "Non-linear optimization techniques", ICI, Edinburgh U.K. (1969).

11. TELLEGEN, B.D.H., "A general network theorem, with applications", Phillips Res. Rept. No. 7, (1952), pp.259-269.

12. DIRECTOR, S.W. and ROHRER, R.A., "A generalized adjoint network and network sensitivites", IEEE Trans. on Circuit Theory, Vol. CT-16 August (1969), pp.330-336.

13. PENFIELD P., SPENCE, R. and DUINKER S., "Tellegen's theorem and electrical networks", M.I.T. Press No. 58 (1970).

14. SPENCE, R., "Small-change sensitivity" as [9].

15. DIRECTOR, S.W. and ROHRER, R.A. "Automated network design, The frequency-domain case", IEEE Trans. on Circuit Theory, Vol. CT-16 No. 3,August (1969), pp.330-337.

16. SANCHES-SINENCIO, E., and TRICK T.N. "CADMIC-Computer-aided design of microwave integrated circuits", IEEE Trans. on Microwave Theory and Techniques, Vol. MTT-22 No. 3, March (1974), pp.309-316.

17. HOSSEINI, N.M., SHURMER, H.V., and SOARES, R.A. "OPTIMAL-A program for optimising microstrip network", Elect. Lett. Vol. 12, No.8 15th April (1976),pp.190-192.

AUTOMATIC ON-LINE MEASUREMENT

The most effective means of dynamically characterising one-or two-port microwave devices is to utilize a network analyzer. An important consideration in these measurements is the form in which the data is made available for future use. Although the manually operated instrumentation provides a variety of displays (i.e. polar, smith chart, rectangular, etc.) as a function of frequency, it is often difficult to accurately interpret the measured data. However, it does provide a visual measure of the effectiveness of network adjustments. The recent trends in network characterization for both active and passive devices, require measurement accuracies not afforded by a manual system. The ability to accurately characterize an unknown device, exclusive of system hardware errors, then store and later represent it in virtually any form mathematically, and

utilize the measured data in CAD and simulation studies has necessitated the use of an automatic computer measurement routine.

Over the past few years there have been significant developments in the application of on-line computing to facilitate the automatic measurement. It also provides recording of microwave characteristics for devices and components freed from errors inherent in the measuring system [1-3]. The basic hardware in this work comprises of a network analyzer together with a digital computer. The latter is used to control a swept-frequency source and to make the necessary corrections to data supplied by the network analyzer.

Errors inherent in the system, together with those arising from transitions, mounting arrangements, etc., are first stored in the computer during a series of preliminary calibration runs. Standard terminations are used, such as a short-circuit or a matched load. During these preliminary runs, the corresponding reflection or transmission coefficients, as measured by the network analyzer, are stored in the computer for a succession of precise frequency steps over a pre-selected bandwidth. Since the true terminating impedances are accurately known, from these stored values, the sum of errors at each frequency can be computed. Subsequent runs, using test pieces to be characterized are carried out at the same precise frequency steps. The computed errors, stored at the time of calibration runs, can be subtracted from the measured data to give a corrected output, (analogue or digital), stepped over the entire pre-determined bandwidth. Here, in the Engineering Department the main facility is based on a XDS-Sigma 5 computer which has 32K storage capacity, backed by a 1.5 Megabytes fixed and 4.6 Megabytes moving head disk, each byte

of which represents one quarter of a 32-bit computer word. This is used in conjunction with Hewlett-Packard microwave equipment, central to which is a network analyzer. A Tekronix visual display unit (V.D.U) is used for manually controlling the program and for instructing the output of results. This Chapter also describes the hardware of automatic on-line measurement to dynamically characterize one-or two-port microwave devices. It also outlines the programming techniques developed to provide a fully time-sharing system. With regard to frequency stabilization some consideration is given to a phase-lock loop system.

4.1 SYSTEM DESCRIPTION.

A simplified block diagram of the measurement system is shown in Fig. 4.1. The system has three major sections, the signal source, the network analyzer, and the computer. The signal source section consists of a sweep oscillator controlling a multiple set of RF signal sources and a signal multiplexer. The sweep oscillator is interfaced to the computer to allow for digital programming of the RF frequency. RF switching is also under computer control. The network analyzer section measures the s-parameters of the device being characterized. A two-port test unit is shown in Fig. 4.1 and in this unit the selection of any one of the four s-parameters is also computer controlled. The network analyzer portion of the sub-system is simply a microwave frequency vector ratio voltmeter which measures the amplitude ratio and phase difference between the reference and test channel. The computer section consists mainly of the interfacing units, this will be described in more detail in the next section.

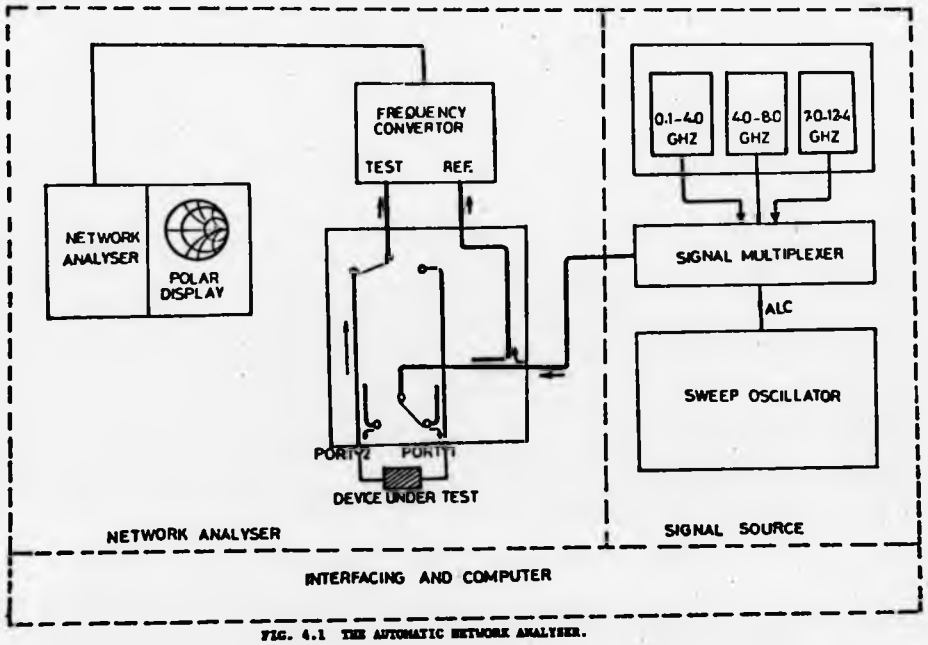

FIG. 4.1 THE AUTOMATIC NETWORK ANALYSER.

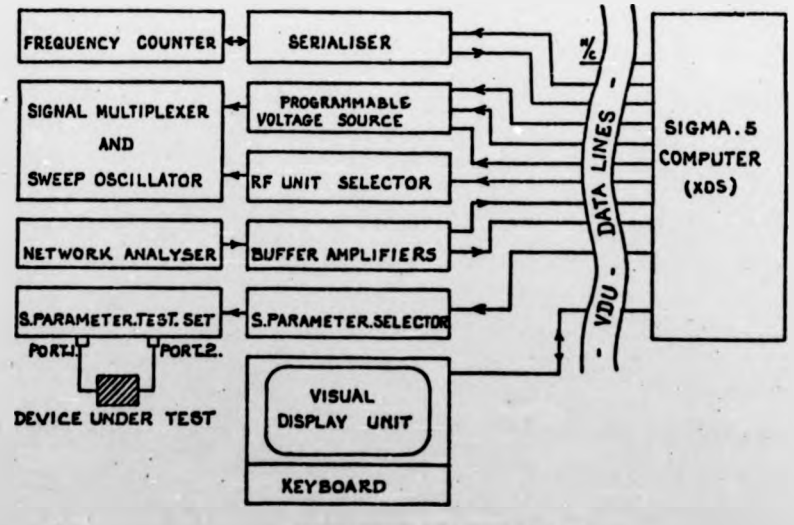

FIG. 4.2 THE INTERFACING UNITS BETWEEN COMPUTER AND NETWORK ANALYSER.

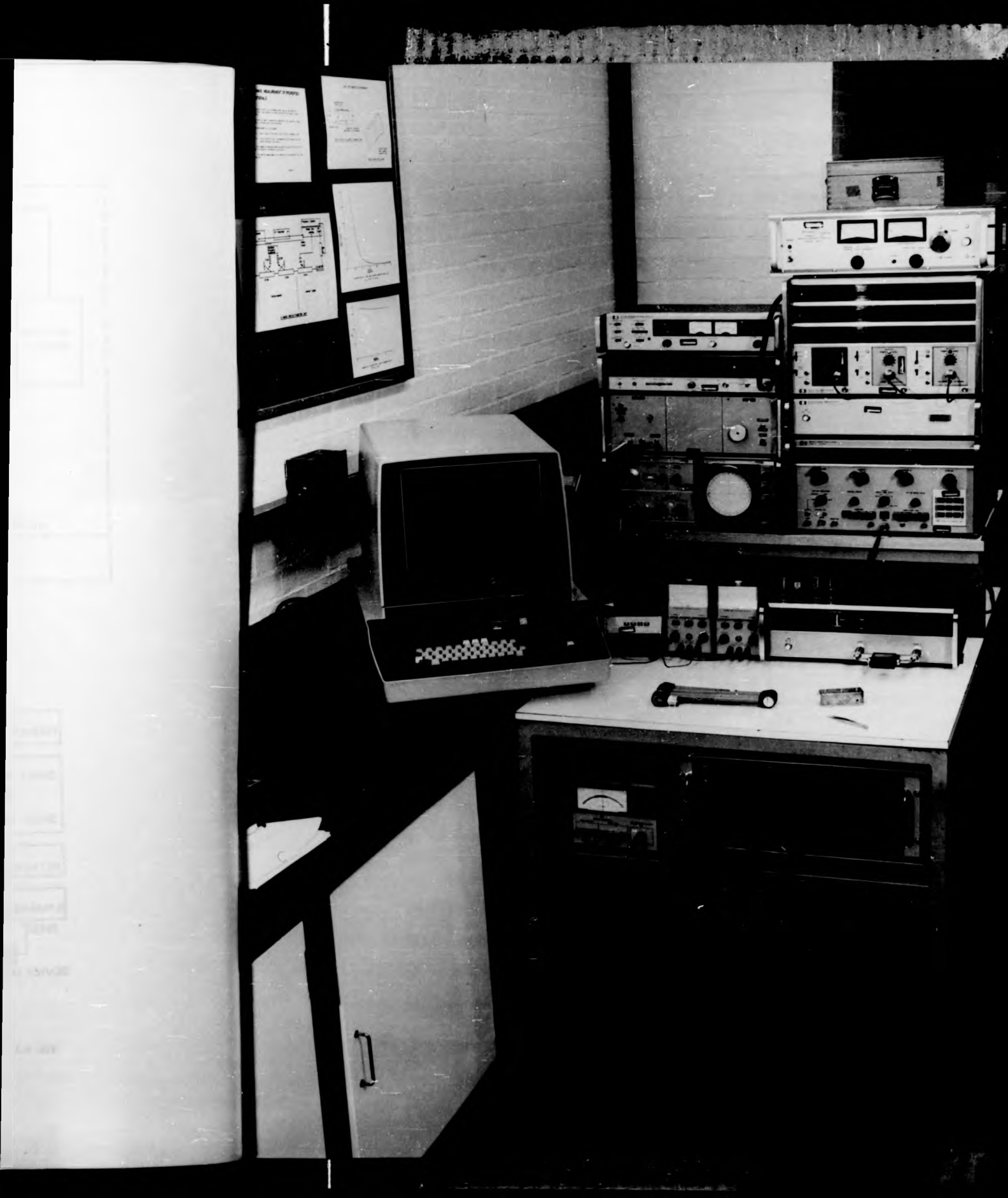

ES 649

The network analyzer is sited remotely from the computer but within the same building. Ten channels for data or control are available, to be shared between individual parts of the system [4]. A basic block diagram of the arrangement is shown in Fig. 4.2.

Communication between measuring set-up and computer was arranged by cable connection. The computer was then linked to the network analyzer system via a patch panel by inserting pins in appropriate positions as indicated in the following table.

Table 4.1 Input and output on the patch panel.

CHANNEL (vertical number)	PINS POSITIONS (horizontal number)	FUNCTION
(1)	(1) Analogue input	X-input from network analyzer
(2)	(2) " "	Y-input from Network analyzer
(3)	(3) " "	Frequency counter input
(4)	(1) Analogue Output	Programmable voltage source pulse
(5)	(2) " "	" " " (convert)
(6)	(3) " "	S-parameters selector
(7)	(4) " "	R.F. units selector
(8)	(0) Relay bit	Programmable voltage source reset
(9)	(5) Analogue Output	Frequency counter reading control
(10)	- Unconnected	-

The vertical number on the panel represents the channel number. The horizontal labels represent the type of analogue connection that is to be made.

As previously stated there are only ten channels available and because this number is insufficient some of them have been multiplexed. This can be done by either employing several levels of direct voltage or by using polarity to distinguish between signals. In the following section some of these interfacings are described briefly.

4.1.1 S-PARAMETER AND R.F. UNIT SELECTOR.

The s-parameter set is used for measurement of all S-parameters of two port networks. For driving the automatic switching of this set a selector network, which interprets the level of an analogue voltage as a 3 bit word, is used. Through this unit the computer can automatically switch to any desired parameter when the appropriate voltage is applied. The procedure only uses a single analogue voltage line for three digital lines.

The R.F. unit selector operates on a principle similar to that of the s-parameter selector, but in this case a 4 bit binary word is required to select one of the R.F. units. The binary word is generated from a single analogue voltage as shown in Fig. 4.3. Presently there are four R.F. units in frequency range of 0.1 - 18 GHZ. In practice, however, at frequencies above 15 GHZ the system is not accurate and the output power drops almost to zero level. This is because, the system including the harmonic mixer, the s-parameter unit and directional couplers were not designed to operate in this band.

4.1.2 PROGRAMMABLE VOLTAGE SOURCE. This unit controls the output frequency of the selected R.F. unit. A block diagram of this unit is shown in Fig. 4.4. The information required to set up the output voltage is fed in serial form, from the computer to the unit, each pulse representing 1 mV. The pulses are fed internally to an accumulating counter as shown. At the start of a test program it is first necessary for the computer to supply a reset signal, which could be done by closure of a set of contacts as shown. This sets up the accumulator to a count of 3000 ensuring that the minimum output voltage is 3V. (This is a requirement of the T.W.T. tube). Following this, it is necessary for the computer to set up the output

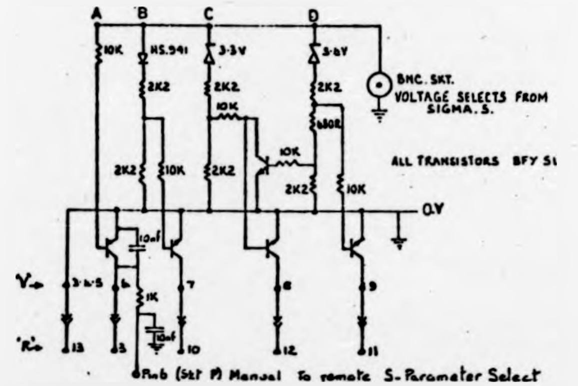

'V'. 9 PIN RS SKT. REAR OF RACK C
'R'. 36PIN 'REMOTE INPUT' SKT ON H/P 8411A. 2PORT TEST SET

THE LEVELS OF DIRECT VOLTAGE AND FREQUENCY RANGES:

A AT 1·5 VOLTS SELECTS RANGE 1. AND AUTO 0·1 TO 2·0 GHZ THRESHOLD P3 ·9 VOLTS
B — 3·0 - - - 2. - - 2·0 - 4·0 - - P10. 2·0 -
C -- 5·0 - - - 3 - - 4·0 - 8·0 - - P12. 3·6 -
D -- 7·5 - - - 4 - - 8·0 - 12·4 - - P11 6·7 -

FIG. 4.3 INTERFACE BETWEEN HEWLETT PACKARD 8707A FREQUENCY MULTIPLEXER AND SIGMA 5 COMPUTER TO ENABLE AUTO RANGE SELECTION.

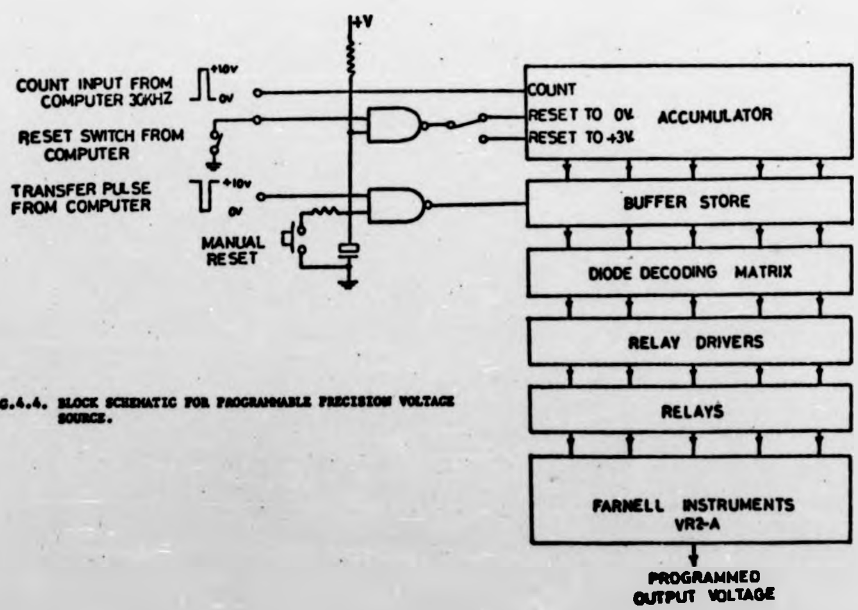

FIG.4.4. BLOCK SCHEMATIC FOR PROGRAMMABLE PRECISION VOLTAGE SOURCE.

voltage for the first test. This is accomplished by feeding pulses into the accumulator, the number being equal to the required output voltage, expressed in mV less 3000. For example, an output of 5 V is required, 5000-3000 = 2000 pulses are fed to the accumulator. This information is then transferred into the buffer store by the transfer pulse. The output from the buffer store is fed to the diode decoding matrix, this decodes the information in the buffer store and operates the appropriate relays via the relay driver circuits. Successive increases in output voltage are similarly achieved by feeding the appropriate number of additional pulses into the accumulator, transferring the information into the buffer store. The normal ramp tuning voltage of the R.F. units is not used. Instead the output from this unit supplies the necessary voltage in steps of 1 mv over the range 3 V to 73 V, corresponding to the full frequency range of each of the R.F. units.

4.1.3 BUFFER AMPLIFIER. Analogue outputs from the network analyzer are in the region between -1.5 and +1.5 volts. As in the case of a reflection measurement on a matched load the outputs are very near zero voltage, and as the noise present on the line could influence final results, provision was made to raise this level by operational amplifiers to between -10, 0, +10 volt. In this case more accurate reading of results in the vicinity of zero voltage could be provided.

4.1.4 VISUAL DISPLAY UNIT (V.D.U). The computer performs operations as instructed by the user via a V.D.U. with an input keyboard. A set of instructions for two-port correction, with typical responses in shown in Fig. 4.5. The questions appear on the screen individually

```
2-PORT FULL CORRECTION PROGRAM.

VERSION OL2/3
INITIALISATION REQUIRED ? TYPE Y OR N >YES
USE OF DATA TAPE REQUIRED ? TYPE Y OR N >NO
ARE AMPLIFIERS IN USE ? TYPE Y OR N !YES
WAVEGUIDE OR COAX - TYPE W OR C  !COAX

STANDARD CALIBRATION USES SLIDING LOAD, SHORT AND OFFSET SHORT.
STANDARD CALIBRATION REQUIRED ? (TYPE Y OR NO) !YES
LENGTH OF OFFSET SHORT (CM) = 0.3
JOYSTICK IS NOT IN USE.
NO. OF READINGS PER POINT =10
TIMING INTERVAL ( N*0.01 SEC). N=30
INPUTS TAKEN FROM POLAR DISPLAY OR PHASE GAIN UNIT ?
TYPE LOG,LIN,OR POL !!! POL
CENTRE BEAM WHILE TYPING ANY CHARACTER Y
MAXIMUM FREQUENCY (GHZ) = 12.0
MINIMUM FREQUENCY (GHZ) = 8.0
NO. OF POINTS = 11
SWITCH TOLEC RESET TO 3U.
MINIMUM FREQUENCY SET UP
CORRECTION TO FREQ. IN MHZ = 8.0
K=1   CONNECT MATCHED LOAD ON PORT 1 >YES
K=2   SLIDE LOAD                    >YES
K=3   SLIDE LOAD                    >YES
K=4   SLIDE LOAD                    >YES
K=5   CONNECT MATCHED LOAD ON PORT 2 >YES
K=6   SLIDE LOAD                    >YES
K=7   SLIDE LOAD                    >YES
K=8   SLIDE LOAD                    >YES
K=9   FWD TRANSM  2 MATCHED LOADS   >YES
K=10  REV TRANSM  2 MATCHED LOADS   >YES
K=11  SHORT CIRCUIT ON PORT 1       >YES
K=12  OFFSET SHORT 1 ON PORT 2      >YES
K=13  SHORT CIRCUIT ON PORT 2       >YES
K=14  OFFSET SHORT 1 ON PORT 1      >YES
K=15  CONNECT THROUGH LINE          >YES

NEW DEVICE ? >YES
TYPE DEVICE IDENTIFICATION & TERMINATE WITH CR
TEST RUN
K=19  CONNECT DEVICE                >YES
```

FIG.4.5. A SET OF INSTRUCTION WITH TYPICAL RESPONSES

```
TASK ? (TYPE LI FOR LIST OF OPTIONS)  !!
TASK OPTIONS - TWO LETTER KEYS REQUIRED
LI  LIST OPTIONS            ZE  RESTART PROGRAM
BG  RESTART CALIBRATION     RE  REPEAT LAST READING
SK  RESET K (SEE BELOW)     ND  GO TO NEW DEVICE
CA  CALCULATE               PR  PRINT
DI  ENTER DISPLAY           DU  DUMP READINGS
UD  UNDUMP READINGS         ST  RELEASE PROGRAM
CO  INSERT COMMENT          CE  CENTRE BEAM
AM  RESET AMPLIFIERS        IN  RESET INPUT TYPE
WA  WAVEGUIDE OR COAX       CL  DEFINE CALIB PIECES
JO  JOYSTICK SWITCH         FR  RESET FREQ RANGE
MF  CORRECT MIN FREQ        NO  RESET NO. READINGS
TI  RESET TIMING INT        TF  UPDATE TAPE FORMAT
DC  DISC FILE CLEAR         LT  LOAD DATA TAPE
UT  UNLOAD DATA TAPE        RS  RESTORE CALIB. DATA

SETTINGS FOR K IN SK OPTION
K=1   CONNECT MATCHED LOAD ON PORT 1
K=2   SLIDE LOAD
K=3   SLIDE LOAD
K=4   SLIDE LOAD
K=5   CONNECT MATCHED LOAD ON PORT 2
K=6   SLIDE LOAD
K=7   SLIDE LOAD
K=8   SLIDE LOAD
K=9   FWD TRANSM  2 MATCHED LOADS
K=10  REV TRANSM  2 MATCHED LOADS
K=11  SHORT CIRCUIT ON PORT 1
K=12  OFFSET SHORT 1 ON PORT 2
K=13  SHORT CIRCUIT ON PORT 2
K=14  OFFSET SHORT 1 ON PORT 1
K=15  CONNECT THROUGH LINE


K=19  CONNECT DEVICE
```

FIG. 4.6 THE FULL SET OF OPTIONS.

and after each one the computer waits until one of three instructions is entered via the keyboard, these are: (a) by a number followed by "CR" (Carriage Return); (b) typing a 'Y', which is automatically completed to a 'yes' on the screen; (c) typing an 'N', which is likewise completed to a 'No'. The answer is stored and the next question appears. The various procedures in the calibration routine are identified by the 'K' values 1-15, which facilitates the repeating of any particular stage. This can be effected by typing 'N' in response to a question, whereupon the V.D.U. displays 'Task'? For example, typing of 'SK' permits a repeat run corresponding to any particular selection of 'K', which is then entered. The full set of options available under 'Task? is shown in the list of Fig. 4.6, which is displayed on the V.D.U. in response to typing the letters 'LI'. The subsequent entering of any of the listed letter-pairs will permit the related function to be accomplished.

4.2 PROGRAMMING TECHNIQUE

The programming is almost entirely in FORTRAN IV, with some interjection of machine code. The programmes are each written as a series of subroutines, which greatly facilitates versatility. The main programme covers the full set of s-parameters for a 2-port device, and this has been overlaid for use in a time-sharing environment. Certain other correction programmes are also available, without overlaying, which are intended for special applications. Programming is done via punched cards and the information is subsequently transferred to magnetic tape. The user controls the programme through a series of questions and answers of the form already described (Fig. 4.5).

The main program comprises of four principal sections:-

(a) Calibration and reading control-calls correction and reading sub-routines.

(b) Line printer routine-available for tabulated results.

(c) V.D.U. Display control-calls graph plotting sub-routines.

(d) Initialization and task control. Calls data set-up, initialization, tape-dumping sub-routines, etc.

Fig. 4.7 shows the general flow-chart which applies to the measurement of scattering parameters, and Fig. 4.8 illustrates in more detail that part of the programme relating to frequency and signal measurement.

4.3 CALIBRATION AND CORRECTION PROCESSES.

All measurement systems introduce errors into the results. For precision measurements those errors which are predictable must be evaluated by a series of preliminary calibration runs[5-11]. During these preliminary runs the corresponding reflection or transmission coefficients, as measured by the network analyser, are stored in the computer for a succession of precise frequency steps over a pre-selected bandwidth. As the true terminating impedances of calibration pieces are known, it is possible to compute from the recorded values the errors at each frequency of measurement. Subsequent runs using the test pieces to be characterized are carried out at exactly the same sequence of frequencies. The computed error can then be subtracted from the measured data to give a sequence of corrected results for each of the set frequencies over the entire predetermined bandwidth.

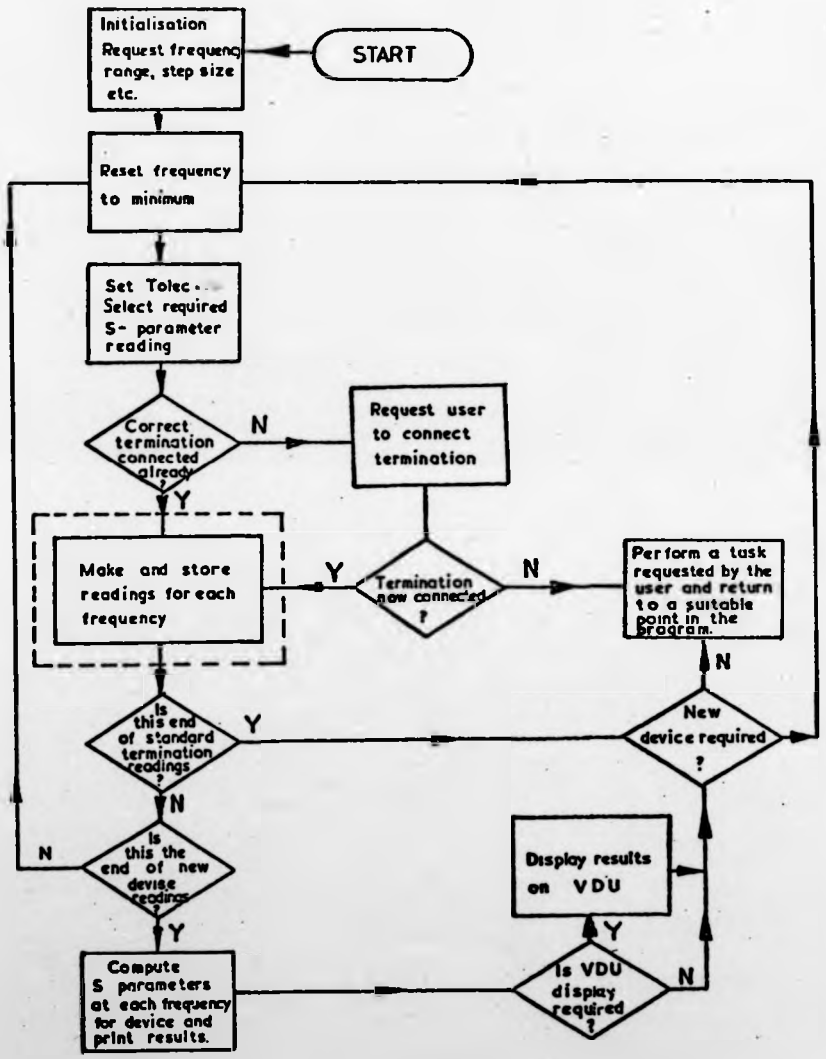

FIG. 4.7 THE GENERAL FLOW-CHART OF SCATTERING PARAMETERS MEASUREMENT.

The calibration pieces for either one-or-two-port are indicated in Appendix (B). The correction techniques which were employed are described in Appendix (C).

4.4 MEASUREMENT EXAMPLES

The measurement examples shown are used to illustrate the types of measurements which can be made, the accuracies which can be achieved, and the type of display and readout which are provided. Fig. 4.9 shows a polar plot of the corrected and uncorrected reflection s-parameters, s_{11} and u_{11} respectively. This is a hard copy of a V.D.U. display and pertains to an off-set short circuit measured over the bandwidth 7-12GHZ. In all of the displays, the uncorrected

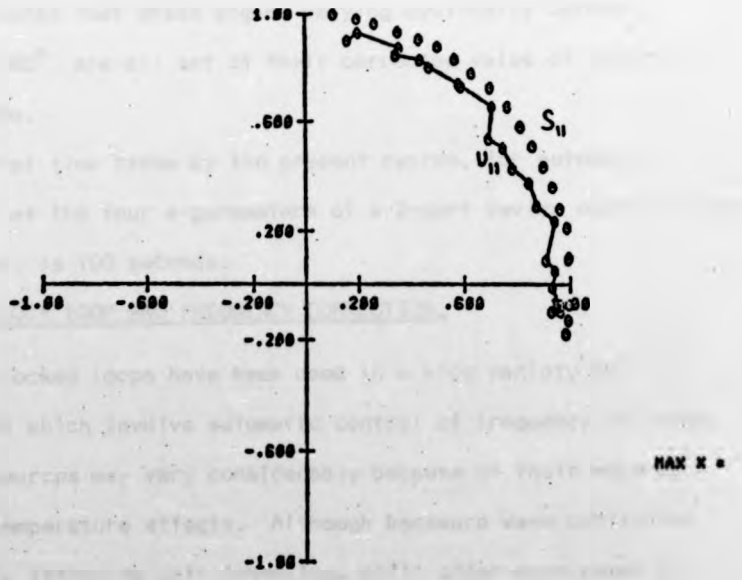

FIG. 4.9 CORRECTED (S_{11}) AND UNCORRECTED (U_{11}) REFLECTION S-PARAMETERS FOR AN OFF-SET SHORT CIRCUIT.

s-parameters are shown with the points jointed by straight lines and the corrected S-parameters as isolated points. It will be noted that in Fig. 4.9 an uncorrected plot with significant errors has been correctly modified

by the computer giving the theoretical arc of circle of unity radius appropriate to an off-set short circuit.

An alternative form of plot, using rectangular co-ordinates with linear scales is illustrated in Fig. 4.10. This pertains to measurements on a section of a 50-ohm air-line with both corrected and uncorrected reverse transmission(s_{12}) and input reflection coefficients (s_{11}) over 7-12 GHZ. This time, the irregular uncorrected curves are correctly modified to horizontal straight lines at y-co-ordinate levels of unity and zero , respectively. An even more impressive example of correction is shown in Fig. 4.11 which relates to the same set of reverse transmission s-parameters as in Fig. 4.10, but this time showing only phase angle as a function of frequency. It will be noted that phase angles varying cyclically between zero and $\pm 180^{\circ}$ are all set at their corrected value of zero by the programme.

The total time taken by the present system, for automatic measurement of the four s-parameters of a 2-port device over 50 steps in frequency, is 100 seconds.

4.5 PHASE-LOCK LOOP AND FREQUENCY CORRECTION.

Phase-locked loops have been used in a wide variety of applications which involve automatic control of frequency or phase. Tube-type sources may vary considerably because of their warm-up and other temperature effects. Although backward wave oscillator (BWO) units, featuring grid levelling, still offer more power at microwave frequencies, they cannot be used in many applications where good measurement accuracy and frequency stability are required.

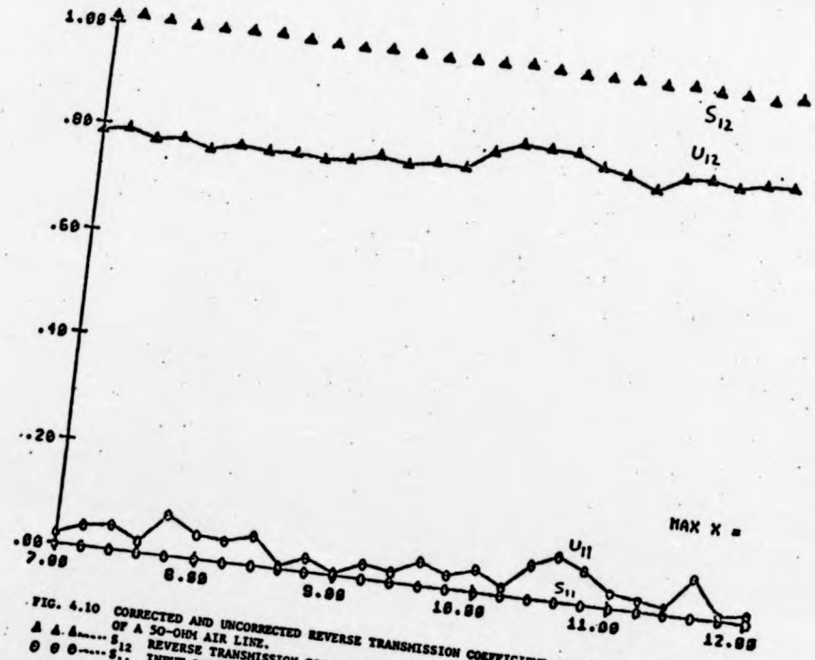

FIG. 4.10 CORRECTED AND UNCORRECTED REVERSE TRANSMISSION COEFFICIENT AND INPUT REFLECTION COEFFICIENT OF A 50-OHM AIR LINE.
Δ Δ Δ------ S_{12} REVERSE TRANSMISSION COEFFICIENT
0 0 0------ S_{11} INPUT REFLECTION COEFFICIENT

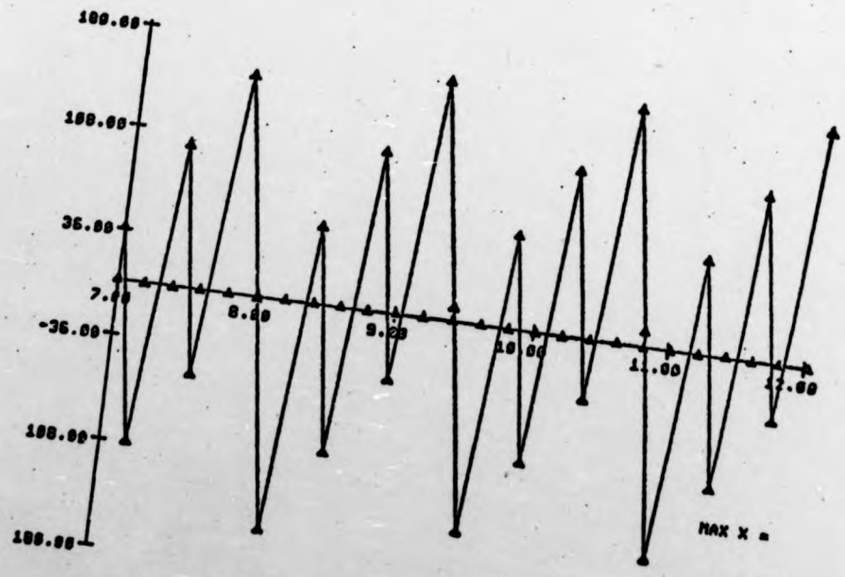

FIG. 4.11 CORRECTED AND UNCORRECTED PHASE ANGLE OF REVERSE TRANSMISSION COEFFICIENT FOR A 50-OHM AIR LINE.

This is because of their inferior frequency-pulling performance caused by the levelling-loop action. Thus, it is preferable to use solid-state sources. As an example, some manufacturers[12] offer solid state sweep oscillators where typical values for a 10-dB level change are less than 1 MHZ frequency shift, while for a grid levelled BWO source typical values are 20-70 MHZ.[13]. A simplified block diagram for the phase-locked loop system is shown in Fig. 4.12.

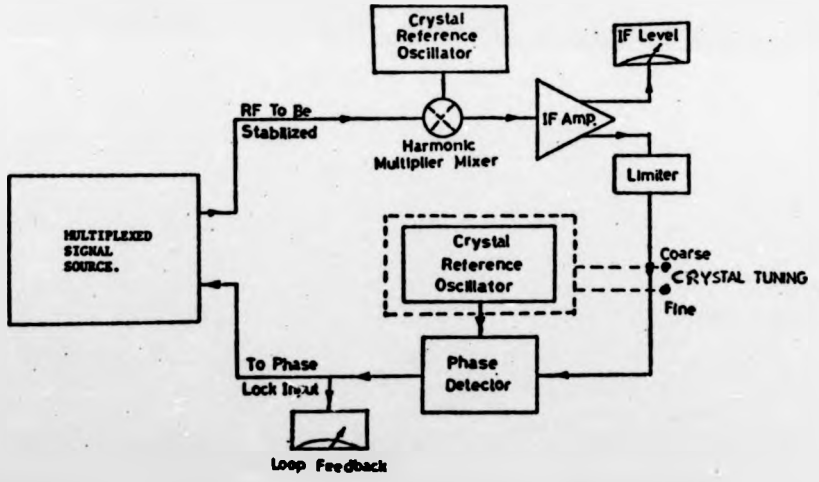

FIG.4.12. BLOCK DIAGRAM OF PHASE LOCK LOOP SYSTEM.

The object of the arrangement is to produce a sinusoidally varying output voltage, of defined frequency f_o, in accordance with a reference signal of frequency f_r. This is achieved by mixing the RF oscillator to be stabilized with harmonics of the internal RF reference providing an intermediate frequency IF. This in turn is compared in phase with a reference signal derived from a

crystal oscillator. The resultant is an error voltage v_e related to the difference in phase between the reference signal and feedback (IF) signal. Then after processing this produces the voltage v_c which is added in series to the voltage control of oscillator frequency f_o.

As the signal source must cover a range from 0.5 to 18 GHZ and the reference oscillator cannot cover a bandwidth this broad, then the signal source must phase-lock to harmonics of the reference oscillator[14]. The computer arranges a source frequency f_s by the user, and the reference oscillator then phase-locks with the accuracy and long-term stability of a crystal standard. This accurately defines the comb spectrum nf_r shown in Fig. 4.13.

FIG. 4.13 THE COMB SPECTRUM OF REFERENCE OSCILLATOR.

The computer also controls the coarse tuning of the source frequency f_s. As frequency errors in coarse tuning may be large, a search generator must be added to the phase loop, which increases its frequency locking range. The search generator systematically

changes f_s about the coarse tuned frequency. When f_s passes a possible lock point, phase lock occurs and the search generator is turned off. To prevent the phase lock loop from locking on the wrong harmonic, the search generator should search less than $\pm f_r$ about the coarse tuning frequency, and the coarse tuning must be closer than $\pm f_r$. These constraints are most important at the lowest reference frequency used. If harmonic skipping occurs, the source frequency f_s is offset by an amount f_r. This offset is typically 15MHZ in the model MOS Series[15] which is used by the author. However, a possible flow chart for the search generator is depicted in Fig. 4.14.

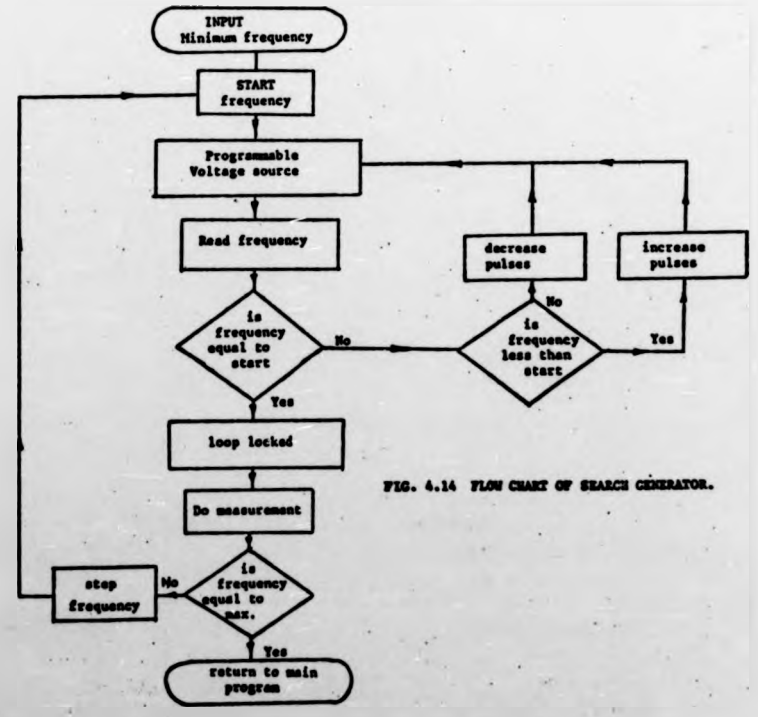

FIG. 4.14 FLOW CHART OF SEARCH GENERATOR.

In this system the signal frequencies at which locking will occur, with a particular crystal, are given by the formula

$$f_o = Nf_r \pm 40.884 \qquad (4.1)$$

where 40.884 MHZ is the intermediate frequency (IF) and f_o's are the lock points in MHZ; N is an integer greater than 65; f_r is the reference oscillator frequency in MHZ. In the MOS model f_r may be tuned from 14.9875 MHZ to 15.1125 MHZ ± 1%. Fig. 4.15 shows the phase of forward transmission for a 10dB attenuator both with and without the phase lock loop over the

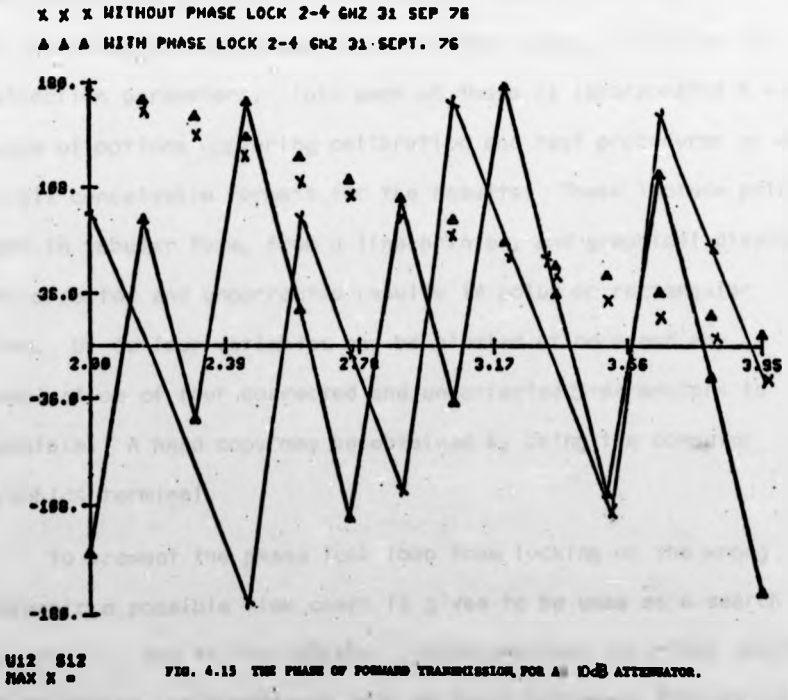

FIG. 4.15 THE PHASE OF FORWARD TRANSMISSION FOR A 10dB ATTENUATOR.

frequency range 2-3.95 GHZ. In general the phase-lock has been achieved only at the lower frequency range (0.1 - 4.GHZ), as at higher

frequencies the above phase-loop system is inapplicable due to the lack of a D C phase comparator network compatible with the BWO tubes

4.6 CONCLUSIONS.

The on-line computer measurements and S-parameters correction system has been described. The basic hardware consists of a network analyzer linked by some interfacing units to a digital computer. The programming is almost entirely in FORTRAN IV in a time-sharing mode, that is, two foreground jobs and the background area may be operated simultaneously. Currently, two programs are available, one giving the full two-port correction facility for all four scattering parameters, the other being limited to the reflection parameters. Into each of these is incorporated a wide range of options covering calibration and test procedures as well as all conceivable formats for the results. These include print-outs in tabular form, from a line-printer, and graphical displays of corrected and uncorrected results in polar or rectangular form. Up to four variables may be plotted at once and any combination of four corrected and uncorrected S-parameters is possible. A hard copy may be obtained by using the computer graphics terminal.

To prevent the phase lock loop from locking on the wrong harmonic a possible flow chart is given to be used as a search generator. Due to the lack of a phase comparator compatible with the BWO tubes phase lock has been achieved only at lower microwave frequencies (0.1 - 4GHZ). At frequencies above 15GHZ accuracy becomes limited

owing to the large errors arising from the harmonic mixer, s-parameter test set and directional coupler. This is because the associated network analyzer has not been designed to operate much above 12.4 GHZ.

REFERENCES

1. SHURMER, H.V., "Low-level programming for the on-line correction of microwave measurements", Radio and Electron. Engr., Vol. 41, August (1971), pp.357-364.

2. SHURMER, H.V., LUXTON, H.E.G., HOSSEINI, N.M., and STONEMAN, K.A., "The application of an on-line computer to microwave measurement". IMEKO VII , Vol. No. 2, 10-14 May (1976) London, paper BEL/211.

3. HACKBORN, R.A. "An automatic network analyzer system", Microwave J., Vol. 11, May (1968), pp.45-52.

4. ABBOTT , D.A., HOSSEINI, N.M., and SHURMER H.V.," Programmable interfacing for microwave gain and noise figure measurements", submitted to the Conference on Programmable Instruments, to be held at the National Physical Laboratory, Teddington, Middlesex, on 22nd and 23rd November (1977).

5. SHURMER, H.V., "Corrections of a Smith-chart display through bilinear transformations", Electron. Lett. Vol. 5, (1969) p.209.

6. SHURMER, H.V., "Calibration procedure for computer-corrected s-parameter characterisation of device mounted in microstrip". Electron. Lett. Vol. 9. (1973) p.323.

7. HAND, B.P., "Developing accuracy specifications for automatic network analyzer systems", Hewlett Packard J. Vol. 21, February (1970) pp.16-19.

8. DaSILVA, E.F., and McPHUN, M.K. "A new method of calibrating a microwave network analyzer for computer-corrected s-parameter measurements." Electron. Lett. Vol. 9 (1973) p. 126.

9. WOODS, D. "Rigorous derivation of computer corrected network analyzer calibration equations" ibid , Vol. 11, (1975), p. 403.

10. DaSILVA, E.F. "Calibration of an automatic network analyzer using transmission lines of unknown properties", University of Warwick, Private communication.

11. FRANZEN, N.R., and SPECIALE, R.A. "A new procedure for system calibration and error removal in automated s-parameter measurements", in Proc. 1976 European Microwave Conf. (Hamburg, Germany), pp.69-73.

12. PRODUCT FRONTIERS, "High-power solid-state m/w sweep oscillator", Microwave J. Vol. 19, October (1976), p. 18.

13. BAPRAWSKI, J., SMITH, C., and BERNUES, E.J. "Phase-locked solid state mm-wave sources", idid, Vol. 19, October (1976), pp. 41-44.

14. RYTTING, D.K. and SANDERS, S.N., A system for Automatic Network Analysis, as reference 7 , pp. 2-10.

15. MOS Microwave Oscillator frequency stabilizer, Handbook Model MOS Series, Microwave Systems Inc..

5

DEVICE CHARACTERIZATION

Accurate measurement of two-or one-port -parameters of active or passive devices at any frequency requires precise calibration of the system. Besides inherent errors in the basic hardware, which was discussed in Chapter 4, additional errors are introduced by the parasitics of coaxial-to-microstrip adaptors. One of the more difficult problems in any active device characterization is the definition of a reference plane. It is important to characterize the device in a fixture that gives a close approximation to the final circuit, so as to avoid a shift in reference planes when changing from the test fixture to a desired circuit. The test fixtures must be completely characterized to account for all parasitics. Naturally, the test fixture must also have minimum parasitics.

This Chapter first describes the problems associated with existing techniques for characterizing the launchers. Then follows a discussion

on an improved and practical method, which has been used by the author and others [1.2]. In order to reduce the parasitics associated with the launcher, a three dimensional movable holder for the microstrip circuits has been developed. Utilization of this holder has enabled successful calibration of transition errors to be made for microstrip lines. Finally, the results of measuring s-parameters for typical Plessey 1 μm gate-length GaAs MESFET'S are given.

5.1 CHARACTERIZATION OF LAUNCHERS

For devices mounted in a conventional microstrip jig, in addition to the hardware errors, the test fixture introduces its own error parameters due to the coaxial-to-microstrip adaptor. Therefore, for more accurate measurement, the calibration procedure must permit the elimination of all significant errors up to references planes in the microstrip. In making computer-corrected measurements on a one-or two-port device, it has, hitherto been common practice to perform a series of calibration runs in which the use of a sliding matched load as a standard termination is a principal feature [3] (see also Chapter 4).

Utilization of a microstrip short circuit, off-set short circuit and the sliding load enable successful calibration of transition errors to be made up to the reference plane. The microstrip sliding load simply consists of a high-dielectric lossy ceramic [4] of special construction, as shown in Fig. 5.1.

The microstrip sliding load is about 35 mm long and this precludes the preceding method, particularly when sufficient space is not available in a conventional microstrip test fixture.

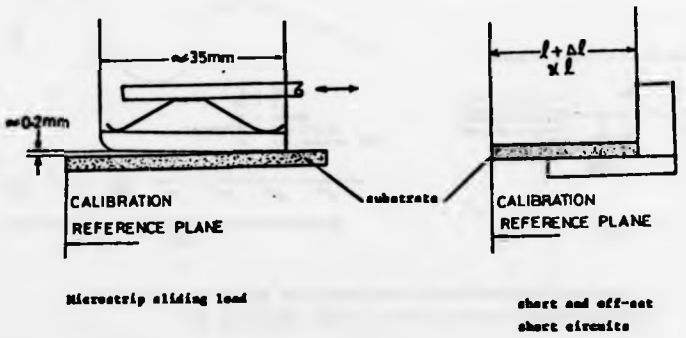

Fig. 5.1 MICROSTRIP CALIBRATION PIECES

An alternative procedure that permits the characterization of the launcher rather than elimination of the errors has been described in [5]. The method consists of using the launcher to make input impedance measurements on various lengths of open-circuited 50 ohm line ($\lambda/8 < \ell < \lambda$). The variation of the excess phase angle (i.e. measured input reflection-coefficient phase angle minus calculated input reflection-coefficient phase angle) versus the electrical length of the open-circuited line, has a cyclical variation, as shown in Fig. 5.2(a). The equivalent circuit shown in Fig. 5.2(b) follows from the knowledge that the excess phase angle at a line length of $\lambda/2$ is due almost entirely to the launcher shunt capacitance, whilst at $\lambda/4$ it is due almost entirely to the launcher series inductance, a constant phase value in

both cases being accounted for by the open-end effect (see Chapter 9).

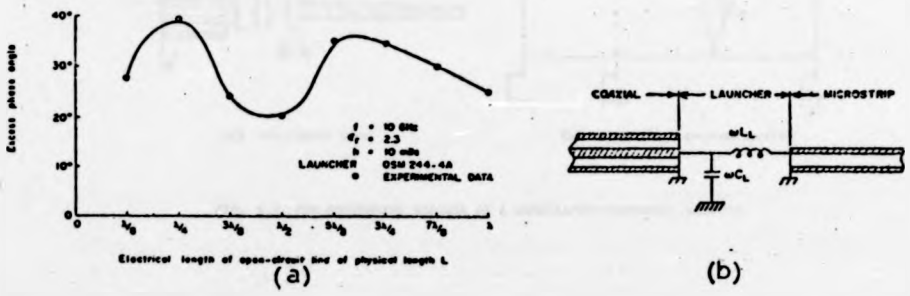

Fig. 5.2 (a) EXCESS PHASE ANGLE FOR AN OPEN-CIRCUITED LINE. [REF. 5].
(b) EQUIVALENT CIRCUIT OF THE MICROSTRIP LAUNCHER INTERFACE.

Numerical values for ωL_L and ωC_L can be conveniently obtained by superimposing the data for the electrical lengths $\lambda/4$ and $\lambda/2$ on a transmission line chart. There are some limitations worth mentioning. First, no correction is made for the radiation loss associated with the transition region from coaxial line-to-microstrip; secondly, the numerical evaluation of ωL_L and ωC_L for a large range of frequencies is rather tedious.

A more accurate method has been described in [6], which overcomes these problems. Consider Fig. 5.3(a) which shows a cross section of an APC-7 launcher feeding a 50 ohm open-circuited microstrip line. The overall fixture may be divided into three sections, which are from left to right; (a) a 50Ω dielectric-filled coaxial line (AA′ to BB′) which is taken to be lossless; (b) a transition region (BB′ to CC′) which is represented as a reciprocal T-network; (c) a microstrip line as load. A suitable electrical representation for the fixture is shown in Fig. 5.3(b).

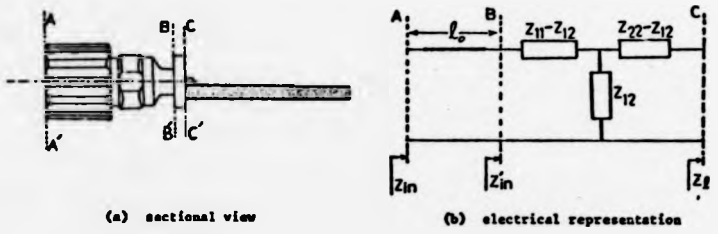

(a) sectional view (b) electrical representation

FIG. 5.3 THE EQUIVALENT CIRCUIT OF A COAXIAL-TO-MICROSTRIP ADAPTOR.

The input impedance of the transition region of the plane (BB'), at a particular frequency, is given by:

$$Z'_{in} = \frac{Z_{11}Z_2 + (Z_{11}Z_{22} - Z_{12}^2)}{Z_\ell + Z_{22}} \qquad (5.1)$$

where Z_{11}, Z_{22} and Z_{12} are indicated in Fig. 5.3(b), and Z_ℓ is the terminating impedance of the open-circuited microstrip line.

On the other hand, the impedance Z'_{in} is related to the measured input impedance Z_{in} via the transmission-line equation:

$$Z'_{in} = Z_o \left[\frac{Z_{in} - J\,Z_o \tan \beta_o \ell_o}{Z_o - J\,Z_{in} \tan \beta_o \ell_o}\right] \qquad (5.2)$$

To obtain values of Z_{11}, Z_{12} and Z_{22}, three different terminating impedances are then required.

The adaptors, type OSI4493A, are characterized by the author, using the above method, over the frequency band 8-12GHZ, the equivalent circuit of the launcher is shown in Fig. 5.4.

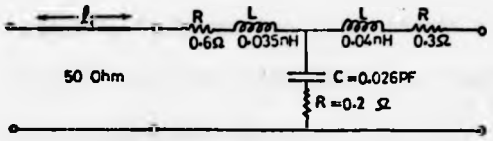

FIG. 5.4 LAUNCHER EQUIVALENT CIRCUIT PARAMETERS.

The launcher lengths from the APC-7 plane to the microstrip plane are depicted in Table 5.1 for various frequencies. The lengths are given in terms of equivalent air line, which is taken to be lossless.

TABLE 5.1 Equivalent air line lengths for launchers.

Frequency (GHZ)	2	4	8	10	12
Air length in cm (ℓ_o)	4.11	4.10	4.07	4.06	4.05

In evaluating equivalent circuit parameters, the end effect at an open circuit was taken into account. The other corrections made are for the losses and dispersion in the microstrip line using the computer programme "MICPA", which was developed by the author [7]. (see also Chapter 8).

The devices which were to be used in the amplifier design are unencapsulated chips mounted on 0.025" alumina substrates, so it was desirable to characterize them in the same mounting configuation with 50 ohm lines at the input and output ports of the device. A practical means of achieving this was to employ the full two-port correction procedure in the normal way, using precision coaxial standards, the transistor fixture, including adaptors, then being accurately measured as a two-port network. The measurement plane

was then moved from the APC-7 plane to the transistor reference plane by "subtracting" the effects of the adapters and the microstrip lines via a computer program.

5.2 MICROSTRIP HOLDER

A significant error arising in the transition from coaxial-line to microstrip results from bad contact between the fixture and ground plane. Because a nominally flat jig might only make contact at a few isolated points, and also for its convenience in handling microstrip lines, the jig of Fig. 5.5 was developed. Contact between the ground plane, comprising two narrow strips, and the jig is formed by moving the former upwards, vice versa for release, thus ensuring good contact to the substrate ground plane. Two launchers are provided, one being movable in two directions so that the test jig can be used for all substrate sizes. This is very useful, especially in cases where the input and output microstrip circuits are asymmetrical, utilization of this holder enabled successful elimination of transition errors to be made for various circuits, via the calibration runs.

5.3 GaAs MESFET's S-PARAMETERS AND THE EFFECTS OF CORRECTION.

The x-band GaAs MESFET's used here were typical Plessey 1 μm gate-length devices, with a drain saturation current, I_{dss}, of 30 mA. Such devices, for microwave amplifier design, typically assumed to be operated at 5V drain-to source bias, have a transconductance, g_m, of 16 mS and a gate pinch-off voltage of -4V at 10μA drain current.

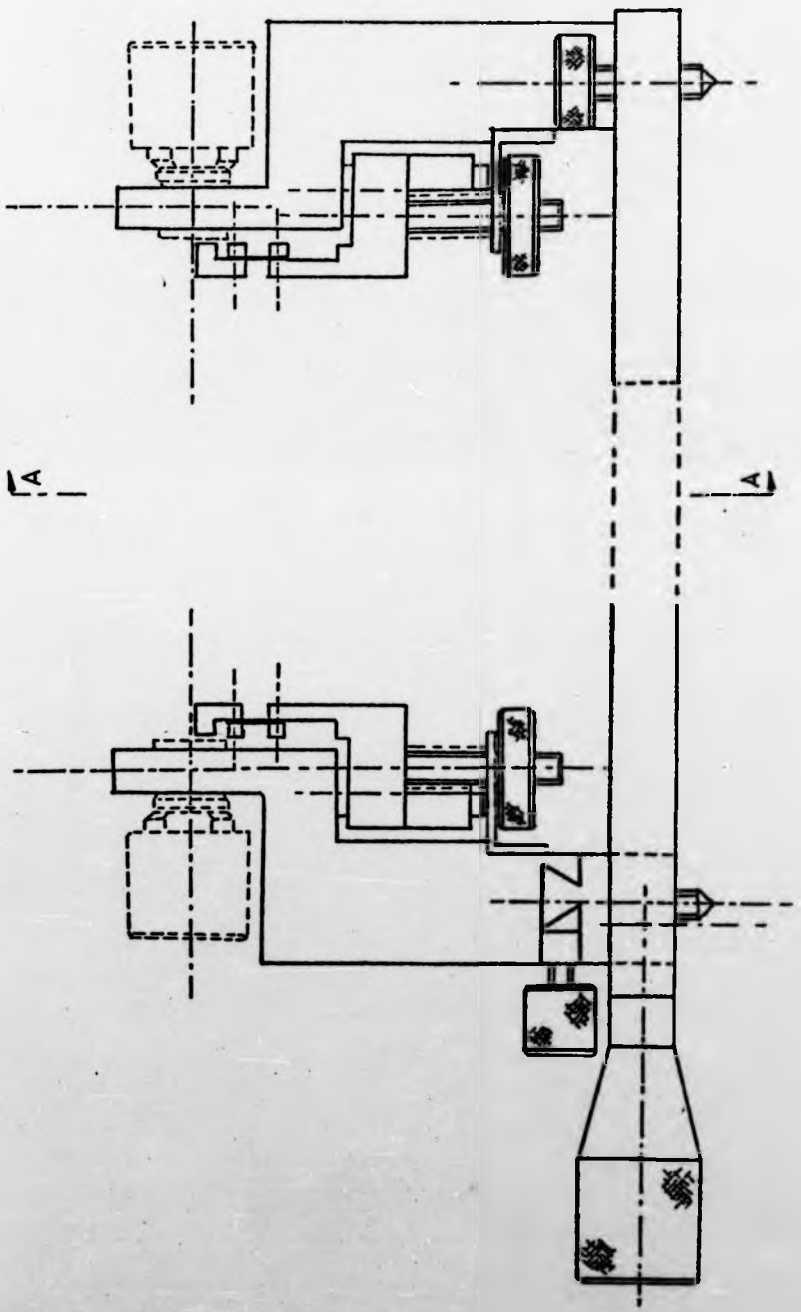

FIG.5.5 MICROSTRIP HOLDER

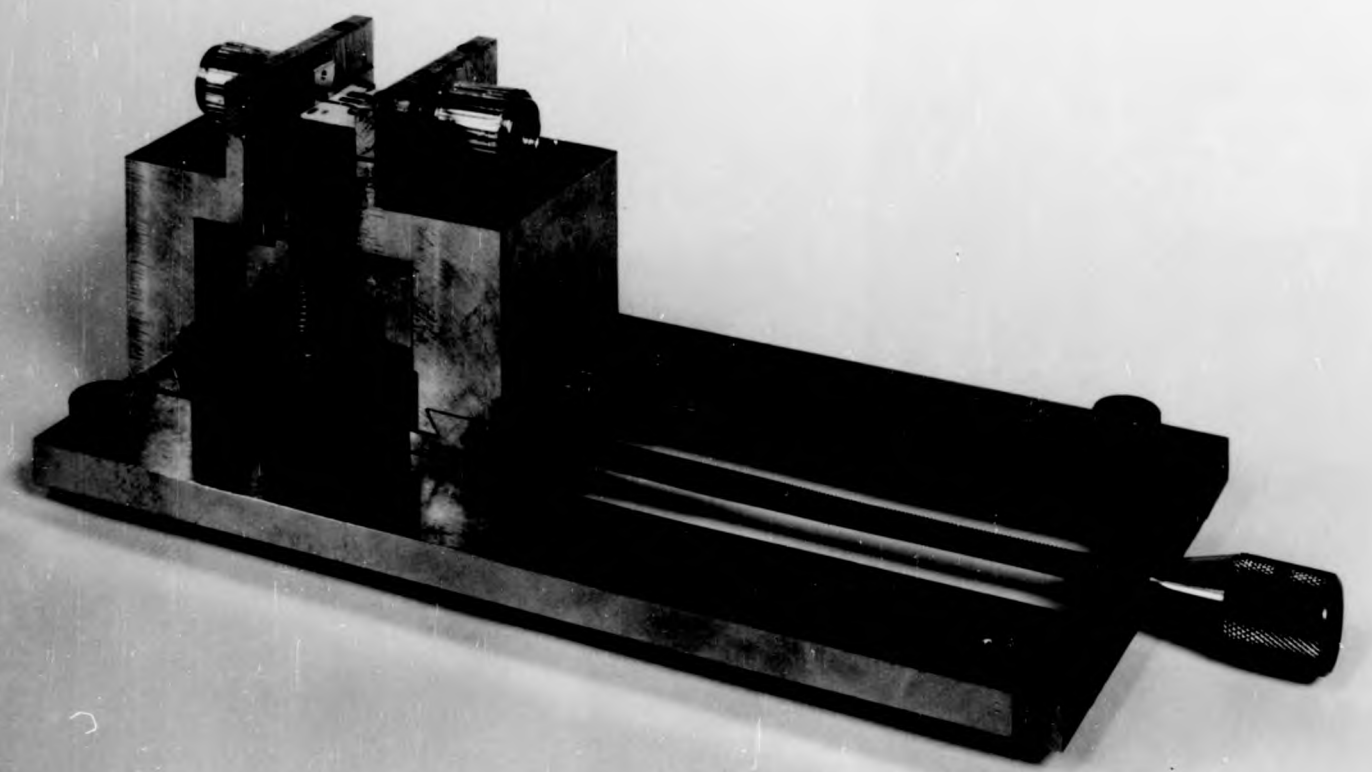

The device was mounted in 1" × 1" alumina substrate of 0.020" thickness and included a reference through-line and two microstrip open circuits. These open circuits were used to set the reference plane of the network analyzer to a plane corresponding to that of the bond wires leading to the transistor. Fig. 5.6a shows the results of measurements, without correction for launchers, whilst Fig. 5.6b shows the corresponding results with correction.

The effect of correction is mainly seen in the reflection coefficients, although $|S_{21}|$ is slightly increased also. If no correction for the adapter parasitics is made, errors of 7^{o} in $\angle S_{11}$ and $\angle S_{22}$ can result. The correction makes S_{11} and S_{22} monotonic and causes S_{11} and S_{22} to fall more nearly on the circles of constant resistance and conductance respectively. Gains computed from the two sets of S-parameters agree very closely.

University of Warwick
Engineering Dept.

SMITH CHART

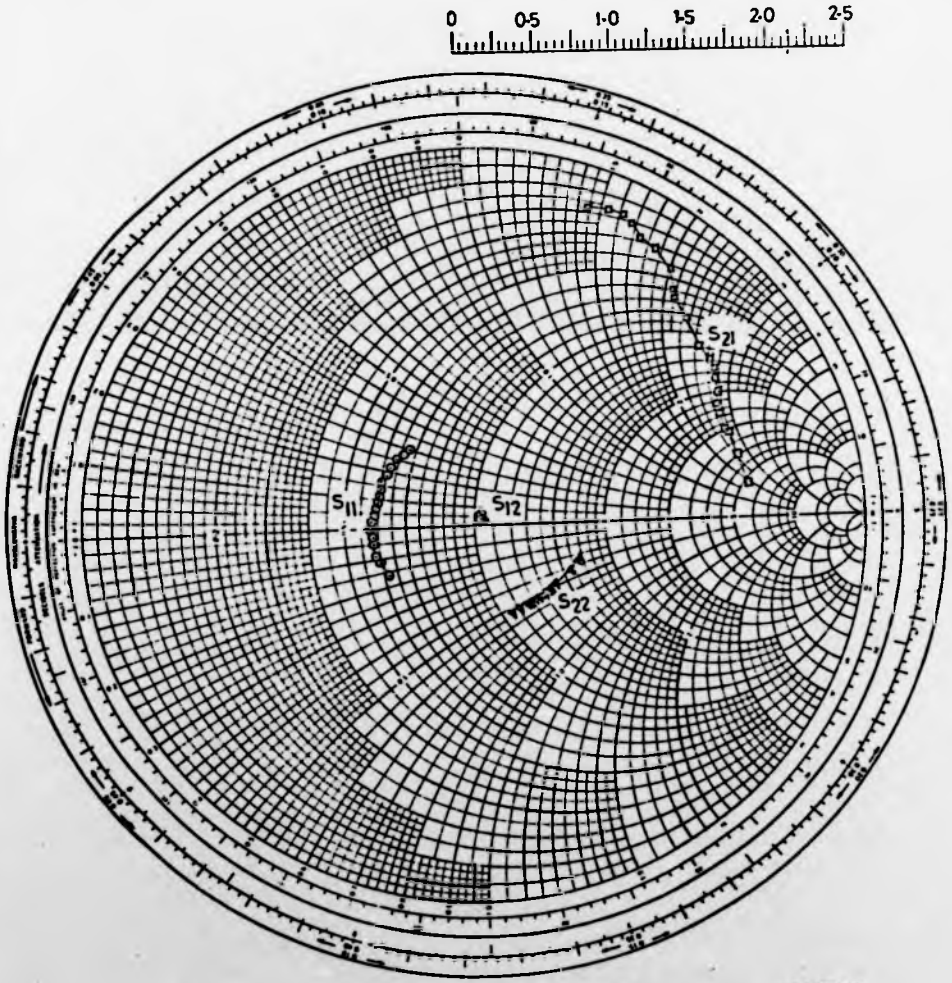

FIG. 5.6a MEASURED S-PARAMETERS OF A GaAs MESFET, WHEN THE LAUNCHER PARASITIC EFFECTS ARE NOT TAKEN INTO ACCOUNT.

University of Warwick
Engineering Dept.

SMITH CHART

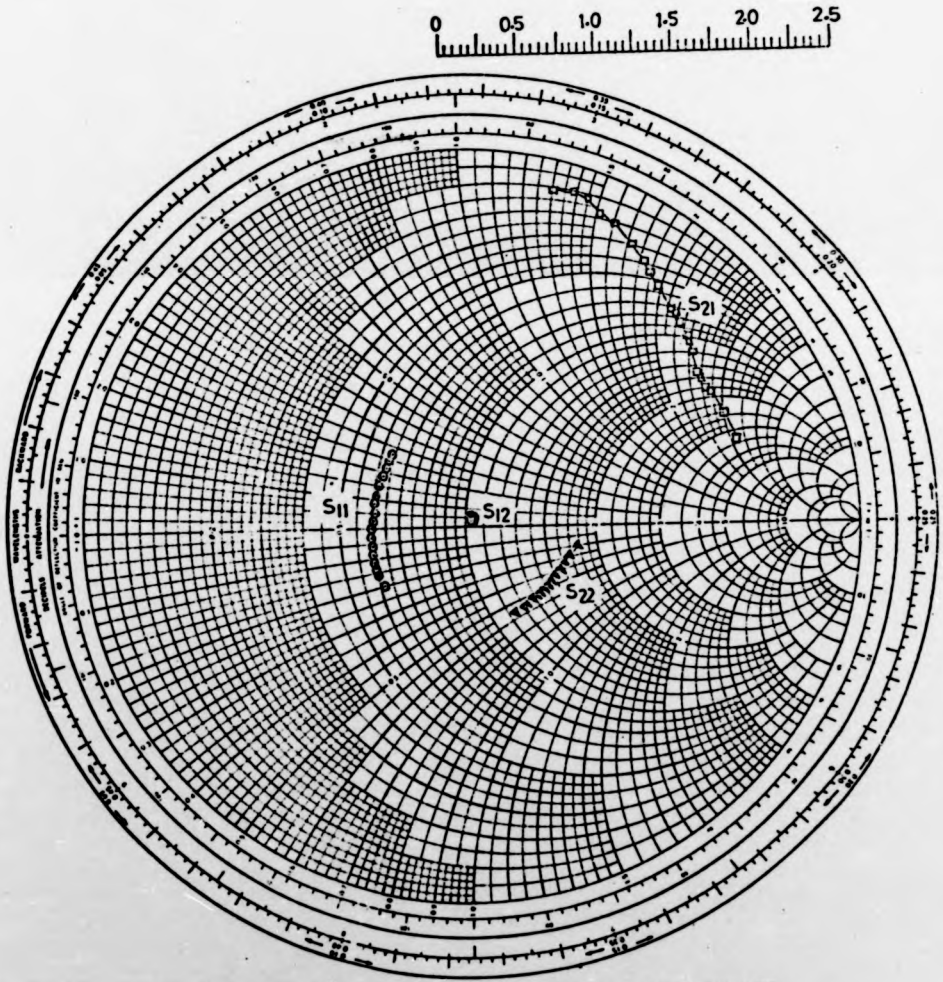

FIG. 5.6b MEASURED S-PARAMETERS OF A GaAs MESFET, WHEN THE LAUNCHER PARASITIC EFFECTS ARE TAKEN INTO ACCOUNT.

REFERENCES

1. SOARES, R.A., and CRIPPS, S.C."Some novel characterisation techniques used in the design of x-band GaAs FET amplifier" in Proc. 1976 European Microwave Conf. (Rome, Italy), Paper, SSI.4.

2. SLAYMAKER, N.A., SOARES, R.A. and TURNER, J.A., "GaAs MESFET small-signal x-band amplifiers", I.E.E.E. Trans. on Microwave Theory & Tech. Vol. MTT-24, June (1976), pp. 329-337.

3. SHURMER, H.V., "Calibration procedure for computer corrected s-parameter characterisation of devices mounted in microstrip", Electron. Lett. Vol. 9, No. 14, 12th July (1973), pp. 323-324.

4. SIEPRATH, W., and ULBRICHT, J. "Meßverfahren zur bestimmung von MIC- Parametern bei verwendung eines automatischen netzwerkanalysators", Nachrichtentechn. Z.27(1974) H.5, S.161-166.

5. WIGHT, J., et al., "Equivalent circuits of microstrip impedance discontinuities and launchers", I.E.E.E. Trans. on Microwave Theory & Tech. Vol. MTT-22, Jan. (1974) pp.48-52.

6. AJOSE, S.O., etal "Characterisation of coaxial-to-microstrip connectors suitable for evaluation of microstrip 2-port", Electron. Lett. Vol. 12., No. 17, 19th August (1976), pp. 430-431.

7. HOSSEINI, N.M.,and SHURMER, H.V., "MICPA-evaluation of microstrip line parameters" ibid, Vol. 12, No. 19 15th September (1976), pp. 496-497.

FABRICATION OF INTEGRATED CIRCUITS ON ALUMINA

The fabrication of microstrip circuits, starting with a schematic diagram, usually involves thin or thick film techniques. Thin films range from $\sim 100A^{\circ}$ to $\sim 1\mu$ in thickness and thick films from $\sim 10\mu$ upwards, the range $1-10\mu$ being classified either as thin or thick. There is no sharp dividing line between thick and thin films in practice, the distinction being usually based on the method of manufacture.

The most widely used methods for thin film deposition are vacuum evaporation and sputtering both of which may be applied to glass or ceramic substrates and the final pattern usually involves a photolithographic process. Subsequent electroplating may be used to increase the thickness.

The completed techniques are direct carry-overs from low frequency integrated circuits and will not be covered in detail since the literature contains many excellent works on these subjects. Thus, the methods of producing thin films by evaporation and sputtering, will not be covered. Some references for standard integrated circuit technology, are given in the bibliography[1-4]. The following method was adopted and used by the author as it satisfies the requirements of simplicity, speed, and accuracy of producing integrated circuits on high-purity alumina (99.5% Al_2O_3).

Probably the cheapest way of producing integrated circuits is to start with ready metallized substrates and etch out the circuit pattern. This procedure, however, involves the disadvantages of reduced accuracy and higher loss due to underetching. The alternative method which is adopted by the author is to start with gold-sputtered substrates, and then apply the following steps.

6.1 Maskmaking

6.2 Photolithography

6.3 Plating

6.4 Etching and removing photo resist.

The utmost care and cleanliness must be observed at all stages and therefore most of the work must be carried out in a 'clean-room'. The complete processing stages will now be described in turn.

6.1 MASKMAKING.

The method described here utilizes "cut 'N' strip" two layered plastic film[5]. The cutting has to be precisely controlled and this

was carried out on a special machine known as a 'co-ordinatograph'. The large scale artwork is photographically reduced, both the camera and screen carrying the artwork are mounted on a shock and vibration free base.

Variable reductions are achieved by moving the camera position relative to the artwork holder on the light box. The positioning error of the camera, on the optical bench, was within ±0.025 mm, which has a negligible effect on the reduction accuracy.

The majority of maskmaking is carried out for 1" × 1" substrates, using 2" × 2" 'KODAK' high resolution photographic plates[6].

6.2 PHOTOLITHOGRAPHY.

The application of the photo-resist is one of many critical steps in the process. The resist is filtered immediately before being applied as a coat on the substrate, the standard method of applying photo resist was carried out in this stage. In general, it has been found that cleaning procedures, given here, are suitable for most kinds of photo-resists which are supplied by different manufacturers. Because ultrasonic facilities exist, the majority of stages as indicated in Fig. 6.1 are ultrasonerated. The final drying was done by either filtered air or spinning dry.

The pre-and post-bake were carried out in a closed oven, time depending on the photo-resist used.,

(a) Trichloroethylene (5 min.)
(b) 2% Decon 73 (5 min.)
(c) D.I. water (2 min.)
(d) Tricholorethylene (2 min.)
(e) Isopropyl alchohol (2 min.)
(f) Dry.

Fig. 6.1 The cleaning procedures.

6.3 GOLD PLATING.

For general purposes gold plating is used and the author employed laboratory type built-in plating units. The substrate to be electroplated is immersed in a solution known as the electrolyte and connected to the negative lead of a low voltage D.C. supply. The positive lead which is called the anode may be of the same metal to be deposited or of an inert insoluble conductive material. There is no standard process for gold plating; any distinction is usually based on the method used by the manufacturer who supplies the gold solutions. It is usual to apply an initial deposit of gold prior to the main gold plating [7]. This prior deposition gives a flash gilding on the substrate, then the heavy gold plating solution may be employed. However, the common equipment, regardless of the manufacturing processes, could be as follows:

CATHODE - The negatively charged electrode, which is the object to be plated, is mounted on this electrode. All electrical connections, except the substrate, should be covered with plastic and the

substrate holder must not be metal, so as to prevent deposition of gold on an unwanted area.

ANODES - Insoluble anodes should be used, but platinised titanium, in the form of mesh, with an area sufficient to provide a maximum anode current density is recommended.

TANKS - For most solutions, teflon, natural polypropylene, or high density polythene lined, glass tanks, supported externally, should be used. Since the operating conditions are at a temperature more than 70 C° a well fitting lid should be used to prevent evaporation of the solutions in free air.

AGITATION & TEMPERATURE. Moderate to vigorous agitation is necessary to maintain uniform metal distribution. The solution should be maintained at an optimum temperature according to the data sheet.

6.4 ETCHING AND REMOVING THE PHOTO-RESIST

The unwanted circuit patterns were etched out, as the author started with ready sputtered gold; therefore the only etchants which will be mentioned at this stage are the metal etchants. It is advisable that all etchants be made immediately prior to use.

GOLD ETCHANT. This is a solution of 32 grams potassium iodide, 8 grams iodine and 200 ml water. The etch rate is approximately 1µm/minute.

CHROMIUM ETCHANT. This is a solution of 40 grams potassium ferricyanide and 12 grams sodium hydroxide dissolved in 200 ml water. The etch rate is 0.075 µm/minute approximately.

COPPER ETCHANT. This is a solution of 10 grams ferric chloride in 200 ml. water. The etch rate is 0.5 μm/minute approximately.

REMOVING PHOTO RESIST. The negative photo-resist may be removed by immersing the substrate in the stripper solution according to the data sheet [8]. The stripper is then removed by washing the substrate thoroughly in a stream of cold water. The positive photo-resist may be removed by immersion in 'REMOVER' solution, but normally it can be removed by immersion in a suitable organic solvent such as acetone.

REFERENCES

1. MAISSEL, L.I., and GLANG, M.M. "Handbook of thin film technology", McGraw-Hill, New York, 1970.
2. MEHMET, K., Ph.D. Thesis, University of Warwick, Chapter 9, October (1970) pp.151-182.
3. BUTLIN, R.S. Ph.D. Thesis, University of Warwick, Chapter 3, September (1973), pp.20-51.
4. MICHIE, D., Ph.D. Thesis, University of Warwick, Chapter 2, March (1974), pp.31-63.
5. KEUFFEL and ESSER publication, "Uses of stabiline CUT 'N' STRIP film" Data sheet (1964).
6. KODAK Publication "Kodak high resolution plate", Data sheet.
7. Handbook on Electroplating. W. Canning & Co. Ltd., Birmingham, 20th Edition, January (1966).
8. 13/LS Resist stripper, Data sheet,Chemical Processes Ltd., Chedburgh, Suffolk.

7

DISPERSION MEASUREMENT TECHNIQUES

The usefulness of theoretical calculations for microstrip parameters is severely limited by the accuracy with which the dielectric constant of the substrate material can be specified at microwave frequencies. This is particularly so with new substrates, such as anisotropic materials, e.g. flexible ceramic filled Teflen, so the microwave engineer is still heavily dependent on measurements to complement his design data. Thus, before choosing a particular theory, for the purpose of CAD, it was decided to measure accurately, as a function of frequency, the dispersion and any variation of the effective relative permittivity (ε_{eff}). The particular transmission structure considered here, and through the remainder of this thesis, is standard microstrip, i.e. an open structure comprising a single

metallized strip deposited on a dielectric substrate backed by a metallic ground plane Fig. 7.1.

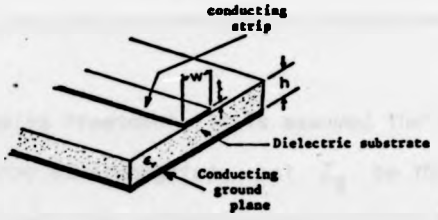

FIG. 7.1 MICROSTRIP TRANSMISSION LINE, SHOWING THE VARIOUS PARAMETERS.

Among several techniques for measuring ε_{eff}, e.g. open or short circuited resonators [1,2], ring resonator [3], transmission measurement [4] and nodal shift technique [5], the following technique (which is based on idea [6] and has been described in [7]), was used to check the effect of dispersion. This technique is ideally suited to the computer on-line measurements described in Chapter 4. The same technique has also been developed by one of the author's colleagues [8], but with different mathematical representations.

7.1 MEASUREMENT OF PHASE VELOCITY.

The measurement technique uses four open-ended microstrip lines, which must have identical physical and geometrical characteristics, except in relation to line lengths. Fig. 7.2 illustrates the cross-section of a launcher together with one of the test pieces. The plane AA' is the reference plane of the APC-7 connector.

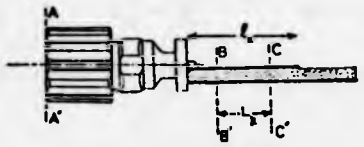

FIG. 7.2 THE LAUNCHER AND REFERENCE PLANES FOR DISPERSION MEASUREMENT.

In the following treatment, it is assumed that only the fundamental mode may be propagated. Let Z_L be the impedance seen at plane CC′, ρ_L' the reflection coefficient at the same plane, normalised with respect to the line impedance Z_1 and ρ_k' the corresponding normalised reflection coefficient at plane BB′. At plane BB′ the reflection coefficient will be as follows:

$$\rho_k' = \rho_L' \exp(-2\gamma L_k) \tag{7.1}$$

where L_K is the length between planes BB′ and CC′.

Now suppose each test piece is terminated in the identical reactance of an open circuit. Using bilinear transformations[8] (see Appendix D) ρ_k' (k = 1, 2, 3, 4) may be expressed as

$$(\rho_1, \rho_2, \rho_3, \rho_4) = (\rho_1', \rho_2', \rho_3', \rho_4') \tag{7.2}$$

where ρ_k (k = 1, 2, 3, 4) is normalized to 50 ohms.

This in turn may be related to the measured reflection coefficient (Γ_k) at the plane AA′ by a bilinear transformation, viz:

$$(\Gamma_1, \Gamma_2, \Gamma_3, \Gamma_4) = (\rho_1', \rho_2', \rho_3', \rho_4') \tag{7.3}$$

By taking the crossratio and then a few manipulations the following results are obtained:

$$\frac{(\Gamma_1 - \Gamma_4)(\Gamma_2 - \Gamma_4)}{(\Gamma_1 - \Gamma_2)(\Gamma_3 - \Gamma_4)} = \frac{[1-\exp(-2\gamma a_4)][\exp(-2\gamma a_2) - \exp(-2\gamma a_4)]}{[1-\exp(-2\gamma a_2)][\exp(-2\gamma a_3) - \exp(-2\gamma a_4)]} \tag{7.4}$$

where $a_k = L_k - L_1 = \ell_k - \ell_1 \qquad k = 2, 3, 4$

For the special case of $\ell_2 - \ell_1 = \ell_3 - \ell_2 = \ell_4 - \ell_3$, equation (7.4) reducesto:

$$\cosh^2 \gamma a_2 = \frac{(\Gamma_1 - \Gamma_3)(\Gamma_2 - \Gamma_4)}{4(\Gamma_1 - \Gamma_2)(\Gamma_3 - \Gamma_4)} \tag{7.5}$$

Solving equation (7.5) leads to a complex root and the imaginary part will be β, the phase constant. The values of ε_{eff} and hence v_p, the phase velocity may be calculated from the equations:

$$\varepsilon_{eff} = \frac{(c\beta)^2}{\omega^2} \quad \text{and} \quad v_p = \frac{c}{\sqrt{\varepsilon_{eff}}} \tag{7.6}$$

where c is the velocity of light in free space and $\omega = 2\pi f$, f being the operating frequency.

Twelve open-circuited terminations in 50Ω line were fabricated on three alumina substratesof 0.025" thickness. The fixed physical length a_2 was approximately $\lambda/8$ at mid-band.

Before the measurements of reflection coefficient were started the errors of the system at each frequency point were measured. In subsequent measurementsof the reflection coefficients the errorswere vectorially substracted from the measurement data, thus leaving only the true characteristics of the device. The error model of the automatic network analyzer was constructed by measuring the appropriate standard terminations, as described in Chapter 4 and 5.

For the purpose of evaluating ε_{eff}, each of the open-circuited terminations is connected in turn to the network analyzer and the corrected reflection coefficients Γ_1, Γ_2, Γ_3, Γ_4 are stored on a

magnetic tape. From this data the ε_{eff} is calculated at each frequency and the results are shown in Fig. 7.3.

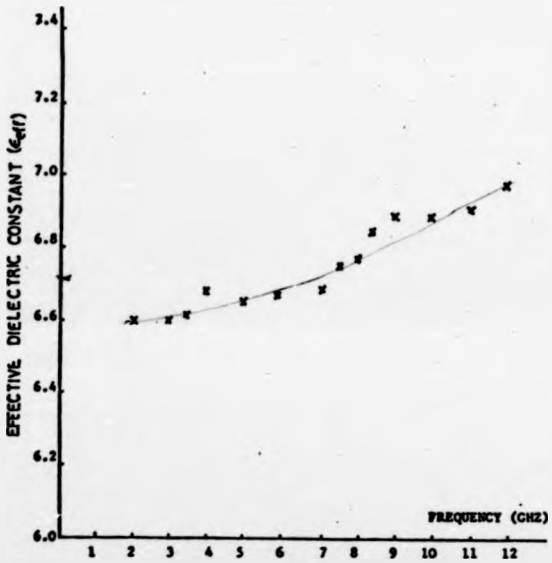

FIG. 7.3 THE MEASURED ε_{eff} AGAINST FREQUENCY FOR 50Ω ALUMINA OF 0.025" THICKNESS AND DIELECTRIC CONSTANT $\varepsilon_r = 9.8$.

In solving equation 7.5, the square root of a complex number is involved and usually, with a small computer the associated 'Library' subroutine does not exist and iteration may alternatively be used to evaluate the square root.

REFERENCES

1. HARTWIG, C.P. MASSE, D.,and PUCEL, R.A. "Frequency dependent behaviour of microstrip", Proceedings of The G-M.T.T. Microwave Symposium, Detroit (1968), pp. 110-116.

2. MEHMET, K., McPHUN, M.K., and MICHIE, D.F. "Simple resonator method for measuring dispersion of Microstrip", Elect. Lett., Vol. 8, No. 6, March (1972), pp. 165-166.

3. TROUGHTON, P. "Measurement techniques in microstrip", Elect. Lett. Vol. 5, No. 2, Jan. (1969), pp.25-26.

4. NAPOLI L.S., HUGHES J.J., "High frequency behaviour of microstrip transmission lines", R.C.A. Review, June (1969), pp.268-276.

5. SECKELMAN R., "Nodal shift measurements to determine transmission line properties", Microwave J., Vol. 11, No. 4, April (1968), pp.69-72.

6. DESCHAMPS, G.A. "Determination of reflection coefficients and insertion loss of a wave guide junction", J. App. Phys. Vol. 24, August (1953), pp. 1046-1050.

7. BIANCO, B., and PARODI, M. "Measurement of the effective relative permittivities of micrsostrip ", Elect. Lett. Vol. 11, No. 3, February (1975), pp. 71-72.

8. SHURMER, H.V. "Correction of a Smith-chart display through bilinear transformations", Elect. Lett. Vol. 5,.15th May (1969), pp.209-210.

9. DaSILVA, E.F., "Measurement of attenuation and phase constants of transmission lines through a mismatched junction", private communication. University of Warwick, Feb. (1976).

EVALUATION OF MICROSTRIP PARAMETERS

High speed digital computers have prompted the development of new techniques for analyzing microstrip lines. A large number of papers on computerized methods of evaluating microstrip parameters has been presented during the last few years. A majority of these works [1-4] are based on semi-analytical and numerical techniques, but these procedures have the disadvantages of being difficult to incorporate into a computer-aided design (CAD) package. Serious problems arise when the numerical technique routines are used in conjunction with an analysis/optimization programme[5]. As the routines are called upon hundreds, possibly thousands of times, during a run, it is important to use a simple and accurate algorithm, especially as this permits simpler programming, reduced execution time and memory size[6].

This Chapter presents a discussion of some of the representative algorithms for evaluating the parameters of open microstrip line. The topics discussed include analysis and dispersion effects as well as evaluation of conductor and dielectric losses. Finally, the chapter

ends with some results which have been evaluated by the author's computer programme.

8.1 CONDUCTOR LOSS.

In practice, losses are always present and it may be important to obtain a quantitative estimate of these for accurate design work. Losses due to finite conductivity in the strip and ground plane can be calculated, using Schneider's[7] approximation, from the following expressions:

(a) Narrow strips

$$\alpha_c h = \frac{10R_s}{\pi \ln 10} \frac{(8h/w - \frac{w}{4h})(1 + \frac{h}{w} + \frac{h}{w}\frac{\partial w}{\partial t})}{Z_1 \exp(Z_1/60)}, \quad w/h \leq 1 \tag{8.1}$$

where $Z_1 = 60\ln(8\,h/w + w/4h)$

(b) Wide strips

$$\alpha_c h = \frac{R_s Z_o}{720\pi^2 \ln 10} \left[1 + 0.44(\frac{h}{w})^2 + 6(\frac{h}{w})^2(1-\frac{h}{w})^5\right](1 + w/h + \frac{\partial w}{\partial t}), \quad w/h \geq 1 \tag{8.2}$$

The partial derivative of the strip width (w) with respect to strip thickness t is found from:

$$\frac{\partial w}{\partial t} = \frac{1}{\pi} \ln(4\pi w/t), \qquad w/h \leq \frac{1}{2\pi}$$

$$\frac{\partial w}{\partial t} = \frac{1}{\pi} \ln(2h/t), \qquad w/h \geq \frac{1}{2\pi}$$

The skin resistance R_s is given by:

$$R_s = (\pi f \mu_o/\sigma_c)^{\frac{1}{2}} \tag{8.3}$$

where f is the frequency (HZ), σ_c is the strip conductivity (S/m) and $\mu_o = 4\pi \times 10^{-7}$(H/m).

8.2 DIELECTRIC LOSS.

Dielectric loss in microstrip may be calculated if one knows the loss tangent of the substrate and the field distribution. Computation of the electric field is complicated and not practical for present purposes, so the author has used an empirical equation by fitting the data into a least squares optimization programme. For convenience, a normalization factor has been introduced, defined by:

$$\alpha_{dn} = \frac{\alpha_d}{\sigma_s} \tag{8.4}$$

where α_d is the dielectric loss and σ_s is the substrate conductivity. The dielectric loss of microstrip may be defined also as follows:

$$\alpha_d = \frac{\text{power loss in the dielectric material}}{2 \times \text{power transmitted}} \tag{8.5}$$

Assuming that the dominant mode is quasi TEM, the expression for α_{dn} is given in [8] by:

$$\alpha_{dn} = \frac{\iint (\nabla\phi)^2 dx dy}{2V^2/Z_o} \tag{8.6}$$

where the integrals are defined over the cross-sectional area. In (8.6) V is the voltage across the strip and ground plane, Z_o the characteristic impedance and ϕ is the potential distribution.

There are a number of quasi-TEM techniques for evaluating the above quantities. Some of these, viz: the modified conformal mapping[9] and the variational method[10], find their principal use in the case where the centre strip is thin. However, for our purpose, the effect of finite thickness of the centre strip cannot be neglected. Since the relaxation method[4] is principally a numerical

technique, it can be applied to the case of the arbitrarily thick centre strip. But the procedure has the disadvantage that its numerical convergence is rather slow.

This part utilizes the results of an extension of the moment method[11] which has been described in[2]. In applying the moment method to calculate microstrip impedance, the charge density distribution on the centre conductor is obtained as an intermediate result[16]. Once this charge density distribution $\sigma(x_o y_o)$ is known, the potential $\phi(x,y)$ at a point $P(x,y)$ inside the dielectric can be written as:[12] (See Appendix E)

$$\phi(x,y) = \int G(x,y|x_o,y_o)\ \sigma(x_o,y_o)d\ell_o \qquad (8.7)$$

where $G(x,y|x_o,y_o)$ is the Green's function, and the integral is defined over the conductor surface.

If the centre conductor is divided into N sufficiently narrow strips, Fig. 8.1, then the charge density on each strip can be considered as a constant, and we can rewrite (8.7) as:

$$\phi(x,y) = \sum_{i=1}^{N} \sigma^i(x_o y_o) \int G(x,y|x_o,y_o)d\ell_o^i \qquad (8.8)$$

where the integral is defined over the ith strip.

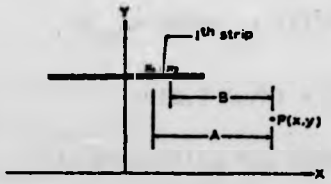

FIG. 8.1 THE CENTRE CONDUCTOR IS DIVIDED INTO N SUFFICIENTLY NARROW STRIPS.

The normalized dielectric losses α_{dn}, and characteristic impedances, Z_o, obtained by this method, utilizing a computer program , for several different dielectric constants are given in Table 8.1.

Table 8.1 Normalized dielectric loss and characteristic impedance for alumina, silicon and gallium arsenide substrates.

w/h	Alumina $\varepsilon_r = 9.8$		Silicon $\varepsilon_r = 11.7$		GaAs $\varepsilon_r = 12.7$	
	α_{dn}	Z_o	α_{dn}	Z_o	α_{dn}	Z_o
0.4	389.3	72.62	357.8	66.85	344.0	64.32
0.6	395.9	62.33	363.8	57.36	349.6	55.18
0.8	401.6	55.15	369.1	50.74	354.6	48.80
1.0	406.9	49.69	373.9	45.70	359.3	43.96
2.0	425.9	33.83	391.0	31.09	375.7	89.89
3.0	439.2	25.90	403.1	23.79	387.2	22.87
4.0	448.5	21.05	411.6	19.32	395.4	18.57
5.0	456.0	17.76	418.3	16.30	401.7	15.66
6.0	461.6	15.38	423.3	14.11	406.7	13.55

However, the computation results are fitted into a least squares curve fitting computer program (see Appendix G), to estimate the unknown coefficient of the following model. The model was based on a function of w/h and ε_r with arbitrary coefficients viz:

$$\alpha_{dn} = F(\varepsilon_r, w/h)$$

The final form was obtained by the least squares procedure over the ranges $0.3 \leq w/h \leq 6$ and $1 \leq \varepsilon_r \leq 14$ and is given as follows

$$\alpha_{dn} = 960/\varepsilon_r + 171(\varepsilon_r)^{-\frac{1}{2}} + 4.6 \ln(w/h) + (225 - 7.7\varepsilon_r)(1-w/h)^{\frac{1}{2}} - 18.7\,(w/h) + (10w/2h)^2 \qquad (8.9)$$

In evaluating the dielectric loss, it is assumed that the substrate conductivity is substantially frequency independent.

8.3 EFFECTIVE DIELECTRIC CONSTANT.

The effective dielectric constant is defined by $\varepsilon_{eff} = C/C_o$, where the static capacitance per unit length is C, inclusive of the dielectric material, and C_o without the dielectric. This may be written, following Schneider[7], as:

$$\varepsilon_{eff} = \frac{\varepsilon_r + 1}{2} + \frac{\varepsilon_r - 1}{2} (1 + 10\ h/w)^{-\frac{1}{2}} \qquad (8.10)$$

This gives an accuracy of ±2 per cent for ε_{eff} and an accuracy of ±1 per cent for $(\varepsilon_{eff})^{\frac{1}{2}}$.

8.4 DISPERSION.

In the gigahertz frequency range, the effects of dispersion for microstrip lines are no longer negligible, making a simple TEM model inaccurate. Indeed, the method of formulation as well as the solution here differs substantially from the TEM or quasi-TEM approach.

In many engineering applications of microstrip, dispersion can be treated as a correction factor to the zero-frequency effective dielectric constant (ε_{eff}), so that only approximate values are required. The experimental results of the previous chapter indicated that Getsinger's model[14] was the most appropriate for computer programs. These express the effective dielectric constant at any frequency as a fixed zero frequency contribution from which must be subtracted a frequency correction term, viz:-

$$\varepsilon_{rd} = \varepsilon_r - \frac{\varepsilon_r - \varepsilon_{eff}}{1+G(f/f_p)^2} \qquad (8.11)$$

where

$$G = 0.6 + 0.009\ Z_o \quad \text{and} \quad f_p = Z_o/2\mu_o h$$

The normalized phase velocity, defined by $v_n = \lambda_g/\lambda_o$ (where λ_g and λ_o are guide and free-space wavelengths, respectively) is given by:-

$$v_n = 1.0/\sqrt{\varepsilon_{rd}} \tag{8.12}$$

The effective line length is then given by:-

$$\ell_{eff} = \ell v_n \tag{8.13}$$

The phase constant, defined by $\beta = \omega/v_p$ (where v_p is the phase velocity) is given by:-

$$\beta = 2.0959 \times 10^{-2}\ f/v_n \tag{8.14}$$

where f is the operating frequency (GHZ).

8.5 MICROSTRIP DIMENSIONS.

For determining strip width in terms of other parameters in Fig. (7.1), the following expressions, based on Wheeler's method of analysis[9], have been used:-

(a) Narrow strips.

$$h/w = 0.25e^{D} - 0.5\ e^{-D} \tag{8.15}$$

where: $$D = \frac{Z_o}{60}\left(\frac{\varepsilon_r + 1}{2}\right)^{\frac{1}{2}} + \frac{\varepsilon_r - 1}{\varepsilon_r + 1}\left(0.226 + \frac{0.121}{\varepsilon_r}\right)$$

(b) Wide strips

$$w/h = \frac{2}{\pi}\left[B - 1 - \ell n(2B - 1)\right] + \frac{\varepsilon_r - 1}{\varepsilon_r \pi}\left[\ell n(B-1) + 0.293 - 0.517/\varepsilon_r\right] \tag{8.16}$$

where:

$$B = \Gamma_o \pi/2Z_o(\varepsilon_r)^{\frac{1}{2}} \quad \text{and} \quad \Gamma_o = 376.73$$

For the characteristic impedance Z_o, the following expressions in terms a given strip width are due to Schneider[7], which have a maximum relative error of ±0.25 per cent in the range $0 \leq w/h \leq 10$, for a single dielectric microstrip:

$$Z_o = 60 \ln (8h/w + w/4h) \text{ ohm} \qquad w/h \leq 1 \tag{8.17}$$

$$Z_o = \frac{120\pi}{w/h + 2.42 - 0.44\, h/w + (1 - h/w)^6} \text{ ohm} \quad w/h \geq 1 \tag{8.18}$$

The above expressions are valid for zero-thickness strips. In the case of finite thickness an approximate width correction must be incorporated to compensate for the effect of fringing fields. The effective width w_e may be written as follows:

$$w_e = w + \frac{t}{\pi}\left[1 + \ln\left(\frac{2h}{t}\right)\right] \qquad w/h > \frac{1}{2\pi} > \frac{2t}{h}$$

and

$$w_e = w + \frac{t}{\pi}\left[1 + \ln\left(\frac{4\pi w}{t}\right)\right] \qquad \frac{1}{2\pi} > w/h > \frac{2t}{h}$$

In using the expressions (8.15) and (8.16) with a CAD package, there could be uncertainty as to which of the above categories (i.e. narrow or wide) was applicable. This, however, may be resolved by considering the value of B in Eqn. (8.16). If this value is less than 2π, then Eqn. (8.15) applies; otherwise Eqn. (8.16) should be used.

8.6 COMPUTER PROGRAM AND CONCLUSIONS

A computer subroutine to evaluate the parameter discussed in this chapter has already been published by the author[6]. A Fortran source listing of the subroutine and instructions that are needed for running it may be found in Appendix (F). However, a flow chart outlining the procedure is given in Fig. (8.2). As

previously, in evaluating the dielectric loss, it is assumed that the conductivity of the substrate is substantially frequency independent.

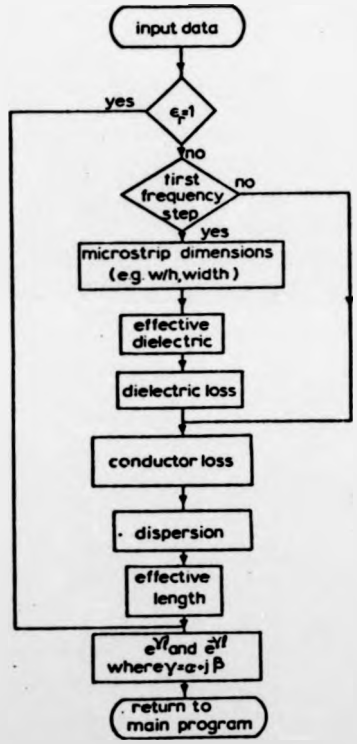

FIG.8.2 THE FLOW DIAGRAM OF COMPUTER PROGRAM 'MICPA'

Fig. (8.3) shows the dispersion diagram for the effective relative permitivity of a 50Ω microstrip line on alumina 0.025" thickness and similar lines on silicon and gallium arsenide substrates of 0.01" thickness.

In order to show how the line lengths vary with frequency, owing to dispersion, results for a 20 mm length of each of the above substrates are indicated in Fig. 8.4.

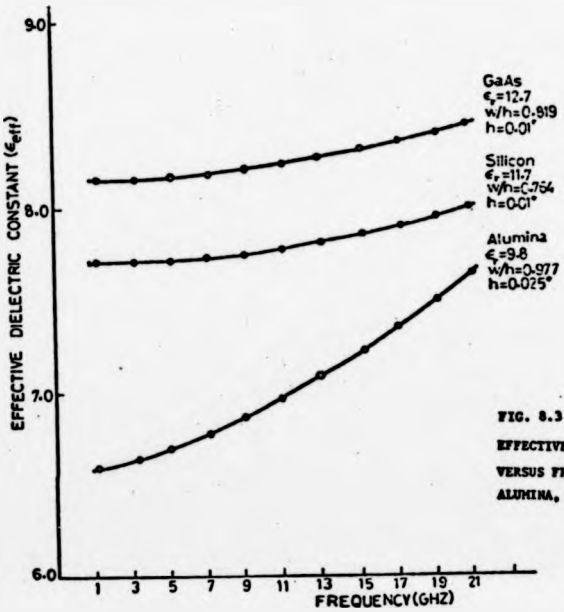

FIG. 8.3
EFFECTIVE DIELECTRIC CONSTANT VERSUS FREQUENCY FOR 50 OHM ALUMINA, SILICON AND GaAs SUBSTRATE.

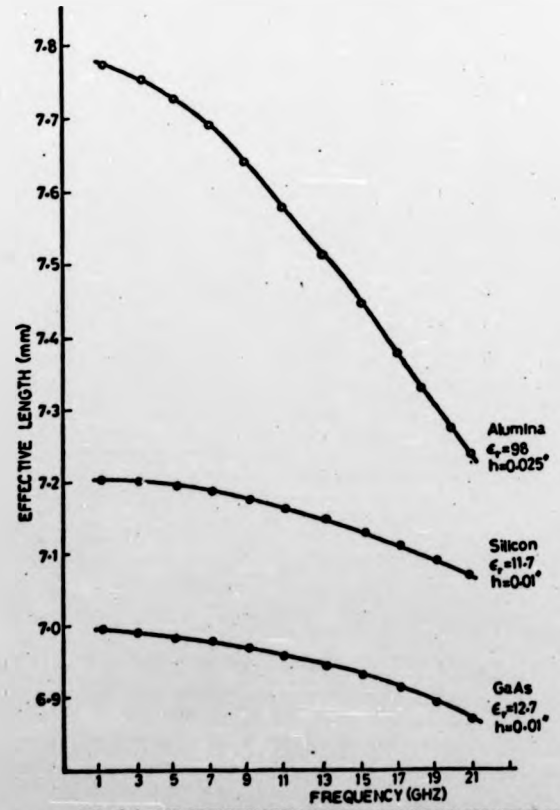

FIG. 8.4 THE EFFECTIVE MICROSTRIP LENGTH VERSUS FREQUENCY FOR 20 mm LONG AIR LENGTHS OF ALUMINA, SILICON AND GaAs SUBSTRATES

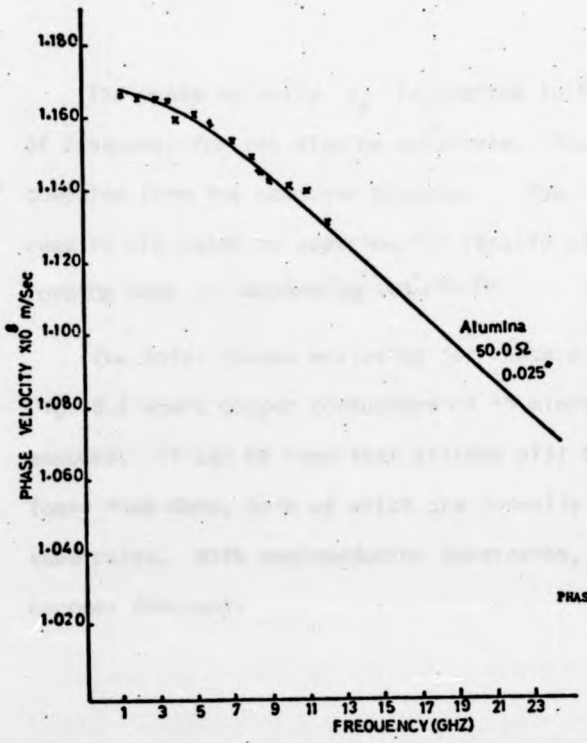

FIG. 8.5 CALCULATED AND MEASURED PHASE VELOCITY ON 0.025" THICK ALUMINA.

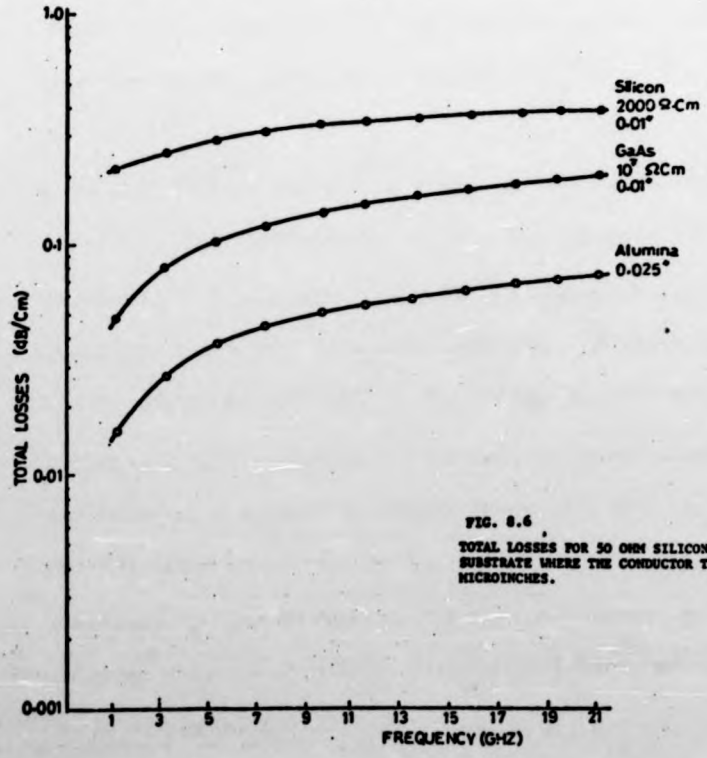

FIG. 8.6

TOTAL LOSSES FOR 50 OHM SILICON, GaAs AND ALUMINA SUBSTRATE WHERE THE CONDUCTOR THICKNESS IS 15 MICROINCHES.

The phase velocity v_p is plotted in Fig. 8.5 as a function of frequency for the alumina substrate. The solid lines are computed from the computer program. The isolated points (x-mark) results are based on experimental results of the previous chapter for a 50Ω line on an alumina substrate.

The total losses evaluated for these substrates are given in Fig. 8.6 where copper conductors of 15 microinch thickness were assumed. It can be seen that silicon will be considerably more lossy than GaAs, both of which are normally more lossy than alumina substrates. With semiconductor substrates, dielectric loss becomes dominant.

REFERENCES

1. BRANT, T.G., "MSTRIP-Parameters of microstrip", IEEE Trans. Microwave Theory and Tech., Vol. MTT-19, April (1971), pp.415-416.

2. SIMPSON, T.L. and TSENG, B., "Dielectric loss in microstrip lines", ibid, Vol. MTT-24, Feb. (1976), pp. 106-108.

3. DENLINGER, E.J., "A frequency dependent solution for microstrip transmission lines", ibid, Vol. MTT-19, Jan. (1971), pp. 30-39.

4. GREEN, H.E., "The numerical solution of some important transmission line problems" ibid, Vol. MTT-13, Sept. (1965), pp. 676-692.

5. HOSSEINI, N.M., SHURMER, H.V. and SOARES, R.A., "OPTIMAL-a program for optimising microstrip networks", Electron. Lett., Vol. 12, No. 8, 15th April (1976), pp.190-192.

6. HOSSEINI, N.M. and SHURMER, H.V., "MICPA-evaluation of microstrip line parameters", ibid, Vol. 12, No. 19, 15th Sept. (1976), pp. 496-497.

7. SCHNEIDER, M.V., "Microstrip lines for microwave integrated circuits", Bell Syst. Tech. J. Vol. 48, May-June (1969) pp. 1421-1444.

8. YAMASHITA, E., and ATSUKI, K., "Strip line with rectangular outer conductor and three dielectric layers", IEEE Trans. Microwave Theory and Tech. Vol. MTT-18 May (1970), pp.238-244.

9. WHEELER, H.A. "Transmission-line properties of parallel strips separated by a dielectric sheet" ibid, Vol. MTT-13, March (1965) pp. 172-185.

10. YAMASHITA, E. and MITTRA, R. "Variational method for the analysis of microstrip line" ibid, Vol. MTT-16, (1968), pp. 251-256.

11. HARRINGTON, R.F. "Field Computation by Moment Methods", Macmillan Co., New York (1968), pp. 1-41.

12. COLLIN, R.E. "Field Theory of Guided waves", McGraw Hill, New York (1960), pp. 43-64.

13. DAVIES, OWEN L., "The Design and Analysis of Industrial Experiments", Oliver and Boyd, London (1956).

14. GETSINGER, W.J. "Microstrip dispersion model", IEEE Trans. Microwave Theory and Tech., Vol. MTT-21, Jan. (1973), pp. 34-39.

15. SILVESTER, P. "TEM Wave properties of microstrip transmission lines", Proc. Inst. Elec. Eng. Vol. 115, Jan. (1968), pp. 43-48.

16. FARRAR A., and ADAMS, A.T. "Characteristic Impedance of microstrip by the method of moments", IEEE Trans. Microwave Theory and Tech. (Corresp.) Vol. MTT-18, Jan. (1970), pp.65-66.

MICROSTRIP DISCONTINUITIES FOR COMPUTER AIDED-DESIGN

In microwave circuits, using microstrip, the line sections are necessarily finite in width and length; consequently this introduces the problems of discontinuities. These present a considerable challenge, making the realization of microwave circuits difficult. Thus for design purposes, the microstrip-lines must be characterized, and the effects of junction parasitics evaluated in useful terms and parameters. If the circuit designer is not relying on "cut-and-try" methods, he requires accurate information concerning the discontinuity effects, as these are needed in the alternative method of CAD. To incorporate this information, within CAD packages, it is necessary to present results by formulae rather than by tables and curves.

This chapter presents a method for calculating the transmission properties of the discontinuities, considering also the frequency dependence of the microstrip lines. The method can be made far more powerful in application through the aid of an automatic computer

corrected s-parameter measurement facility. Here, the network analyzer is utilized to characterize the discontinuity in terms of its properties at the external terminals, while attention to the details of an exact equivalent circuit for the parasitic junction is not required. The procedure involves first assuming an approximate model and then modifying this to match its predicted performance to that measured by the network analyzer.

The text also covers a discussion of some of the representative techniques for calculating discontinuity effects and outlines the basic principles underlying the procedures. A subsidiary objective of this chapter is to establish the effects of various discontinuities that frequently occur in microwave amplifier circuits. Typical discontinuities of interest are; open-ended stub , step in width, right-angle bend and T-junction in the centre conductor of microstrip line.

9.1 METHODS OF CALCULATING DISCONTINUITIES

Theoretical and experimental techniques for calculating microstrip line discontinuities, which are available in the literature, fall broadly into three categories. First, there is a growing body of information on the quasi-static capacitance of microstrip structures, supplemented more recently by studies of the associated inductance. A second source of data derives from the use of a uniform plane-wave parallel plate model for the microstrip-cross section. Finally, the third method is based on an experimental method of determining microstrip junction parameters. The above methods are first described and the results for a particular discontinuity are presented subsequently.

9.1.1 QUASI-STATIC METHODS. The effects of a discontinuity in a microstrip line may be represented by a lumped shunt capacitance [1-6] and a series inductance[7-9]. The shunt capacitance is calculated by obtaining the total capacitance, C, of the desired structure for a given length (ℓ), and the capacitance of a uniform length, C_o, of the infinite structure, per unit length. The excess of these two capacitances is then associated with the discontinuity effects. As an example, the equivalent circuit of an open-circuited microstrip is shown in Fig. 9.1, where C_{oc} is the fringing capacitance.

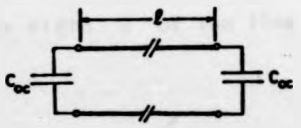

FIG. 9.1 EQUIVALENT CIRCUIT OF AN OPEN-CIRCUITED MICROSTRIP LINE WITH FRINGING CAPACITANCE AT EACH END.

This capacitance may then be defined as

$$C_{oc} = \lim_{\ell \to \infty} \tfrac{1}{2}(C(\ell) - \ell C_o) \qquad (9.1)$$

where $C(\ell)$ is the total capacitance of a section of length ℓ and width w, C_o is the line capacitance, per unit length, of a uniform line of the same width, and the factor $\frac{1}{2}$ accounts for the discontinuities at both ends of the strip.

9.1.2 WAVEGUIDE MODEL. This method is based on the use of a uniform plane-wave parallel plate model for microstrip. The following treatment comprises two approaches. The first is based on the

Babinet's principle; the second discusses a field matching technique.

A-BABINET'S PRINCIPLE. This approach has been described in [10-11]. It begins by considering a balanced strip transmission line having an inner conductor of zero thickness, as indicated in Fig. 9.2.

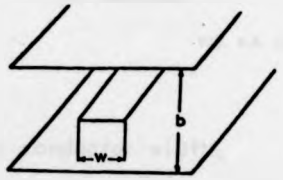

FIG. 9.2 THE BALANCED STRIP TRANSMISSION LINE.

Because of the formidable task of solving for this geometry, the approximate model of Fig. 9.3 has been employed in the determination of equivalent circuit parameters for discontinuities in the line. The width D of the line is related to the actual centre strip width w,

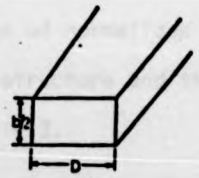

FIG. 9.3 THE APPROXIMATE MODEL WITH MAGNETIC SIDE WALLS.

and this is given in [10] to a good approximation by:

$$D = w + (2b/\pi)\ln 2 \qquad (9.2)$$

The model has electric walls (short circuits) for the top and bottom plates and magnetic walls (open circuits) for the side walls. In effect, the approximate model is a portion, of width D, of a parallel plate transmission line of an infinite width. The evolution of this model, from the actual geometry, is shown in Fig. 9.4. The fringing of the electric field lines for the dominant

mode, shown in Fig. 9.4(a), may be compensated for by extending the

(a) ACTUAL-LINE

(b) EQUIVALENT PARALLEL PLATE LINE

FIG. 9.4 ACTUAL AND APPROXIMATE MODEL

inner conductor width. Structure 9.4(b) may be viewed as two identical portions of parallel plate transmission lines placed back to back, and any incident wave will be divided equally between both portions. Since any balanced discontinuity in the line will reflect the same proportion, it is not necessary, when dealing with normalized quantities, to retain both halves of the line. Thus, in the analysis of balanced discontinuities, which are described in terms of normalized quantities, one need consider only one-half of the structure and therefore employ the approximate model of Fig. 9.3.

The magnetic field lines of this model are similar to the electric field lines of a parallel plate waveguide, so, by reference to Babinet's principle, we may apply standard rectangular waveguide data[12]. The Babinet equivalent of a structure is found by replacing all magnetic walls by electric walls and vice-versa, the magnetic and electric lines are also interchanged. The equivalent circuit of the original discontinuity structure is then the same as the dual Babinet equivalent discontinuity structure, the numerical values of the corresponding dual elements being identical. The line which is the Babinet equivalent of the approximate model of

Fig. 9.3 is shown in Fig. 9.5. This is seen to be another section

(a) APPROXIMATE MODEL (b) BABINET EQUIVALENT LINE

FIG. 9.5 THE BABINET EQUIVALENT LINE

of parallel plate line rotated through 90^{o}. As another example, a top view of a right angle bend in a microstrip-line is shown in Fig. 9.6(a). The bend in the Babinet equivalent line is illustrated in Fig. 9.6(b). The equivalent circuit for the E-plane corner of

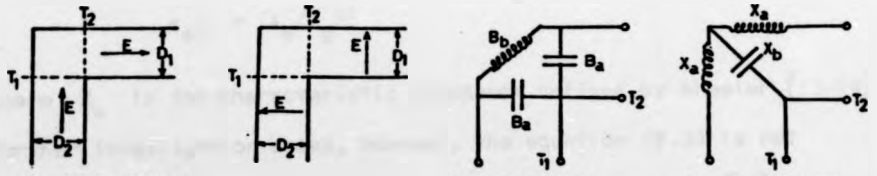

(a) APPROXIMATE MODEL (b) BABINET'S EQUIVALENT (c) E-PLANE CORNER (d) STRIP LINE BEND

FIG. 9.6 DUAL EQUIVALENT CIRCUITS OF RIGHT-ANGLE BEND

the rectangular waveguide at the terminal planes T_1 and T_2, as indicated in [12-p.312], is shown in Fig. 9.6(c). The equivalent circuit appropriate to the right angle bend at the terminal planes T_1 and T_2 is thus the dual of that of Fig. 9.6(c) and is given in Fig. 9.6(d).

B - MODE-MATCHING METHOD. The waveguide model used here consists of a parallel plate waveguide of effective width w_{eff} and height h with plates of infinite conductivity at the top and bottom. It also has magnetic side walls and is filled with a dielectric medium of dielectric constant ε_{eff}. The model is indicated in Fig. 9.7

and was used by Wheeler for the lowest-order mode, which approximates

(a) ACTUAL MICROSTRIP (b) THE MODEL

FIG. 9.7 ACTUAL AND PLANAR WAVEGUIDE MODEL OF A MICROSTRIP LINE

to a TEM mode. In this case the width w_{eff} and relative permittivity ε_{eff} may be obtained from

$$w_{eff} = \frac{h}{Z_w}\sqrt{\mu_o/(\varepsilon_{eff}\cdot\varepsilon_o)}$$
$$\varepsilon_{eff} = (\lambda_o/\lambda_g)^2 \qquad (9.3)$$

where Z_w is the characteristic impedance defined by Wheeler [13-14]. Further investigation shows, however, the equation (9.3) is not suitable if higher-order modes are going to be considered[15]. This arises from the physical aspect that the electric field becomes more and more concentrated in the dielectric material with increasing frequency, thereby reducing the fringing field, so a frequency dependent equation for w_{eff} may be deduced:

$$w_{eff}(f) = w + \frac{w_{eff}(0) - w}{1 + f/f_g} \qquad (9.4)$$

where $f_g = c_o/2w\sqrt{\varepsilon_r}$ and $w_{eff}(0)$ is the effective width calculated from 9.3. Babinet's principle has also been applied to this model for solving the problem of the discontinuity at a T-junction [24]. In contrast to the Babinet's principle, there are well tested methods for calculating the effects of discontinuities

and junctions using waveguide techniques. These methods use orthogonal-series expansions of the fields in the waveguide [16-17]. A necessary condition for applying orthogonal-series-expansion methods is that a complete set of field solutions for the problem considered must be known. A typical discontinuity structure which may be used to formulate the mode-matching technique is indicated in Fig. 9.8.

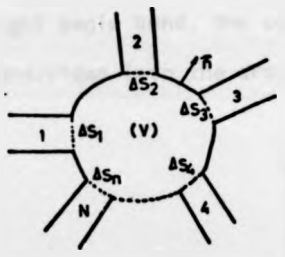

FIG. 9.8 GENERALIZED MODEL OF A PASSIVE MICROWAVE CIRCUIT WITH DISCONTINUITIES.

The structure consists of N waveguides exciting a closed region of a certain shape. The cavity may be characterized by a volume V having a unit vector $\vec{n}$ normal to its closed surface S. The closed surface S is composed of a metallic part s_m and apertures having arbitrary cross section Δs_n (n = 1,....,N). In each waveguide two sets of both incident and reflected E- and H- modes must be considered. In the cavity a unique set-up is obtained by superimposing the solutions for the transverse electric field $\vec{E}_t$ and magnetic field $\vec{H}_t$ of the simplified boundary value problem. By combining the two infinite systems of linear algebraic equations, derived from the continuity conditions for the tangential components

of electric and magnetic field across the boundary of the cavity, sufficient relationships are obtained for their solution. From these equations all unknown expansion coefficients can be determined as a function of the incident waveguide-mode amplitudes, which are assumed to be given. To demonstrate this method, a right angle bend is investigated in the following example.

To formulate the electromagnetic field representation for the right angle bend, the configuration in Fig. 9.9is first of all subdivided into the cross-sectional regions I, II and III .

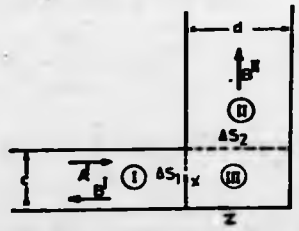

FIG. 9.9 · RIGHT ANGLE BEND OF THE MICROSTRIP LINE

Region III forms a cavity connected to the two transmission lines I and II Due to the geometry of the arrangement, the fields in all regions have uniform transverse distributions with respect to the y-axis. It is also assumed that as the height h of the waveguide model is sufficiently small, then the fields are independent of the y-coordinate. Therefore, only TEM and TE_{no}-modes with E_y-, H_x-, and H_z - components exist. The transverse electromagnetic field of the Fig. 9.7 structure may be described using a scalar potential [16].

$$\phi_n = \sqrt{\frac{e_n}{w_{eff} \cdot h}} \; \frac{\sin(n\pi x/w_{eff})}{n\pi/w_{eff}} \qquad e_n = \begin{cases} 1 & \text{for } n = o \\ 2 & \text{for } n \neq o \end{cases}$$

by the equations

$$E_t = \sum_{n=0}^{\infty} (A_n e^{-\gamma z} + B_n e^{\gamma z})(\hat{z} \times \nabla_t \phi_n)$$
$$H_t = -\sum_{n=0}^{\infty} Y_n (A_n e^{-\gamma z} - B_n e^{\gamma z}) \nabla_t \phi_n \qquad (9.5)$$

where A_n, and B_n are the amplitude coefficients.

$\gamma = \left[(n\pi/w_{eff})^2 - \omega^2 \varepsilon_o \varepsilon_{eff} \mu_o\right]^{\frac{1}{2}}$ is the propagation constant, $\hat{z}$ is the unit vector of the z-coordinate, ∇_t is the transverse Nabla-operator and $Y_n = \frac{1}{Z_n} = \gamma / j\omega\mu_o$ is the complex characteristic wave admittance. Using a normalized wave amplitude and introducing the potential function, the transverse components of electric and magnetic fields are given by:

$$E_y = \sum_{n=0}^{\infty} (a_n e^{-\gamma z} + b_n e^{+\gamma z}) \sqrt{Z_n} \sqrt{\frac{e_n}{w_{eff} \cdot h}} \cos\left(\frac{n\pi}{w_{eff}} x\right)$$
$$H_x = -\sum_{n=0}^{\infty} (a_n e^{-\gamma z} - b_n e^{\gamma z}) \sqrt{Y_n} \sqrt{\frac{e_n}{w_{eff} \cdot h}} \cos\left(\frac{n\pi}{w_{eff}} x\right) \qquad (9.6)$$

where $a_n = Z_n^{\frac{1}{2}} A_n$ and $b_n = Z_n^{\frac{1}{2}} \cdot B_n$.

Suppose now a unit wave is incident from the left in region I of Fig. 9.9. The field then can be written

$$H^{I}_x = -e^{-jkz} + \sum_{n=0}^{\infty} R_n e^{+\gamma z} \cos(n\pi x/c) \qquad (9.7)$$

where $K = 2\pi/\lambda$ and $R_n = \sqrt{\frac{e_n}{c.h}} \cdot b_n \sqrt{Y_n}$

In region II only transmitted waves occur, since the guide is assumed infinite (or matched). Thus

$$H^{II}_x = To\, e^{-jkx} + \sum_{n=1}^{\infty} T_n e^{-\gamma x} \cos(n\pi z/d) \qquad (9.8)$$

The magnetic field in region III is obtained in a similar way and this may be written as follows[18]:

$$H^{III}_x = \int_0^\infty f(\gamma z) \cos(n\pi x/c) \sin[\gamma(z-d)]dz \qquad (9.9)$$

The function $f(\gamma z)$ can be chosen so that the boundary conditions between region I and III are satisfied and the tangential magnetic field strength vanishes at the magnetic walls of region II. The coefficients R_n and T_n can be computed so that the boundary conditions in the discontinuity are met. This is so if equations (9.9) and (9.7), together with their electric fields are matched at $z = o$, and similarly (9.9) and (9.8) with their electric fields are matched at $z = c$.

9.1.3 EXPERIMENTAL METHOD.

To check the validity of theoretical data and provide data where theory is not yet established, an experimental method may be used. The measurement data which is available in the literature shows considerable discrepancies between values given by different authors. As an example, the range of values for the correction of an open-end effect for a 50Ω line on 0.025" thick alumina is 0.100-0.264 mm[19]. An error of about 0.160 mm in the value would result in an open circuit stub designed to be a quarter wave long at 12GHZ actually being a quarter wave length long at 12.9 GHZ. This emphasizes the importance of presenting the microstrip circuit designer, particularly at X-band, with reliable values for the parameters of interest. In the following, two approaches will be presented: one uses a resonant technique and the other is the general modelling method which has been extended to microstrip circuits by the author.

A - THE RESONANT TECHNIQUE - In this method the discontinuity effect can be determined from the component under test in a microstrip resonator [20-21]. The resonator is loosely coupled, via a microstrip

line, to test equipment which is only used to measure the resonant frequency of the system. By the use of various circuit test patterns, and different modes of resonance, the equivalent circuit of the component under test may be found. Although the method has been used by the author for a particular discontinuity, and produced accurate results, its extension to a complex discontinuity is not practical.

B. MODELLING METHOD. In this method, the parasitic elements arising at junctions are dealt with by first assuming an approximate model for discontinuity effects. Of course, the model for particular discontinuities is not unique, since a specific junction can be described by any one of a number of models. The ultimate preference for one model over another arises as a result of compromise between simplicity and the accuracy with which the microstrip under consideration can be described.

The performance corresponding to the initial element values for the model is computed and compared with the required performance via a predetermined error criterion. The corresponding error function is fed to an optimization programme and thereby minimized until the model performance falls within a specified norm, or else the number of iterations exceeds some pre-established value. The required performance is determined by measuring certain properties of the microstrip junction (e.g. input impedance), using automatic computer corrected s-parameters measurements, described in Chapters 4 and 5.

9.2 END EFFECT DISCONTINUITY.

The open-circuit termination occurs extensively in microstrip circuits. It offers a relatively easy method of precise fabrication as compared to the alternative short-circuit termination of stubs and resonant sections. This end region will store considerably more accumulated charge than the remaining portion of the strip. The present available equivalent of the end-effect circuit is presented either as a capacitor or as an excess of line length. The value of the capacitor has been calculated from the quasi-static capacitance of the microstrip structure [1,4,6,22]. The alternative one, which is an extension of the effective electrical length of line, has been measured using the resonator configuration [19,20,23]. In this method the end-effect may be determined from the physical length and resonant frequency of an open-circuit microstrip resonator, provided that the phase velocity is known accurately. The resonator is loosely coupled, via a line, to the test equipment which is then only used to measure the resonant frequency of the structure.

Consider the resonator of Fig. 9.10a with a pnysical length; ℓ , $\Delta\ell$, ℓ_g are the end-effects at the right hand and the input coupling gap, respectively. The equivalent of the coupling gap may be represented by a capacitive Π-section and this in turn, can be represented by an inverter and two line lengths Figs. 9.10b, 9.10c.

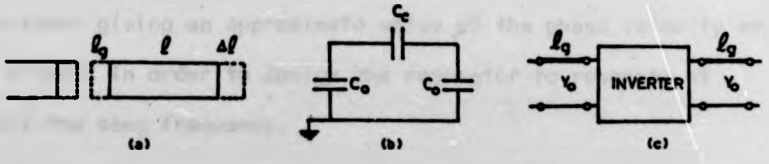

FIG. 9.10. (a) MICROSTRIP OPEN CIRCUIT RESONATOR. (b) and (c) EQUIVALENT CIRCUIT OF A CAPACITIVE COUPLING GAP.

The resonant frequency f_1 of this structure can be determined by observing a display of the complex reflection coefficient in the input line, for which:

$$n\, v_p(f) = 2(\ell + 2\ell_g + \Delta\ell) f_1 \qquad (9.10)$$

where v_p is the phase velocity and n is the resonant mode. The reference plane is set to the effective open end at the coupling gap. By measuring the resonant frequency, f_o, of the circuit shown in Fig. 9.11, $\Delta\ell$ and ℓ_g can be distinguished.

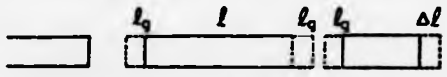

FIG. 9.11 MODIFIED OPEN CIRCUIT RESONATOR.

Here the resonator is gap coupled to a second resonator, which, together with its end effect, is $\lambda/4$ long at the frequency f_o. The open circuit at the right hand end of Fig. 9.11 will be transformed to an effective short-circuit at the terminals of the inverter of the second gap, so that the resonance condition will be given by:

$$n\, v_p(f_o) = (\ell + 2\ell_g) f_o \qquad (9.11)$$

In practice, it may be necessary to perform a preliminary experiment giving an approximate value of the phase velocity and end effects in order to design the resonator to resonate at nearly the same frequency.

A number of circuits were fabricated on 1"x 1" of nominally

0.025" thick alumina substrate (MRC superstrate) with nichrome/gold conducting films of 5 microns approximate thickness. The accuracy of the circuit dimension was (± 0.1%, ± 5μm) and the length ℓ of the resonator which were individually measured to an accuracy of ± 1μm. Experimental results for the end-effect $\Delta\ell/h$ as a function of (w/h) using the configurations of Fig. 9.10 and 9.11 are presented in Table 9.1.

TABLE 5.1 The end-effect $\Delta\ell/h$ as a function of w/h at about 6-7GHZ.

$(\Delta\ell/h)$ End-effect ± 0.03	0.254	0.315	0.348	0.371	0.401	0.433
Ratio of w/h	0.5	1.0	1.5	2.0	2.5	3.0

These experimental results are also depicted in Fig. 9.12 and for comparison the results of some other authors are illustrated in this figure.

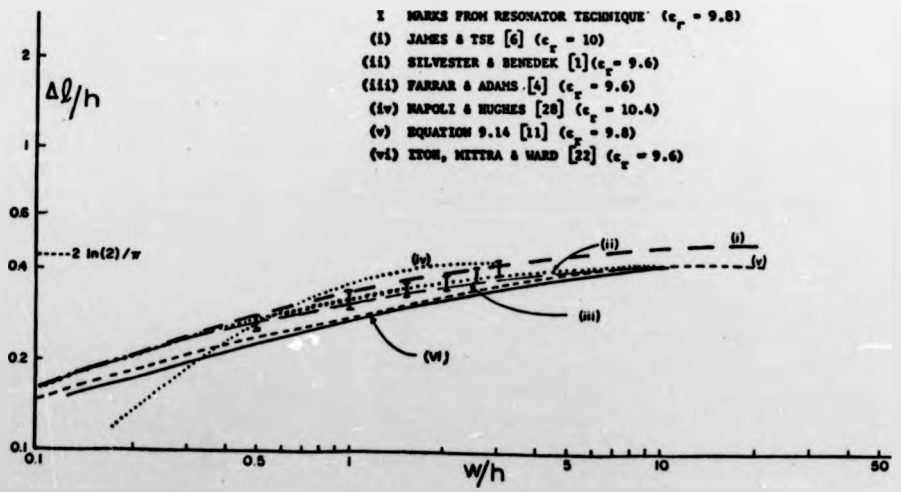

Fig. 9.12 END EFFECT OF THE OPEN-CIRCUIT TERMINATION [REF. 22]

The results of curves (i,iii,vi) are based on theoretical computation using the quasi-static method [6,4,22]. Curve (ii) is also based on the quasi-static method, but using different approaches from previous techniques. Here, an integral equation was found for the charge distribution near an open-circuited microstrip end, and it was solved to find the fringing capacitance [1]. Curve (iv) is the result of experimental work [28], except for low values of w/h, it follows the measured one well through the midrange and up to broad strip widths. Finally, the results of curve (v) are evaluated from equation 9.14.

In order to use these results, in a CAD package, the empirical formula that has been developed in [1] may be used. This gives the fringing capacitance in terms of w/h as follows:

$$C/w = \exp\left[(\ell\log_e 10)\sum_{i=1}^{5} c_i(\varepsilon_r)(\ell\log_{10} w/h)^{i-1}\right] \quad (pF/m) \qquad (9.12)$$

when the coefficients c_i are as tabulated in Table 9.2.

TABLE 9.2 Coefficients c_i for the empirical equation 9.12 (Ref.1)

i \ ε_r	1.0	2.5	4.2	9.6	16.0	51.0
1	1.110	1.295	1.443	1.738	1.938	2.403
2	−0.2892	−0.2817	−0.2535	−0.2538	−0.2233	−0.2220
3	0.1815	0.1367	0.1062	0.1308	0.1317	0.2170
4	−0.0033	−0.0133	−0.0260	−0.0087	−0.0267	−0.0240
5	−0.0540	−0.0267	−0.0073	−0.0113	−0.0147	−0.0840

An alternative expression for the end-effect in terms of excess length of line has been given in [11]. The formula is

$$\Delta\ell = \frac{1}{k}\cot^{-1}\left[\frac{4c + 2w}{c + 2w}\cot(kc)\right] \qquad (9.13)$$

where $k = 2\pi/\lambda_g$ and $c = h(\ell n2)/\pi$.

For most practical dimensions (k_c small), one can approximate 9.13) by the following expression:

$$\Delta\ell = c\left(\frac{c + 2w}{4c + 2w}\right) \tag{9.14}$$

which is a good approximation for $\varepsilon_r = 9.8$. In order to use this expression for various dielectric constants, the following formula given in [24], may be used;

$$\frac{\Delta\ell}{h} = 0.412\,\frac{\varepsilon_r + 0.3}{\varepsilon_r - 0.258}\,\frac{w/h + 0.262}{w/h + 0.813} \tag{9.15}$$

The maximum error here is less than 5% of h for $\varepsilon_r = 1$ and 1% for other values of ε_r.

9.3 STEP DISCONTINUITY

The step in impedance, resulting from an abrupt change in the width of the upper conductor of the microstrip configuration, is shown in Fig. 9.13a and the equivalent circuit is shown in Fig. 9.13b.

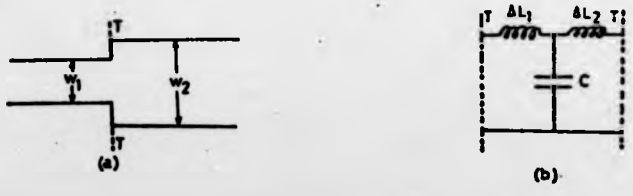

FIG. 9.13 (a) UPPER-STRIP CONFIGURATION OF AN IMPEDANCE STEP.
(b) THE EQUIVALENT CIRCUIT.

The parasitic reactancesthat are associated with this discontinuity have been considered by a number of authors [3, 4, 9, 10, 11, 16, 25]. The shunt capacitance has been calculated by the quasi-static method and is given in [3,4]; calculation of series inductances by the same method has been given in [9].

In general, these numerical techniques are difficult to incorporate into an analysis/optimization package as the numerical routine has to be called upon numerous times. Further, each method is able to evaluate only certain parameters either the shunt capacitance or series inductance of microstrip discontinuities.

The technique which the author advocates is that of modelling, which obviates the need to represent junction parasitics by an exact equivalent circuit. Initially, an approximate model is assumed, which is subsequently modified to match its predicted performance to that obtained for the circuit structure, using the on-line automatic computer-corrected S-parameters measurement system described in Chapter 4. For evaluation of the discontinuity parameters with step junctions a test fixture of the form illustrated in Fig. 9.14a has been used. The full equivalent circuit is shown in Fig. 9.14b.

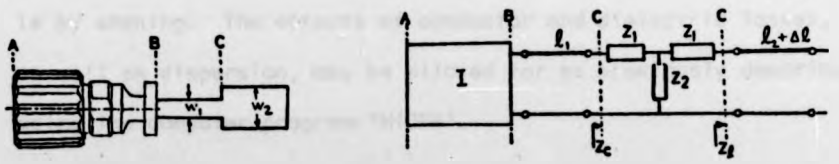

(a) THE TEST FIXTURE (b) EQUIVALENT CIRCUIT

FIG. 9.14 THE TEST FIXTURE AND FULL EQUIVALENT CIRCUIT OF THE STEP JUNCTION

The test fixture introduces its own error parameters due to the coaxial-to-microstrip adaptor, represented by the error box I. There is also an end-effect represented by the additional line length $\Delta\ell$.

A high quality APC-7 launcher was used and its error parameters evaluated as outlined in Chapter 5, data for the end-

effect correction being obtained from previous section on resonator measurements. The input impedance of the test fixture was obtained with the aid of the computer-corrected measurement facility. From the equivalent circuit of Fig. 9.14b, this impedance Z_c, at any particular frequency, is given by

$$Z_c = \frac{Z_1^2 + 2Z_1Z_2 + Z_1Z_\ell + Z_2Z_\ell}{Z_1 + Z_2 + Z_\ell} \qquad (9.16)$$

where Z_ℓ is the terminating impedance of an open-circuited micro-strip line. By incorporating into an equivalent T-network the parasitics associated with the coaxial to microstrip transition, Z_c may readily be related to the measured input impedance (see Appendix F). To obtain the values for Z_1 and Z_2, it is clearly necessary to obtain first two separate values of Z_c, corresponding to different terminating impedances. A convenient practical way of changing the terminating impedance is by etching. The effects of conductor and dielectric losses, as well as dispersion, may be allowed for as previously described, using the computer program 'MICPA'.

In normal practice, discontinuity steps are adequately small to validate neglecting the effects of any higher modes which may be generated [16,26]. Therefore Z_1 may be chosen as an inductive reactance $L\omega/2$ and Z_2 as a capacitive reactance $1/C\omega$

In order to find a function, which approximates the measured data, the following models were chosen for the junction reactances associated with step discontinuities.

$$\frac{L}{w_1} = F_1(w_1, w_2) = \sum_{m=0}^{n} c_m (w_2/w_1)^m \, \ell n(\operatorname{cosec} (\pi w_1/2w_2)) \quad nH/m \qquad (9.17a)$$

$$\frac{C}{w_1} = F_2(w_1, w_2) = \sum_{m=0}^{n} c_m (w_2/w_1)^m \, \ell n (\operatorname{cosec} (\pi w_1/2w_2)) \quad pF/m \qquad (9.17b)$$

In order to estimate the unknown coefficients, c_m, from the above models a non-linear least squares procedure was employed. The technique estimates the coefficients of the models and minimizes $\varepsilon = (e)^2$, where $e = L/w_1 - F_1$ or $e = C/w_1 - F_2$ are the residuals. The Gauss-Newton method was used to minimize ε. The technique and more details about the least-squares method are given in Appendix (E). The coefficients c_m, which have been obtained by the above method, are tabulated in 9.3, taking $\varepsilon_r = 9.8$.

Table 9.3 Coefficients c_m for the model equations 9.17a and 9.17b.

Function	Coefficients c_m				
	m=0	m=1	m=2	m=3	m=4
F_1 (L/w_1)	25.7	20.1	-1.5	0.09	0.0
F_2 (C/w_1)	95.8	-42.0	14.2	-1.5	0.06

The values of L and C in equations 9.17a and 9.17b are not very sensitive to small variations in these coefficients, so that computer word length should not be a consideration in using these formulae.

The values of calculated series inductance and shunt capacitance from the above equations are given in Table 9.4 for a variety of step width ratios. For comparison are quoted the corresponding experimental results of Easter[9] for the series inductance.

TABLE 9.4 Equivalent series inductance and shunt capacitance for various step width ratios.

W_2/h	(a) Shunt Capacitance ($F \times 10^{-14}$)	(a) Series Inductance ($H \times 10^{-11}$)	(b) Series Inductance ($H \times 10^{-11}$)	(b) Frequency (GHz)
2.0	1.2	1.3	1.4	10
3.24	2.9	3.4	3.1	7.5
4.0	4.5	5.3	6.0	6.8
5.0	6.7	7.5	8.0	6.8
6.0	9.2	9.7	9.6	6.7
7.0	12.0	12.1	-	-
8.0	15.0	14.5	-	-

(a) Results obtained from Eqn. 9.17 at 4 GHz.

(b) Experimental results reported by Easter [9].

In Figs. 9.15a and 9.15b are shown the computed results for L/w_1 and C/w_1 respectively, as functions of various ratios of w_2/h, taking $\varepsilon_r = 9.8$. The next chapter will illustrate the effect of this discontinuity in the gain of an amplifier.

9.4 RIGHT-ANGLE BENDS

For the case of a microstrip right-angle bend, two equivalent circuits have been discussed in the literature [27,28] . One equivalent circuit includes a shunt capacitance to account for charge accumulation at the corner, as well as series lengths of transmission lines on either side to account for the increase in current path length around the corner. The other is again a shunt capacitance but with a series inductance on either side of the corner. These circuits, together with the reference planes are shown in Fig. 9.16.

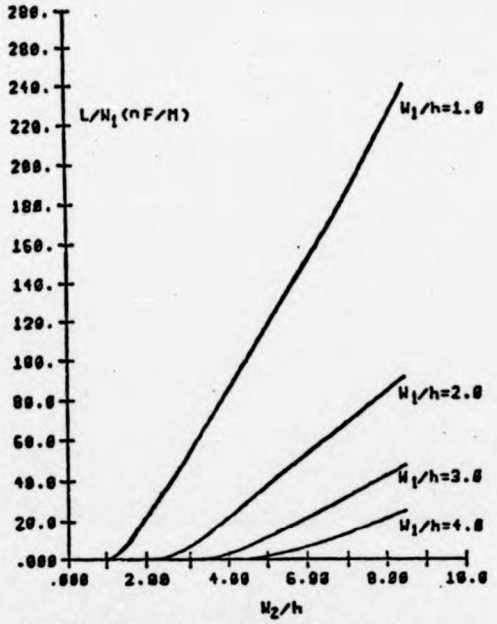

FIG. 4(a) THE NORMALIZED SERIES INDUCTANCE OF STEP DISCONTINUITY

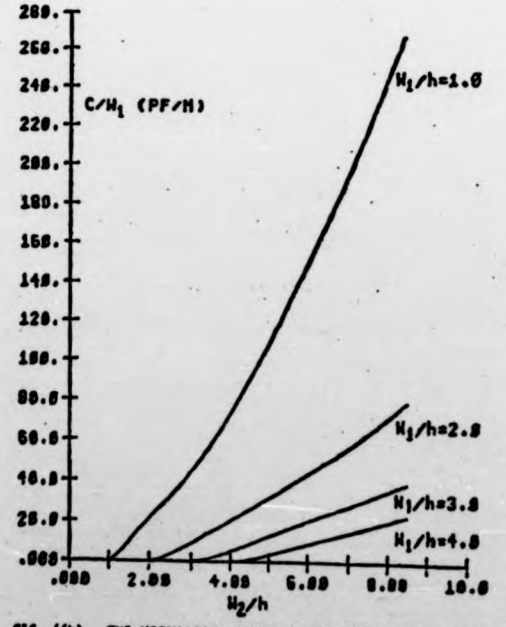

FIG. 4(b) THE NORMALIZED SHUNT CAPACITANCE OF STEP DISCONTINUITY

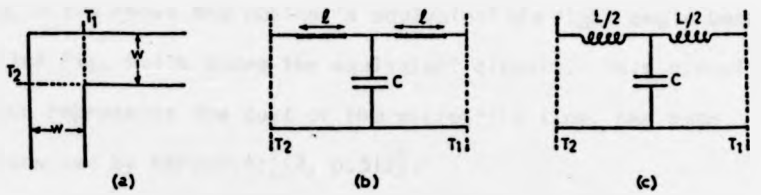

FIG. 9.16 MICROSTRIP RIGHT-ANGLE BEND, (a) PHYSICAL STRUCTURE WITH REFERENCE PLANES; (b) and (c) EQUIVALENT CIRCUITS.

The shunt capacitance has been calculated by Silver [2], and experimentally this, with the series transmission line, has been obtained by Stephenson and Easter [27], utilizing the resonant configuration method.

Let ℓ_1 and ℓ_2 be the two lengths of right-angle bend along the central axis up to terminal planes T_1' and T_2', as shown in Fig. 9.17a. Utilizing a conformal mapping technique, it easily may be seen that the total length, $\ell_1 + \ell_2$, is reduced by an amount of $0.441\, w_{eff}$ (see Appendix I). This is a good approximation for the transmission line in the model of 9.16b. In general, however, the junction parasitics of the right angle bend may be obtained using Babinet's principle.

In determining the junction parameters, by Babinet's principle, an approximate model, similar to a model previously used by Oliner [10], Altchuler and Oliner [11] is used, to calculate junction effects in symmetric strip lines. The cross section of the microstrip and its waveguide model were given in Fig. 9.7a and 9.7b. The effective line width (w_{eff}) is:

$$w_{eff}(f) = w + \frac{w_{eff}(0) - w}{1 + f/f_g} \qquad (9.18)$$

where $f_g = \frac{c_o}{2W\sqrt{\varepsilon_r}}$ and $w_{eff}(0) = \frac{h}{z_w}\sqrt{(\mu_o/\varepsilon_{eff})\cdot\varepsilon_o}$

Fig. 9.17a shows the Babinet's equivalent of a right angle bend, whilst Fig. 9.17b shows the equivalent circuit. This circuit, which represents the dual of the microstrip line, has been determined by Marcuvitz[12, p.312].

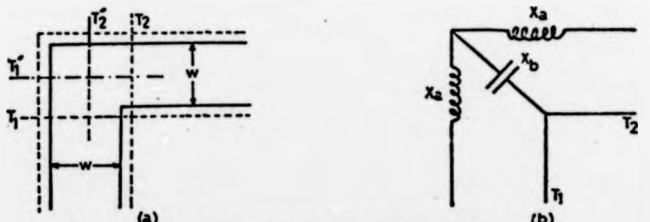

FIG. 9.17 (a) THE APPROXIMATE MODEL OF RIGHT-ANGLE BEND.
(b) THE EQUIVALENT CIRCUIT.

The results, analogous to those obtained by Altschuler and Oliner[11], for the X_a and X_b are as follows:

$$\frac{X_a}{Z_o} = \frac{2w_{eff}}{\lambda}\left(0.878 + 0.498\left(\frac{2w_{eff}}{\lambda}\right)^2\right) \qquad (9.20a)$$

$$\frac{X_b}{Z_o} = -\frac{\lambda}{2\pi w_{eff}}\left(1 - 0.114\left(\frac{2w_{eff}}{\lambda}\right)^2\right) \qquad (9.20b)$$

9.5 T-JUNCTIONS

Several sources of data were located for the equivalent circuit and parameter values. The author has already discussed the end-effect of a stub, so this section considers only the T-junction. The simplest equivalent circuit, for the T-junction, may be represented as Fig. 9.18b where the value of the capacitance has been calculated theoretically by Silvester and Benedek[2].

This capacitance with the lines lengths ℓ_1 and ℓ_2 has also been measured by Easter[21], using the resonator configuration. The impedance ratio values of n^2 were also

determined by the same technique, and pronounced frequency dependence especially at higher frequencies is seen.

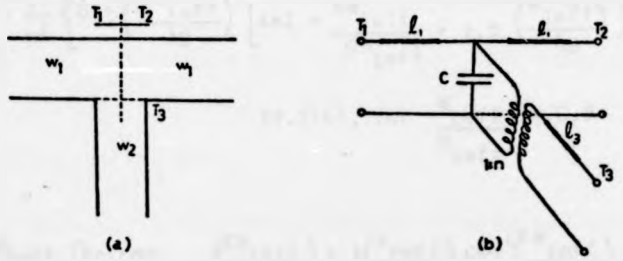

FIG. 9.18 MICROSTRIP T-JUNCTION; (a) ACTUAL STRUCTURE; (b) THE EQUIVALENT CIRCUIT

In order to incorporate the results into a CAD package, it may be useful to consider an approximate model that is similar to the right-angle bend. Fig. 9.19 shows the equivalent circuit of a symmetric T-junction which has been derived via Babinet's principle, using the results of an E-plane waveguide, derived in[11].

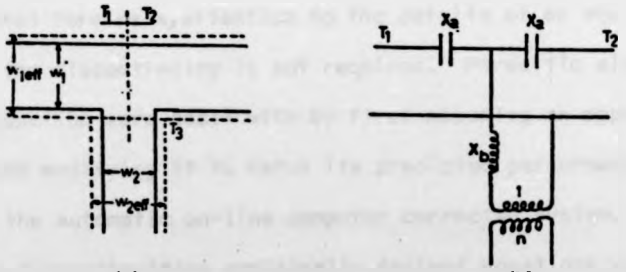

FIG. 9.19 THE EQUIVALENT CIRCUIT FOR A SYMMETRIC MICROSTRIP T-JUNCTION; (a) THE ACTUAL STRUCTURE; (b) EQUIVALENT CIRCUIT.

In this case the parameter values are obtained by the following equations

$$n = \frac{\sin(w_{2eff}/\lambda_g)}{\pi w_{1eff}/\lambda_g} \qquad (9.21a)$$

$$\frac{X_a}{Z_1} = -\frac{w_{2eff}}{\lambda_g}(n\pi/4)^2$$

$$\frac{X_b}{Z_1} = -\frac{X_a}{2Z_1} + \frac{2w_{1eff}}{n^2\lambda_g}\left[\ln\left(\frac{1.43w_{1eff}}{w_{2eff}}\right) + 2\left(\frac{w_{1eff}}{\lambda g}\right)^2\right], \text{ for } \frac{w_{2eff}}{w_{1eff}} > 0.5 \qquad (9.21b)$$

$$\frac{X_b}{Z_1} = -\frac{X_a}{2Z_1} + \frac{1}{n^2}\left\{B + \left(\frac{2W_{1eff}}{\lambda g}\right)\left[\ell n 2 + \frac{\pi W_{1eff}}{6W_{1eff}} + 1.5\left(\frac{W_{1eff}}{\lambda g}\right)^2\right]\right\}$$

(9.21c), for $\frac{W_{2eff}}{W_{1eff}} < 0.5$

where

$$B = \frac{2W_{1eff}}{\lambda g}\left[\ell n \cos\left(\frac{\pi W_{2eff}}{2W_{1eff}}\right) + \frac{1}{2}\left(\frac{W_{1eff}}{\lambda g}\right)\cos^4\left(\frac{\pi W_{2eff}}{2W_{1eff}}\right)\right]$$

9.6 CONCLUSIONS

The present computerized methods for evaluating microstrip discontinuity effects have been described. As these numerical techniques were difficult to incorporate into CAD packages, a modelling technique has been extended to discontinuities in microstrip lines. By using a network analyzer to characterize a network in terms of its properties at the external terminals, attention to the details of an equivalent circuit for the discontinuity is not required. Parasitic elements arising at a junction were dealt with by first assuming an approximate model and then modifying it to match its predicted performance to that measured by the automatic on-line computer corrected system. In the case of step discontinuities empirically derived equations were presented which are suitable for incorporation into CAD packages. For the right angle-bend and symmetric T-junction, the approximate model of the E-plane waveguide, utilizing Babinet's Principle, was used for CAD purposes. Considerable improvement in accuracy over former procedures was demonstrated, without sacrifice of simplicity.

REFERENCES

1. SILVESTER P. and BENEDEK P. "Equivalent capacitance of microstrip open circuits". IEEE Trans. Microwave theory and Tech. , Vol. MTT-20 Nov. (1972) pp.511-516.

2. ——— ," Microstrip Discontinuity Capacitance for Right-Angle Bends, T Junction, and crossing", ibid, Vol. MTT-21 May (1973) pp.341-346.

3. BENEDEK P. and SILVESTER, P. "Equivalent capacitances of microstrip gaps and steps", ibid Vol. MTT-20 Nov. (1972) pp.729-733.

4. FARRAR, A. and ADAMS, A.T. "Computation of lumped microstrip capacitance by matrix method. Rectangular sections and end effect" ibid (corresp.) Vol. MTT-19 May (1971) pp.495-497.

5. ——— ," Matrix method for microstrip three-dimensional problems" ibid, Vol. MTT-20, Aug. (1972) pp.497-504.

6. JAMES, D.S. and TSE,S.H. "Microstrip end effects". Electron Lett, Vol. 8, Jan. (1972), pp.46-47.

7. GOPINATH, A. and EASTER, B. "Moment method of calculating discontinuity inductance of microstrip right-angle bends", IEEE Tran. Microwave Theory Tech. (Short papers) Vol. MTT-22, Oct. (1974), pp.880-883.

8. THOMPSON, A.F. and GOPINATH, A. "Calculation of microstrip discontinuity inductance" ibid Vol. MTT-23, Aug.(1975) pp.648-655.

9. GOPINATH, A., THOMSON, A.F. and STEPHENSON, I.M. "Equivalent circuit parameters of microstrip step change in width and cross junctions" ibid (short papers) Vol. MTT-24 March (1976) pp.142-144.

10. OLINER, A.A. "Equivalent circuits for discontinuities in balanced strip transmission line", IRE Trans. Vol. MTT-3 (1955) pp.134-143.

11. ALTSCHULER, H.M. and OLINER, A.A. "Discontinuities in the centre conductor of symmetric strip transmission line" ibid, Vol. MTT-8 May (1960) pp.328-338.

12. MARCUVITZ, N. "Waveguide handbook" MIT Radiation Laboratory Series 1950.

13. WHEELER, H.A. "Transmission-line properties of parallel wide strips separated by a dielectric sheet", IEEE Trans. Microwave Theory Tech. Vol. MTT-13 March (1965) pp.172-185.

14. ——— ,"Transmission-line properties of parallel wide strips by a conformal mapping approximation" ibid, Vol. MTT-12 May (1964) pp.280-289.

15. KOMPA, G. "Planar waveguide model for calculating microstrip components", Electron. Lett. Vol. 11, Sept. (1975) pp.459-460.

16. MENZEL, W. and WOLFE, I. "A method for calculating the frequency-dependent properties of microstrip discontinuities", Vol. MTT-25 No. 2 Feb. (1977) pp.107-112.

17. KÜHN, E. "A mode-matching method for solving field problem in waveguide and resonator circuits", Arch. Elek. Übertrangung, Vol. 27, Dec. (1973) pp.511-513.

18. LEWIN, L. "On the inadequacy of discrete mode-matching techniques in some waveguide discontinuity problems", IEEE Trans. Microwave theory Tech. Vol. MTT-18, July (1970) pp.364-372.

19. RICHINGS, J.G. "An accurate experimental method for determining the important properties of microstrip transmission lines", The Marconi Review Vol. 37 (1974) pp.209-216.

20. EASTER, B., RICHINGS, J.G. and STEPHENSON, I.M. "Resonant techniques for the accurate measurement of microstrip properties and equivalent circuits" in Proc. 1973 European Microwave Conf. (Brussels, Belgium), paper B.7.5.

21. EASTER B. "The equivalent circuit of some microstrip discontinuities", IEEE Trans. Microwave Theory Tech. Vol. MTT-23, Aug (1975) pp. 655-660.

22. ITOH, T., MITTRA, R. and WARD, R.D. "A Method for computing edge capacitance of finite and semi-infinite microstrip lines" Idid (short papers), Vol. MTT-20 pp.847-849.

23. TROUGHTON, P. "Design of complex microstrip circuits by measurement and computer modelling", Proc. IEE, Vol. 118, March/April (1971) pp.469-474.

24. Hammerstad, E.O. "Equation for microstrip circuit design" in Proc. 1975 European Microwave Conf. (Hamburg, Germany) pp.268-271.

25. NALBANDIAN, V. and STEENAART, W. "Discontinuities in symmetric striplines due to impedance steps and their compensations", IEEE Trans. Microwave Theory Tech. Vol. MTT-20, Sept. (1972) pp.573-578.

26. KOMPA, G., "Excitation and propagation on higher order modes in microstrip discontinuities" in Proc. 1973 European Microwave Conf. (Brussel, Belgium) Paper B.7.6.

27. STEPHENSON I.M. and EASTER B. "Resonant Techniques for establishing the equivalent circuits of small discontinuities in microstrip", Electron. Lett. Vol. 7, 23rd Sept. (1971) pp.582-584.

28. NAPOLI, L.S. and HUGHES, J.J. "Foreshortening of microstrip open circuits on alumina substrates", IEEE Trans. Microwave Theory Tech. (Corresp.) Vol. MTT-19 June (1971) pp. 559-561.

29. KOBER, H. "Dictionary of conformal representations" Dover Publication, Inc. (1957).

10

COMPUTER PROGRAMS AND CONCLUSIONS

In the past few years several analysis programs have been adopted for microstrip circuits, assuming that the normal mode of operation for the microstrip line may be adequately described in terms of a TEM mode[1-14]. This approach works well up to S-band, but at higher frequencies spurious propagating modes introduce dispersive effects which make the simple TEM model unacceptable. Discontinuity effects are another problem which makes the analysis of microwave integrated circuits difficult. Some of these analysis programs are linked to optimization routines making use of direct search techniques [5-11]. The latter are in general based on 'sequential' or 'linear search algorithms', in which previously generated points are used to determine the new direction of search. Although extremely efficient in determining the minima of unimodal functions, in the case of multivariable, multimodal problems as encountered in amplifier

optimization, a sequential search program will converge to the nearest local minimum, ignoring neighbouring minima which may be superior.

By using two different strategies of optimization we may increase the accuracy of approach to the true minimum. One may also aim to reduce the execution time, particularly when the starting points are near to the position of the optimum, or have poor starting values[19].

Currently two programs have been developed by the author and his colleagues[14-15]. One uses the two-port chain matrix method in the analysis subroutine for handling the microstrip circuits and the other utilizes the nodal analysis algorithm, as described in Chapter 3 Section 3, dealing mainly with the modelling of devices.

The first program, which is called 'OPTIMAL', has several novel features, as follows:

(a) The analysis routine incorporates an algorithm for dispersion effects, conductor and dielectric losses in the microstrip.

(b) The analysis routine also takes into account the junction parasitics for various discontinuities, as described in Chapter 9, as well as radiation loss due to open terminations.

(c) The optimization routine makes use of a large-step pseudo-random search technique in order to increase the chances of finding a global minimum.

(d) If a promising valley is located, the program switches to an efficient conjugate gradient technique in order to converge quickly to the minimum.

As 'OPTIMAL' is designed mainly to deal with active two-port devices, this Chapter concludes by showing the results for the design optimization of various amplifiers using GaAs F.E.T.'s and silicon bipolar transistors.

10.1 PROGRAM DESCRIPTION.

The program 'OPTIMAL' is written in Fortran IV with a length of nearly 800 Fortran statements. OPTIMAL is loaded on the XDS-Sigma 5 computer by using overlay. The program requires less than 13000 words of core storage and uses single precision variables.

The various responses which may be optimized by 'OPTIMAL' are: (a) transducer gain, (b) input VSWR, (c) output VSWR, (d) a weighted combination of all three. The least pth objective function formulation was selected as follows:

$$\epsilon = \frac{1}{P} \sum_f (W_1 |\rho_{in}|^P + W_2 |\rho_{out}|^P + W_3 |G_t - G_d|^P) \qquad (10.1)$$

where

f is the set of frequencies.

W_1, W_2, W_3 are weighting factors, ≥ 0.

ρ_{in}, ρ_{out} are the input and output reflection coefficients.

G_t is the network transducer gain.

G_d is the desired transducer gain.

P is a positive, nonzero integer value, which is even.

The various network configurations which may be cascaded are eight basic types of circuit elements, each type being classified by a number, as indicated in Fig. 10.1.

Normally, all of the circuit elements which are represented by

Element Type	Description	Symbol	Parameters (Units)
1	General		S_{11} S_{12} S_{21} S_{22}
2	Transmission Line	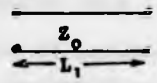	Z_o (ohms) L_1 (mm)
3	Short circuit Shunt Stub	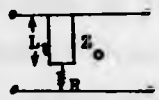	R, Z_o (ohms) L_1 (mm)
4	Series Parallel L, C, R		L (nH) C (pF) R (ohms)
5	Series Series L, C, R	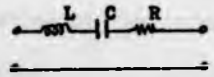	L (nH) C (pF) R (ohms)
6	Shunt Parallel L, C, R	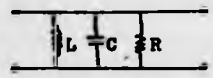	L (nH) C (pF) R (ohms)
7	Shunt Series L, C, R	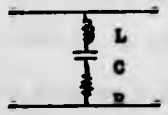	L (nH) C (pF) R (ohms)
8	Shunt L-section of transmission line	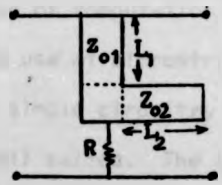	Z_{o1}, Z_{o2} (ohms) L_1, L_2 (mm) R (ohms)

FIG. 10.1 THE EIGHT ELEMENT TYPES

S-parameters are optimized, except transistors. If desired, however, certain elements may be frozen at their initial values, a negative initial value for any parameter value indicating that this parameter is to be varied during optimization. Thus - lower and upper bound for each varied element shoud be punched subsequently on the same card.

To avoid using excessive computer core storage, it was necessary to place upper limits on the number of network elements and frequencies that 'OPTIMAL' could handle. The number of frequency points must not exceed 20 and the maximum number of circuit elements was chosen to be 60. However, it is a simple matter to increase these limits by altering the appropriate 'DIMENSION' statements, as required.

A simplified flow chart of 'OPTIMAL' is shown in Fig. 10.2. It depicts the general organization of the program without detailing the role of individual subroutines.

10.2 ANALYSIS

In the course of development for any computer program, two conflicting requirements emerge - one is to perform the analysis as quickly as possible, by making the program highly specific, the other being to relate the method of computation to the general usage capability of the program. The use of microstrip for microwave amplifiers implies essentially simple circuitry for which the S-parameters [S] approach is well suited. The inability to use S-parameters in chain matrices is the result of the decision to take reflected waves as dependent variables and incident waves as independent. Rearranging the relationship between these waves, we

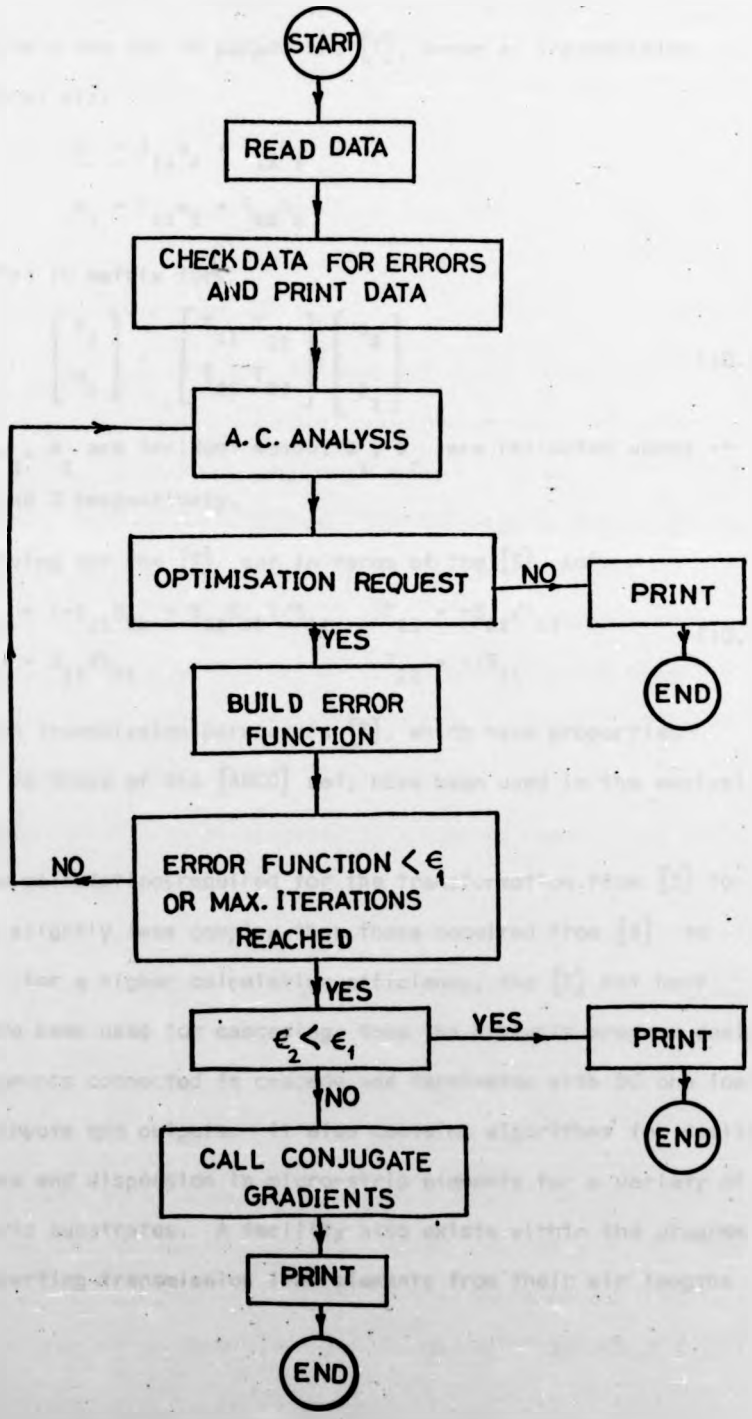

FIG.10-2. FLOW DIAGRAM OF 'OPTIMAL' PROGRAM

may define a new set of parameters $[T]$, known as transmission parameters, viz:

$$b_1 = T_{11}a_2 + T_{12}b_2$$

$$a_1 = T_{21}a_2 + T_{22}b_2$$

or written in matrix form

$$\begin{bmatrix} b_1 \\ a_1 \end{bmatrix} = \begin{bmatrix} T_{11} & T_{12} \\ T_{21} & T_{22} \end{bmatrix} \begin{bmatrix} a_2 \\ b_2 \end{bmatrix} \qquad (10.2)$$

where a_1, a_2 are incident waves, b_1, b_2 are reflected waves at port 1 and 2 respectively.

Solving for the $[T]$ set in terms of the $[S]$ set:

$$T_{11} = (-S_{11}S_{22} + S_{12}S_{21})/S_{21} \qquad T_{21} = -S_{22}/S_{21}$$
$$T_{12} = S_{11}/S_{21} \qquad T_{22} = 1/S_{21} \qquad (10.3)$$

Therefore transmission parameters $[T]$, which have properties similar to those of the $[ABCD]$ set, have been used in the analysis routine.

The calculations required for the transformation from $[S]$ to $[T]$ are slightly less complex than those required from $[S]$ to $[ABCD]$. For a higher calculation efficiency, the $[T]$ set have therefore been used for cascading; thus the analysis program deals with elements connected in cascade and terminated with 50 ohm loads at the inputs and outputs. It also contains algorithms for dealing with loss and dispersion in micro-strip elements for a variety of dielectric substrates. A facility also exists within the program for converting transmission line elements from their air lengths

and characteristic impedances to dimensions compatible with microstrip substrates.

10.3 OPTIMIZATION.

This section of the program has two parts: the large step pseudo-random search algorithm, and a conjugate gradient search, to locate the final minimum.

10.3.1 LARGE STEP-METHOD. The non-unilateral properties of the GaAs FET and bipolar transistor in microwave amplifier circuits means that no element is entirely isolated from any other in its effects on the overall response. For this reason the author has used an approach similar to Emery and O'Hagan's 'spider method'[9] in which the variables are selected in a pseudo-random sequence. This reduces the possibility of the optimum-following algorithm concentrating on certain variables to the exclusion of others, thereby causing false minima to be obtained.

The variable to be examined is chosen by means of an algorithm in which a random number is obtained by multiplying the error between computed and specified circuit performance by 10^6 and selecting the last two integers. Since the chances that the error will be identical for any two values of variable are extremely remote, this simple technique guarantees a number sufficiently random for the purposes of the program.

Oncethe first element is chosen, a combination of successive error multiplication by 10^6 and modular arithmetic will ensure that each of the remaining variables will be examined once in as random a manner as possible. Initially,element values are varied

by 4% for distributed elements and 8% for discrete elements, although this step size is automatically varied within the program, depending on the success rate in minimising the objective function. A flow chart of the procedure is shown in Fig. 10.3 without detailing the role of individual subroutines.

The criterion for the initial step size is as follows: It is desirable to choose a large step size, since this decreases the execution time for poor starting points. Fig. 10.4, relating to the gain of an amplifier, shows the final error function versus step size. It can be seen that when the step size is too large the routine has converged to a local minimum and has ignored the neighbours which were superior. Of course, it is not practical to choose a step size smaller than the limiting value to which the network could be adjusted. The criterion stated above is a reasonable compromise between too large or too small intervals.

10.3.2 CONJUGATE GRADIENT METHOD. Having located a promising valley, by the pseudo-random search technique, the program switches to the conjugate gradient method, [16] and the objective function is then minimized. With the conjugate gradient technique each new direction of search is calculated as part of the iteration cycle.

The method of steepest descent [17] uses the direction of the negative gradient, and the method of alternating direction [18] uses cyclically the direction of the n coordinate axes. Methods which calculate each new direction of search as part of the iteration cycle are inherently more powerful than those in which the directions are assigned in advance, in that any accumulated knowledge

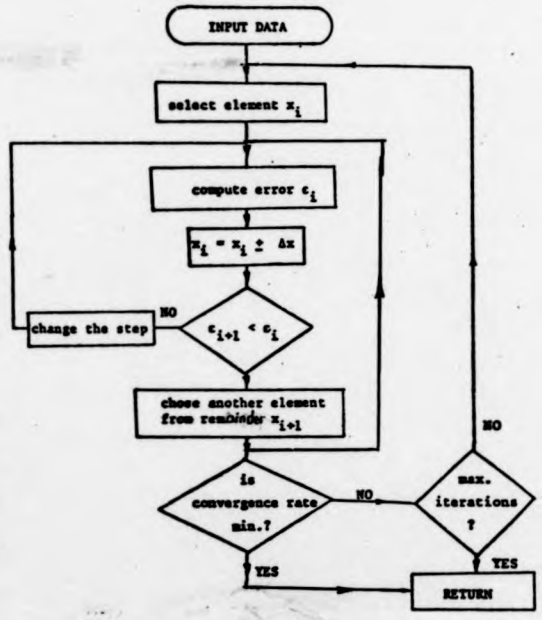

FIG. 10.3 THE FLOW CHART OF THE LARGE-STEP DIRECT SEARCH METHOD.

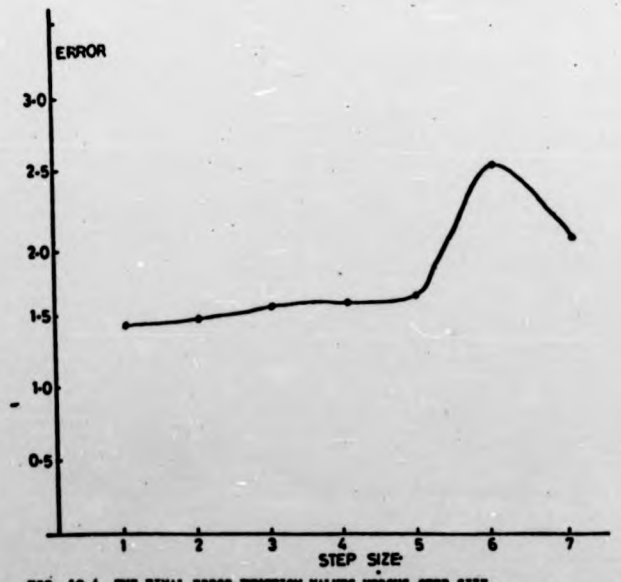

FIG. 10.4 THE FINAL ERROR FUNCTION VALUES VERSUS STEP SIZE.

of the local behaviour of the function can be taken into account.

In particular, if we assume the error function of n variables, whose value $\varepsilon(\tilde{x})$ and gradient vector $g(\tilde{x})$ can be calculated at any point $\tilde{x}$, the directions $\tilde{P}_0$, $\tilde{P}_1$... are generated, such that $\tilde{P}_{i+1}$ is a linear combination of $-g(\tilde{x})_{i+1}$ and $\tilde{P}_0$, $\tilde{P}_i$,...$\tilde{P}_1$, such that the G-orthogonality conditions, as described in Appendix A are satisfied.

A linear search is used to minimize the error function along the $\tilde{P}$ direction. The point at which the one-dimensional minimum occurs becomes the new base point and the previous network parameter values are updated to the new base point values. Since a new base point is defined at the end of each iteration, the new direction is also defined and the above procedure can be repeated indefinitely, until the optimum value of ε is located. In any practical application the time spent evaluating the function and gradient at the various points required may well dominate the time for the whole minimization process. It is therefore desirable to limit the number of such evaluation procedures as much as possible. Thus an upper limit to the number of iterations is specified to avoid wasting computer time. This number is represented by LIMIT and is read as part of the input data. Execution is also terminated when a given iteration reduces the objective function insignificantly. Finally, the method leads to the following general minimization algorithm:

$\tilde{x}_o$ = arbitrary

g_o = $g(\tilde{x}_o)$, $\tilde{P}_o = -g_o$

$\tilde{x}_{i+1}$ = position of minimum of $\varepsilon(\tilde{x})$ on the line through $\tilde{x}_i$ in the direction $\tilde{P}_i$.

g_{i+1} = $g(\tilde{x}_{i+1})$

β_i = g_{i+1}^2/g_i^2

$\tilde{P}_{i+1}$ = $g_{i+1} + \beta_i \tilde{P}_i$

This process is guaranteed (apart from rounding errors) to locate the minimum of any quadratic function of n arguments in n iterations at most. The functions used are not normally quadratic, so the process is iterative rather than n-step and a test for convergence is required. This test value is represented by EST as a part of data.

In applying this algorithm to a general error function, four main points require attention. These are the choice of $\tilde{x}_o$ or starting values, the linear search to locate each $\tilde{x}_{i+1}$ as described before, the overall rate of convergence, and the final convergence criterion.

10.4 'OPTIMAL' APPLICATION TO AMPLIFIER DESIGN.

This section illustrates the method of design for some optimized amplifiers and the effects of varying their parameters. Three different circuits of varying complexity were programmed for optimization. The first amplifier circuit is shown in Fig. 10.5. The listing of output results for initial values is given in Fig. 10.6a, whilst Fig. 10.6b shows the optimized output results given by the large-step routine. This was improved

by the final optimization routine, i.e. conjugate gradient, to give a better response over the desired bandwidth and the final optimized results are given in Fig. 10.6c.

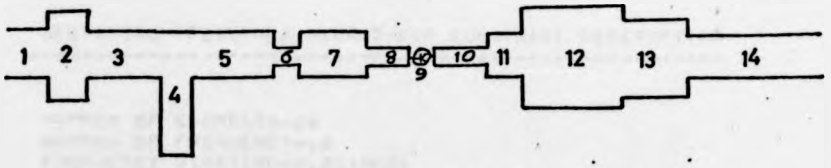

FIG. 10.5 X-BAND GaAS F.E.T. AMPLIFIER CIRCUIT

The aim was to achieve a flat 7dB power gain and 2:1 VSWR at both input and output over a frequency range of 8-11.6GHZ. The transistors incorporated were early Plessey GaAs F.E.T.'s. In Table 10.1 the initial parameter values together with the final values of the elements are shown.

TABLE 10.1

The (-) sign means this element varies during optimization.

Element	Initial values (Length mm)	(Impedance Ohms)	Final values (Length mm)	(Impedance Ohms)
1	3.85	50.0	3.85	50.0
2	-4.40	-16.0	2.00	16.9
3	-5.40	50.0	5.03	50.0
4	-4.17	-43.0	3.07	42.8
5	-5.13	50.0	4.85	50.0
6	1.96	95.0	1.96	95.0
7	-5.27	-30.0	3.10	30.1
8	-2.52	95.0	4.25	95.0
9 (TRANSISTOR)	-	-	-	-
10	-1.22	-95.0	3.99	95.0
11	-4.93	43.0	4.12	43.0
12	-2.88	-19.0	3.61	18.6
13	-8.60	-30.0	9.78	29.6
14	13.60	50.0	13.60	50.0

FREQUENCY RESPONSE
****

FREQ	GAIN	VSWR1	VSWR2	K
8.200	8.719	2.845	2.485	.745
8.400	8.661	2.668	2.535	.796
8.600	8.726	2.832	3.729	.668
8.800	7.908	2.569	3.289	.833
9.000	6.570	2.272	3.456	1.205
9.200	5.493	2.218	2.700	1.524
9.400	5.663	2.463	3.137	1.401
9.600	5.352	2.327	3.672	1.400
9.800	5.638	2.350	3.120	1.432
10.000	6.219	2.556	3.130	1.166
10.200	6.474	2.356	2.878	1.105
10.400	5.991	2.040	2.250	1.376
10.600	5.788	2.021	2.074	1.472
10.800	6.419	1.924	2.297	1.286
11.000	6.593	2.214	2.473	1.147
11.200	5.953	2.418	2.215	1.302
11.400	5.536	2.418	3.670	1.131
11.600	5.399	2.725	2.633	1.250

FIG. 10.6b THE OPTIMIZED RESULTS OF THE X-BAND AMPLIFIER BY LARGE-STEP ROUTINE.

FREQUENCY RESPONSE
****

FREQ	GAIN	VSWR1	VSWR2	K
8.200	7.214	2.358	4.304	.745
8.400	7.447	2.082	4.115	.796
8.600	7.946	1.911	4.985	.668
8.800	7.459	1.667	4.279	.833
9.000	7.092	1.482	3.070	1.205
9.200	5.973	1.504	2.447	1.524
9.400	6.102	1.671	3.073	1.401
9.600	6.234	1.666	2.973	1.400
9.800	6.350	1.718	2.641	1.432
10.000	6.730	1.777	3.142	1.166
10.200	6.987	1.616	3.004	1.105
10.400	6.672	1.499	2.072	1.376
10.600	6.521	1.608	1.787	1.472
10.800	7.208	1.706	1.903	1.286
11.000	7.551	2.100	1.977	1.147
11.200	6.996	2.316	1.446	1.302
11.400	7.594	2.342	1.476	1.131
11.600	6.795	2.791	1.530	1.250

FIG. 10.6c THE FINAL OPTIMIZED RESULTS OF THE X-BAND AMPLIFIER.

Fig. 10.6d shows the frequency response for both the initial and the final designs. The initial circuit performance gave 1.2 dB gain at 8GHz, going up to 5.8 dB at 8.8 GHz and falling to -6 dB at 11.6 GHz. This was improved by the optimization program to give a gain of 7dB ± 0.5 dB and a VSWR better than 2:1 over the desired bandwidth. The total time taken to run the submitted example was approximately 15 minutes on the Sigma5 computer.

Experimental results obtained by using the microstrip line dimensions from the optimized circuit are also included in Fig. 10.6d. Although the experimental results follow the predicted gain response shape, there are significant differences between the two curves. These have been traced to dispersion effects, losses and junction parasitics, for which no corrections have been made. Fig. 10.6e shows again the optimized power gain with and without taking into account the above parameters. The results indicated by the solid line are obtained when conductor and dielectric losses as well as dispersion effects are included. The dotted line results are obtained when, in addition to these parameters, junction parasitic effects are taken into account. It is to be noted from Fig. 10.6e that these are of much smaller importance here than losses and dispersion in the microstrip.

If the input and output matching networks consist of only a few sections, then the junction introduces mismatching as illustrated in [20], which tends to enhance the effects of the parasitic reactances. Here, however, a multi-section microstrip arrangement was used, mainly for reducing the VSWR of the amplifier.

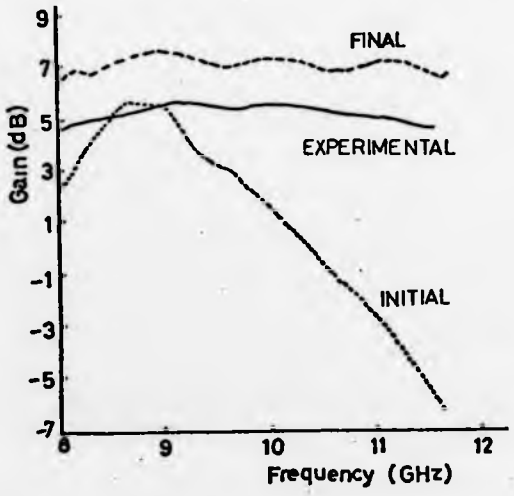

FIG. 10.6d. FREQUENCY RESPONSE OF BOTH INITIAL AND FINAL DESIGN.

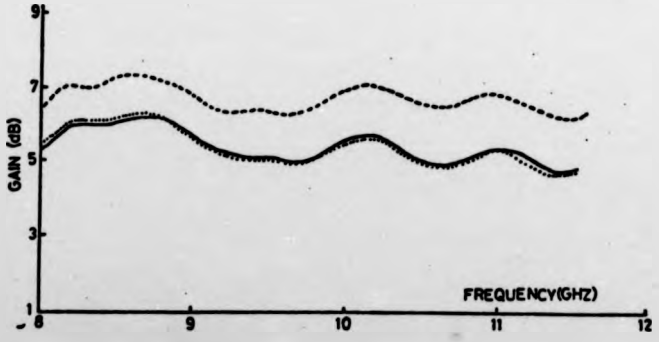

FIG. 10.6e. FREQUENCY RESPONSE OF X-BAND AMPLIFIER
———— NO CORRECTION
———— CORRECTION FOR DISPERSION EFFECTS AND LOSSES
..... CORRECTION FOR DISPERSION, LOSSES AND JUNCTION PARASITIC EFFECTS.

The second example is that of a three stage amplifier utilizing bipolar transistors. The amplifier circuit is shown in Fig. 10.7a and the results are summarised in Fig. 10.7b for the frequency range 2.5 -3.5 GHz. The results for optimized power gain are shown as a dashed line in Fig. 10.7c for the case when no correction for microstrip parameters and junction reactances has been included in the analysis of the amplifier. The results indicated by the solid line are obtained when the above parameters are taken into account. It is to be noted from Fig. 10.7c that the power gain has been reduced by almost 1 dB. The junction reactances have virtually no effect on the power gain, but result in slightly increased input and output VSWR.

The third example is that of a simple narrow band amplifier utilizing Plessey GaAs F.E.T.'s. The circuit diagram is indicated in Fig. 10.8a, which shows that there are here only two stubs. The dotted and solid lines in Fig. 10.b are computed for initial and final optimized power gain, respectively. In Fig. 10.8a the final parameter values for the microstrip lines on alumina substrate are shown. The objective of this example was to examine the effect on microstrip parameters using different substrate material. (The previous examples used alumina substrate, for which $\varepsilon_r = 9.8$). Fig. 10.8c shows the results for both alumina and 'polyguide' substrates. In the case of 'polyguide', the power gain of the amplifier is higher than with alumina.

10.5 COMPUTER ANALYSIS OF TRANSISTOR MODELLING.

In a vast number of network problems, such as the equivalent circuit of a transistor, the relationship between electrical

FIG. 10.7a. A THREE STAGE AMPLIFIER CIRCUIT

Initial Circuit Performance			After 1 Cycle			After 2 cycles			After 3 cycles			Frequency
Gain dB	VSWR In	Out	Gain dB	VSWR In	Out	Gain dB	VSWR In	Out	Gain dB	VSWR In	Out	GHz
17.7	1.7	1.5	19.1	1.5	1.5	18.9	1.6	1.5	18.9	1.62	1.5	2.5
18.0	1.4	1.4	19.4	1.2	1.5	19.2	1.2	1.5	19.2	1.3	1.5	2.7
18.7	1.0	1.4	20.1	1.1	1.4	20.0	1.1	1.4	20.0	1.0	1.4	2.9
19.1	1.2	1.3	20.5	1.4	1.3	20.4	1.3	1.3	20.4	1.3	1.3	3.1
19.4	1.4	1.3	20.8	1.6	1.2	20.7	1.5	1.2	20.7	1.5	1.2	3.3
19.1	1.6	1.1	20.4	2.0	1.1	20.3	1.9	1.1	20.4	1.8	1.1	3.5
Specified Performance: 2.7-3.3 GHz. Gain 20 dB ± 0.5 dB. VSWR 1.5:1												

FIG. 10.7b. PERFORMANCE OF 'OPTIMAL' ON S-BAND AMPLIFIER.

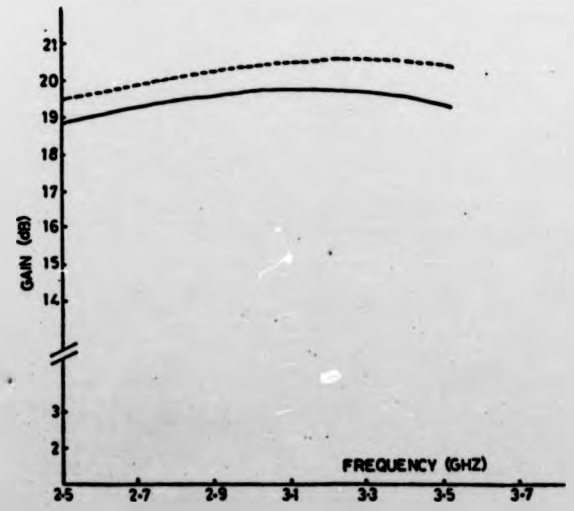

FIG. 10.7a. FREQUENCY RESPONSE OF S-BAND AMPLIFIER
---------- NO CORRECTION.
———————— CORRECTION FOR DISPERSION EFFECTS AND LOSSES.

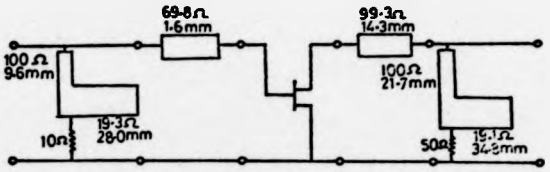

FIG. 10.8a. A S. BAND AMPLIFIER CIRCUIT.

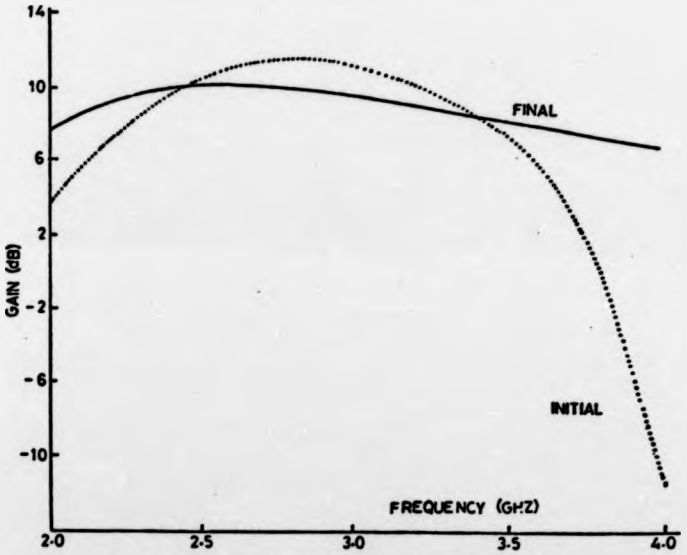

FIG. 10.8b. FREQUENCY RESPONSE OF BOTH INITIAL AND FINAL DESIGN.

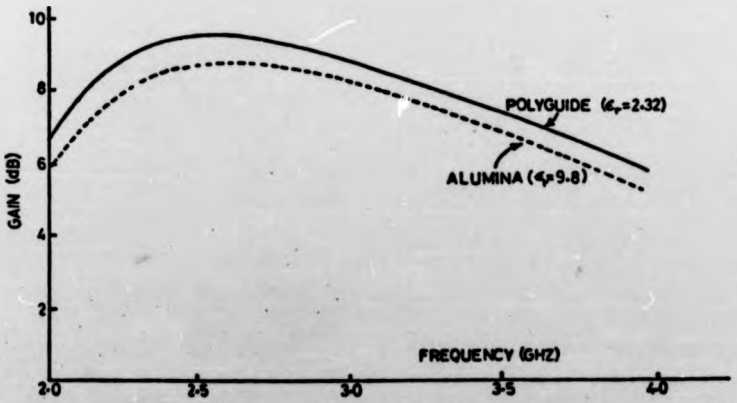

FIG. 10.8c. FREQUENCY RESPONSE OF S-BAND AMPLIFIER USING POLYGUIDE AND ALUMINA AS SUBSTRATE MATERIAL.

properties at the output and input ports is of predominant interest. It is therefore desirable to compute the two-port parameters of such a network, in order to present a model for active as well as passive devices. The author has already described such an algorithm, Chapter 3 Section 3.1.2, which halves the number of iterations compared to a conventional nodal analysis routine. This Section describes a computer program developed by the author and based on this algorithm.

10.5.1 DESCRIPTION OF THE PROGRAM

The program is written in Fortran IV, with a length of nearly 1200 Fortran statements. The program is loaded on to the Sigma 5 computer by using overlay. It requires about 14000 words of core storage and uses single precision variables. It can handle 50 nodes, 170 parameter values of the following kind of components, resistors, capacitors, inductors and controlled current sources. The above elements are keyed in the program as R, C, L, and GM respectively.

One of the most powerful features of the program is the free format form of specification. The free-format input is the same as that used in the "CADMIC" computer program[12]. The first card of the data deck is the title card and the last one is an end card. The cards between them can be arbitrarily ordered. Table 10.3 illustrates how easily circuit data can be supplied. Columns 1-4 must contain an element name of up to four characters; "A" stands for any alphanumeric character. Thus elements can be described with a meaningful name, e.g., RG, CDS. The numbers of the

nodes between which the element is connected are NI and N2, NG being the controlling node for the voltage-controlled current source. Node numbers must be integers and all data fields must be separated by one or more blanks.

TABLE 10.3 INPUT DATA INFORMATION.

RAAA	NI	N2	VALUE	
CAAA	NI	N2	VALUE	
LAAA	NI	N2	VALUE	
GMAA	NI	N2	NG	VALUE
SPA	NIN^-	$N2N^+$	NIO^+	NIO^-
ZPA	NIN^-	$N2N^+$	NIO^+	NIO^-
YPA	NIN^-	$N2N^+$	NIO^+	NIO^-
FRE	F(1)	F(2)	.....F(N-3)	
+ F(N-2)	f(N-1)	F(N)		
END				

The output specification cards are designated SPA, ZPA, YPA for S-parameters, Z-parameters and Y-parameters, respectively. NIN^- and NIN^+ are the nodes associated with the input port, NIO^+ and NIO^- are the nodes associated with the output port. The negative sign stands for the ground and positive sign indicates the non-ground node. The frequency card is FRE, for which values of frequencies must be specified. Continuation cards, specified by the symbol + in Column 1, can be used if necessary. Engineering abbreviations to describe noninteger values in this program are shown in Table 10.4.

TABLE 10.4 ABBREVIATION ALLOWED FOR INPUT OF DATA VALUES.

Symbols	P	N	U	M	K	ME	G
Values	1E-12	1E-09	1E-06	1E-03	1E+03	1E+06	1E+09

10.5.2 EXAMPLE

As an example, the equivalent circuit of a F.E.T. is shown in Fig. 10.9a. The listing of the input data in Fig. 10.9b shows how convenient it is to use the program. The output results are given in Fig. 10.9c in the form of S-parameters over a frequency range of 2-4GHZ, using complex format. The total time taken to run the submitted example is about 60 seconds.

10.6 THESIS CONCLUSIONS.

In problems where the synthesis procedures of classical circuit theory are inapplicable, optimization techniques may often provide a solution. These are generally iterative in nature, the network being analyzed repeatedly, performance being compared with the specification and the parameters adjusted systematically until success is achieved.

In the past few years several general-purpose microwave a.c. analysis/optimization programs have been developed. Most of these make use of a direct search method to optimize the error function. This method is essentially a sequential one, in which the next points are determined by the previously generated points, through the function values and/or gradient vectors. Although sequential methods may be used, they are efficient only in unimodal problems.

Mathematical functions which describe microwave circuit behaviour are in general non-linear and are complex, often with many local minima. Incorporation of these into sequential search methods leads to convergence to the nearest local minimum, ignoring

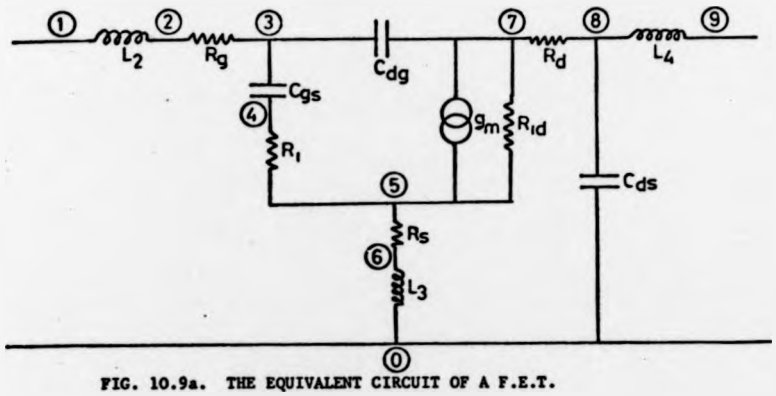

FIG. 10.9a. THE EQUIVALENT CIRCUIT OF A F.E.T.

```
EQUIVALENT CIRCUIT OF F.E. TRANSISTOR
 L2  1 2 0.5N
 RG  2 3 3.6
 CGS 3 4 0.6P
 RI  4 5 1.76
 RS  5 6 1.4
 L3  6 0 0.7N
 GM  7 5 3 0.02
 CDG 3 7 0.1P
 RID 7 5 0.5K
 RD  7 8 1.4
 CDS 8 0 0.1P
 L4  8 9 0.5N
 SPA 0 1 9 0
 FRE 3.0G 2.0G 2.2G 2.4G 2.6G 2.8G 3.0G 3.2G 3.4G 3.6G
+3.8G 4.0G
 END
```

FIG. 10.9b. THE LISTING OF INPUT DATA.

S-PARAMETER

FREQUENCY	S_{11}		S_{12}		S_{21}		S_{22}	
.20E 10	.443	-.687	.050	.090	-1.050	1.244	.735	-.253
.22E 10	.378	-.702	.058	.095	-.931	1.304	.720	-.272
.24E 10	.293	-.707	.066	.098	-.811	1.351	.703	-.290
.26E 10	.211	-.702	.073	.101	-.690	1.385	.687	-.307
.28E 10	.132	-.687	.081	.103	-.572	1.407	.670	-.322
.30E 10	.057	-.664	.088	.104	-.457	1.418	.653	-.337
.32E 10	-.012	-.634	.094	.105	-.345	1.418	.636	-.350
.34E 10	-.076	-.598	.101	.105	-.239	1.409	.618	-.362
.36E 10	-.134	-.556	.106	.105	-.138	1.392	.601	-.374
.38E 10	-.186	-.510	.112	.105	-.044	1.367	.584	-.385
.40E 10	-.231	-.461	.117	.104	.045	1.337	.567	-.395

FIG. 10.9c. THE COMPUTED S-PARAMETERS FOR THE EQUIVALENT CIRCUIT OF THE F.E.T.

neighbours which may be superior.

As cost is also a very important consideration in the selection of an optimization algorithm for use in an industrial application, various modifications have been made to speed up the direct search methods by varying the step size in the success or failure program. The algorithms still have a tendency to slow down, particularly when the starting point is too far from the optimum or very close to it.

The author has first described how, by combining two or three different strategies of optimization, some of the problems may be overcome, particularly the accuracy of approach to the true minimum. It is also desirable to reduce the execution time, especially when the starting point is near to the position of the minimum, or with poor starting values.

The non-unilateral properties of transistors in microwave amplifier circuits means that the elements all interact in some degree with each other in determining the overall response. With these effects in mind, the author has adopted the pseudo-random sequence technique for chosen variables. This reduces the possibility of the optimum-following algorithm concentrating on certain variables to the exclusion of others, and thereby yielding false minima. The optimization strategies are a combination of "large step direct search" with "conjugate gradient pattern search" techniques. To improve the chance of finding a global minimum solution to multi-modal problems (as encountered in amplifier optimization), a limited number of random searches are also employed.

While the use of a good analysis program is essential, the limited capabilities associated with fast analysis often significantly reducesthe efficiency of the design procedure. The methods most frequently adopted by frequency domain analysis programs for linear circuits have been described, giving greater attention to those best suited for use in microwave circuits. A comparison of the methods has been made, emphasizing execution speed as well as limitations imposed by the nature of the components and by circuit topology. The author has described how, with the aid of a simple algorithm, a relatively inexperienced computer programmer can apply the relevant procedures to typical multi-terminal circuit analysis. This is very useful, particularly for modelling transistors and various other active and passive devices. It has also been demonstrated how this algorithm may be used to evaluate any two-port parameters, thereby halving the number of iterations required in a typical analysis/optimization program.

A realistic design approach, devised especially for microwave integrated circuits, involves the representation of complex devices using data obtained from measurements made on them. The designer may employ the computer to perform the measurement characterization of an unknown device and then reduce the data to a form suitable for further processing. One of the outstanding examples of device characterization involves the automatic network analyzer. The technique of employing automatic on-line measurement for characterizing one-or two-port microwave device has been described.

It was demonstated also how to characterize accurately an unknown device, exclusive of system hardware errors, together with those arising from transitions, mounting arrangements etc. It has also been described how the results may be corrected, stored and later presented in virtually any mathematical form.

In applying optimization techniques to the design of microwave circuits, the designer requires accurate information concerning any discontinuity effects and other parameters to be compatible with the CAD packages. The majority of computerized methods for discontinuity effects have resulted in procedures employing numerical techniques. These, however, are difficult to incorporate into such packages and further, each method is able to evaluate only certain parameters.

A method has been presented for calculating the transmission properties at discontinuities, allowing for dispersion effects in microstrip lines. The method, found to be of considerable value, employs modelling techniques, in which attention to the details of an exact equivalent circuit for parasitic junction effects is not required. The procedure is first to assume an approximate model and then to modify it so as to match its predicted performance to that measured by an automatic computer on-line computerized S-parameters systems.

The various methods of calculating discontinuity effects have been presented. Some practical problems encountered in the actual design, such as measuring effective dielectric constant and the computation of losses has been included.

Finally, for the designer's benefit, empirical equations for step discontinuities are given. An algorithm has also been presented for evaluating the parameters most frequently required in designing microwave integrated circuits. The algorithm allows for the evaluation of conductor and dielectric losses, as well as dispersion effects. It has been applied to the design of amplifiers using alumina and polyguide substrates, at S- and X-band frequencies.

REFERENCES.

1. McPHUN, M.K. "A computer program for the analysis of branched distributed and lumped circuits", I.E.E. Conference Publication, No. 23 (1966) pp.89-124.

2. GREEN, R.E. "General purpose programs for the frequency domain analysis of microwave circuits", I.E.E.E. Trans. Microwave Theory and Tech. Vol. MTT-17, August (1969), pp.506-514.

3. PARKER, W.N. "DIPNET- A general distributed parameters network analysis program" ibid, Vol. MTT-17, August (1969), pp. 495-505.

4. MARCHENT, B.G. "MICRO2 - A frequency domain circuit analysis program for microwave circuits using mixed matrices". University of Warwick, School of Engineering Science, June (1971), Report No. 65.

5. MONACO, V.A. and TIBERIO P. "Automatic scattering matrix computation of microwave circuits", Alta Frequenza, Vol. XXXIX, Feb. (1970) pp.165-170.

6. HOUSTON, T.W. and READ, L.W., "Computer-aided design of broad-band and low noise amplifier", I.E.E.E. Trans. Microwave Theory and Tech. Vol. MTT-17, August (1969), pp.612-614.

7. MURRAY-LASSO M.A. and KOZEMCHAK, E.B., "Microwave circuit design by digital computer", ibid, Vol. MTT-17 August (1969) pp.514-526.

8. GELNOVATCH, V.G. and CHASE I.L. "DEMON-An optimal seeking computer program for the design of microwave circuits". I.E.E.E. Trans. Solid-state circuits, Vol. SC-5 Dec. (1970) pp.303-309.

9. EMERY, F.E. and O'HAGAN M. "Optimal design of matching network for microwave transistor", I.E.E.E. Trans. Microwave Theory and Tech. Vol. MTT-14 Dec. (1966) pp.696-698.

10. TRICK, T.N. and VLACH, J. "Computer-aided design of broad-band amplifiers with Complex loads" ibid Vol. MTT-18 Sept. (1970) pp.541-614.

11. CISCO, T.C. "Design of microstrip components by computer" NASA-Contractor Report (NASA-CR-1982) March (1972) p.205.

12. SANCHEZ-SINENCIO, E. and TRICK, T.N. "CADMIC-Computer-aided design of microwave integrated circuits", IEEE Trans. Microwave Theory and Techn. Vol. MTT-22, March (1974) pp.309-316.

13. HERRICK, D.L. "NOVA-Network optimization via adjoints" ibid Vol. MTT-23 Oct. (1975) pp. 849-850.

14. SOARES, R.A. "Amplifier design using bipolar transistor" London University Ph.D. Thesis (1974).

15. HOSSEINI, N.M.,SHURMER H.V., and SOARES, R.A. "OPTIMAL- A program for optimizing microstrip networks", Electron Lett. Vol. 12, No. 8, 15th April (1976), pp. 190-192.

16. FLETCHER, R., and REEVES, C.M. "Function minimisation by conjugate gradients", Computer Journal, Vol. 7, ISS.2. (1964) p.149.

17. FLETCHER, R. and POWELL, M.J.D. "A rapidly convergent descent method for minimisation", Computer Journal, Vol. 6 (1963) pp. 163-168.

18. ROSENBROCK, H.H. "An automatic method for finding the greatest or the least value of a function", Computer Journal, Vol. 3, (1960), p. 175.

19. HOSSEINI, N.M. and SHURMER, H.V. "Parameter evaluation and optimisation for microstrip", I.E.E. Colloquium on Microwave Integrated circuits, Digest No. 1976193 London 28 Oct. (1976).

20. AKELLO, R.J., EASTER B., and STEPHENSON, I.M. "Effects of

microstrip discontinuities on GaAs-M.E.S.F.E.T. Amplifier gain performance", Electron. Lett. Vol. 13, No. 6, 17th March (1977), pp. 160-162.

APPENDICES

(A) G-CONJUGATE VECTORS

(B) CALIBRATION PIECES

(C) TWO-PORT AND ONE-PORT CORRECTION

(D) BILINEAR TRANSFORMATION

(E) GREEN'S FUNCTION AND MOMENT METHOD

(F) MICPA-EVALUATION OF MICROSTRIP PARAMETERS

(G) CURVE FITTING TECHNIQUES

(H) EVALUATION OF PARASITIC JUNCTION PARAMETERS FOR STEP DISCONTINUITIES

(I) JUNCTION PARASITIC OF RIGHT-ANGLE BEND IN MICROSTRIP LINE

APPENDIX (A)

G-CONJUGATE VECTORS

Two vectors $\tilde{x}$ and $\tilde{y}$ are G-conjugate with respect of matrix G when $\tilde{x}^T G \tilde{y} = 0$, where $\tilde{x}^T$ represents the n-dimensional column and $\tilde{y}$ the row vectors, respectively. In fact the orthogonality is a special case of conjugacy, with G being the identity matrix.

Given a set of m linearly independent n-dimensional vectors ($m \leq n$), it is always possible to form a suitable linear combination of them that will transform into a set of m, G-Conjugate vectors spanning the same space. This process is known as Gram-schmidt orthogonalization, viz:-

Let $\tilde{x}_1, \ldots . \tilde{x}_n$ be linearly independent. We may construct an array $\tilde{y}_1, \ldots, \tilde{y}_n$ such that:

$$\tilde{x}_i^T G \tilde{y}_j = 0 \quad \text{for} \quad i \neq j \tag{a.1}$$

Let $\tilde{y}_1 = \tilde{x}_1$ and $\tilde{y}_2 = \tilde{x}_2 + a_{21} \tilde{y}_1$, where the scalar a_{21} is chosen to make $\tilde{y}_1$ and $\tilde{y}_2$ G-conjugate; i.e.

$$\tilde{y}_2^T G \tilde{y}_1 = \tilde{x}_2^T G \tilde{y}_1 + a_{21} \tilde{y}_1^T G \tilde{y}_1 \tag{a.2}$$

or

$$a_{21} = - (\tilde{x}_2^T G \tilde{y}_1)/(\tilde{y}_1^T G \tilde{y}_1) \tag{a.3}$$

Finally, dealing with all the a's, by construction G-conjugate vectors, $\tilde{y}_1, \tilde{y}_2, \ldots . \tilde{y}_k$ we may obtain

$$\tilde{y}_{k+1} = \tilde{x}_{k+1} + \sum_{j=1}^{k} a_{kj} \tilde{y}_j \tag{a.4}$$

or

$$a_{kj} = - (\tilde{x}_{k+1}^T G \tilde{y}_j)/(\tilde{y}_j^T G \tilde{y}_j) \tag{a.5}$$

For the generation of G^{-1}, a matrix H is used which may initially be chosen to be any positive definite symmetric matrix. This matrix is modified after the ith iteration using the information gained by moving down the direction.

$$\underset{\sim}{d}_i = - H_i g_i(\underset{\sim}{x}) \qquad (a.6)$$

The modification is such that $\underset{\sim}{d}_i$ is effectively an eigenvector of the matrix $H_{i+1} G$. This ensures that as the procedure converges H tends to G^{-1} evaluated at the minimum. It is convenient to take the unit matrix initially for H, so that the first direction is down the line of steepest descent.

APPENDIX (B)

CALIBRATION PIECES.

Before running the correction programs, the devices to be tested plus a suitable mount to enable connection to the s-parameter test set should be assembled. Calibration pieces which can be accommodated in the same mount are also required. The following options are available for the calibration pieces.

2-port correction:

Four terminations are required:

(1) Sliding or matched loads. Necessary for all calibrations.

(2) Short circuit or offset short circuit. If an offset short is used, the offset length (cm) will be required.

(3) Offset short or open circuit. The length (cm) of the offset will be required, and it must be different from the offset length of (2). For the open, the discontinuity capacitance (pf) and characteristic impedance (ohms) are required.

(4) Through connection - necessary for all calibrations. Some mounts are such that the two ports cannot be directly connected at the measurement planes, thus the length (cm) of any connecting line should be ascertained, as it can be taken into account.

Reflection coefficient:

Three terminations are required. If one of these is to be a matched load the options are as follows:

(1) Sliding or matched load

(2) Short or offset short circuit

(3) Offset short or open circuit

If no matched load is to be used, the options are as follows:

(1) Short circuit

(2) Offset short circuit

(3) Offset short or open circuit

Use of offset shorts requires the lengths (cm) to be known; for the open circuits the discontinuity capacitance (pf) and the characteristic impedance (ohms) are required.

APPENDIX (C)

TWO-PORT AND ONE-PORT CORRECTION

(a) Two port.

The correction methods used are based on the references. [4-7] in Chapter 4. A signal flow graph which is used to represent the system is shown in Fig. 1.c and 2.c.

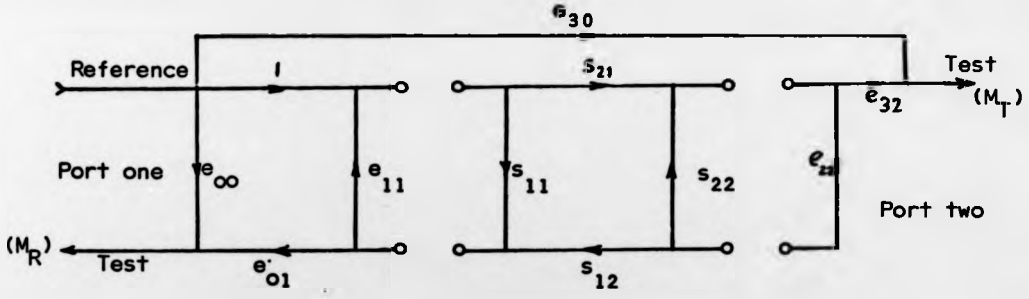

Fig. 1.c. Port one as reference.

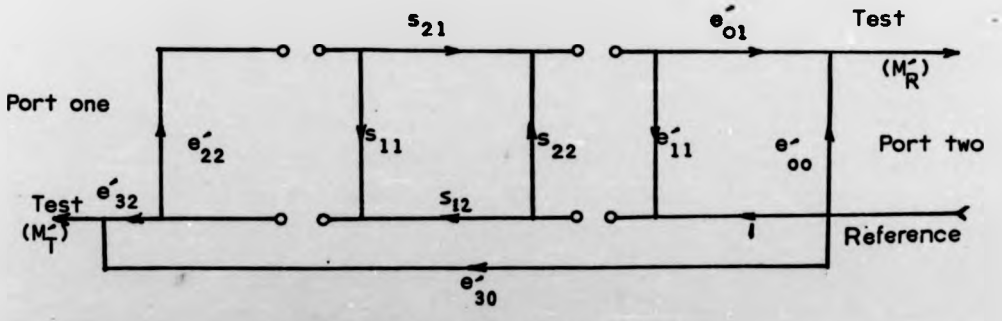

Fig. 2.c Port two as reference

The S-parameters of any device connected between the two ports are represented by s_{11}, s_{21}, s_{12}, s_{22}. The properties of the test unit, plus some of the errors due to transitions and mounting arrangements are represented by the e parameters. It has not been assumed that the e parameters are independent of which port is being used as the reference. Flow graph analysis results in the following general expressions for the measured values of reflection and transmission:

$$M_R = e_{oo} + \frac{s_{11}e_{o1}(1 - s_{22}e_{22}) + s_{21}s_{12}e_{22}e_{o1}}{1 - s_{11}e_{11} - s_{22}e_{22} - s_{21}s_{12}e_{11}e_{22} + s_{11}e_{11}s_{22}e_{22}} \quad (c.1)$$

$$M_T = e_{30} + \frac{s_{21}\, e_{32}}{1 - s_{11}e_{11} - s_{22}e_{22} - s_{21}s_{12}e_{11}e_{22} + s_{11}e_{11}s_{22}e_{22}} \quad (c.2)$$

$$M_R' = e_{oo}' + \frac{s_{22}e_{o1}'(1 - s_{11}e_{22}') + s_{12}s_{21}e_{22}'e_{o1}'}{1 - s_{22}e_{11}' - s_{11}e_{22}' - s_{12}s_{21}e_{11}'e_{22}' + s_{22}e_{11}'s_{11}e_{22}'} \quad (c.3)$$

$$M_T' = e_{30}' + \frac{s_{12}\, e_{32}'}{1 - s_{22}e_{11}' - s_{11}\, e_{22}' - s_{12}s_{21}e_{11}'e_{22}' + s_{22}e_{11}'s_{11}e_{22}'} \quad (c.4)$$

The calibration process involves making sufficient measurements with standards and conditions of known characteristics to determine all the e parameters.

The calibration measurements are as follows:

(1) Reflection with a sliding load. The computer measures the reflection three times, instructing the user to slide the load between measurements. It then constructs a circle through the three values and finds the centre of the circle. Thus we have

$$s_{11} = s_{21} = s_{12} = s_{22} = 0$$

so $M_1 = e_{oo}$ and $M_1' = e_{oo}'$

(2) Transmission without a through connection, both measurement ports terminated.

$$s_{11} = s_{21} = s_{12} = s_{22} = 0$$

so $M_2 = e_{30}$ and $M_2' = e_{30}'$

(3) Reflection with a short or offset short

$s_{11} = -e^{-j2\beta\ell}$; $s_{21} = s_{12} = s_{22} = 0$; where ℓ is the length of the offset short.

If we let $A = -1$ for short circuit ($\ell = 0$)

$= -e^{-j2\beta\ell}$ for offset short circuit

then we have $$M_3 = e_{oo} + \frac{Ae_{01}}{1-Ae_{11}}$$

similarly for $s_{22} = -e^{-j2\beta\ell'}$, $s_{21} = s_{12} = s_{11} = 0$, we get

$$M_3' = e_{oo}' + \frac{A'e_{01}'}{1-A'e_{11}'}$$

(4) Reflection with an offset short or open circuit

have $s_{21} = s_{12} = s_{22} = 0$

$s_{11} = -e^{-j2\beta\ell}$ for the offset short, ℓ is length

$= e^{-j2\theta}$ for the open, $\theta = \tan^{-1}(\omega CZ_o)$

If we let $B = -e^{-j2\beta\ell}$ for an offset short

$= e^{-j2\theta}$ for an open circuit

then we have $$M_4 = e_{oo} + \frac{Be_{01}}{1-Be_{11}}$$

similarly for $s_{22} = -e^{-j2\beta\ell'}$ or $e^{-j2\theta'}$, $s_{21} = s_{12} = s_{11} = 0$

we get $$M_4' = e_{oo}' + \frac{B'e_{o1}'}{1-B'e_{11}'}$$

(5) Reflection with a through connection

we have $s_{11} = s_{22} = 0$, $s_{21} = s_{12} = e^{-j\beta\ell}$, where ℓ is the through length.

If we let $L = e^{-j\beta\ell}$ $\quad$ ($L = 1$ if $\ell = 0$)

then we have $$M_5 = e_{oo} + \frac{L^2 e_{22}e_{o1}}{1-L^2e_{11}e_{22}}$$

and $$M_5' = e_{oo}' + \frac{L^2e_{22}'e_{o1}'}{1-L^2e_{11}'e_{22}'}$$

(6) Transmission with a through connection

we have $s_{11} = s_{22} = 0$, $s_{21} = s_{12} = e^{-j\beta\ell}$, where ℓ is the through length.

If we let $L = e^{-j\beta\ell}$ $\quad$ ($L = 1$ if $\ell = o$)

then we have $$M_6 = e_{30} + \frac{Le_{32}}{1-L^2e_{11}e_{22}}$$

and $$M_6' = e_{30}' + \frac{Le_{32}'}{1 - L^2e_{11}'e_{22}'}$$

The equation for $M_1 \rightarrow M_6$ and $M_1' \rightarrow M_6'$ can be solved to give the desired e parameters:

Let $X_1 = M_3 - M_1$
$X_2 = M_4 - M_1$
$X_3 = M_4 - M_3$
$X_4 = M_5 - M_1$
$X_5 = M_6 - M_2$

then we have:

$$e_{oo} = M_1$$

$$e_{11} = \frac{AX_2 - BX_1}{ABX_3}$$

$$e_{01} = \frac{X_1 X_2 (B-A)}{ABX_3}$$

$$e_{3o} = M_2$$

$$e_{22} = \frac{X_4}{L^2(e_{o1} + X_4 e_{11})}$$

$$e_{32} = \frac{X_5(1 - L^2 e_{11} e_{22})}{L}$$

Similar equations can be obtained for e'_{oo}, e'_{11}, e'_{o_1}, e'_{30}, e'_{22}, e'_{32}. Different e parameters will be obtained for each frequency point; they will be used by the computer for correcting all subsequent measurements of that frequency.

Values for A, B and L are computed from information provided by the user.

When an unknown device is connected to the system, reflection and transmission measurements are made at each port. As before, flow graph analysis gives the following expressions for these measurements:

$$M_R = e_{oo} + \frac{s_{11}e_{o1} + e_{o1}e_{22}(s_{21}s_{12} - s_{11}s_{22})}{D} \qquad (c.5)$$

$$M_T = e_{30} + \frac{s_{21}e_{32}}{D} \qquad (c.6)$$

where $D = 1 - s_{11}e_{11} - s_{22}e_{22} - e_{11}e_{22}(s_{21}s_{12} - s_{11}s_{22})$ and,

$$M'_R = e_{oo} + \frac{s_{22}e'_{o1} + e'_{o1}e'_{22}(s_{21}s_{12} - s_{11}s_{22})}{D'} \qquad (c.7)$$

$$M_T' = e_{30}' + \frac{s_{12}e_{32}'}{D'} \qquad (c.8)$$

where $D' = 1 - s_{22}e_{11}' - s_{11}e_{22}' - e_{11}'e_{22}'(s_{21}s_{12} - s_{11}s_{22})$

Let $Q = s_{21}s_{12} - s_{11}s_{22}$

Then we can obtain from (c.6) ...(c.8)

$$s_{11} = \frac{(M_R - e_{oo})D}{e_{01}} - e_{22}Q \qquad (c.9)$$

$$s_{21} = \frac{(M_T - e_{30})D}{e_{32}} \qquad (c.10)$$

$$s_{22} = \frac{(M_R' - e_{oo}')D'}{e_{01}'} - e_{22}'Q \qquad (c.11)$$

$$s_{12} = \frac{(M_T' - e_{30}')D'}{e_{32}'} \qquad (c.12)$$

An explicit solution to equations (c.9 to c.12), although theoretically feasible, has proved an intractable problem. Thus an iterative method of solution is used, which has been shown to have negligible error. The process is as follows:

Initially set

$$\hat{s}_{11} = M_R \qquad \hat{s}_{21} = M_T \qquad \hat{s}_{22} = M_R' \qquad \hat{s}_{12} = M_T'$$

Then:

(1) Calculate Q, D, D' from $\hat{s}_{11}$, $\hat{s}_{21}$, $\hat{s}_{22}$, $\hat{s}_{12}$ and the e parameters.

(2) Calculate new values for $\hat{s}_{11}$, $\hat{s}_{21}$, $\hat{s}_{22}$, $\hat{s}_{12}$ as follows:

$$\hat{s}_{11} = \frac{(M_R - e_{oo})D}{e_{01}} - e_{22}Q \qquad \hat{s}_{21} = \frac{(M_T - e_{30})D}{e_{32}}$$

$$\hat{s}_{22} = \frac{(M_T' - e_{oo}')D'}{e_{01}'} - e_{22}'Q \qquad \hat{s}_{12} = \frac{(M_T' - e_{30}')D'}{e_{32}'}$$

(3) Return to (1).

This cycle is repeated until a convergence is obtained (ten times).

The final values for $\hat{s}_{11}$, $\hat{s}_{21}$, $\hat{s}_{22}$ and $\hat{s}_{12}$ are the corrected s-parameters for the unknown device.

The relationship between the reading sequence of the 2-port correction program and the measurement parameters is given below.

Program K setting	Type of measurement	Device to be measured	Equation parameters
1	s_{11}	Sliding load	M_1
2	s_{11}		
3	s_{11}		
4	not used		
5	s_{22}	Sliding load	M'_1
6	s_{22}		
7	s_{22}		
8	not used		
9	s_{21}	Match	M_2
10	s_{12}	Match	M'_2
11	s_{11}	Short or offset	M_3
12	s_{22}	offset or open	M'_4
13	s_{22}	offset or open	M'_3
14	s_{11}	short or offset	M_4
15	s_{11}	Through connection	M_5
16	s_{21}		M_6
17	s_{22}		M'_5
18	s_{12}		M'_6
19	s_{11}	Unknown Device	M_R
20	s_{21}		M_T
21	s_{22}		M'_R
22	s_{12}		M'_T

b-One-port

The correction method used is really just a sub-set of the 2-port correction method. In practice, the results have never proved quite as accurate as reflections obtained using the 2-port correction, one theory being that the leakage is not accounted for. However, the programme is much quicker to use due to the reduced reading times for calibration and devices.

The system can be represented by the following system flow diagram:

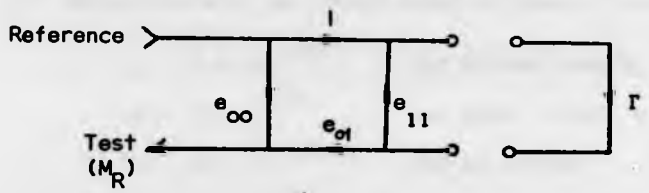

Fig. 3.C The flow diagram for reflection coefficient.

The e parameters represent the properties of the test unit plus some transition and mounting errors. Flowgraph analysis gives the following general expression for the measured reflection:

$$M_R = e_{oo} + \frac{\Gamma e_{01}}{1-\Gamma e_{11}}$$

The calibration process involves making sufficient measurements with standards and conditions of known characteristics to determine all the e parameters. There are two sets of calibration equations, depending on whether a matched load is used or not.

Calibration with a matched load:

Measurements are:

(1) Reflection with a sliding load. The computer measures the reflection three times, instructing the user to slide the load between measurements. It then constructs a circle through the three values and finds the centre of the circle. We thus have:

$$\Gamma = 0$$

so $M_1 = e_{oo}$

(2) Reflection with a direct or offset short

we have $\Gamma = -e^{-J2\beta\ell}$ when ℓ is the length of the offset

let $A = -e^{-J2\beta\ell}$, if $\ell = 0$ (i.e. a direct short)

then $A = -1$

then $M_2 = e_{oo} + \dfrac{Ae_{o1}}{1-Ae_{11}}$

(3) Reflection with an offset short or open circuit have

$\Gamma = -e^{-J2\beta\ell}$ for offset length ℓ

or $\Gamma = e^{-J2\theta}$ for open circuit with $\theta = \tan^{-1}(\omega CZ_o)$

let $B = -e^{-J2\beta\ell}$ for an offset

or $B = e^{-J2\theta}$ for an open

then $M_3 = e_{oo} + \dfrac{Be_{o1}}{1 - Be_{11}}$

The equations for M_1, M_2 and M_3 can be solved to give the following:

$$e_{oo} = M_1$$

$$e_{11} = \frac{AX_2 - BX_1}{ABX_3}$$

$$e_{o1} = \frac{X_1X_2(B-A)}{ABX_3}$$

where $X_1 = M_2 - M_1$

$X_2 = M_3 - M_1$

$X_3 = M_3 - M_2$

Calibration using short and open circuits only.

Measurements are:

(1) Reflection with a direct short:

we have $\Gamma = -1$, thus

$$M_1 = e_{oo} - \frac{e_{o1}}{1+e_{11}}$$

(2) Reflection with an offset short:

we have $\Gamma = -e^{-j2\beta\ell}$ ℓ is length of offset

let $A = -e^{-j2\beta\ell}$, then

$$M_2 = e_{oo} + \frac{A e_{o1}}{1-Ae_{11}}$$

(3) Reflection with an offset short or open circuit:

we have $\Gamma = -e^{-j2\beta\ell}$ for offset length ℓ

or $\Gamma = e^{-j2\theta}$ for open circuit $\theta = \tan^{-1}(\omega C Z_o)$

let $B = -e^{-j2\beta\ell}$ for an offset

or $B = e^{-j2\theta}$ for an open

then $M_3 = e_{oo} + \frac{Be_{o1}}{1-Be_{11}}$

The above equations for M_1, M_2 and M_3 can be solved to give the following:

$$e_{oo} = \frac{A M_3 X_1 - BM_2 X_2 - ABM_1 X_3}{AX_1 - BX_2 - ABX_3}$$

$$e_{11} = \frac{BX_1 - AX_2 - X_3}{AX_1 - BX_2 - ABX_3}$$

$$e_{o1} = \frac{-X_1 X_2 X_3 (1 + A)(1 + B)(A - B)}{[AX_1 - BX_2 - ABX_3]^2}$$

where $X_1 = M_2 - M_1$

$X_2 = M_3 - M_1$

$X_3 = M_3 - M_2$

Either type of calibration gives a set of equations for the e parameters. Values for A and B are computed from information provided by the user. Different e parameters will be obtained

for each frequency point; they will be used by the computer for correcting all subsequent measurements at that frequency.

When an unknown device is connected to the system, a reflection measurement is taken. As before, flowgraph analysis gives the following expressions for this measurement:

$$M_R = e_{oo} + \frac{\Gamma e_{o1}}{1-\Gamma e_{11}}$$

This can be solved to give the corrected result Γ for the reflection coefficient of the unknown device as:

$$\Gamma = \frac{M_R - e_{oo}}{e_{11}(\Gamma - e_{oo}) + e_{o1}}$$

APPENDIX (D)

BILINEAR TRANSFORMATION

A one-to-one transformation between the W and Z planes is given by

$$W = \frac{aZ + b}{cZ + d} \qquad (1.d)$$

It is a so-called bilinear transformation or bilinear mapping, where the constant a, b, c and d are real or complex.

It may be easily shown that W is analytic except where $cZ + d = 0$. Assuming $Z = x + jy$ then the left hand side of Eqn. (1.d) may be rewritten as follows:

$$\frac{aZ + b}{cZ + d} = \frac{a(x + jy) + b}{c(x + jy) + d}$$

$$= \frac{(ax + b)(cx + d) + acy^2 + j[ay(cx + d) - cy(ax + b)]}{(cx + d)^2 + c^2y^2} \qquad (2.d)$$

Now, assuming $W = U + jV$ then from (2.d), U, and V will hold the following values:

$$U = \frac{(ax + b)(cx + d) + acy^2}{(cx + d)^2 + c^2y^2} \quad \text{and} \quad V = \frac{y(ad - bc)}{(cx + d)^2 + c^2y^2}$$

Hence

$$\frac{\partial U}{\partial x} = \frac{(ad - bc)[(cx + d)^2 - c^2y^2]}{[(cx + d)^2 + c^2y^2]^2} \quad \text{and} \quad \frac{\partial V}{\partial x} = \frac{2cy(ad - bc)(cx + d)}{[(cx + d)^2 + c^2y^2]^2}$$

$$\frac{\partial U}{\partial y} = \frac{-2cy(ad - bc)(cx + d)}{[(cx + d)^2 + c^2y^2]^2} \quad \text{and} \quad \frac{\partial V}{\partial y} = \frac{(ad-bc)[(cx + d)^2-c^2y^2]}{[(cx+d)^2 + c^2y^2]^2}$$

Therefore the Cauchy-Rieman conditions $\left(\text{i.e. } \frac{\partial U}{\partial x} = \frac{\partial V}{\partial y} \text{ and } \frac{\partial V}{\partial x} = -\frac{\partial U}{\partial y} \right)$

are satisfied and partial derivatives are continuous, hence:

$$\frac{dW}{dZ} = \frac{ad - bc}{(cZ + d)^2}$$

Thus, if $ad-bc \neq 0$ each point Z is such that $cZ + d \neq 0$ and these correspond to one and only one point W.

Suppose that the reflection coefficient for both planes 2 and 1 of a junction (Fig. 1.d), looking toward the right are:

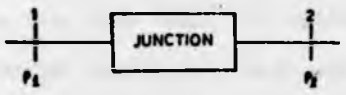

Fig. 1.d. The reflection coefficient ρ_2 and ρ_1 at terminal 2 and 1 respectively.

$$\rho_1 = \frac{b_1}{a_1} \qquad (3.d)$$

$$\rho_2 = \frac{a_2}{b_2}$$

$$\text{Then } \rho_1 = \frac{-\Delta s\rho_2 + s_{11}}{-s_{22}\rho_2 + 1} \qquad (4.d)$$

So it can be seen from equation (4.d) there is a bilinear relationship between reflection coefficient (ρ_2) at terminal 2 and (ρ_1) at terminal 1. Where the constants a, b, c, d are; $a = -\Delta_s$, $b = s_{11}$, $c = -s_{22}$, $d = 1$ and $\Delta_s = s_{11}s_{22} - s_{12}^2$. The symbols in equations (3.d) and (4.d); a_1 and a_2 are incident, b_1 and b_2 are reflected voltage waves on ports 1 and 2, respectively.

APPENDIX (E)

GREEN's FUNCTION AND MOMENT METHOD.

The Green's function for a particular geometrical arrangement is the solution for the associated potential problem with a specific arrangement of grounded conducting boundaries when the only charge present is a unit point charge. Let ϕ be the desired solution of the problem and let $\psi = G$ be the Green's function with this particular geometry. Utilizing Green's identity, viz:-

$$\int(\phi\nabla^2\psi - \psi\nabla^2\phi)dv = \int(\phi\nabla\psi - \psi\nabla\phi).ds \qquad (1.e)$$

On the other hand, the solution of the problem of a unit point charge located at $r = 0$ with surface s grounded is the Green's function of the form:

$$G = \frac{1}{4\pi\varepsilon_o r} \qquad (2.e)$$

Since G has a singularity only at $r = 0$, which may be handled by means of the δ-function viz:-

$$\nabla^2 G = -\frac{\delta(r)}{\varepsilon_o} \qquad (3.e)$$

Substituting Eqn. (3.e) into Eqn. (1.e), we obtain:

$$\int\left[G\nabla^2\phi + \frac{\phi\delta(r)}{\varepsilon_o}\right] dv = \int(G\nabla\phi - \phi\nabla G).ds \qquad (4.e)$$

The Green's function is zero at the surface S and if the potential over the surface is represented by ϕ_s, then (4.e) reduces to:

$$\phi = -\varepsilon_o\left(\int G\nabla^2\phi dv + \int\phi_s\nabla.ds\right) \qquad (5.e)$$

In the case of microstrip, the potential over the surrounding surface is zero (i.e. $\phi_s = 0$) and $\nabla^2\phi = -\rho/\varepsilon_o$ due to the charge distribution ρ throughout the volume v. Eqn. (5.e) may be

rewritten as follows:

$$\phi = \int G(x,y|x_o,y_o)\sigma(x_o,y_o)d\ell_o \qquad (7.e)$$

where the integral is defined over the conductor surface.

The Green's function for the open microstrip line may be obtained from extended image theory [as illustrated by Silvester [Chapter 8, ref. 15]] by superimposing the potential distributions caused by the two opposite line charges acting individually Fig. 1.e.

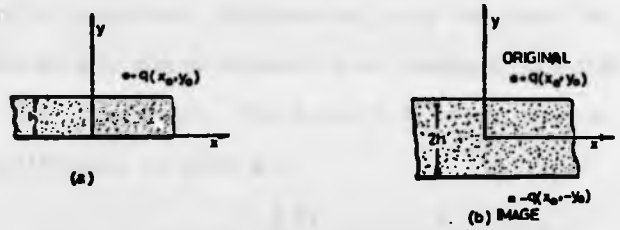

FIG. 1.e (a) - LINE CHARGE NEAR DIELECTRIC SHEET ABOVE GROUND PLANE.
(b) - ELECTROSTATIC EQUIVALENT

The potential distribution of a single line charge of Fig. 1.e in the upper region, i.e. $y > h$ is given by

$$V(x,y) = \frac{-q}{4\pi\varepsilon_o}\{[(x-x_o)^2 + (y-y_o)^2] + K\,\ell n[(x-x_o)^2 + (y-y_o-2h)^2] - (1-K^2)\sum_{n=o}^{\infty} K^{2n+1}\,\ell n[(x-x_o)^2 + (y+y_o+2(2n+1)h)^2] \qquad (8.e)$$

The three terms in this equation refer to the source charge itself, the primary image and the infinite set of secondary images, respectively. In a similar manner, the potential distribution in the centre region (i.e. $-h<y<h$) is given by

$$V(x,y) = -\frac{(1-K)q}{4\pi\varepsilon_o\varepsilon_r}\sum_{n=o}^{\infty} K^{2n}\,\ell n[(x-x_o)^2 + (y-y_o-2nh)^2] \qquad (9.e)$$

and in the lower region (i.e. $y \leq -h$) by

$$V(x,y) = -\frac{(1-K)^2 q}{4\pi\varepsilon_o} \sum_{n=o}^{\infty} K^{2n} \ln\left[(x-x_o)^2 + (y-y_o-4nh)^2\right] \qquad (10.e)$$

where K, the image coefficient, is defined as $K = (1-\varepsilon_r)/(1+\varepsilon_r)$.

The required Green's function may be found by superimposing the potential distributions, caused by the two opposite line charges acting individually. Depending on the region in which a solution is sought, a two-fold expression of type of equations (8.e), (9.e) and (10.e) results. If the strip is assumed to be very thin, all the charge elements will be very near the dielectric interface. Furthermore, only the potential at the location of any charge element is of interest, not the potential at any arbitrary point. The Green's function, however, for the upper half-space is given by:

$$G(x,y|x_o,y_o) = \begin{cases} G_1 & y \geq h \quad y_o \geq h \\ G_2 & y \leq h \quad y_o \geq h \\ G_3 & y \geq h \quad y_o < h \\ G_4 & y \leq h \quad y_o > h \end{cases}$$

The expressions for G_1, G_2, G_3 and G_4 are respectively:

$$G_1 = -\frac{1}{4\pi\varepsilon_o}\left\{\ln\left[(x-x_o)^2 + (y-y_o)^2\right] + k\ln\left[(x-x_o)^2 + (y+y_o+2h)^2\right] - (1-K^2)\sum_{n=o}^{\infty} K^n \ln\left[(x-x_o)^2 + (y-y_o+2nh)^2\right]\right\} \qquad (11.e)$$

$$G_2 = \frac{1}{4\pi\varepsilon_o}(1-K)\sum_{n=o}^{\infty} K^n \ln\left[\frac{(x-x_o)^2 + (y+y_o+2nh)^2}{(x-x_o)^2 + (y-y_o-2nh)^2}\right] \qquad (12.e)$$

$$G_3 = \frac{1}{4\pi\varepsilon_o}(1+K)\sum_{n=o}^{\infty} K^n \ln\left[\frac{(x-x_o)^2 + (y+y_o+2nh)^2}{(x-x_o)^2 + (y-y_o+2nh)^2}\right] \qquad (13.e)$$

$$G_4 = \frac{1}{4\pi\varepsilon_o\varepsilon_r}\left\{\sum_{n=o}^{\infty} K^n \ln\left[\frac{(x-x_o)^2 + (y+y_o+2nh)^2}{(x-x_o)^2 + (y-y_o+2nh)^2}\right] + \sum_{n=o}^{\infty} K^n \ln\left[\frac{(x-x_o)^2 + (y+y_o-2(n+1)h)^2}{(x-x_o)^2 + (y-y_o-2(n+1)h)^2}\right]\right\} \qquad (14.e)$$

MOMENT METHOD

In accordance with Equation 8.8, the potential at any point p(x,y) is given by:

$$\phi(x,y) = \sum_{i=1}^{N} \sigma^{i}(x_o,y_o) \int_{w_i} G(x,y|x_o,y_o)d\ell_o^{i} \qquad (15.e)$$

If the strips w_i are small, the potential ϕ^i on each strip may be approximated by the average of all potential values on the strip

$$\phi^{i}(x,y) = \sum_{j} \sigma^{j}(x,y) \frac{1}{w_i} \int_{w_i}\int_{w_j} G(x,y|x_o,y_o)d\ell_o^{i}\, d\ell^{j}$$

$$= \sum_{j}\left[\frac{1}{w_i}\frac{1}{w_j}\int_{w_i}\int_{w_j} G(x,y|x_o,y_o)d\ell_o^{i}d\ell^{j}\right]q_j \qquad (16.e)$$

where $q_j = \sigma_j w_j$, the charge per unit length on the jth strip. Letting D_{ij} denote the typical integral, Equation (16.e) may be written as follows

$$\phi^{i} = D_{ij}\, q_j \qquad (17.e)$$

since the conductors may be presumed to be at known potentials V, Eq. 17.e may be written as the matrix equation.

$$[V] = [D][q] \qquad (18.e)$$

The unknown charge densities [q] are obtained by matrix inversion:

$$[q] = [D]^{-1}[V] \qquad (19.e)$$

The capacitance of microstrip line is:

$$C = \sum_{i=1}^{m} q_i = \sum_{i}^{m}\sum_{j}^{m} [D_{ij}]^{-1} \qquad (20.e)$$

The characteristic impedance is then given by:

$$Z_o = \frac{1}{v_o\sqrt{C_o C}} \qquad (21.e)$$

where C_o is the capacitance of air filled microstrip line and v_o is the velocity of light.

Finally the integral of 8.8 may be expressed as

$$\phi(x,y|\frac{x_1+x_2}{2}, h) = \frac{-1}{2\Pi(\varepsilon_o+\varepsilon)}\sum_{n=o}^{\infty}(-K)^n\left\{B\,\ell n\frac{(y+H_n)^2+B^2}{(y-H_n)^2+B^2}\right.$$

$$-A\ell n\frac{(y+H_n)^2+A^2}{(y-H_n)^2+A^2} + 2(y+H_n)\left[\arctan\frac{B}{y+H_n} - \arctan\frac{A}{y+H_n}\right]$$

$$\left. + 2(y-H_n)\left[\arctan\frac{B}{y-H_n} - \arctan\frac{A}{y-H_n}\right]\right\} \qquad (22.e)$$

where $K = \frac{\varepsilon_r - 1}{\varepsilon_r + 1}$, $H_n = (2n+1)\,h$

and $A = x - x_1$, $B = x - x_2$

as shown in Fig. 8.1. (Chapter 8).

The value of $\nabla\phi$ in equation 8.6 can be obtained by differentiating (22.e).

COMPUTER PROGRAM DESCRIPTION.

The following program computes the characteristic impedance and the line capacitance using the above method. Where the centre conductor is divided into 'NSE' equal subsections, DEW, along the cross section.

The infinite series summation is terminated when the total is changed by less than 10^{-4} upon addition of a term. For the results given at the end of the Program the centre conductor was divided into 20 subsections in each case. This number is automatically increased by the program as w, the centre conductor width, increases according to the following relationship:

$$NSE = 2[2.5(w/h - 1.0) + 0.5]$$

The input data and output are indicated in the beginning of the program. However the output is a feature of the Sigma 5 Computer. For other computers, use 'READ' or 'WRITE' statement with the appropriate format.

PROGRAM DETAILS.

(a) FORTRAN IV

(b) A maximum of 20 subsections.

(c) Only single precision.

(d) 135 cards including comments.

PERFORMANCE GUIDE

(a) It is loaded on the XDS-Sigma 5 Computer.

(b) Core-size requirements: 4866 bytes.

(c) Input medium: cards

(d) Output medium: line printer.

(e) Work or data files needed: None.

(f) Time taken to run submitted examples:
Compilation 59 seconds, run 67 seconds.

```
C
C.....INPUT DATA
C     NSEC:   NUMBER OF NARROW STRIPS
C     H:      DIELECTRIC THICKNESS
C     W:      CENTRE CONDUCTOR WIDTHNESS
C     ER:     DIELECTRIC CONSTANT
C.....VARIABLE DIMENSION
C             D(NSEC/2,NSEC/2) , G1(NSEC) , V(NSEC/2),SIGM(NSEC/2)
C.....OUTPUT
C     WOH:    RATIO OF W/H
C     ZO:     CARACTERISTIC IMPEDANCE
C     C:      LINE CAPACITANCE
C     EFF:    EFFECTIVE DIELECTRIC CONSTANT
C**************************************************
C
C..... MICROSTRIP CHARACTERISTIC  IMPEDANCE AND LINE CAPACITANCE
C..... USING GREEN'S FUNCTION (MOMENT METHODE)
C
      DIMENSION D(30,30),G1(60),V(30),SIGM(30)
      DATA PI,ERO/3.14159,8.854E-12/
      WRITE(108,1)
1     FORMAT(1H ,1X,'RATIO OF',4X,'CHARACTERISTIC',4X,
     1'LINE CAPACITANCE',4X,'EFFECTIVE DIELECTRIC'/1H 3X,
     2'W/H',7X,'IMPEDANCE(OHM)',9X,'( F/M)',15X,'CONSTANT'/)
7     READ(105,3,END=100) NSEC,H,W,ER
3     FORMAT(I,3F)
      N=NSEC/2
      IF(W/H.GT.1.0) N=10.5+2.5*(W/H-1.0)
      NSEC=2*N
      ASEC=NSEC
      DW=W/ASEC
      DEW=DW/2.0
      IND=0
C
C     BOUNDRY CONDITION
C
      DO 10 I=1,N
10    V(I)=1.0
5     CONTINUE
      EK=(ER-1.0)/(ER+1.0)
      CST=1.0/(2.0*PI*(1.0+ER)*ERO)
      X0=0.0
      DO 15 J=1,NSEC
      X1=X0-DEW
      X2=X0+DEW
C
C     CALL GREEN FUNCTION
C
       CALL GREEN(X1,X2,EK,H,G)
      G1(J)=CST*G
      X0=X0+DW
15    CONTINUE
C
C     USING SYMMERTY ARGUT THE CENTRE CONDUCTOR
C
      K=2*N+1
      DO 20 J=1,N
      DO 20 I=1,N
      M=IABS(J-I)+1
      L=IABS(J+I-K)+1
20    D(J,I)=G1(M)+G1(L)
      CALL SOLVE(D,V,SIGM,N)
      Q=0.0
      DO 25 J=1,N
25    Q=Q+SIGM(J)
      Q=2.0*Q*DW
      IF(IND.NE.0) GO TO 30
      C=Q
      ER=1.0
      IND=1
      GO TO 5
30    CO=Q
```

```
      EFF=C/CO
      ZO=SQRT(C*CO)*3.0E8
      ZO=1.0/ZO
      WOH=W/H
      WRITE(102,2) WOH,ZO,C,EFF
2     FORMAT(1H ,1X,F4.1,10X,F6.2,14X,E9.2,16X,F6.3)
      GO TO 7
100   STOP
      END

      SUBROUTINE SOLVE (A,C,X,N)
C     THIS SUBROUTINE SOLVES SIMULTANEOUS EQATIONS
C     MATRIX(A)*MATRIX (X) =MATRIX(C)
C
      DIMENSION A(30,30),C(30),X(30)
      INTEGER P
      P=N+1
      A(1,P)=1.
      DO 120 K=2,N
120   A(K,P)=0.
      DO 150 J=1,N
      DO 160 L=1,N
160   A(P,L)=A(1,L+1)/A(1,1)
      DO 170 K=2,N
      DO 170 L=1,N
170   A(K-1,L)=A(K,L+1)-A(K,1)*A(P,L)
      DO 150 L=1,N
150   A(N,L)=A(P,L)
      DO 180 I=1,N
      X(I)=0.
      DO 180 L=1,N
180   X(I)=X(I)+A(I,L)*C(L)
      RETURN
      END

      SUBROUTINE GREEN(X,Y,EK,H,G)
      FC=1.0
      A1=(Y*Y+4.0*H)/(Y*Y)
      G1=Y*ALOG(A1)
      A2=(X*X+4.0*H)/(X*X)
      G2=X*ALOG(A2)
      H2=H*2.0
      G3=ATAN2(Y,H2)-ATAN2(X,H2)
      G3=4.0*H*G3
      G=G1-G2+G3
      IF(EK.EQ.0.0) GO TO 2
      DO 1 I=2,200
      FC=-FC*EK
      B=2.0*FLOAT(I)
      BH=B*H
      C=B*B
      CH=(B-2.0)*H
      D=(B-2.0)*(B-2.0)
      A1=(Y*Y+C*H*H)/(Y*Y+D*H*H)
      G1=Y*ALOG(A1)
      A2=(X*X+C*H*H)/(X*X+D*H*H)
      G2=X*ALOG(A2)
      G3=2.0*BH*(ATAN2(Y,BH)-ATAN2(X,BH))
      G4=2.0*CH*(ATAN2(Y,CH)-ATAN2(X,CH))
      TEM=FC*(G1-G2+G3-G4)
      G=G+TEM
      IF(ABS(TEM/G).LE.1.0E-4) GO TO 2
1     CONTINUE
2     RETURN
      END
```

EXTENDED FIV-H, VERSION 001

RATIO OF W/H	CHARACTERISTIC IMPEDANCE (OHM)	LINE CAPACITANCE (F/M)	EFFECTIVE DIELECTRIC CONSTANT
.4	72.63	.11E-09	6.199
.5	66.95	.12E-09	6.269
.6	62.34	.13E-09	6.334
.7	58.47	.14E-09	6.396
.8	55.15	.15E-09	6.455
.9	52.26	.16E-09	6.511
1.0	49.69	.17E-09	6.565
2.0	33.84	.26E-09	7.020
3.0	25.91	.35E-09	7.352
4.0	21.05	.44E-09	7.605
5.0	17.77	.52E-09	7.804
6.0	15.38	.61E-09	7.965

COMPUTED PARAMETERS- The following parameters are computed via the associated algorithms.

(a) Conductor loss

(b) Dielectric loss

(c) Line dimensions

(d) Dispersion.

PROGRAM DETAILS

(a) Fortran IV

(b) A maximum of 30 microstrip lines

(c) Complex and only single-precision arithmetic

(d) 139 cards, including comments.

PERFORMANCE GUIDE

(a) It is loaded on the XDS-Sigma 5 computer

(b) Core size requirements: 17928 bytes

(c) Input medium: cards

(d) Output medium: line printer

(e) Work or data files needed - none

(f) Time taken to run submitted examples: Compilation 01:07 min. run 19 seconds

```
14:25 NOV 08,'76
!JOB N.N.M. MICROSTRIP PARAMETERS
!FORTRANH LS,GO
    EXTENDED FIV-H, VERSION 001
      1                 COMMAN/MICP/FR,H,T,RESD,SIGC,ZO,AL
      2                 DIMENSION W(30,2),WOH(30,2),EEF(30,2),AO(30,2),ALPHDI(30,2)
      3                 READ(105,1) FSTART,FINCR,NF
      4           1     FORMAT(2F,I)
      5                 READ(105,7) ZO,AL,RESD,SIGC,H,T,ER
      6           7     FORMAT(7F)
      7                 WRITE(108,6)
      8           6     FORMAT(1H1,10X,'MICROSTRIP LINE PARAMETERS'/10X,26(1H*))
      9                 OUTPUT RESD,SIGC,H,T,ER,FSTART,FINCR,NF
     10                 I=1
     11                 WRITE(108,4) ZO,AL
     12           4     FORMAT(//1H ,'CHARACTERISTIC IMPA.=',F5.1,'(OHMS)',5X,
     13                1'AIR LENGTH=',F4.1,'(MM)'///
     14                21H ,'FREQUENCY',3X,'EFF. LENGTH',3X,'EFFECTIVE',3X,
     15                4'TOTAL LOSSES',4X,'WAVE-LENGTH',3X,'PHASE VELOCITY'/1H ,2X,
     16                5'(GHZ)',8X,'(MM)',7X,'DIELECTRIC',5X,'(DB/CM)',9X,'(MM)',8X,
     17                7'(1E+M/SEC)'/)
     18                 FR=FSTART
     19                 DO 3 J=1,NF
     20                 CALL MICPA(EAL,EFD,ALPH,ALAN,VP,VN,FR,J,I,1,W)
     21                 WRITE(108,5)FR,EAL,EFD,ALPH,ALAN,VP
     22           5     FORMAT(1H ,2X,F5.1,6X,F7.3,7X,F6.3,8X,F8.5,6X,FR.3,9X,F7.4)
     23                 FR=FR+FINCR
     24           3     CONTINUE
     25                 WRITE(108,9) W(I,1)
     26           9     FORMAT(/1H ,'MICROSTRIP WIDTH=',F6.3,'(MM)')
     27                 STOP
     28                 END


      1           C
      2           C
      3           C     ***************************************************************
      4           C
      5           C.........THE ALGORITHM CALCULATES DIMENSION,OHMIC LOSS,DIELECTRIC
      6           C.........LOSS,DISPERSIVE EFFECT OF MICROSTRIP LINE
      7           C
      8           C     ***************************************************************
      9           C
     10           C
     11           C     INPUT DATA
     12           C
     13           C.....ZO=CHARACTERISTIC IMPEDANCE (OHMS)
     14           C.....AL=AIR LENGTH OF MICROSTRIP LINE (MM)
     15           C.....ER=RELATIVE DIELECTRIC CONSTANT.
     16           C.....H=SUBSTRATE THICKNESS (THOUSANDTHS OF AN INCH).
     17           C.....T=CONDUCTOR STRIP THICKNESS (MICROINCHES)
     18           C.....RESD=RESISTIVITY OF THE SUBSTRATE (OHM-CM)
     19           C.....SIGC=CONDUCTIVITY OF THE CONDUCTORS(S/M).
     20           C.....FR=FREQUENCY IN GHZ.
     21           C.....NF=NUMBER OF FREQUENCY STEPS.
     22           C.....L =IDENTIFICATION NUMBER FOR DIFFERENT MICROSTRIP LINE
     23           C.....M=IDENTIFICATION FOR L-SECTION
     24           C
     25           C     OUTPUT
     26           C
     27           C.....EAL=EFFECTIVE LENGTH OF MICROSTRIP(MM).
     28           C.....W=MICROSTRIP WIDTH(MM)
     29           C.....ALPHC=OHMIC LOSS (DB/CM)
```

```
C.....ALPHD=DIELECTRIC LOSS (DB/CM)
C.....ALPH=TOTAL LOSSES
C.....ALAN=WAVELENGTH(MM)
C.....VP=VELOCITY(M/SEC) PHASE VELOCITY
C.....VN=NORMALIZED PHASE VELOCITY
C.....CNUM1,CNUM2 ARE EXP(GAMA*EAL),EXP(-GAMA*EAL) WHERE
C          GAMA=ALPH+J*BETA
C
      SUBROUTINE MICPA(EAL,EFO,ALPH,ALAN,VP,VN,FR,NF,L,M,W)
      COMMON/MICP/FR,W,T,RESD,SIGC,ZO,AL
      DIMENSION W(30,21),WOH(30,21),EEF(30,21),AO(30,21),ALPHDI(30,21)
      COMPLEX CNUM1,CNUM2
      DATA AT,PI/376.73,3.14159/
      VN=1.0
      DNP=1.0/8.686
      ALPH=0.0
C
C     DIMENSION OF MICROSTRIP (WHEELER'S ALGORITHM).
C
      IF(ER.LE.1.) GO TO 30
      IF(NF.GT.1) GO TO 20
C
      B=PI*AT/(2.*ZO*SQRT(ER))
      IF(B.GT.(2.*PI)) GO TO 1
      ER1=(ER+1.0)/2.0
      D=ZO*SQRT(ER1)/60.*((ER-1)/(ER+1))*(0.226+(0.121/ER))
      WH=4./(0.5*EXP(D)-EXP(-D))
      WOH(L,M)=WH
      GO TO 2
1     WH=(2./PI)*(B-1-ALOG(2.*B-1.)+(ER-1.)/(2.*ER)*(ALOG(B-1.)
     1+0.293-(0.517/ER)))
      WOH(L,M)=WH
2     CONTINUE
      W1=WOH(L,M)*W
      W(L,M)=WOH(L,M)*W+0.0254
C
C     EFFECTIVE DIELECTRIC CONSTANT
C
      IF(WH.GT.1.) GO TO 3
      EE=.5*(ER+1.)+.5*(ER-1)*(1./SQRT(1.+12./WH)
     1   + 0.04*(1-WH)**2)
      EEF(L,M)=EE
      GO TO 4
3     EE=.5*(ER+1.) + .5*(ER-1)/SQRT(1.+12./WH)
      EEF(L,M)=EE
4     CONTINUE
C
C     DIELECTRIC LOSS
C
      ALPHDN=A90./ER+171./SQRT(ER)+4.*ALOG(WH)+(225.-7.7*ER)
     1+SQRT(1.+WH)-13.7*WH+(10.-WH/2.)**2
      ALPHD=ALPHDN/RESD
      ALPHDI(L,M)=ALPHD
C
C     OHMIC LOSS  SCHNEIDER'S METHOD
C
      PS=1.0/(2.0*PI)
      PII=1.0/PI
      IF(WH.GT.PS) GO TO 5
      WHT=1000.0*W1/T
      WT=PII*ALOG(4.*PI*WHT)
      GO TO 6
5     WHT=1000.0*W/T
```

```
      93                WT=PII*ALOG(2.0*WHT)
      94          6     CONTINUE
      95                HW=1./WH
      96                IF(WH.GT.1.) GO TO 7
      97                Z2=60.*ALOG(8.0*HW*WH/4.)
      98                Z1=Z2*EXP(Z2/60.)
      99                A1=10./(PI*ALOG(10.0))
     100                AO(L,M)=(A1*(8.*HW-WH/4.)*(1.0+HW+HW*WT))/Z1
     101                GO TO 8
     102          7     CONTINUE
     103                HW1=HW*HW
     104                HW2=(1.+HW)**5
     105                A2=20/(720.0*PI*PI*ALOG(10.0))
     106                AO(L,M)=A2*(1.0+0.44*HW1+6.0*HW1*HW2)*(1.0+WH*WT)
     107          8     CONTINUE
     108          C
     109          20    CONTINUE
     110                RS=PI*SQRT(4CO.*FR/SIGC)
     111                ALPHCO=RS*AO(L,M)/(10.0254*H)
     112                ALPHC=10.*ALPHCO*SQRT(EEF(L,M))
     113          C
     114          C     TOTAL LOSSES
     115          C
     116                ALPH=ALPHDI(L,M)+ALPHC
     117          C
     118          C     DISPERSIVE EFFECT
     119          C
     120                G=0.6+0.CO9*70
     121                FP=70*1.25/(10.0254*H*PI)
     122                FK=(FR/FP)**2
     123                EFD=ER-(ER-EEF(L,M))/(1.0+G*FK)
     124                VN=1./SQRT(EFD)
     125          C
     126          C     EFFECTIVE AIR LENGTH
     127                ALANO=299.8/FR
     128                ALAN=VN*ALANO
     129          30    CONTINUE
     130                EAL=AL*VN
     131                VP=ALAN*FR*0.01
     132          C
     133                PE=2.09579E-2*FR/VN
     134                COSPF=COS(PE*EAL)
     135                SINPF=SIN(PE*EAL)
     136                CNUM1=EXP(ALPH*EAL*ONP)*CMPLX(COSPE,SINPE)
     137                CNUM2=EXP(-ALPH*EAL*ONP)*CMPLX(COSPE,-SINPE)
     138                RETURN
     139                END

!GLOAD GO
LOADING WAS COMPLETED
!RGV
```

MICROSTRIP LINE PARAMETERS

RESD = 1.000000E 13
SIGC = 5.800000E 07
H = 25.0000
T = 15.0000
ER = 9.80000
FSTART = 1.00000
FINCR = 2.00000
NF = 11

Alumina

CHARACTERISTIC IMPA.= 50.0(OHMS) AIR LENGTH=20.0(MM)

FREQUENCY (GHZ)	EFF. LENGTH (MM)	EFFECTIVE DIELECTRIC	TOTAL LOSSES (DB/CM)	WAVE-LENGTH (MM)	PHASE VELOCITY (1E8*M/SEC)
1.0	7.778	4.611	.01586	116.599	1.1660
3.0	7.763	4.638	.02747	38.787	1.1636
5.0	7.732	4.691	.03547	23.180	1.1590
7.0	7.688	4.767	.04196	16.464	1.1525
9.0	7.635	4.862	.04758	12.716	1.1445
11.0	7.574	4.974	.05261	10.321	1.1353
13.0	7.508	7.094	.05719	8.657	1.1254
15.0	7.440	7.227	.06143	7.435	1.1152
17.0	7.371	7.362	.06540	6.500	1.1050
19.0	7.304	7.497	.06914	5.763	1.0949
21.0	7.240	7.631	.07268	5.168	1.0853

MICROSTRIP WIDTH= .621(MM)
STOP 0
!ROV

MICROSTRIP LINE PARAMETERS

RESD = 2000.00
SIGC = 5.800000E 07
H = 10.0000
T = 15.0000
ER = 11.7000
FSTART = 1.00000
FINCR = 2.00000
NF = 11

Silicon

CHARACTERISTIC IMPA.= 50.0(OHMS) AIR LENGTH=20.0(MM)

FREQUENCY (GHZ)	EFF. LENGTH (MM)	EFFECTIVE DIELECTRIC	TOTAL LOSSES (DB/CM)	WAVE-LENGTH (MM)	PHASE VELOCITY (1E8*M/SEC)
1.0	7.203	7.710	.22680	107.969	1.0797
3.0	7.200	7.714	.25862	35.977	1.0793
5.0	7.195	7.727	.28052	21.571	1.0785
7.0	7.188	7.743	.29833	15.392	1.0774
9.0	7.178	7.764	.31373	11.958	1.0759
11.0	7.166	7.790	.32749	9.765	1.0741
13.0	7.151	7.822	.34005	8.246	1.0720
15.0	7.135	7.858	.35167	7.130	1.0695
17.0	7.117	7.898	.36254	6.275	1.0668
19.0	7.097	7.942	.37279	5.599	1.0638
21.0	7.076	7.990	.38251	5.051	1.0606

MICROSTRIP WIDTH= .208(MM)
STOP 0
!ROV

MICROSTRIP LINE PARAMETERS

RESD = 1.000000E 07
SIGC = 5.800000E 07
H = 10.0000
T = 15.0000
ER = 12.5000
FSTART = 1.00000
FINCR = 2.00000
NF = 11

Gallium Arsenide

CHARACTERISTIC IMPA.= 50.0(OHMS) AIR LENGTH=20.0(MM)

FREQUENCY (GHZ)	EFF. LENGTH (MM)	EFFECTIVE DIELECTRIC	TOTAL LOSSES (DB/CM)	WAVE-LENGTH (MM)	PHASE VELOCITY (1E8*M/SEC)
1.0	6.997	8.171	.04627	104.883	1.0488
3.0	6.994	8.177	.08011	34.948	1.0484
5.0	6.989	8.188	.10341	20.954	1.0477
7.0	6.982	8.204	.12235	14.951	1.0466
9.0	6.972	8.224	.13873	11.612	1.0451
11.0	6.960	8.248	.15337	9.484	1.0433
13.0	6.946	8.277	.16673	8.009	1.0411
15.0	6.929	8.310	.17909	6.925	1.0387
17.0	6.911	8.346	.19066	6.094	1.0360
19.0	6.892	8.386	.20156	5.437	1.0331
21.0	6.871	8.429	.21190	4.904	1.0299

MICROSTRIP WIDTH= .194(MM)
STOP 0

APPENDIX (G)

CURVE FITTING TECHNIQUES

The problem is to choose the values of the unknown coefficients b to fit the set of measurements by a nonlinear function. The model is:

$$y_t = f(z_t, \beta) + \varepsilon_t \,, \quad t = 1, 2, \ldots m \qquad (1.9)$$

The least squares estimator of the parameters, b values, minimize $\phi(b) = \frac{1}{2}\underset{\sim}{e}'\underset{\sim}{e}$, where $e_t = y_t - f(z_t, b)$ are the residuals, $\underset{\sim}{e}$ and $\underset{\sim}{e}'$ are the column vector and row vector of m function e_t, respectively.

A gradient optimization technique may be used to minimize ϕ as a function of b's. In Chapter 8 and 9, the Gauss-Newton method [13-Chapter 8] was used in the following way: The gradient of ϕ is

$$\frac{\partial \phi(b)}{\partial b} = -G'\underset{\sim}{e} \,, \quad \text{where } G = \frac{\partial f}{\partial \beta} \qquad (2.9)$$

Gauss noticed that if the e_t are all linear functions of the b, so that ϕ is quadratic, then G' does not change from one point to another. Thus he suggested approximating the gradient at a point $b + \Delta b$ as follows

$$\frac{\partial \phi(b + \Delta b)}{\partial b} \approx -G'\underset{\sim}{e}(b + \Delta b) \qquad (3.9)$$

An approximation for $\underset{\sim}{e}(b + \Delta b)$ is obtained from the linear terms of the Taylor expansion about b.

$$\underset{\sim}{e}(b + \Delta b) \approx \underset{\sim}{e} + G\Delta b \qquad (4.9)$$

Combination of Equations (3.9) and (4.9) gives an estimate of the gradient at $b + \Delta b$.

$$\frac{\partial \phi(b+\Delta b)}{\partial b} \approx -G'(\underset{\sim}{e} + G\,\Delta b) = -(G'\underset{\sim}{e} + G'G\,\Delta b) \qquad (5.9)$$

Assuming $G'G$ is nonsingular and has an inverse $(G'G)^{-1}$, one can solve equation (5.9) for the correction Δb which drives all components of the gradient to zero and hence obtain:

$$\Delta b = d = (G'G)^{-1} G' \tilde{e} \qquad (6.9)$$

The point $b + \Delta b$ is where Gauss approximation predicts the minimum to be, since the gradient $\frac{\partial \phi}{\partial b}$ would vanish there. Gauss method is to measure the true values of $\tilde{e}(b + \lambda b)$ and $G'(b + \lambda d)$ to see whether the gradient $-G' \tilde{e}$ really vanishes. If it does, a stationary point has been found; if not, the information is used to generate a new approximation and further correction. The procedure calculates d from b^{I-1} and the corresponding residuals. If $|d_j / b_j^{I-1}| \leq$ TOLB, $J = 1, \ldots, m$, the procedure has converged, where TOLB is the convergence criterion for the parameters. If not, λ is searched over, starting at $\lambda = 1, \frac{1}{2}, \ldots \frac{1}{2}, \ldots$, until $\phi^I < \phi^{I-1}$, b^I is set equal to $b^{I-1} + \lambda d$ and the process is repeated.

APPENDIX(H)

EVALUATION OF PARASITIC JUNCTION PARAMETERS FOR STEP DISCONTINUITIES.

The equivalent circuit of Fig. 9.20 is redrawn for convenience as follows:-

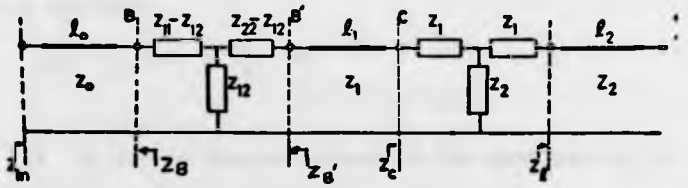

FIG. 1.h. THE EQUIVALENT CIRCUIT OF THE STEP JUNCTION WITH THE LAUNCHER.

Here, ℓ_o is the equivalent air length of the launcher; the first T-network represents the parasitic junction of the launcher to-microstrip, the second one represents the discontinuity effect for two microstrips ℓ_1 and ℓ_2 having widths w_1 and w_2 respectively.

Assuming Z_{in} is the input impedance, measured by the network analyzer, then the impedance at plane B is given by:

$$Z_B = Z_o \left[\frac{Z_{in} - jZ_o \tan \beta_o \ell_o}{Z_o - j Z_{in} \tan \beta_o \ell_o} \right] \qquad (1.h)$$

The impedance at plane B' then may be related to that of the B plane viz:

$$Z_{B'} = \frac{-Z_B Z_{22} + Z_{11} Z_{22} - Z_{12}^2}{Z_B - Z_{11}} \qquad (2.h)$$

Again the impedance at plane C is related via the following relationship: (looking towards generator)

$$Z_C = Z_1 \left[\frac{Z_{B'} - Z_1 \tanh \gamma \ell_1}{Z_1 - Z_{B'} \tanh \gamma \ell_1} \right] \qquad (3.h)$$

On the other hand this impedance is related to open circuit termination via the following relationship.

$$Z_c = \frac{Z_\ell Z_2 + Z_1^2 + 2Z_1 Z_2 + Z_1 Z_2}{Z_1 + Z_2 + Z_\ell} \qquad (4.h)$$

where Z_ℓ is the load impedance of an open circuit which is given as follows:

$$Z_\ell = Z_2 \coth \gamma(\ell_2 + \Delta\ell) \qquad (5.h)$$

where $\Delta\ell$ is due to the end effect of the open microstrip line.

APPENDIX (I).

JUNCTION PARASITIC OF RIGHT-ANGLE BEND IN MICROSTRIP LINE.

Let ℓ_1 and ℓ_2 be the two lengths of right-angle bend along the central axis up to terminal planes T_1' and T_2', as shown in Fig. I.Ia. Utilizing a conformal mapping technique, we may transfer the area inside of the right-angle bend at plane Z to the upper half of another plane, W, by the following transformations [Ref. 28, p.157 of Chapter 9].

$$Z = \cos^{-1}\frac{b-2W}{b} + \sqrt{b-1}\ \cosh^{-1}\frac{bW + b - 2W}{b(1-W)} \qquad (1.1)$$

where the strip width is $\pi\sqrt{b-1}$. For convenience we may assume the strip width is π, hence transformation of (1.1) reduce to:

$$Z = \cos^{-1}(1-W) + \cosh^{-1}\left[1/(1-W)\right] \qquad (2.1)$$

using an intermediate transformation $W = \tanh\xi$, this upper half W-plane may be transformed into an infinite long strip $\pi/2$ wide Fig.(I.Ic).

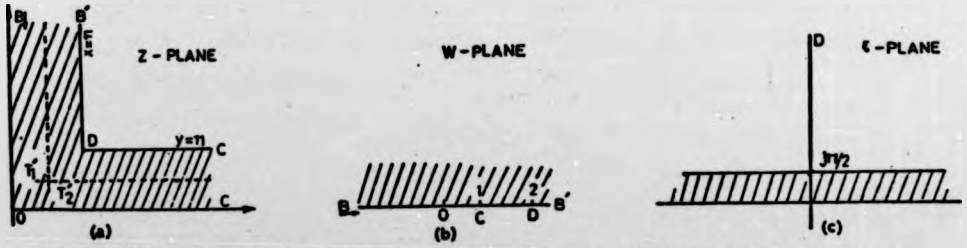

FIG. 1.1 (a) THE RIGHT-ANGLE BEND ON THE Z-PLANE; (b) Z-PLANE TRANSFORMED TO UPPER HALF OF THE W-PLANE; (c) UPPER HALF OF W-PLANE TRANSFORMED TO A STRIP $\pi/2$ WIDE IN THE ζ-PLANE.

Substituting this intermediate transformation into (2.1) we obtain:

$$Z = \cos^{-1}(1 - \tanh\xi) + \cosh^{-1}\left[1/(1 - \tanh\xi)\right] \qquad (3.1)$$

Suppose now ξ is a real. Taking two large values of x_1 and $-y_1$, then since $1-\tanh x = 2e^{-2x}$, (3.1) for x_1 value reduces to:

$$Z = \cos^{-1}(2e^{-2x_1}) + \cosh^{-1}(e^{2x_1}/2) = \Pi/2 + 2x_1 \qquad (4.1)$$

similarly, for $-y_1$:

$$Z = \cos^{-1}(2e^{2y_1}) + \cosh^{-1}(e^{-2y_1}/2) = j(\ell n 4 + 2y_1 + \Pi/2) \qquad (5.1)$$

By comparing (4.1) and (5.1), it easily follows that the total length on the long side is reduced by $\ell n 4$ for the strip of width Π. More generally, for a strip of w width the reduction is:

$$\frac{w\ell n 4}{\Pi} = 0.441w.$$

PUBLICATIONS

(I) Electron. Lett. Vol. 12, No. 8, 15th April (1976) pp. 190-192.

(II) IMEKO VII , Vol. No. 2, 10-14 May (1976) London paper, BEL/211.

(III) Electron. Lett. Vol. 12, No. 19, 15th Sept. (1976) pp. 496-497.

(IV) IEE Colloquium on microwave integrated circuit, Digest No. 1976/93, London 28 Oct. (1976) paper 4.

(V) Submitted to the Conference on Programmable Instrument, to be held at The National Physical Laboratory, Teddington, Middlesex, on 22nd and 23rd Nov. (1977).

(1) Electron. Lett. Vol. 12, No. 8, 15th April (1976) pp. 190-192.

OPTIMAL: A PROGRAM FOR OPTIMISING MICROSTRIP NETWORKS*

Indexing terms: Electronics applications of computers, Microwave amplifiers, Optimisation, Solid-state microwave circuits, Striplines

An optimisation program OPTIMAL is described which includes algorithms for dispersion and loss in microstrip. The optimisation routine combines pseudorandom and conjugate gradient pattern-search techniques to improve the chances of finding a global-minimum solution to multimodal problems. The optimisation of a GaAs f.e.t. amplifier shows the program's ability to produce good results from poor starting values.

Introduction: Microstrip, because of its light weight, small dimensions and easy processing capability, is being increasingly used for microwave circuit design up to J-band. General-purpose transmission-line analysis programs have been adapted for microstrip circuits by specifying microstrip elements as operating in a TEM mode. This approach works well up to S-band,[1,2] but at higher frequencies spurious propagating modes introduce dispersive effects which make the simple TEM model inaccurate.

Many optimisation programs are now available which make use of these general circuit analysis programs.[3] In general, the optimisation programs are based on 'sequential' or 'linear search algorithms', in which previously generated points are used to determine the new direction of search. Although extremely efficient in determining the minima of unimodal functions, for multivariable, multimodal problems, such as those encountered in amplifier optimisation, a sequential search program will converge to the nearest local minimum, ignoring neighbouring, but possibly better, minima.

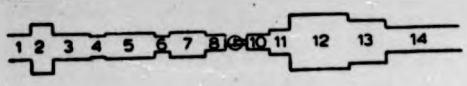

Fig. 1

* The program listing and accompanying documentation are held in the IEE Library, Savoy Place, London WC2R 0BL, England. For further information, please contact the Library, quoting CP131

Table 1

Elements		1	2	3	4	5	6	7	8	9	10	11	12	13	14
Initial values	Ω	50	−16	50	−43	50	95	−30	95	Tr.	−95	−43	−19	−30	50
	mm	3·8	−4·4	−5·4	−4·1	−5·1	1·9	−5·2	−2·5		−1·2	−4·4	−2·8	−8·6	13·6
Final values	Ω	50	23	50	49·9	50	95	46	95	Tr.	100	44·5	20·9	27·5	50
	mm	3·8	2·8	5·5	2·4	8·7	1·9	6·6	2·9		4·3	2·1	8·8	7·2	13·6

This letter describes a microstrip analysis and optimisation program OPTIMAL which has several novel features:

(*a*) The analysis routine incorporates Getsinger's model for microstrip dispersion[4] and includes an algorithm for determining conductor loss in microstrip lines.

(*b*) The optimisation routine makes use of a large-step pseudorandom search technique to increase the chances of finding a global minimum.

(*c*) Having located a promising valley, the program switches to efficient conjugate gradient technique to converge quickly to the minimum.

As this program is designed mainly to deal with active 2-port devices, the letter concludes by showing the results of the optimisation of an X-band GaAs f.e.t. amplifier design.

Program description: The program OPTIMAL has been written for cascades of 2-port circuit elements. It employs a least *p*th objective function based on the following network responses: (*a*) transducer gain, (*b*) ripple gain and (*c*) input/output reflection coefficient.

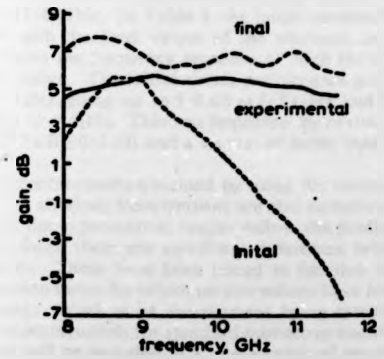

Fig. 2

Eight basic types of circuit element are available. They include transistors which are not optimised and represented by their *s*-parameters, transmission lines, short- or open-circuited shunt stubs, series series, series parallel, shunt series, shunt parallel of inductor-capacitor-resistor, L-section of transmission line. A negative initial value for any parameter indicates that this parameter is to be varied during optimisation and thus a lower and upper bound for each varied element will be punched afterwards in the same card (see also program details).

Analysis: In the course of development of any computer program, two conflicting requirements emerge: one is to perform the analysis as quickly as possible, by making the program highly specific, the other is to relate the method of computation to the general usage capability of the program. The *s*-parameters (*S*) approach was chosen, since it is ideally suited to these requirements. It is obvious that the inability to use *s*-parameters in chain matrices is the result of the decision to take reflected waves as dependent variables and incident waves as independent. Therefore transmission parameters (*T*), which have properties similar to those of the (*ABCD*) set, have been used in the analysis routine.

The calculations required for the transformation from (*S*) to (*T*) are slightly less complex than those required from (*S*) to (*ABCD*). For a higher calculation efficiency, the (*T*) set have therefore been used for cascading; thus the analysis program deals with elements connected in cascade and terminated with 50 Ω loads at the inputs and outputs. It also contains algorithms for dealing with loss and dispersion in microstrip elements for a variety of dielectric substrates. A facility also exists within the program for converting transmission-line elements from their air lengths and characteristic impedances to dimensions compatible with microstrip substrates.

Optimisation: This section of the program has two parts; the large-step pseudorandom search algorithm known as PRANCE and a conjugate gradient search to locate the final minimum.

PRANCE: The nonunilateral properties of the GaAs f.e.t. and bipolar transistor in microwave amplifier circuits means that no element is entirely isolated from any other in its effects on the overall response. For this reason the authors have used an approach similar to Emery and O'Hagan's 'spider method',[5] in which the variables are chosen in a pseudorandom sequence. This reduces the possibility of the

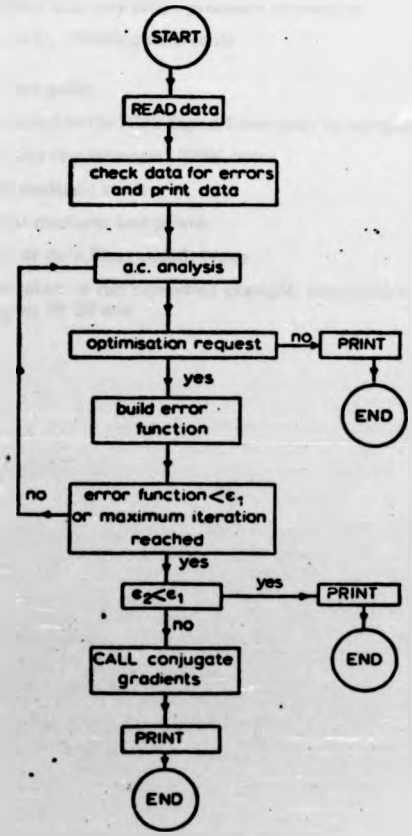

Fig. 3 *Flow diagram*

optimum-following algorithm concentrating on certain variables to the exclusion of others, thereby causing false minima to be obtained.

The variable to be examined is chosen by an algorithm in which a random number is obtained by multiplying the error between computed and specified circuit performance by 10^6 and selecting the last two integers. Since the chances that the error will be identical for any two values of variable are extremely remote, this simple technique guarantees a number sufficiently random for the purposes of PRANCE.

Once the first element is chosen, a combination of successive error multiplication by 10^6 and modular arithmetic will ensure that each of the remaining variables will be examined once in as random a manner as possible.

The objective function is the least pth form, where p can have any value between 6 and 60. Initially, element values are varied by 4% for distributed elements and 8% for discrete elements, although this step size is automatically varied within the program, depending on the success rate in minimising the objective function.

Conjugate gradient: In the last stage, the objective function is minimised by the Fletcher-and-Reeves algorithm[6] which the new circuit values select, by a conjugate gradient pattern search. By this technique, each new direction of search is calculated as part of the iteration cycle. The method is inherently more powerful than those in which the directions are assigned in advance.

OPTIMAL application to GaAs-f.e.t.-amplifier design: This provides a good example of the ability of OPTIMAL to produce results from poor starting values. The amplifier circuit is shown in Fig. 1. The goal was to achieve a flat 7 dB power gain and 1·5:1 v.s.w.r. at both input and output over the range 8–11·6 GHz. In Table 1, the initial parameter values, together with the final values of the elements, are shown. Fig. 2 shows the frequency response of both the initial and the final design. The initial circuit performance gave 1·2 dB gain at 8 GHz, going up to 5·8 dB at 8·8 GHz, and falling to −6 dB at 11·6 GHz. This was improved by OPTIMAL to give a gain of 7 dB ± 0·5 dB and a v.s.w.r. of better than 2:1 over the band.

Experimental results obtained by using the microstrip line dimensions obtained from OPTIMAL are also included in Fig. 2. Although the experimental results follow the predicted gain response shape there are significant differences between the two curves. These have been traced to junction parasitics and radiation losses for which no corrections have been made in OPTIMAL. Work is at the moment being carried out to obtain accurate models for standard microstrip discontinuities and these will be included in a new version of OPTIMAL.

Acknowledgments: Some part of this work is supported by the UK Science Research Council. The authors wish to thank A. J. Tebby for developing the pseudorandom search technique. The letter is published by kind permission of the Directors of The Plessey Company Ltd.

N. M. HOSSEINI
V. H. SHURMER

Department of Engineering
University of Warwick
Coventry CV4 7AL, England

R. A. SOARES

The Plessey Company Ltd.
Towcester, England

8th March 1976

References

1 GELNOVATCH, V. G., and CHASE, I. L.: 'DEMON—an optimal seeking computer program for the design of microwave circuits', *J. Solid-State Circuits*, 1970, SC-5, pp. 303–309
2 HOUSTON, T. W., and READ, L.W.: 'Computer aided design of broad and low noise microwave amplifiers', *IEEE Trans.*, 1969, MTT-17, pp. 612–619
3 SOARES, R. A.: 'Amplifier design using bipolar transistors' Ph.D. Thesis, London University, 1974
4 GETSINGER, W. J.: 'Microstrip dispersions model', *IEEE Trans.*, 1973, MTT-21, p. 34
5 EMERY, F. E., and O'HAGAN, M.: 'Optimal design of matching network for microwave transistor', *ibid.*, 1966, MTT-14, pp. 696–698
6 FLETCHER, R., and REEVES, C. M.: 'Function minimisation by conjugate gradients', *Comput. J.*, 1964, 7, (2), p. 149

Program details

(*a*) FORTRAN IV

(*b*) A maximum of 60 network types

(*c*) Complex and only single precision arithmetic

(*d*) 963 cards, including comments

Performance guide

(*a*) It is loaded on the XDS-Sigma 5 computer by using overlay

(*b*) Core-size requirements: 50896 bytes

(*c*) Input medium: cards

(*d*) Output medium: line printer

(*e*) Work or data files needed: None

(*f*) Time taken to run submitted example: compilation 4·10 min, run 19·20 min

IMEKO VII

(II) IMEKO IIV, Vol. No. 2, 10-14 May (1976) London paper, BEL/211.

THE APPLICATION OF AN ON-LINE COMPUTER TO MICROWAVE MEASUREMENT

H.V. Shurmer*, H.E.G. Luxton*, N.M. Hosseini*, Katie A. Stoneman*

Some of the many problems encountered in setting up an automatic computer-corrected s-parameter measurements facility are discussed for a system which has been developed from standard commercial items of equipment. The programming techniques which have been employed to provide a time-sharing capability are described, together with the various options made available to the operator. Examples of applications to device development are given and results pertaining to optimization studies in component design are also presented. The latest work on an extension of the facility to include optimised automatic noise figure measurements is also outlined.

INTRODUCTION

Automatic network analyser packaged systems, first described by Hackborn (1), have now become an an accepted part of the facilities of major standards laboratories throughout the world. Such systems, which include a dedicated computer, provide excellent service but they require a very high initial capital outlay and tend to be relatively inflexible with restricted peripherals (e.g. a punched paper tape reader input and a teleprinter output). This arises because the peripherals are also dedicated to the packaged system and inflexibility is enhanced as the users are not usually anxious to become involved in the complexities of modifying the computer programmes supplied by the equipment manufacturers. A significant fraction of the cost of such systems arises from their use of frequency synthesis, which although desirable, is not essential, except where standards laboratory levels of accuracy are demanded.

The alternative to such packages, which has been adopted at Warwick, is to develop systems based on computers intended for process control, incorporating assemblages of separate component items and making maximum use of facilities already available. Initial development here started in 1969 with a GEC 90/2 computer, a Hewlett-Packard network analyser Type 8410, with reflection test unit, and an ASR 35 teletype for input keying and output listing (2). At this early stage the programming was performed in the assembly language SYMBOL and the correction procedure was based on the theory of bilinear transformations (3). A visual record of corrected reflection parameters was obtained by photographing graphical plots obtained on a storage oscilloscope.

When an XDS Sigma 5 control computer became available within the Engineering Department in 1970, this enabled programmes to be written in FORTRAN and the potential of the facility was immediately greatly increased. It was decided then to re-model the facility along the general lines already adopted in the U.S.A. (4) and present results in the form of sets of corrected two-port s-parameters, but at the same time aiming at maximum flexibility with regard to options and programme extension.

Additional significant items of hardware have subsequently been assimilated into this facility, which today represents a powerful research tool for the characterisation of components and devices in terms of wide-band s-parameters, which are automatically corrected for system and transition errors. The present equipment permits a frequency coverage from 100 MHz up to about 16 GHz, but plans to increase the upper limit are in hand. The results, for any chosen option, may be shown graphically on a visual display unit (from which hard copies may be taken), tabulated by a line printer or dumped on to magnetic tape for further analysis or subsequent processing as a background activity within the time-sharing arrangements of the computer.

Close attention to the requirements of industry has been maintained, particularly with regard

*Department of Engineering, University of Warwick, Coventry, England.

to the need for special options, level of accuracy and novel strip-line device mounting arrangements, involving new calibration procedures. Members of industrial organisations are currently making significant use of the facility in developing microwave oscillators and amplifiers.

BASIC PRINCIPLES

With on-line computer correction of s-parameter measurements, errors inherent in the system, together with those arising from transitions, mounting arrangements, etc., are first stored in the computer during a series of preliminary calibration runs, in which standard terminations are used, such as a short-circuit, off-set short circuit, matched load or a 'through-line'. In general, there will need to be as many calibration runs as there are error parameters to be corrected (5), (6), (7).

During the preliminary runs, the corresponding s-parameters, as measured by the network analyser, are stored by the computer for a succession of precise frequency steps over a pre-selected bandwidth. Since the true impedance values are accurately known, from these results the values of the error parameters may be computed through the solution of a corresponding number of simultaneous equations. Subsequent runs, using the test sample to be characterised, are carried out at the same precise frequency steps. The results thus obtained may be used in conjunction with the stored values of the error parameters to compute corrected values of the various s-parameters of the test sample, stepped over the entire predetermined bandwidth. Subsequent test samples of the same form may be measured without further calibration.

COMPUTER OPERATIONS

Three basic requirements in the system are fulfilled by the computer, viz:

1. Control of the measurement procedure.
2. Storage and processing of data to obtain the corrected results.
3. Presentation of output data.

The computer performs operations as instructed by the operator via a V.D.U. (Visual Display Unit) with an input keyboard. A set of instructions for two-port correction, with typical responses, is shown in Fig. 1. The questions appear on the screen one at a time and after each one the computer waits until there is entered on the keyboard either a number plus C.R. (carriage return), or a 'Y', which is automatically completed to a 'YES' on the screen, or an 'N', which is likewise completed to a 'NO'. The answer is stored and the next question appears. The various procedures in the calibration routine are identified by the 'K' values 1-15, which facilitates the repeating of any particular stage. This can be effected by typing 'N' in response to a question, whereupon the V.D.U. displays 'TASK?'. The typing of 'SK' at this stage permits a repeat run corresponding to any particular selection of K, which is then entered. The full set of options available under 'TASK?' is shown in the list of Fig. 2, which is displayed on the V.D.U. in response to typing the letters 'LI'. The subsequent entering of any of the listed letter pairs will permit the related function to be accomplished.

The network analyser is sited remotely from the computer but within the same building. Ten channels for data or control are available, to be shared between individual parts of the system. As this is less than the number of functions to be provided, some of the lines have been multiplexed, either by employing several levels of direct voltage or by using polarity to distinguish between signals.

CONTROL OF THE NETWORK ANALYSER

Using receipt of a given instruction, the computer will select the s-parameter corresponding to the desired reflection or transmission measurement. It will then set the frequency and read the output from the network analyser. These functions are performed via the interface units, which are illustrated in Fig. 3. The s-parameter test set is controlled through application of a direct voltage, whose level it interprets as a 3-bit binary word and thus a single analogue line substitutes for three digital lines.

The sweep oscillators are multiplexed in groups of three, which can be changed at will. Any particular one of these units may be chosen by the s-parameter selector, again through application of a direct voltage, but this time interpreted as a 4-bit binary word. The frequency which is output by the selected unit is set by the programmable voltage source. This is an item specially developed for the purpose from a stabilised power unit whose output was controlled by manual decade switching. In the present unit, the switching is accomplished electronically and the voltage increased progressively in steps of 1mV over the range 3V to 73V, corresponding to the full frequency range of each of the sweep oscillators. Each step requires one voltage pulse from the computer and the rate at which these are supplied is 30,000 p.p.s. The particular step of voltage

which is required to output the next frequency, at any stage of the calibration or testing, is determined by data stored in the computer. This data is obtained from preliminary calibration of the sweep oscillators. Operation of the programmable voltage source requires three separate lines from the computer, which provide initialization, output and cancellation of the tuning voltage, respectively.

As each particular frequency is set up, it is read by the automatic frequency counter, which has now replaced an earlier counter requiring semi-manual tuning and for which a servo control system had been developed, but which was relatively slow in operation. The reading from the automatic counter is fed back to the computer along a single channel, after conversion of the counter output from eight parallel bits into a serialized form. By using both positive and negative analogue voltages, a second channel serves to carry either clock pulses for the serializer or control instructions for the computer. The circuit arrangement of the interface units is illustrated schematically in Fig. 4.

The output from the network analyser to the computer comprises two analogue voltages, which correspond to the real and imaginary parts, respectively, of the s-parameter being measured. These voltages are stepped up via buffer amplifiers before being transmitted, in order to give improved signal-to-noise ratios at the analogue inputs of the computer.

In the present system, nine of the ten channels available are used. Work is, however, proceeding on the introduction of a phase-locked loop system to improve both the frequency accuracy and frequency stability of the microwave sources. As this would normally be expected to require at least two channels, in order to keep the total number within the ten available, the solution adopted will probably be to multiplex the inputs to the programmable voltage source. It has been demonstrated already that stepping through a given frequency range with phase locking can be accomplished at the lower microwave frequencies, but problems are encountered in the vicinity of 10 GHz due to the high orders of crystal harmonic which are involved.

The introduction of a phase-locking system will undoubtedly extend the measurement 'read' times, at present some 300 ms per point, since a significant pause is required at each step for the locking to be effected. There is additionally a waiting period of 2 s at the start of each sweep over the frequency bandwidth, which is just sufficient to ensure that transient effects in the system have died away by the time the next set of readings from the network analyser is transmitted to the computer. The total time taken by the present system for automatic measurement of the four s-parameters of a 2-port device over 50 steps in frequency is 100 s.

PROGRAMMING

The Sigma 5 computer has 32 K storage capacity, backed by an R.A.D. (rapid access disc) of 1.5 Megabytes, each of which represents one quarter of a 32-bit computer word. There are foreground and background areas to the core, tasks in the former area being executed according to a priority interrupt system. The background area is available for batch processing.

The programming is almost entirely in FORTRAN IV, with some interjection of machine code. The programmes are each written as a series of subroutines, which greatly facilitates versatility. The main programme covers the full set of s-parameters for a 2-port device, but a shorter version has also been prepared for use when reflection parameters only are required. Both of these have been overlayed for use in a time-sharing environment. Certain other correction programmes are also available, without overlaying, which are intended for special applications. Programming is done via punched cards and the information is subsequently transferred to magnetic tape. The user controls the programme through a series of questions and answers of the form already described (Fig. 1).

The main programme comprises four principal sections:-

(a) Calibration and Reading Control - calls correction and reading sub-routines.

(b) Line Printer Routine - available for tabulated results.

(c) V.D.U. Display Control - calls graph plotting sub-routines.

(d) Initialization and Task Control - calls data set-up, initialization, tape-dumping sub-routines, etc.

A general flow-chart of the routine for s-parameter measurements is shown in Fig. 5. That part of it which relates to the setting up of each frequency and the recording of network analyser readings is shown in more detail in Fig. 6.

FORMS OF GRAPHICAL DISPLAY

The display options are made available under 'TASK?' by entering the letters DI on the keyboard (Fig. 1). They include the choice of polar or rectangular form. Up to four variables may be plotted at once and any combination of the four uncorrected s-parameters with the four corrected s-parameters is possible, with the main programme.

An example of a polar plot for the corrected and uncorrected reflection s-parameter, s_{11} and U_{11} respectively, is shown in Fig. 7, which is a hard copy of a V.D.U. display and pertains to an off-set short-circuit measured over the bandwidth 7-12 GHz. In all of the displays, the uncorrected s-parameters are shown with the points joined by straight lines and the corrected s-parameters as isolated points. Circles are used to indicate the forward reflection parameters and triangles the reverse transmission parameters. In a similar manner the programme makes available squares and crosses, which are used to represent the reverse reflection and forward transmission parameters,repsectively. It will be noted that in Fig. 7 an uncorrected plot with significant errors has been correctly modified by the computer to give the theoretical arc of circle of unity radius appropriate to an off-set short circuit.

The uncompleted message 'MAX X =' in Fig. 7 is inviting a response in the form of a number to be typed on the V.D.U. keyboard, should it be desired to have the plots expanded. The number to be entered is the maximum value of the x-coordinate. Upon provision of this information a similar uncompleted message requests the minimum value for the X- coordinate, whereupon the procedures are repeated for the Y- coordinates. After entering the four numbers, the corresponding expanded plot appears and the whole process can be repeated indefinitely for different values, or dispensed with altogether.

An alternative form of plot, using rectangular coordinates with linear scales, is illustrated in Fig. 8 which pertains to measurements on a section of 50-ohm air-line both corrected and uncorrected forward reflection and reverse transmission s-parameters over 7-12 GHz. This time, the irregular uncorrected curves are correctly modified to horizontal straight lines at Y- coordinate levels of zero and unity, respectively. An even more impressive example of correction is shown in Fig. 9, which pertains to the same set of reverse transmission s-parameters as in Fig. 8, but this time showing phase angle only, as a function of frequency. It will be noted that phase angles varying cyclically between zero and ± 180° are all set at their correct value of zero by the programme.

APPLICATIONS

Much use has been made of the system in characterising Plessey gallium arsenide field-effect transistors at frequencies extending beyond 11 GHz. One method is to mount the transistors on alumina substrates with 50 ohm input and output lines, calibration being effected by means of a combination of microstrip and coaxial terminations.

Following calibration, the transistor under test is measured and a print-out is obtained of the various corrected s-parameters, together with gain and stability computations, if required. The latter form particularly useful data in comparing the potential amplifier performance of different devices.

A predicted gain of 6 dB at 11 GHz for a F.E.T. of 1 micron gate length was achieved within 0.5 dB. For two similar F.E.T.'s in cascade the initial measured overall gain was 9 dB, which compared unfavourably with the predicted value of 12 dB. Subsequent adjustment of the output tuning, however, resulted in the overall gain being increased to 11.5 dB - a very satisfactory result.

In Fig. 10 are shown results obtained with the aid of the present system in seeking to optimize the gain of a single-stage gallium arsenide field effect transistor amplifier over the bandwidth 8-11.6 GHz. The extent of the optimization process involved is indicated by Fig. 11, each of the numbered blocks representing a section of transmission line of different characteristic impedance and length, the lengths being disposable variables. The initial results are shown by the curve A and the predicted optimized results by the curve B. After modifying the circuit in accordance with the values derived via the optimization programme (known as 'OPTIMAL') the experimental curve C was obtained. The differences between curves B and C are accounted for by junction parasitics and radiation losses, which were not allowed for in the present programme but will be included in a new version which is in hand.

It has been demonstrated that the computerized system can be controlled from a distant terminal via G.P.O. telephone lines. The present system has in fact been controlled from the University of Sussex, where corrected graphical displays of s-parameters have been received on-line from the Warwick equipment. It is hoped eventually to extend this aspect of the facility via radio links overseas and plans for achieving this are under active considersideration.

Work is now in progress aimed at establishing a computer-controlled automatic noise measure-

ment system to obviate the slow and tedious procedures traditionally involved in the measurement of noise figures, especially where the noise contribution of the second stage precludes a direct measurement of the noise figure of the first stage.

In this exercise, a noise figure/gain monitor (AILTECH 7380) is being used in conjunction with the XDS Sigma 5 computer and Tektronix V.D.U. to provide a virtually instantaneous calculation and display of the noise figures and subsidiary parameters for microwave devices over the frequency range 1-12 GHz. A double-balanced image-rejection mixer is being used to obviate the need for separate filters at each frequency of measurement. Slide-screw tuners, servo-operated via stepping motors, are to be incorporated to match the amplifying devices. The positioning of the tuning elements, and hence the impedance mismatch presented to the test device, will be controlled by the computer. With this type of arrangement it will be possible to search for noise minima, gain maxima and Smith Chart contours of specified noise figure or gain.

Using the above system, calibrated values of impedance and loss for the slide-screw tuners can be stored, to be used in subsequent determination and display of automatically corrected values of the various parameters. These techniques offer the prospect of significant improvements in accuracy and consistency compared with present-day manual arrangements, in addition to a striking saving in effort, as well as extending the scope of measurements into regions which are unjustifiable for conventional techniques.

Finally, we would mention the work being done at Warwick on microprocessors by our colleague Mr. J.F. Craine, who is aiming to apply the latest integrated circuits offered in this area to extensions of the overall facility. Where subsidiary functions, such as phase-locking, can be divorced from the main computer, these will in due course be taken over by microprocessors incorporated into the system, thereby increasing further the scope of conceivable operations.

ACKNOWLEDGEMENTS

The authors gratefully acknowledge the contributions of their colleagues, past and present, at the University of Warwick, with support from the Science Research Council, Plessey Allen Clark Research Centre and G.E.C. Ltd.

REFERENCES

1. Hackborn, R.A., An automatic network analyser system. Microwave J. 1968, 11, 45.

2. Shurmer, H.V., Low-level programming for the on-line correction of microwave measurements. Radio and Electron Engr. 1971, 41, 357.

3. Shurmer, H.V., Corrections of a Smith-Chart display through bilinear transformations. Electron. Lett., 1969, 5, 209.

4. Hand, B.P., Developing accuracy specifications for automatic network analyser systems. Hewlett-Packard J., 1972, 21, 16.

5. DaSilva, E.F., and McPhun, M.K., A new method of calibrating a microwave network analyser for computer-corrected s-parameter measurements. Electron. Lett., 1973, 9, 126.

6. Shurmer, H.V., Calibration procedure for computer-corrected s-parameter characterisation of device mounted in microstrip. Electron. Lett., 1973, 9, 323.

7. Woods, D., Rigorous derivation of computer corrected network analyser calibration equations. Electron. Lett., 1975, 11, 403.

```
2-PORT FULL CORRECTION PROGRAM
ARE AMPLIFIERS IN USE? TYPE Y OR N YES
WAVEGUIDE OR COAX - TYPE W OR C '' COAX
LENGTH OF OFFSET SHORT  C11  = 1.0
IS JOYSTIK IN USE? TYPE Y OR N NO
NO. OF POINTS PER READING   10
TIMING INTERVAL (N   0.01 SEC).  N = 30
INPUTS TAKEN FROM POLAR DISPLAY OR PHASE GAIN UNIT
TYPE LOG. LIN. OR POL  POL
CENTRE BEAM WHILE TYPING ANY CHARACTER k
MAXIMUM FREQUENCY (GHZ) = 2.0
MINIMUM FREQUENCY (GHZ) = 1.0
NO. OF POINTS = 5
MINIMUM FREQUENCY SET UP
CORRECTION TO FREQ. IN MHZ = N.N
CORRECTION TO FREQ. IN MHZ = 0

K=1   CONNECT MATCHED LOAD''YES
K=2   SLIDE LOAD''YES
K=3   SLIDE LOAD''YES
K=4   SLIDE LOAD''YES
K=5    CONNECT MATCHED LOAD''YES
K=6    SLIDE LOAD''YES
K=7    SLIDE LOAD''YES
K=8    SLIDE LOAD''YES
K=9    FWD TRANSM  2 MATCHED LOADS''YES
K=10   REV TRANSM  2 MATCHED LOADS''YES
K=11   S/C ON PART 1''YES
K=12   OFFSET SHORT ON PORT  2''YES
K=13   SHORT CIRCUIT ON PORT 2''YES
K=14   OFFSET SHORT ON PORT 1''YES
K=15   CONNECT THRO LINE''YES
NEW DEVICE? ''YES
IDENTIFY DEVICE & TERMINATE WITH CR
TEST RUN ONLY

K=19   CONNECT DEVICE''
```

FIG.1. INSTRUCTIONS FOR 2 PORT CORRECTION

```
TASK    (TYPE L1 FOR LIST OF OPTIONS) ''
TASK OPTIONS - TWO LETTER KEYS REQUIRED
L1   LIST OPTIONS            ZE  RESTART PROGRAM
BG   RESTART CALIBRATION     RE  REPEAT LAST READING
SK   RESET K (SEE BELOW)     ND  GO TO NEW DEVICE
CA   CALCULATE               PR  PRINT
DI   ENTER DISPLAY           DU  DUMP READINGS
UD   UNDUMP READINGS         ST  RELEASE PROGRAM
CO   INSERT COMMENT          CE  CENTRE BEAM
AM   RESET AMPLIFIERS        IN  RESET INPUT TYPE
WA   WAVEGUIDE OR COA        CL  DEFINE CALIB PIECES
JO   JOYSTICK SWITCH         FR  RESET FREQ RANGE
MF   CORRECT MIN FREQ        NO  RESET NO. POINTS
TI   RESET TIMING INT        TP  UPDATE TAPE FORMAT
DC   DISC FILE CLEAR

SETTINGS FOR K IN SK OPTION
K=1   CONNECT MATCHED LOAD ON PORT 1
K=2   SLIDE LOAD
K=3   SLIDE LOAD
K=4   SLIDE LOAD
K=5   CONNECT MATCHED LOAD ON PORT 2
K=6   SLIDE LOAD
K=7   SLIDE LOAD
K=8   SLIDE LOAD
K=9   FWD TRANSM  2 MATCHED LOADS
K=10  REV TRANSM  2 MATCHED LOADS
K=11  SHORT CIRCUIT ON PORT 1
K=12  OFFSET SHORT 1 ON PORT 2
K=13  SHORT CIRCUIT ON PORT 2
K=14  OFFSET SHORT 1 ON PORT 1
K=15  CONNECT THROUGH LINE

K=19  CONNECT DEVICE
```

FIG 2 'TASK OPERATIONS'

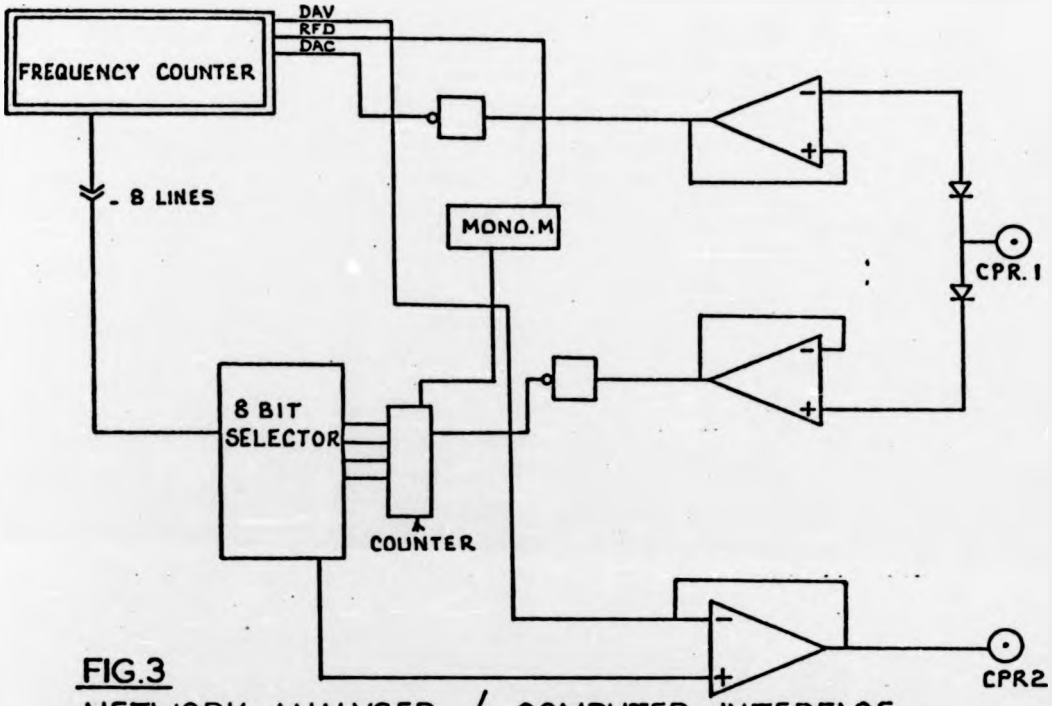

FIG.3
NETWORK ANALYSER / COMPUTER INTERFACE

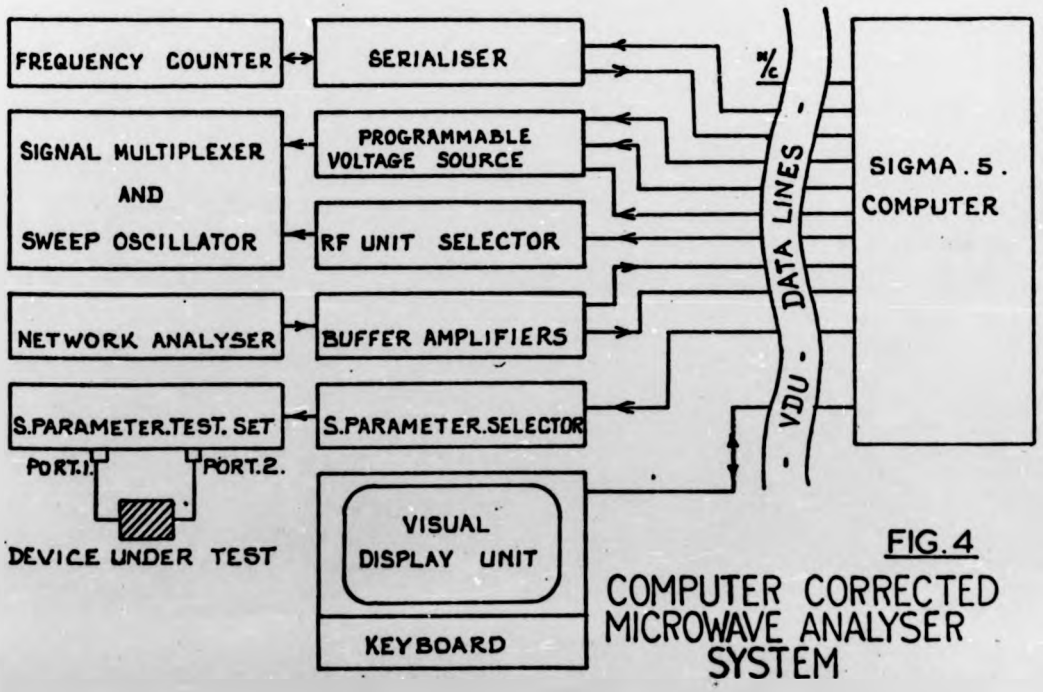

FIG.4
COMPUTER CORRECTED MICROWAVE ANALYSER SYSTEM

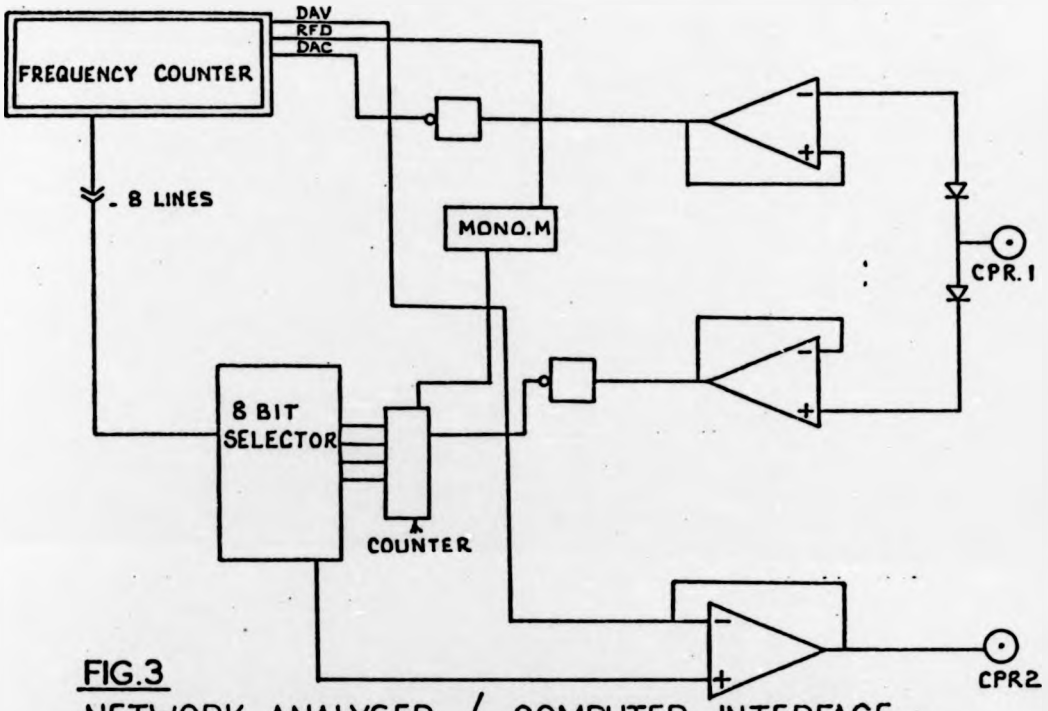

FIG.3
NETWORK ANALYSER / COMPUTER INTERFACE

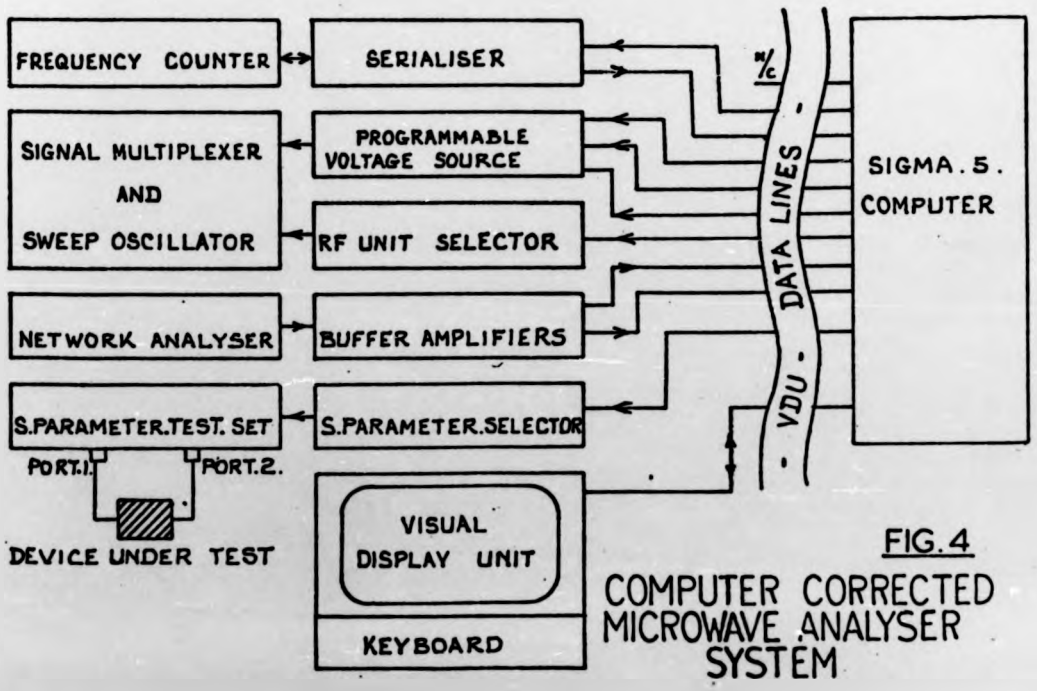

FIG.4
COMPUTER CORRECTED MICROWAVE ANALYSER SYSTEM

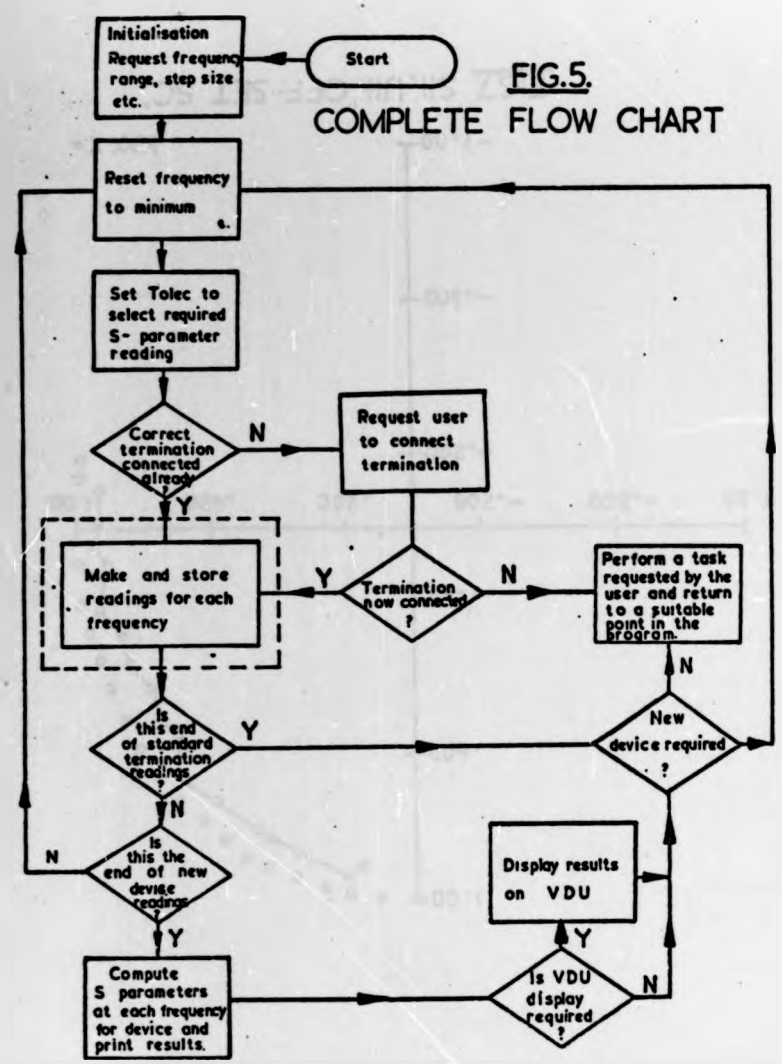

FIG.5.
COMPLETE FLOW CHART

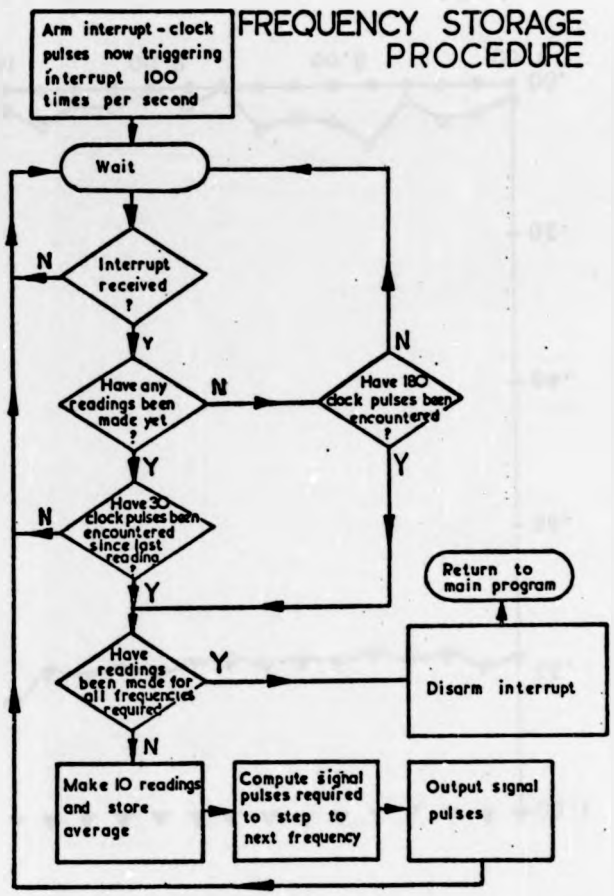

FIG.6.
FREQUENCY STORAGE PROCEDURE

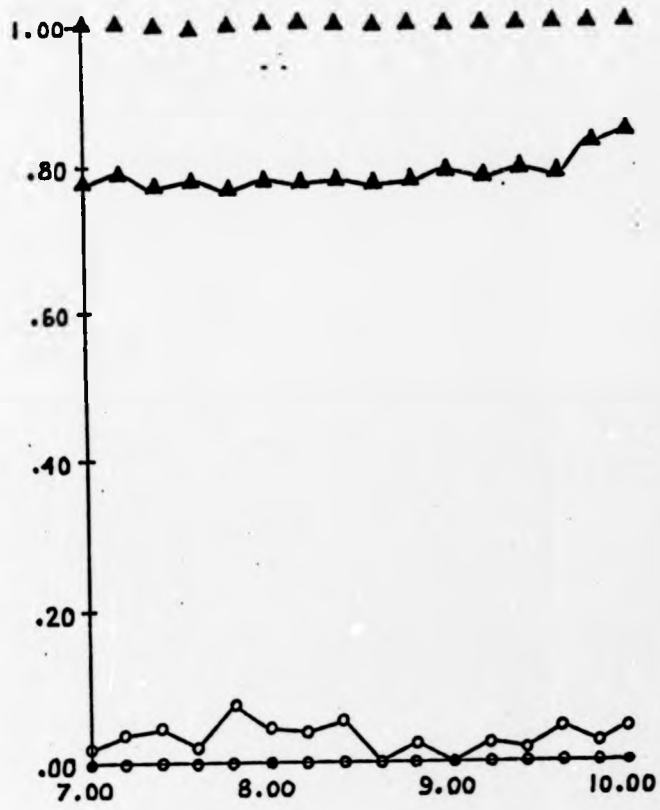

FIG.8. SII.SI2.UII.UI2:'THROUGH LINE'

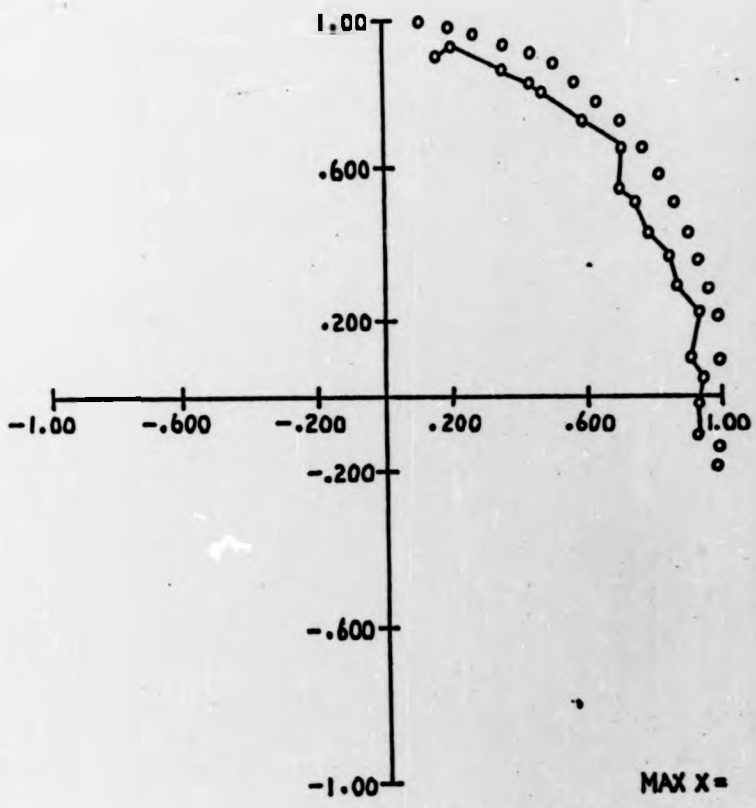

FIG.7. SII.UII.'OFF-SET S.C.'

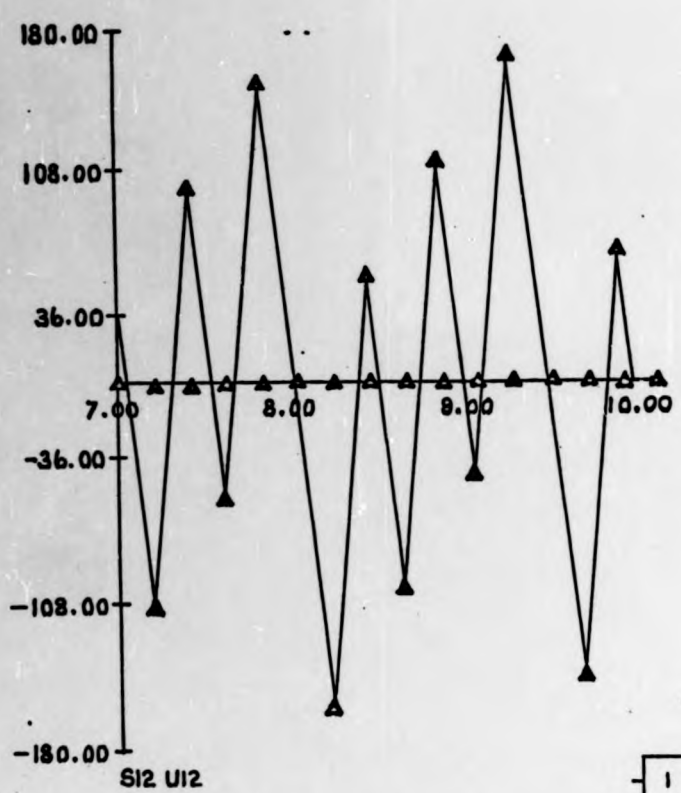

FIG.9
REVERSE TRANSMISSION_PHASE ANGLES_
'THROUGH LINE'

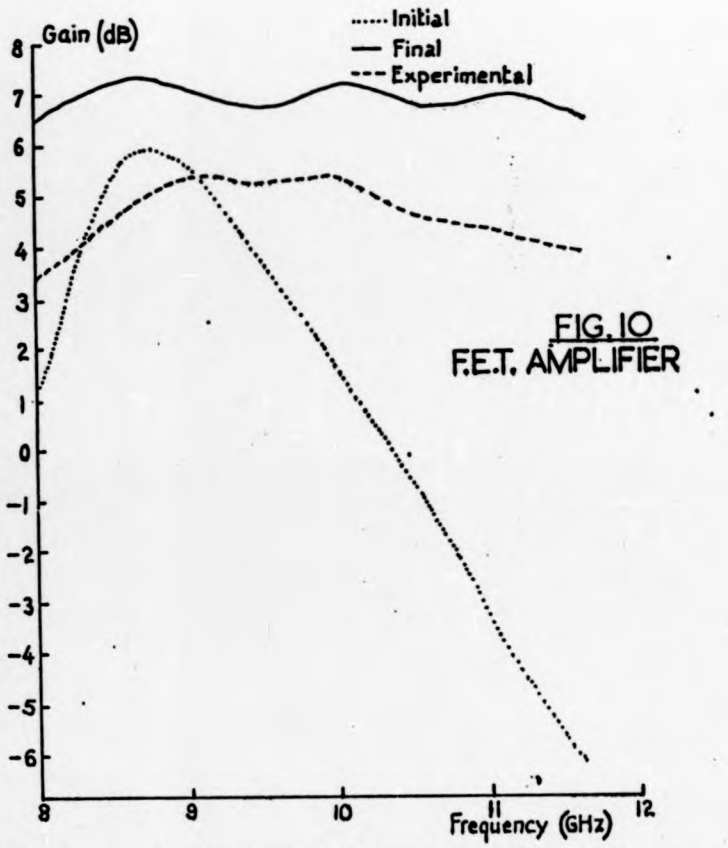

FIG.10
F.E.T. AMPLIFIER

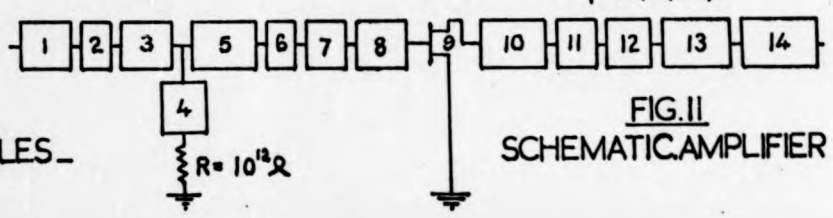

FIG.11
SCHEMATIC.AMPLIFIER

(III)Electron. Lett. Vol. 12, No. 19,
15th Sept. (1976) pp. 496-497.

MICPA: EVALUATION OF MICROSTRIP-LINE PARAMETERS*

Indexing terms: Computer-aided analysis, Striplines

A subroutine for microstrip-line parameters is described which evaluates dispersive effects, microstrip dimensions, conductor attenuation and dielectric loss.

Introduction: During the last few years, a large number of papers on computerised methods of evaluating microstrip parameters have been presented. These usually require extensive subroutines to compute individual parameters, so that the associated programs are rendered expensive in terms of computer time. They are also invariably cumbersome for incorporation into a computer analysis/optimisation package.[1] It is therefore particularly desirable to seek alternatives which are efficient and this consideration, in turn, influences the choice of associated algorithms for the microstrip parameters.

In this letter, a subroutine is presented which computes the parameters most frequently required in designing microwave integrated circuits. The particular transmission structure considered is standard microstrip, i.e. an open structure comprising a single stripline deposited on a dielectric substrate backed by a metallic ground plane. The subroutine, however, may be used in conjunction with programs or independently. This subroutine represents an improvement over OPTIMAL, described previously.[1]

Input data: In computing the various parameters, the following are assumed to be known:

characteristic impedance Z_0, Ω

air length of microstrip l, mm

substrate thickness, h, mils

relative permittivity of substrate, ε_r

conductor thickness t, microinches

metalised conductivity of strip σ_c, S/m

dielectric resistivity of substrate ρ_d, Ωcm

Computed parameters: The following parameters are computed via the associated algorithms

(*a*) Conductor loss

(*b*) Dielectric Loss

(*c*) Line dimensions

(*d*) Dispersion

In the subroutine, the above parameters are evaluated by reference to the methods indicated below:

(*a*) Conductor loss: Schneider's approximation,[4] being simple and explicit, is used to estimate conductor losses in the strip and ground plane.

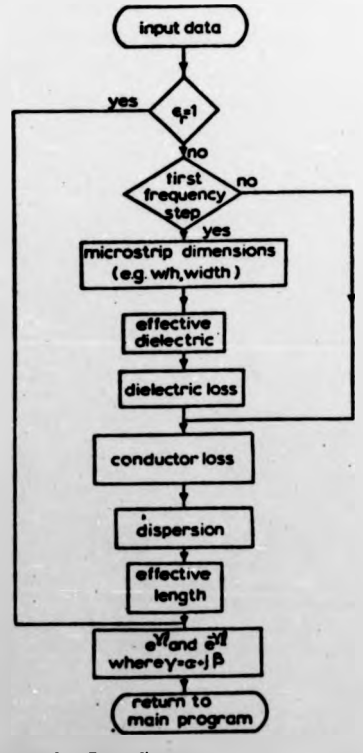

Fig. 1 *Flow diagram*

* The program listing and accompanying documentation are held in the IEE Library, Savoy Place, London WC2R 0BL, England. For further information, please contact the Library, quoting CP155

(b) Dielectric loss: this may be calculated if the loss tangent and also the electric-field distribution are known. Computation of the electric field is complicated and not practical for present purposes, so here we have used an empirical method, details of which will be published in due course.

(c) Line dimensions: the results of Wheeler[2] have been employed, expressing the ratio of width to thickness in terms of the characteristic impedance.

(d) Dispersion: of the many experimental and theoretical approaches reported, we have chosen the Gesinger model[3] as being the most appropriate for computer analysis.

A flow chart outlining the procedures is given in Fig. 1. In evaluating the dielectric loss, it is assumed that the conductivity of the substrate is substantially frequency independent.

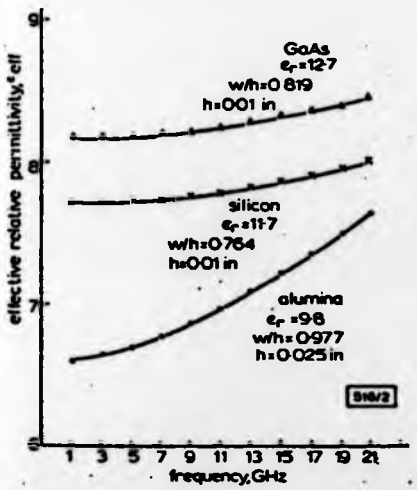

Fig. 2 *Effective relative permittivity against frequency for 50 Ω alumina, silicon and GaAs substrate*

To show how the substrate relative permittivity varies with frequency owing to dispersion, results are presented in Fig. 2 for 50 Ω, 635 μm (0·025 in) thick alumina microstrip and also for typical 254 μm (0·01 in) thick silicon and GaAs microstrip. Total losses with the above substrates are shown in Fig. 3, for copper conductors of 0·0381 μm ($1·5 \times 10^{-6}$ in) thickness.

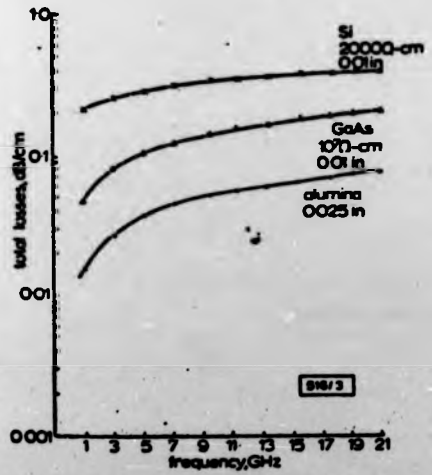

Fig. 3 *Total losses for 50 Ω silicon, GaAs and alumina substrate*
Conductor thickness = 0·0381 μm ($1·5 \times 10^{-6}$ in)

Acknowledgments: This work is supported by the UK Science Research Council. The authors wish to thank K. Halstead of the Computer Unit for many helpful discussions.

N. M. HOSSEINI
H. V. SHURMER

Department of Engineering
University of Warwick
Coventry CV4 7AL, England

9th August 1976

References

1 HOSSEINI, N. M., SHURMER, H. V., and SOARES, R. A.: 'OPTIMAL: a program for optimising microstrip networks', *Electron. Lett.*, 1976, 12, pp. 190–193
2 WHEELER, H. A.: 'Transmission line properties of parallel strips separated by a dielectric sheet', *IEEE Trans.*, 1965, MTT–13, pp. 172–185
3 GETSINGER, W. J.: 'Microstrip dispersion model', *ibid.*, 1973, MTT–21, pp. 34–39
4 SCHNEIDER, M. V.: 'Microstrip lines for microwave integrated circuits', *Bell Syst. Tech. J.*, 1969, 48, pp. 1421–1444

Program Details

(a) FORTRAN IV

(b) A maximum of 30 microstrip lines

(c) Complex and only single-precision arithmetic

(d) 139 cards, including comments

Performance Guide

(a) It is loaded on the XDS-Sigma 5 computer

(b) Core-size requirements: 17928 bytes

(c) Input medium: cards

(d) Output medium: line printer

(e) Work or data files needed: none

(f) Time taken to run submitted examples: compilation 01 : 07 min run 19 s

(IV) IEE Colloquium on microwave integrated circuit, Digest No. 1976/93, London 28 Oct. (1976) paper 4.

PARAMETER EVALUATION AND OPTIMIZATION FOR MICROSTRIP

N.M. Hosseini and H.V. Shurmer

The majority of computerized methods for evaluating microstrip parameters are based on semi-analytical and numerical techniques, but these procedures have the disadvantage of being difficult to incorporate into a computer-aided design (CAD) package. Serious problems arise when numerical techniques are used in conjunction with an analysis/optimization programme, since the routine of a numerical technique may perhaps be called upon thousands of times during a run. It is important to use a simple and accurate algorithm, especially as this permits simpler programming, reduced execution time and memory size. We have therefore developed a routine(1) for evaluating the parameters of open microstrip line, which includes evaluation of conductor and dielectric losses, and dispersion effects. A facility also exists within the programme for converting from the air lengths and characteristic impedances of transmission time elements to dimensions compatible with microstrip substrates. Results showing how dispersion causes the relative permittivity to vary with frequency are presented in Fig. 1 for 50Ω, 0.025 in. thick alumina microstrip, compared with typical 0.01 in. thick silicon and GaAs microstrip. Total losses with the above substrates are shown in Fig. 2, assuming copper conductors of 1.5×10^{-6} in. thickness.

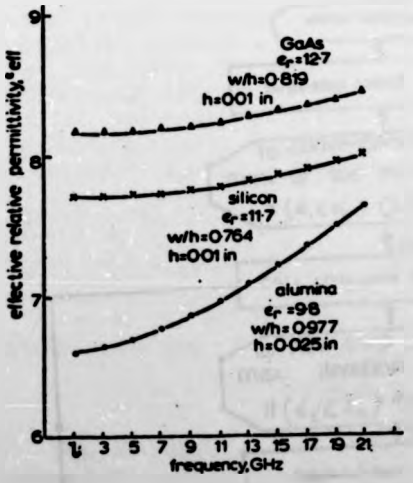

Fig. 1 *Effective relative permittivity against frequency for 50 Ω alumina, silicon and GaAs substrate*

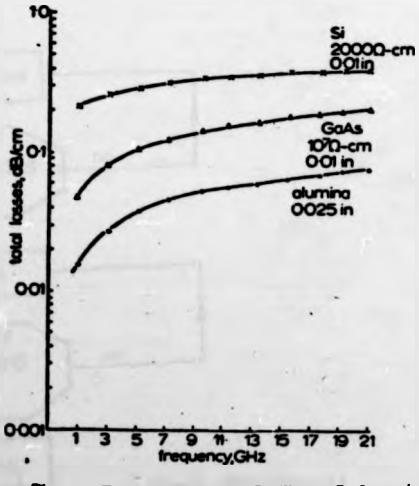

Fig. 2 *Total losses for 50 Ω silicon, GaAs and alumina substrate*

N.M. Hosseini and H.V. Shurmer are at the Engineering Department, University of Warwick.

When a particular substrate and conductor material combination has been chosen for designing a microstrip circuit, the circuit topology must be selected and analyzed. The analytical routine, which must be fast, plays a predominant role in the programme. Here we have employed transmission parameters (T) in the interests of high efficiency.

The choice of optimization technique is also very important. In general, the majority of optimization techniques are based on 'sequential' or linear search algorithms in which points previously generated are used to determine the new direction of search. Although extremely efficient in determining the minima of unimodal functions, (as encountered in amplifier optimization) a sequential search technique will converge to the nearest local minimum, ignoring neighbouring minima, which may be superior. By using two or three different strategies of optimization[2] also we may increase the accuracy of approach to the true minima. We also seek to reduce the execution time, particularly when the starting points are near to the position of the minimum. To these ends the authors have used a combination of large step direct search with conjugate gradient pattern-search techniques. To improve the chance of finding a global minimum solution to multi-modal problems, a limited number of random searches are also employed.

The nonunilateral properties of the GaAs f.e.t. and bipolar transistor in microwave amplifier circuits means that the elements all interact in some degree with each other in the effects on the overall response. For this reason, the authors have used the pseudo-random sequence technique[3] for the chosen variables. This reduces the possibility of the optimum-following algorithm concentrating on certain variables to the exclusion of others, and thereby yielding false minima. A flow chart of procedure is indicated in Fig.3

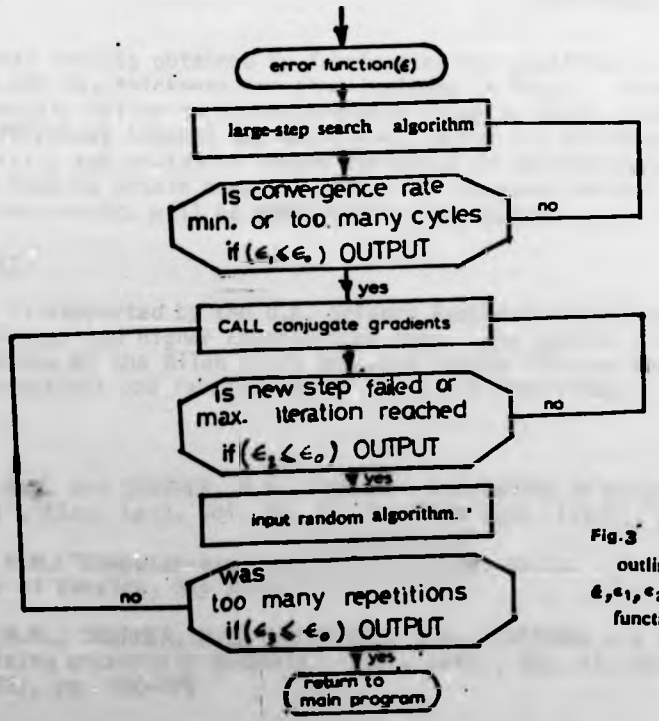

Fig.3 *Flow diagram* outlining the procedures. $\varepsilon, \varepsilon_1, \varepsilon_2$ and ε_3 are the objective functions at each stage.

The programme has been written for cascades of 2-port circuit elements. It employs a 'least-pth' objective function based on the following network responses: (a) transducer gain, (b) ripple gain and (c) input/output reflection coefficient.

As an example of the programme's ability to produce good results from poor starting values, consider the amplifier circuit shown in Fig. 4. The aim was to achieve a flat 7 dB power gain and 1.5:1 VSWR at both input and out ports over the range of 8-11.6 GHz. Fig. 5 shows the frequency response of both the initial and final design. The initial circuit performance gave 1.2 dB gain at 8 GHz, increasing to 5.8 dB at 8.8 GHz, and falling to -6 dB at 11.6 GHz. The final achievement was a gain of 7 dB ± 0.5 dB and a VSWR of better than 2:1 over the band.

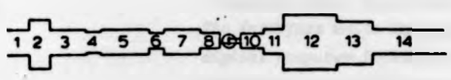

Fig. 4 X-band GaAs f.e.t. amplifier circuit

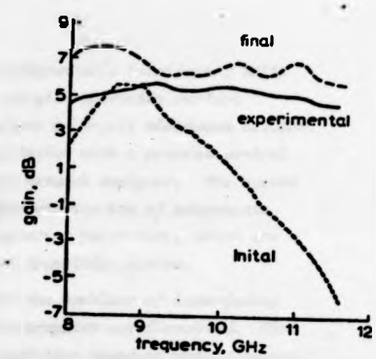

Fig. 5 Frequency response of both initial and final design.

Experimental results obtained by fabricating the amplifier on an alumina substrate of 0.025 in. thickness are also included in Fig. 5. Although the experimental results follow the predicted gain response shape, there are significant differences between the two curves, which are attributable to junction parasitics and radiation losses for which no correction have been made. Work is now in hand to obtain accurate models for standard microstrip discontinuities and the results will be published in due course.

Acknowledgements

This work is supported by the U.K. Science Research Council and by the Ministry of Sciences and Higher Education of Iran. The authors are indebited also to R.A. Soares of the Allen Clark Research Centre, Plessey Company Ltd., for many useful discussions and fabrication of the f.e.t. amplifier.

References

1. HOSSEINI, N.M. and SHURMER, H.V.: "MICPA - evaluation of microstrip line parameters", Elec. Lett. Vol. 12, No. 19, 15th Sept. (1976), pp. 496-497.

2. HOSSEINI, N.M.: "Computer-aided microwave circuit design", Internal report, University of Warwick, May 1976.

3. HOSSEINI, N.M., SHURMER, H.V. and SOARES, R.A.: "OPTIMAL - a programme for optimising microstrip networks", Elec. Lett., Vol. 12, No. 8, 15th April (1976), pp. 190-192.

investigate successively a variety of options. A basic block diagram of interfacing between the network analyzer and the computer is shown in Fig.4.1 Communication between measuring set-up and the computer was arranged by cable connection. A patch panel in the computer room provides this communication by inserting pins in appropriate positions.

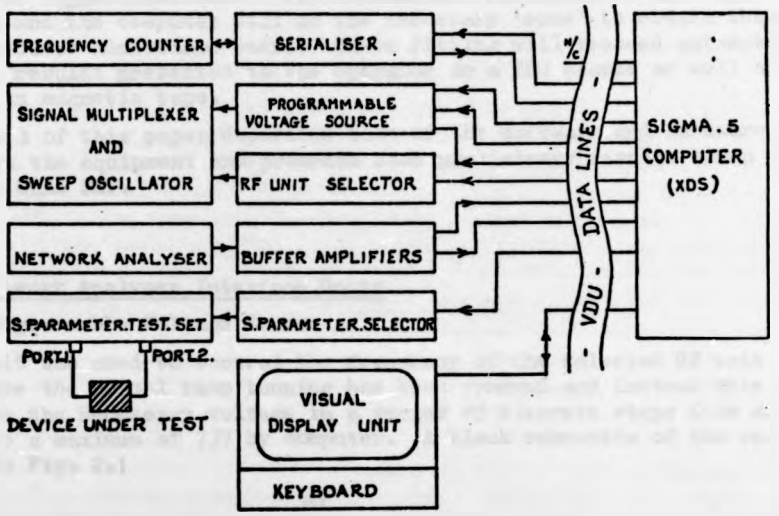

FIG. 4.1 THE INTERFACING UNITS BETWEEN COMPUTER AND NETWORK ANALYSER.

The network analyzer and associated system is controlled by the visual display unit (V.D.U.). The system is sited remotely from the computer, but within the same building. Ten channels for data or control are available, to be shared between individual parts of the system. As this is less than the number of functions to be provided some interfacing units were developed to reduce the number of lines. These are described in the following sections.

Full device characterisation for low noise amplifier design requires a (NF) noise figure measuring system as an essential. The conventional method of determining the noise figure of a two port network is to measure the total (NF) the network in combination with a receiver. Measurement of network gain and receiver noise figure allows the network noise figure to be extracted by use of Friis' formula [7]. However this procedure does not fully characterise the device as it only gives one of the three noise parameters, the noise figure. For full device characterisation, determination of the optimum source admittance and the noise resistance are necessary.

The system under development proposes to extract all these parameters by using a system similar to that described by Lane [8]. A variable impedance tuner sets up a number of source admittances at which system noise figure and gain are measured. Device noise figures are obtained from Friis' formula giving a number of noise figure/source admittance pairs. These are

curve fitted to the noise figure/source admittance equation [9] giving the required parameters.

It is known that this technique is being used in other major microwave laboratories [10-12] but only in a manual or semi-automatic mode. It is intended that the system in our laboratories be entirely computer-controlled and corrected. A computer-controlled trough-line tuner will set up the source admittance, whilst the computer itself will 'read' the results from the noise figure indicator. All corrections for system losses will then be applied and the computer will do the necessary 'sums' to obtain the noise figure/source admittance pairs. Curve fitting will proceed automatically and the results presented to the operator on a VDU source as well as being stored on magnetic tape.

Section 3 of this paper describes some of the software and hardware associated with the equipment and presents some preliminary results taken on a Plessey GaAs FET.

2. Network Analyser Interface Units

2.1 Programmable Voltage Source

This unit was used to control the frequency of the selected RF unit. In this case the normal ramp tunning has been removed and instead this unit supplies the necessary voltage in a series of discrete steps from a minimum of 3V to a maximum of 73V by computer. A block schematic of the unit is shown in Fig. 2.1

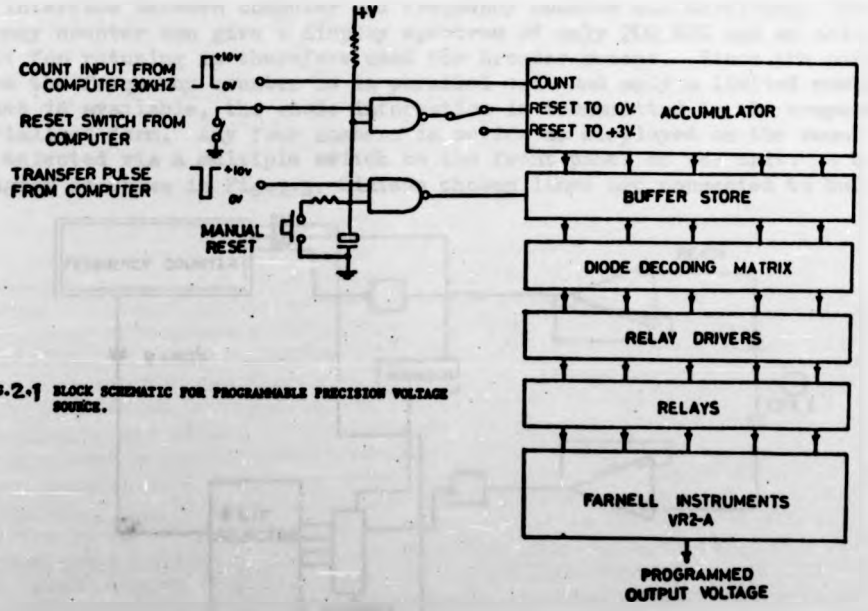

FIG.2.1 BLOCK SCHEMATIC FOR PROGRAMMABLE PRECISION VOLTAGE SOURCE.

The information required to set up the output voltage is fed in serial form from the computer to the unit, by means of pulses, in which each one represents 1mV. The pulses are fed internally to an accumulating counter as shown. At the start of a test programme it is first necessary for the com-

puter to supply a reset signal, which could be by closure of a set of contacts as shown. This sets up the accumulator to a count of 3000 ensuring that the maximum output voltage is 3V (this is a requirement of the T.W.T. tube). Following this, it is necessary for the computer to set up the output voltage for the first test. This is accomplished by feeding pulses into the accumulator, the number being equal to the required output voltage expressed in mV less 3000. For example, if an output of 5V is required, 5000–3000 = 2000 pulses are fed to the accumulator. This information is then transferred into the buffer store and is fed to the diode decoding matrix which decodes the information in the buffer store and operates the appropriate relays via the relay driver circuits.

Successive increases in output voltage are similarly achieved by feeding the appropriate number of additional pulses into the accumulator and transferring the information into the buffer store. The advantage of using a buffer store is twofold: firstly it cuts down the number of operations for the relays, since they only operate when information in the buffer store is changed by the transfer pulse, and secondly the fact that information can be fed into the accumulator ready for the next test whilst the previous test is in progress reduces the overall test time.

The automatic switch-on reset circuitry ensures that the output automatically resets to 3V on switch on. This resetting operation may also be preformed manually by depressing a push button mounted on the front panel.

2.2 Serializer Unit

To enable the computer to read frequency displays from the frequency counter, an interface between computer and frequency counter was developed. The frequency counter can give a display spectrum of only 200 MHZ and an additional unit for retuning is therefore used for broader sweeps. Since the output from the frequency counter is in parallel code and only a limited number of lines is available, the whole information is transmitted to the computer in serialised form. Any four numbers in series as displayed on the counter may be selected via a multiple switch on the front panel of the unit. A block diagram is shown in Fig.2.3. Sixteen chosen lines are connected to buffer

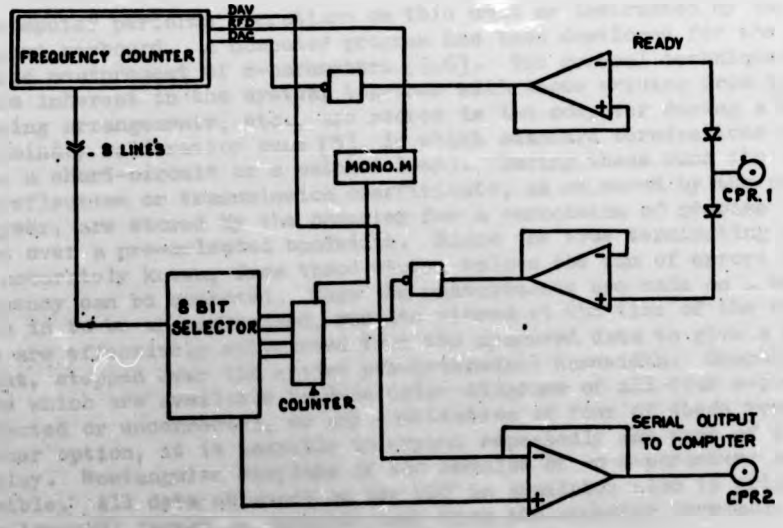

FIG. 2.3 INTERFACING BETWEEN FREQUENCY COUNTER AND COMPUTER

transistor stages in each line to match the high output impedance of the counter and to drive the logic input (output impedance is 100 K). A multiplexer with 16 inputs is used for serialising the information, which is fed through the output operational amplifier to provide suitable output levels for the computer link (0V and 9V).

Information on the availability of the display is fed to the computer via the serialiser by another link, which indicates the 'ready' state. The same signal is used to derive the strobe of the serialiser which enables simultaneous reading of the latter. When this signal is present the computer can send sixteen pulses on a third 'clock line' to read the display. These clock pulses drive the serialiser through a four bit counter, the reading being taken at the serialiser output.

2.3 S-parameter and R.F. Unit Selector

The s-parameter set is used for measurement of all the s-parameters of a two port device. To drive this unit automatically a selector network was developed which interprets the level of an analogue voltage as a 3-bit binary word. Utilising this unit, the computer may be switched automatically to read any desired parameters by applying the appropriate voltage. This procedure also enables a single analogue voltage line to serve for three digital lines.

The R.F. unit selector operates on a principle similar to that of the s-parameter selector in that a 4-bit binary word, required to select one of the three R.F. units, is generated from a single analogue voltage.

2.4 Buffer Amplifier

Analogue outputs from the network analyser are in the region between -1.5 and +1.5 volts. Since, in the case of a matched load, the outputs are very nearly at zero voltage. The noise on the line present could influence final results. Provision was therefore made to raise these levels via operational amplifiers to the range -10.0, +10 volt, thus giving more accurate readings in the vicinity of zero voltage.

2.5 Visual Display Unit

The computer performs operations on this unit as instructed by the user on an input keyboard. A computer program has been developed for the automatic on-line measurement of s-parameters [3,6]. The general technique is that errors inherent in the system, together with those arising from transitions, mounting arrangements, etc., are stored in the computer during a series of preliminary calibration runs [5], in which standard terminations are used (e.g. a short-circuit or a matched load). During these runs the corresponding reflection or transmission coefficients, as measured by the network analyser, are stored by the computer for a succession of precise frequency steps over a pre-selected bandwidth. Since the true terminating impedances are accurately known, from these stored values the sum of errors at each frequency can be computed. When the measurements are made on a test piece which is to be characterised, results stored at the time of the calibration runs are effectively subtracted from the measured data to give a corrected output, stepped over the entire pre-determined bandwidth. Graphical displays which are available include polar diagrams of all four s-parameters, corrected or uncorrected, or any combination of four of these results. As a further option, it is possible to expand repeatedly any part of a polar display. Rectangular displays of the modulus of an s-parameter are also possible. All data obtained on the VDU is available also in printed form or in a 'dumped' format on magnetic tape from the computer terminal. This may be used for further evaluation or stored.

3. Noise Figure Measurement

3.1 Hardware

The noise measurement system is based on the type 7380 System Noise Monitor (SNM) manufactured by the Airborne Instruments Laboratory (AIL). Although less accurate than their Type 75 Precision Automatic Noise Figure Indicator (PANFI) the SNM has the advantage of simultaneous indication for gain and noise figure, and a BCD output of each parameter via a rear panel socket. The other hardware is illustrated in Figure 3.1 and is the same as most conventional noise figure measuring systems.

At present the trough line tuner is a manual one loaned by the Plessey Company, Caswell. It gives accurate control over the vertical and horizontal displacement of a tuning slug, but due to the slug size is only usable up to 8 GHz. A computer-controlled tuner is in the design stage. It comprises two stepping motors controlling the displacement of an interchangeable slug. enabling the tuner to cover a broad bandwidth. The rest of the system will remain as in Figure 3.1.

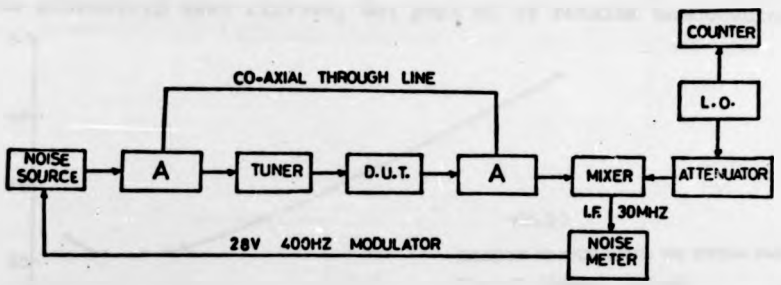

FIG. 3.1 BLOCK DIAGRAM OF NOISE MEASUREMENT SYSTEM, WHERE BLOCK 'A' REPRESENTS FOR BIAS TEE, CO-AXIAL SWITCH AND ISOLATOR.

3.2 Software

The presently available computer programs accept gain and noise figure as a function of source admittance and output the noise parameters and the co-ordinates of the constant noise figure circles on a Smith chart. There are two versions of the program. The first and simplest accepts the data from a card desk and outputs the results to the line printer. The second is an interactive program and runs from a VDU alongside the measurement equipment. Results are available on the VDU screen and can also be dumped onto magnetic tape.

Both programs are built around a minimisation routine which 'curve-fits' the experimental data to the theoretical noise figure/source admittance relationship. The interactive program prompts the user by displaying the order of measurements and accepting the results at the required time. At present, the data is entered on the VDU keyboard, though it is hoped that soon the computer will 'read' the gain and noise figure directly from the back panel of the SNM. Calibration data is also fed to the VDU at the time of measurement. All correction computations are done by the computer prior to entry into the curve-fitting routine.

The output of results on the VDU screen is in tabular form. However, all results are dumped on to magnetic tape and a subsidiary program, run externally from the measured program, can call these off and either tabulate them on the line printer, or give any one of a series of graphical plots. Routines enabling plotting of the results straight on to the VDU screen are under development.

3.3 Results

A few GaAs FETs manufactured by the Plessey Company, Caswell, have been measured on the manually controlled system. Some results are shown in Figures 3.2 to 3.5.

Figure 3.2 gives a plot of noise figure against drain current at 3 GHz, for a constant drain bias. The minimum noise figure is obtained around 10 A and is of the order of 2 dB. A plot of noise figure versus frequency for the same device is shown in Figure 3.3. This is at constant drain bias and current. A theoretical noise figure versus frequency plot has been obtained for this device using reference[13]. The two curves show the same slope but are separated by 0.6 dB. Part of this error can be attributed to the loss in the microstrip test fixture, but part of it remains unaccounted for.

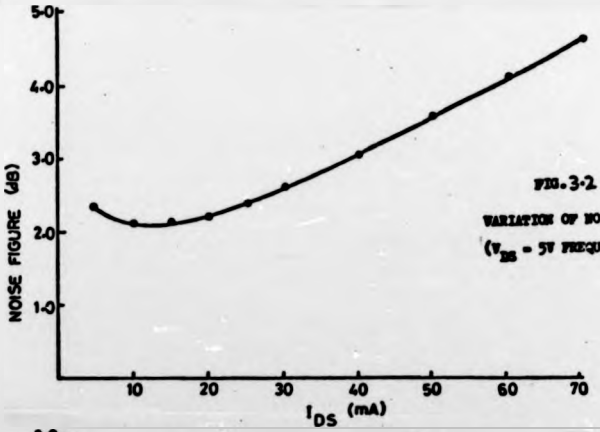

FIG. 3·2
VARIATION OF NOISE FIGURE FOR TYPICAL GaAs FET VERSUS I_{DS}
(V_{DS} = 5V FREQUENCY = 3.0 GHz)

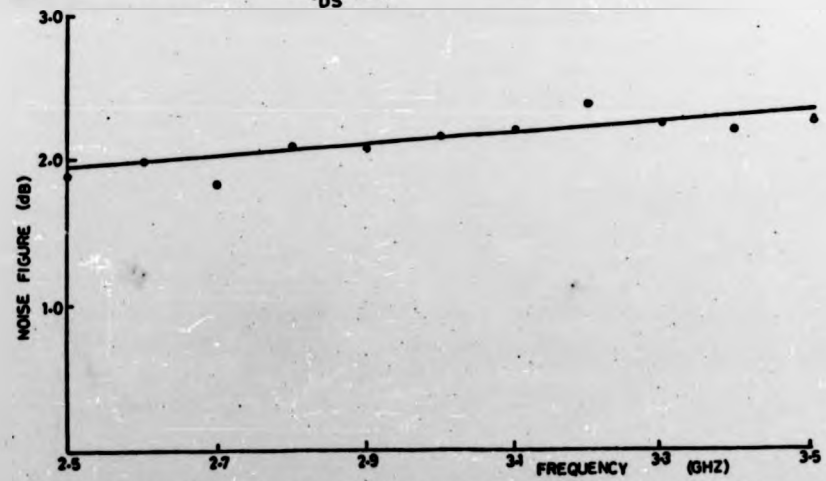

FIG. 3·3 VARIATION OF NOISE FIGURE FOR TYPICAL GaAs FET AGAINST FREQUENCY (V_{DS} = 5.0V AND I_{DS} = 10 mA)

The variation of source admittance for minimum noise figure versus frequency is shown in Figure 3.4, whilst Figure 3.5 shows a set of circles for constant noise figure.

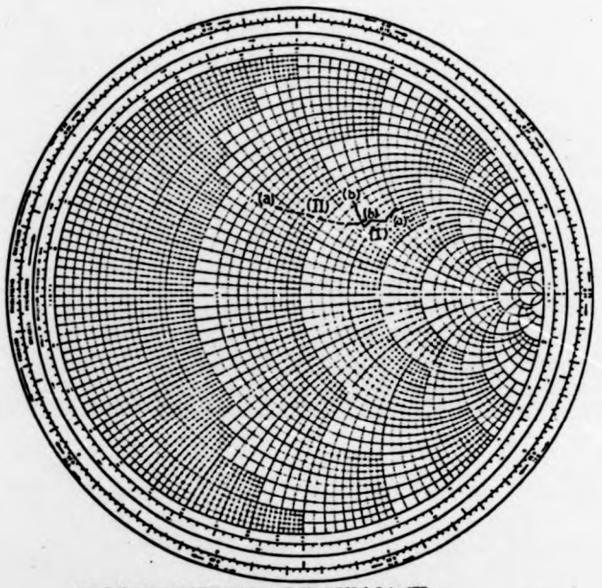

FIG.3.4 OPTIMUM SOURCE ADMITTANCE FOR TYPICAL GaAs FET
(I) FREQUENCY RANGE (a) 2.5 GHz TO (b) 3.5 GHz
(V_{DS} = 5.0V AND I_{DS} = 10 mA)
(II) I_{DS} = 70 mA (a) TO 5mA (b) (FREQUENCY 3.0 GHz AND V_{DS} = 5.0V)

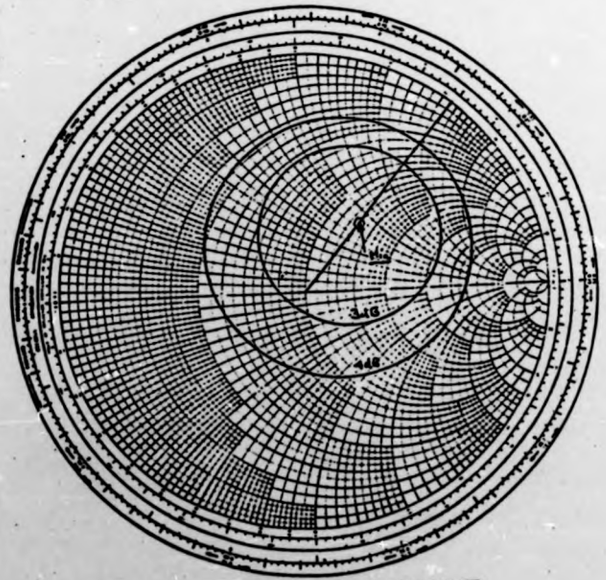

FIG.3.5 CONSTANT NOISE FIGURE CIRCLES FOR TYPICAL GaAs FET
(FREQUENCY = 3.0 GHz, V_{DS} = 3V, I_{DS} = 10 mA AND
NOISE RESISTANCE = 15.3 OHMS).